Chemical oceanography of Irish waters, with particular emphasis on ocean acidification

Triona McGrath

Ph.D

National University of Ireland, Galway

Dr. Rachel Cave[1], Dr. Evin McGovern[2], Dr. Martin White[1]

[1] School of Natural Sciences, National University of Ireland, Galway
[2] Marine Institute, Ireland

June 2012

Table of Contents

Declaration

I, Triona McGrath, declare that the results presented are to the best of my knowledge correct, and that this thesis represents my own original work, carried out during the designated research project period. As the thesis was part of a larger research project, see Appendix 1, other authors made contributions to the articles presented here, as outlined on Page ix.

Signed_____Date:_____

Supervisor(s)

Signed_____Date:_____

Acknowledgements

Firstly I would like to thank my supervisors Rachel Cave, Evin McGovern and Martin White for giving me the opportunity to carry out this research. Special thanks to Rachel and Evin who have been so supportive throughout my PhD and have patiently read and corrected innumerable drafts of papers and chapters. Thank you Evin for securing funding and allowing flexibility throughout the fellowship.

I would like to thank the Marine Institute for the fellowship position which has given me invaluable work experience alongside my research project. Many thanks to the MI staff, in particular everyone in the environmental chemistry team, who I have thoroughly enjoyed sharing an office with over the years. Thanks to the crew of the Celtic Explorer and Voyager, and in particular the fellow scientists who made all the sampling possible and somehow managed to make every survey a good laugh, despite fierce North Atlantic swells! Thank you Tom for all the help with cruise prep and in the lab in general. Glenn Nolan and Kieran Lyons, I thank you for your insights into physical oceanography and help and support with data and tricky Matlab scripts.

Thanks to Caroline Kivimae for the training on our *lovely* VINDTA and for sharing your carbon chemistry knowledge, along with useful feedback on papers and chapters. Thanks to Eileen Joyce for the training and guidance in the sometimes frustrating nutrient analysis.

Last but not least, I'd like to give a massive thank you to my parents for your endless support and encouragement; I couldn't have done it without you. Thank you Caoimhe for keeping me company on the drives home from Galway and allowing me to rant every now and then! A special thanks to Neil, you have supported me in every way possible which I will be forever grateful.

Thank you all so very very much!

Abstract

Strategically positioned along the western margin of the North Atlantic, Irish shelf and offshore waters play a crucial role in the global thermohaline circulation and regional and global climate cycles. The main objective of this study was to investigate the biogeochemical characteristics of the main water masses in the region to generate information on how the marine environment is changing with time. Dissolved oxygen, nutrient and carbon data, collected across the Rockall Trough in February 2009 and 2010, proved useful as chemical tracers of water masses in the region and highlighted processes that could not have been identified using hydrographic data alone. Inorganic carbon data from 2009 and 2010 were compared with WOCE data collected across the Trough in the 1990s to assess the temporal evolution of anthropogenic carbon (ΔC_{ant}) in the region over 2 decades. Two methods were used to calculate ΔC_{ant} between surveys, $C_{T\text{-}abio}$ and extended multiple linear regression, both of which resulted in similar rates of increase in C_{ant} through the water column, with subsequent decrease in pH and saturation state of calcium carbonate minerals. Between 1991 and 2010, pH in subsurface waters has decreased by 0.040±0.003 units and by 0.029±0.002 units in Labrador Sea Water.

Net community production (NCP) was calculated along the western shelf edge between 49.8-55.4ºN. Generally maximum NCP was measured in surface waters over the 500-750m contours, decreasing in both offshore and shallower on-shelf surface waters. Where calculated, there was a net CO_2 uptake from the atmosphere suggesting this region is a CO_2 sink during the productive season.

Due to its influence on the buffer capacity of the surface ocean, the distribution of total alkalinity (A_T) in Irish coastal and shelf waters was investigated. The A_T distribution in outer estuarine and coastal waters is more complex than along the western shelf and through the centre of the Irish Sea due to varying river inputs. Rivers with limestone bedrock catchments had relatively high A_T concentrations which influence the buffer capacity, and hence rate of pH change, of the surrounding coastal waters. Results indicate that the algorithm produced by Lee et al. (2006) to calculate A_T from temperature and salinity should not be used in Irish coastal waters due to variable but substantial riverine inputs of A_T.

List of Articles

This thesis is based on the work presented in the articles listed below. I was involved in preparation for 11 of the 12 of the surveys, and was on board to carry out sample and data collection for 8 of them (exceptions were CV0911, CV0924, CE0919 and CE10014). I was trained by post-doctoral researcher Dr Caroline Kivimae at NUIG in the analysis of carbon samples, and was wholly responsible for all nutrient and salinity analysis. As the lead author on Papers I, II and IV, I was responsible for the data analysis and writing of each paper, while my co-authors contributed in various ways to the sampling programme, method development and sample analysis, and discussion of results. While it was Rachel Cave that was responsible for the concept of Paper IV, I was largely responsible for the writing of the paper and am therefore the first author. Caroline Kivimae was responsible for the concept of Paper III, along with the overall content and calculations, while I was responsible for the nutrient and salinity analysis, some of the data analysis prior to production estimates and assisted in writing the introduction and method sections, as well as participating in discussion of the results.

Articles

I. McGrath, T., Nolan, G., McGovern, E., 2012. Chemical characteristics of water masses in the Rockall Trough. Deep Sea Research Part I: Oceanographic Research Papers 61 (0), 57-73.

II. McGrath, T., Kivimäe, C., Tanhua, T., Cave, R.R., McGovern, E. Inorganic carbon and pH levels in the Rockall Trough 1991-2010. Deep Sea Research Part I: Oceanographic Research Papers 68 (0), 79-91.

III. Kivimäe, C., McGrath, T., Cave, R.R. and White, M. Net community production from biogeochemical parameters along the Irish continental slope from 49.8 - 55.4°N. Submitted to Marine Chemistry.

IV. McGrath, T. Cave, R.R. and Kivimäe, C. and McGovern, E. Total alkalinity in Irish coastal and shelf waters. Submitted to Estuarine Coastal and Shelf Science.

List of Figures

5. (a) $\Delta C_{T\text{-}abio}$ concentration (μmol kg^{-1}) and (b) pH (total) in the subsurface waters of the southern Rockall Trough between 1991 and 2010
6. (a) $\Delta C_{T\text{-}abio}$ concentration (μmol kg^{-1}) (b) pH (total) between 1500-2000m across the southern Rockall Trough between 1991 and 2010
7. ΔC_{ant}^{eMLR} (μmol kg^{-1}) between 200-2200m across the southern Rockall Trough between 1991 and 2010

Paper III

1. Survey and transect numbers for stations used in this paper
2. Potential temperature-salinity plot from CE0911 with water mass abbreviations
3. Cross slope transects from CE0911 sea surface salinity (a), temperature (b) and nitrate (c) vs. transect distance
4. Temperature and salinity versus depth at the CE0911 1500m stations
5. CE0911 nitrate, C_T and oxygen saturation versus depth for all stations
6. Nitrate and C_T concentrations in the top 500m for selected transects from CE0807, CE0911, CE10002 and CE10003
7. Net community production (g C m^{-2}) calculated from C_N^{prod}, C_P^{prod} and ΔC_T vs. station numbers, alongside air-sea CO_2 exchange for CE0911

Paper IV

1. The study area with station positions where A_T measurements were made, labelled bathymetry and principal Irish rivers numbered (1) Corrib, (2) Shannon, (3) Fergus, (4) Lee, (5) Blackwater, (6) Suir, (7) Nore, (8) Barrow, (9) Slaney, (10) Avoca, (11) Liffey, (12) Boyne, (13) Newry, (14) Lagan, (15) Lower Bann, (16) Mourne, (17) Foyle and (18) Erne.
2. Surface distribution of (a) salinity (b) winter TOxN (c) winter phosphate (d) winter silicate and (e) total alkalinity.
3. A_T versus salinity from four separate surveys, with predicted freshwater A_T concentrations from the A_T -salinity regressions.
4. (a) A_T residuals (calculated A_T using L'06 minus measured A_T) vs. salinity, where the dotted lines indicate the full limits to the Lee et al. (2006) algorithm (b) A_T versus salinity for all surveys, the dotted lines indicate where our data fall within the uncertainty given by Lee et al. (2006).

List of Tables

List of Abbreviations

$\Delta\sigma_T$	Delta sigma theta, i.e. density difference
AABW	Antarctic Bottom Water
AAIW	Antarctic Intermediate Water
AOU	Apparent oxygen utilisation
ASH	Aragonite saturation horizon
A_T	Total alkalinity, also called TA
BATS	Bermuda Atlantic Time Series
C:N	Carbon to nitrogen ratio
C:P	Carbon to phosphate ratio
Ca^{2+}	Calcium
$CaCO_3$	Calcium carbonate
C_{ant}	Anthropogenic carbon
C_{ant}^{eMLR}	Anthropogenic carbon calculated using eMLR
CDIAC	Carbon dioxide information analysis centre
CFC	Chlorofluorocarbons
C_N^{prod}	Net community production calculated from nitrate deficit
CO_2	Carbon dioxide
$CO_2(aq)$	Aqueous CO_2
$CO_2(g)$	Gaseous CO_2
CO_2*	The sum of $CO_2(aq)$ and H_2CO_3
CO_3^{2-}	Carbonate ions
C_P^{prod}	Net community production calculated from phosphate deficit
CRM	Certified reference material
CS	Celtic Sea
C_T	Dissolved inorganic carbon, also called DIC or TCO_2
$C_{T\text{-}abio}$	C_T corrected for biological activity
$C_T^{air\text{-}sea}$	Dissolved inorganic carbon due to air-sea exchange
CTD	Conductivity-Temperature-Depth probe
$C_{T\text{-}N}^{air\text{-}sea}$	Air-sea CO_2 exchange calculated from C_N^{prod}
$C_{T\text{-}P}^{air\text{-}sea}$	Air-sea CO_2 exchange calculated from C_P^{prod}
C_T^{pre}	Preformed dissolved inorganic carbon
$C_{T\text{-}prod}$	Integrated deficit of C_T to the euphotic depth
DI	Deionised water
DIC	Dissolved inorganic carbon, also called C_T
DO	Dissolved oxygen
DOC	Dissolved organic carbon
ED	Euphotic depth
EEA	European Environment Agency
eMLR	Extended multiple linear regression
ENAW	Eastern North Atlantic Water
EPA	Environmental Protection Agency
ESTOC	European Station for Time Series in the Ocean
fCO_2	Fugacity of carbon dioxide
GEOSECS	Geochemical Ocean Section Study
GS	Goban Spur
GSI	Geological Survey Ireland
H^+	Hydrogen ion
H_2CO_3	Carbonic acid

H_2O	Water
HB	Hatton Bank
HCO_3^-	Bicarbonate ion
HDPE	High density polyethylene
HOT	Hawaii Ocean Time Series
ICES	International Council for the Exploration of the Sea
INAB	Irish National Accreditation Board
IPCC	Intergovernmental Panel on Climate Change
IS	Irish shelf
ISF	Irish Shelf Front
ISOW	Iceland Scotland Overflow Water
K_0	Temperature dependent solubility coefficient for CO_2 in seawater
K_1	First dissociation constant for carbonic acid
K_2	Second dissociation constant for carbonic acid
KSO_4	Potassium sulphate
K_{sp}*	Solubility product of $CaCO_3$
K_z	Eddy (vertical) diffusivity
LDW	Lower Deep Water
LOD	Limit of detection
LOQ	Limit of quantification
LSW	Labrador Sea Water
MI	Marine Institute, Ireland
MLD	Mixed layer depth
MLR	Multiple linear regression
MOW	Mediterranean Overflow Water
MW	Mediterranean Water
n	Number of samples
NAC	North Atlantic Current
NAO	North Atlantic Oscillation
NA_T	Normalised total alkalinity to constant salinity
NCP	Net community production
NC_T	Normalised dissolved inorganic carbon to constant salinity
NEADW	North East Atlantic Deep Water
NO_2	Nitrite
NO_3	Nitrate
NO_3^o	Preformed nitrate
NO_3^{pre}	Preformed nitrate
NP	Nitrogen to Phosphate ratio
N_{prod}	Integrated deficit of nitrate to the euphotic depth
NROCK	Northern Rockall transect
NUIG	National University of Ireland, Galway
NUT	Dissolved inorganic nutrients
O_2	Oxygen
OH^-	Hydroxide ion
^oN	Degrees North
OSIL	Ocean Scientific International Ltd
^oW	Degrees West
P	Pressure
PA	Practical alkalinity
PAP	Porcupine Abyssal Plain

PB	Porcupine Bank
pCO_2	Partial pressure of carbon dioxide
pH	Describes the acidity of a liquid
pH_F	pH on the free scale
pH_{NBS}	pH on the National Bureau of Standards scale
pH_{SWS}	pH on the seawater scale
pH_T	pH on the total scale
PO_4	Phosphate
PO_4^o	Preformed phosphate
PP	Primary Productivity
ppmv	parts per million volume
P^{pre}	Preformed phosphate
P_{prod}	Integrated deficit of phosphate to the euphotic depth
PSB	Porcupine Sea Bight
RB	Rockall Bank
RPD	Relative percentage difference
RV	Research vessel
S	Practical Salinity
S_A	Absolute salinity
SAIW	Subarctic Intermediate Water
SEC	Shelf Edge Current
Si	Silicate
sML	Summer mixed layer
SOP	Standard Operating Material
S_R	Reference composition salinity
SROCK	Southern Rockall transect
SST	Sea Surface Temperature
SW	Surface water
T	Temperature
t	Time
TA	Total alkalinity, also called A_T
TCO_2	Dissolved inorganic carbon, also called C_T or DIC
THC	Thermohaline Circulation
TOC	Total organic carbon
TOxN	Total oxidised nitrogen
UCM	Uncertainty of measurement
VINDTA	Versatile Instrument for the Determination of Titration Alkalinity
wML	Winter mixed layer
WOCE	World Ocean Circulation Experiment
WTOW	Wyville Thomson Overflow Water
WTR	Wyville Thomson Ridge
z	Depth
Ω	Omega, saturation state of calcium carbonate

1. Introduction

Ocean circulation has a profound influence on the climate system as it regulates the global transport of heat, salt and other properties. The North Atlantic plays an important role in the global thermohaline circulation (THC), a large scale ocean circulation driven by heat and freshwater fluxes. Warm surface water of the Atlantic Ocean is transported northwards towards the poles and is continually cooled through heat loss to the atmosphere, helping to regulate the western European climate. Due to high evaporation rates relative to precipitation, the salinity of the North Atlantic is relatively high compared to the Pacific and the Indian Oceans (Tomczak and Godfrey, 1994). Due to the high salt content and cool temperatures, the northern North Atlantic is an area of deep water formation. The Rockall Trough, a deep sea channel to the west of Ireland, is a pathway for warm and saline North Atlantic waters to reach the Arctic Ocean and therefore contributes to the global THC. There is a complex interaction of a number of water masses of different origins and histories in the Trough and therefore the knowledge of the distribution and variability of environmental parameters in the region can provide valuable information on the changing global climate.

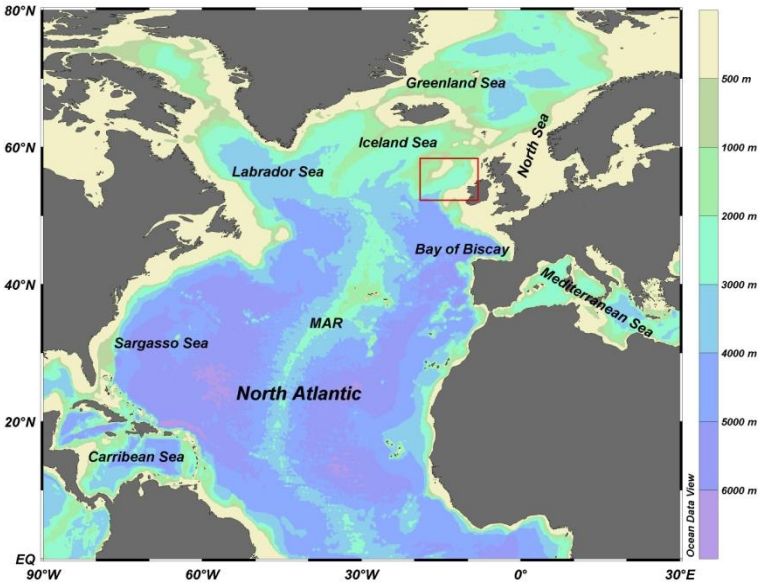

Figure 1.1. Map illustrating the North Atlantic; the red box highlights the Rockall Trough region. MAR: Mid Atlantic Ridge.

1.1 Climate Change

"Climate is usually described in terms of the mean and variability of temperature, precipitation and wind over a period of time, ranging from months to millions of years." (Solomon et al., 2007).

The Earth's climate system is constantly changing due to external forcings, such as relative distance from the sun, volcanic activity and atmospheric composition, along with internal feedback mechanisms. Prior to the Industrial Revolution (1850's), the Earth's climate changed in predictable cycles, such as glacial-interglacial cycles. However since then, human activities have gradually been altering the ocean-atmosphere climate system. Carbon dioxide (CO_2) is one of the primary greenhouse gases responsible for trapping the sun's long wave radiation in the Earth's atmosphere, without which life on Earth as we know it would not survive. However, atmospheric CO_2 concentrations have increased from 280 ppmv (parts per million volume) in the Industrial Revolution to 394 ppmv in February 2012 (Thomas Conway and Pieter Tans, NOAA/ESRL (www.esrl.noaa.gov/gmd/ccgg/trends/), largely due to the combustion of fossil fuels, production of cement and land-use change (Burns, 2008; Guinotte and Fabry, 2008), Fig. 1.2. This is intensifying the natural greenhouse effect and has resulted in an increase in the Earth's global temperature of 0.74°C ±0.18°C between 1906 and 2006, a phenomenon known as global warming (Solomon et al., 2007).

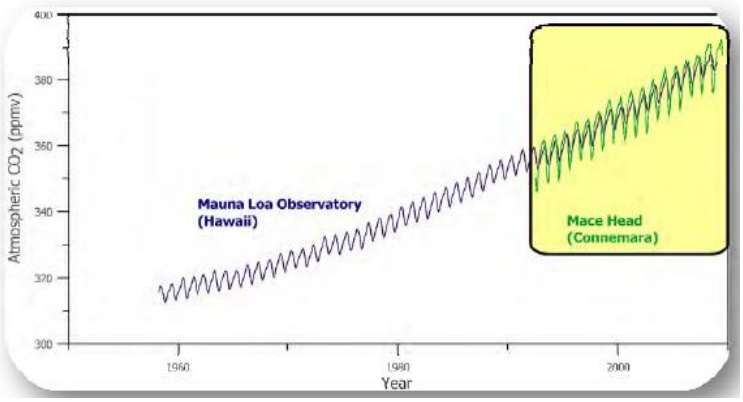

Figure 1.2. Mauna Loa, Hawaii 50 year time series showing steadily increasing atmospheric CO_2 levels. This is mirrored by the measurements taken since 1992 at NUIG's atmospheric research station at Mace Head, County Galway (Ní Longphuirt et al., 2010).

A changing climate affects the ocean through altering the rate of exchange of heat, salt and gases between the ocean and the atmosphere, and subsequent changes to the marine environment influence the global climate through a series of complex feedback mechanisms. Ocean currents and circulation can influence regional climate patterns, while the global thermohaline circulation influences climate on a global scale. The surface ocean has warmed by 0.10°C between 1961 and 2003 (Solomon et al., 2007). In Irish waters, sea surface temperature (SST) time-series between 1900 and 2007 exhibit a warming trend averaging 0.38°C, with strongest warming since 1994 (Cannaby and Hüsrevoğlu, 2009). Higher sea surface temperatures have resulted in the melting of sea ice at the poles, which may in turn affect the global thermohaline circulation by altering the salinity at sites of deep water formation. For example, the Arctic Ocean has exhibited a freshening trend over recent years associated with increased river run-off and ice melt which is expected to influence the rate of deep water formation in the Labrador Sea (Karcher et al., 2005). A number of models have predicted a collapse in the THC due to the build up of the atmosphere's greenhouse blanket, with knock-on impacts on the atmosphere operation and hence global climate (Broecker, 1997). The path of the North Atlantic Current (NAC), which forms the upper limb of the THC is linked to changes in the mean North Atlantic wind field, and a shift in its pathway will have implications for water masses at the European Shelf Edge (Nolan et al., 2009).

1.2 Nutrients and biogeochemical cycles

The availability of nutrients underpins all ecosystem functions as they are essential for the growth of living organisms. A nutrient element is one which is involved in the production of organic matter by photosynthesis in the upper ocean and usually refers to phosphorus, inorganic nitrogen compounds and silicon (Grasshoff et al., 1983). Phosphorus in the ocean exists in the form of ions of phosphoric acid, H_3PO_4. About 10% of inorganic phosphate in seawater is present as PO_4^{3-} and practically all the remaining phosphate exists as HPO_4^{2-}. Nitrogen in the ocean is either in elementary dissolved nitrogen or it is oxidised by biological activity to produce other forms, e.g. ammonia NH_4^+, nitrite NO_2^-,

and nitrate NO_3^-. In coastal waters fixed nitrogen species may be added by artificial fertiliser runoff or sewage inputs. Nitrate is the final oxidation product of nitrogen compounds in seawater and it is the second most abundant form of nitrogen after dissolved elementary nitrogen (Grasshoff et al., 1983). The natural level of nitrite in seawater is low since in the presence of oxygen it should be oxidised to nitrate. Denitrification is the reductive respiration of nitrate or nitrite to N_2O or N_2. Evidence of denitrification in a water body is if winter N:P ratios are lower than source waters suggesting removal of nitrogen relative to phosphorus, or if the nitrate or nitrite concentrations fall below the predicted nitrate/nitrite-salinity dilution line (Hydes et al., 1999). Silicon is brought into solution during the weathering of silicate material, mostly from glacial weathering of rocks in Antarctica and in rivers. Silicon is required for building the frustule of diatoms, which are the most productive and fastest growing of the phytoplankton (Smetacek, 2000).

The utilisation of primary nutrients by phytoplankton in the surface ocean is called photosynthesis, a process which takes up carbon, nitrogen and phosphorus and a range of trace elements, and produces organic matter with oxygen as a by-product. These nutrients are often taken up in a fixed ratio, called the Redfield Ratio (106C:16N:1P) (Redfield et al., 1963) and an analysis of nutrient concentrations relative to this ratio can indicate which nutrients are limiting production in that region. As the sinking organic material becomes remineralised, the dissolved inorganic nutrients are released back into the water column in these almost constant proportions. Oxygen and nitrate/phosphate concentrations can therefore be combined to estimate the effect of remineralisation on the nutrient concentrations to reveal the concentrations initially present in seawater before any remineralisation has occurred. These are called preformed nutrients (Broecker and Peng, 1982);

$$NO_3^o = NO_3 - AOU/a \quad (1)$$

$$PO_4^o = PO_4 - AOU/b \quad (2)$$

where a and b are the equivalence factors between moles of oxygen consumed and nitrate/phosphate released by oxidation of organic material, while AOU is the apparent oxygen utilisation, see section 1.4. Pérez et al. (1993) calculated the

stoichiometric ratios of *a*=10 and *b*=163 for the northeast Atlantic and European margins.

Natural sources of nutrients to the ocean are from atmospheric deposition, nitrogen fixation, land erosion and volcanic activity, while anthropogenic inputs are largely from agricultural runoff, industrial or other point source emissions (such as sewage treatment plants) and fossil fuel consumption and associated emissions. Increased anthropogenic (human-induced) loading of nutrients to a system, both deliberately or as a consequence of other activities, is called fertilisation (Lavelle et al., 2001). Intensification of agriculture, enabled by large scale application of artificial fertiliser, has greatly increased the runoff of macronutrients to coastal waters mainly via rivers. The addition of fertiliser to coastal waters has the potential to increase phytoplankton production and therefore the draw down of atmospheric CO_2. However, excess nutrients in coastal waters can lead to the over-abundant growth of plants and algae, and the subsequent break down of this organic matter can lead to oxygen deficiency and consequent impacts on the ecosystem. This process is called eutrophication and can lead to the displacement or mortality of marine organisms (OSPAR, 2000).

The availability of nutrients in the ocean therefore controls the growth of phytoplankton and hence plays an important role in the global climate through the transport of carbon to deeper waters. This is driven by the production of organic material in surface waters and subsequent remineralisation at depth. Shelf and coastal seas are regions of exceptionally high biological productivity with high rates of biogeochemical cycling and socio-economic importance (Holt et al., 2009). The coastal ocean only accounts for 8% of the global ocean surface area, yet has nearly 30% of oceanic primary production, 80% of organic matter burial and 50% of the deposition of calcium carbonate (Gattuso et al., 1998; Longhurst et al., 1995; Walsh et al., 1988; Walsh et al., 1991). The deep ocean is a large reservoir of nutrients and changes in ocean circulation could affect the transfer of carbon and nutrients between surface and deep waters. Inputs of nutrients to surface waters in the open ocean could be reduced if higher temperatures result in increased ocean stratification, restricting the return of inorganic nutrients from deeper waters back to the surface (Sarmiento et al., 1998). Cermeño et al. (2008) predict a dramatic reduction in the nutrient supply to the surface ocean over the next century due to increased thermal stratification,

with a positive feedback in the climate system. Doney (2006) also predicts a reduction in productivity due to increased stratification in the tropics where nutrients are limited, however, it may increase productivity in high latitude regions by keeping phytoplankton in the surface sun-lit layer of the ocean. This may be counteracted by increased storminess associated with climate change, which could increase wind driven mixing, potentially increasing the nutrient supply from deeper waters to the surface layers. The complex interaction of climate feedback mechanisms make it difficult to predict how the ocean will respond to climate change and therefore requires continued monitoring and research to determine the impacts it will have on ocean chemistry and ecosystems.

1.3 The marine inorganic carbon system and ocean acidification

Carbon in the ocean is present in either inorganic or organic form, either dissolved or particulate. The focus of this thesis is on the inorganic part of the oceanic carbon cycle. The individual species of the carbon dioxide system cannot be measured in seawater directly; it is instead described by the fugacity of carbon dioxide (fCO_2), total dissolved inorganic carbon (C_T), total alkalinity (A_T), and pH. The knowledge of any two of these parameters, along with the temperature, salinity, pressure, phosphate and silicate concentrations, and the relevant equilibrium constants, allows the determination of the other two parameters.

The partial pressure of carbon dioxide, pCO_2, in a seawater sample is the partial pressure of CO_2 in the gas phase that is in equilibrium with that seawater. The net difference of pCO_2 between the ocean and atmosphere indicates the direction and magnitude of air-sea gas exchange, and when in equilibrium, the net exchange is zero. pCO_2 is temperature dependent, with higher pCO_2 in warmer waters. fCO_2 accounts for the non-ideal behaviour of CO_2 and includes the dimension of pressure, it is therefore used instead of pCO_2 in the equilibrium constant definition. The fCO_2 is practically equal to the pCO_2 (within ~1%), and is 0.995-0.997 times the pCO_2 between -2ºC and 25ºC (DOE, 1994). pCO_2 in a seawater sample is defined as the product of the mole fraction of CO_2, xCO_2, (the number

of moles in CO_2(g) divided by the number of moles of all components in the sample) and the total pressure of the sample (P).

$$pCO_2 = xCO_2 \bullet P \quad (3)$$

When atmospheric CO_2 dissolves in seawater it is hydrated to form carbonic acid, H_2CO_3. The carbonic acid can then be dissociated in two steps to bicarbonate ions (HCO_3^-) and carbonate ions (CO_3^{2-}), see Fig.1.3, where K_1 and K_2 are the first and second dissociation constants for carbonic acid.

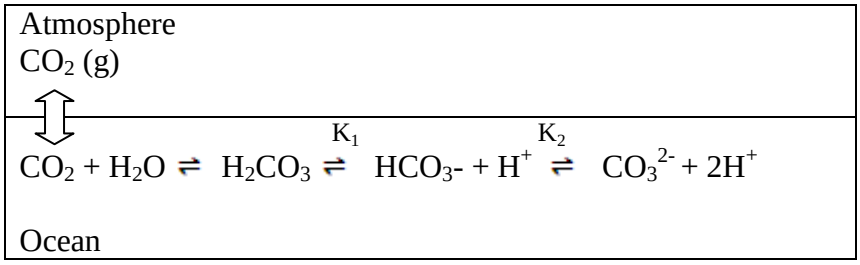

Figure 1.3. Schematic illustration of the exchange of CO_2 between the atmosphere and ocean, via equilibration of CO_2(g) and dissolved CO_2, where K_1 and K_2 are the first and second dissociation constants for carbonic acid. Edited from Zeebe and Wolf-Gladrow (2003).

Dissolved inorganic carbon, C_T, is the sum of dissolved inorganic species, and is mostly present in 3 inorganic forms in seawater, free aqueous carbon dioxide (CO_2(aq)), bicarbonate (HCO_3^-) and carbonate (CO_3^{2-}). True carbonic acid (H_2CO_3) is only a minor form, with a concentration less than 0.3% of [CO_2(aq)], where brackets represent total stoichiometric concentrations. The sum of [CO_2(aq)] and [H_2CO_3] is denoted as [CO_2*]. C_T is therefore defined as

$$C_T = [CO_2^*] + [HCO_3^-] + [CO_3^{2-}] \quad (4)$$

At a pH of <5, [CO_2*] is the dominant carbon dioxide species in solution, however at higher pH it is ionised to bicarbonate and carbonate species, Figure 1.4 (Dickson, 2010). When CO_2 reacts with seawater it reacts with carbonate ion to form bicarbonate ion, with a net effect to increase concentrations of dissolved carbon dioxide and bicarbonate ion, while decreasing the carbonate ion concentration.

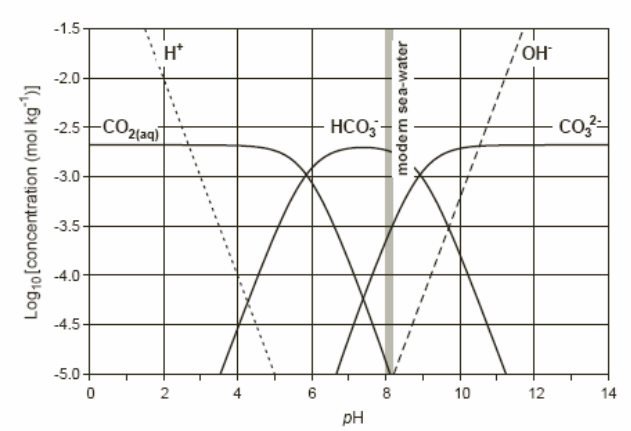

Figure 1.4. The influence of ocean pH on the relative amounts of the carbonate species in seawater. At present day ocean pH, the percentage of the dissolved species is ~86.5% [HCO_3^-], ~13% [CO_3^{2-}] and ~0.5% [CO_2*] (Zeebe and Wolf-Gladrow, 2003).

After reacting with seawater, gaseous CO_2, CO_2(g), is related to [CO_2*] by Henry's law in thermodynamic equilibrium:

$$CO_2(g) \overset{K_0}{=} [CO_2^*] \quad (5)$$

where K_0 is the temperature-dependent solubility coefficient of CO_2 in seawater. The concentration of dissolved CO_2, [CO_2*], and the fugacity of CO_2 in the atmosphere, fCO_2^{atm}, then obey the equation:

$$[CO_2^*] = fCO_2^{atm} \cdot K_0 \quad (6)$$

Total alkalinity, A_T, is a measure of charge balance in seawater, and is determined by titration with a strong acid. It is "the number of moles of hydrogen ions equivalent to the excess of proton acceptors (bases formed from weak acids with a dissociation constant $K \leq 10 - 4.5$ at 25ºC and zero ionic strength) over proton donors (acids with $K > 10 - 4.5$) in one kilogram of seawater" (Dickson, 1981). This corresponds to:

$A_T =$	$[HCO_3^-] + 2[CO_3^{2-}]$ +	$[B(OH)_4^-]$ +	$[OH^-] - [H^+]$ +	minor compounds
	carbonate alkalinity	borate alkalinity	water alkalinity	(7)

If the minor compounds are not included in Equation 7, it is termed practical alkalinity (PA). PA describes the alkalinity of natural seawater at pH values

above 8 and is generally the approximation used in calculations involving alkalinity in the ocean (Zeebe and Wolfe-Gladrow, 2003). Carbonate alkalinity is a measure of the charge concentration of the anions of carbonic acid present in a sample. With the addition of a strong acid to a 'simplified seawater' (without boron, phosphate, silicate and ammonia), the protons will mainly combine with carbonate ion to form bicarbonate, therefore decreasing carbonate ion concentration. Adding more acid to the sample converts the bicarbonate back to CO_2 and ultimately results in all of the bicarbonate and carbonate ions being converted to CO_2. The number of moles of acid required for the whole process is equal to the initial carbonate alkalinity of the sample (Zeebe and Wolfe-Gladrow, 2003). However, it is not only carbonate ions that accept protons; the other two most important acid-base systems that contribute to total alkalinity in many ocean waters are boric acid and water itself.

Like salinity, A_T is conservative in seawater; it stays constant with varying temperature and pressure. A_T is not affected by CO_2 exchange with the atmosphere and concentrations are generally governed by factors that affect salinity, such as precipitation and evaporation (Broecker and Peng, 1982; Lee et al., 2006). It is found to behave conservatively in surface waters of the major oceans (Lee et al., 2006; Millero et al., 1998). A_T decreases with $CaCO_3$ formation, while it increases with the dissolution of $CaCO_3$, with a slight increase with photosynthesis due to the uptake of protons with nitrate by phytoplankton (Zeebe and Wolf-Gladrow, 2003).

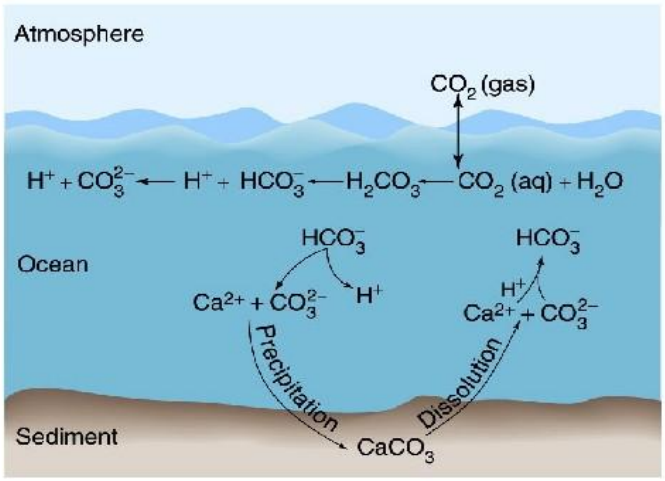

Figure 1.5. Simplified image of the marine inorganic carbon cycle. http://www.jochemnet.de/fiu/OCB3043_28.html (21/03/12).

The term pH describes the acidity of a liquid, defined as the negative logarithm of the hydrogen ion activity, $[H^+]$,

$$pH = - \log_{10}[H^+] \quad (8)$$

Due to several definitions of pH, there are a number of pH scales used, depending on which species are included in the definition; total (pH_T), seawater (pH_{SWS}), free (pH_F) and National Bureau of Standards (pH_{NBS}) scales. The following description of these pH scales has been taken from Zeebe and Wolfe-Gladrow (2003).

The International Union of Pure and Applied Chemistry defined the National Bureau of Standards (NBS) pH scale as a series of standard buffer solutions across a range of pH values. These buffer solutions have very low ionic strength (~0.1) while seawater has a relatively high ionic strength (~0.7). This results in large differences in the electric potential between the solution in the electrode and the sample, and therefore the measurement of pH in seawater using NBS buffers is not recommended. The other three scales, pH_T, pH_{SWS} and pH_F, can be used for the measurement of pH in seawater.

$$pH_F = - \log [H^+]_F \quad (9)$$

$$pH_T = - \log ([H^+]_F + [HSO_4^-]) \quad (10)$$

$$pH_{SWS} = - \log ([H^+]_F + [HSO_4^-] + [HF]) \quad (11)$$

The free scale is the 'free' hydrogen ion concentration, including hydrated forms. Due to the protonation of sulphate ions in seawater ($HSO_4^- \leftrightarrow H^+ + SO_4^{2-}$), the stability constant of HSO_4^-, K_S^*, has to be determined. The total scale includes the effect of sulphate ion and therefore avoids the difficult task of determining the K_S^*. On the total pH scale the standard buffers to measure pH use artificial seawater, therefore reducing the liquid junction potential (electric potential difference) between the buffer and the sample due to similar ionic strength between the two solutions. If the sample solution also contains fluoride ions, the protonation of F^- ($HF \leftrightarrow H^+ + F^-$) must also be considered, which defines the seawater scale. The difference between the total and seawater scale is however small because the concentration of HSO_4^- in seawater is much larger than the concentration of HF.

Due to significant differences in the equilibrium constants between the pH scales, the values of pH in seawater could differ by up to 0.12 units depending on which

scale is used (Zeebe and Wolf-Gladrow, 2003). This is much larger than the desired accuracy of pH measurements given the small annual change in oceanic pH expected. It is therefore critical that when comparing pH from different datasets, that pH is calculated using the same pH scale and equilibrium constants. The total scale (total hydrogen ion concentration scale) is used in this thesis as it is recommended by Dickson (2010) to best describe the pH of seawater.

The addition of an acid to distilled water results in a much larger reduction in pH than if the same amount of acid was added to seawater. This seawater pH buffer is mainly as a result of the capacity of the CO_3^{2-} ions to accept protons, i.e. when CO_2 dissolves in seawater, there is only a slight change in CO_2 concentration because the system is buffered by CO_3^{2-} ions.

$$CO_2 + CO_3^{2-} + H_2O \rightarrow 2HCO_3^- \quad (12)$$

Part of the resulting HCO_3^- dissociates into CO_3^{2-} and H^+, therefore reducing pH (see Eq. 8). The Revelle factor (Revelle and Suess, 1957; Takahashi et al., 1993) is often used to quantify the buffer capacity. It is ratio of the relative change of CO_2 to the relative change of C_T, and typically ranges between 8 and 15 (Zeebe and Wolf-Gladrow, 2003). A low Revelle factor indicates a high buffering capacity, and vice versa. The Revelle factor increases with decreasing temperatures, resulting in relatively low values for warmer waters and higher values for colder waters. The Revelle factor also increases with increasing pCO_2, therefore the buffering capacity of seawater will decrease with increasing levels of atmospheric CO_2.

Calcification is the precipitation of dissolved ions into solid calcium carbonate ($CaCO_3$) and is used by calcifying organisms to produce their shells and skeletons. The precipitation or formation of $CaCO_3$ in the oceans plays an important part in the global carbon cycle, as it effectively transfers CO_2 from surface to deep waters. The formation or dissolution of calcium carbonate is expressed as;

$$CaCO_3 \rightleftharpoons Ca^{2+} + CO_3^{2-} \quad (13)$$

The $CaCO_3$ saturation state of seawater (Ω) is determined from

$$\Omega = [Ca^{2+}]_{SW} \times [CO_3^{2-}]_{SW} / K_{SP}^{*} \quad (14)$$

where $[Ca^{2+}]_{SW}$ is the concentration of calcium and $[CO_3^{2-}]_{SW}$ is the concentration of carbonate in seawater, and K_{SP}^{*} is the solubility product at in situ conditions of temperature, salinity and pressure. An Ω greater than 1 indicates that the seawater is supersaturated with respect to calcium carbonate and would predict $CaCO_3$ precipitation, while Ω less then 1 indicates undersaturation, where $CaCO_3$ tends to dissolve. The depth at which Ω=1 is called the saturation horizon. Ca^{2+} is a major constituent of seawater and concentrations vary only slightly in the open ocean (Feely et al., 2004), therefore the $CaCO_3$ saturation state is mainly determined by the carbonate ion concentration. Aragonite and calcite are naturally occurring polymorphs of calcium carbonate in seawater. The K_{SP}^{*} for the two minerals have different values, i.e. different solubilities, due to differing crystal lattice structures; aragonite is about 1.5 times more soluble than calcite at 25ºC (Dickson, 2010).

Ocean Acidification

Largely due to the burning of fossil fuels since the Industrial Revolution, CO_2 in the atmosphere has reached the highest concentration experienced by the Earth over the past 800,000 years (Lüthi et al., 2008). The oceans have absorbed almost one-third of this anthropogenic CO_2 added to the atmosphere (Sabine et al., 2004), without which atmospheric levels would be considerably higher with more pronounced global climate change. The uptake of CO_2 by the oceans however, is altering our ocean chemistry; it increases the concentration of the bicarbonate ions and dissolved inorganic carbon (C_T) and lowers the pH, the concentration of carbonate ions and the saturation state of the main biogenic calcium carbonate minerals (aragonite, calcite and magnesian calcite). This process is referred to as ocean acidification. It is estimated that surface ocean pH has decreased by 0.1 units, from approximately 8.21 to 8.10 since preindustrial time (Raven et al., 2005) and is expected to decrease by a further 0.3-0.4 pH units by the end of the century under IPCC business-as-usual emission scenario (Orr et al., 2005). Due to the buffer capacity of seawater, the dissolved CO_2 concentration in the surface ocean increases proportionally to the increase of CO_2

in the atmosphere, however the increase in C_T is at a slower rate. However, the buffer capacity of the ocean is expected to decrease with increasing atmospheric CO_2, with a positive feedback to the climate cycle enhancing atmospheric CO_2 levels and hence global warming. Since climate change and ocean acidification are both caused by increasing atmospheric CO_2, ocean acidification is often referred to as the "other CO_2 problem" (Doney et al., 2009a).

One of the major concerns associated with ocean acidification is a decrease in the global saturation state of calcium carbonate and shoaling of saturation horizons due to a decrease in carbonate ions with increasing CO_2. There has been a 20% decrease in the calcium carbonate saturation state between 1766 and 2007 (Caldeira and Wickett, 2003; Gattuso and Lavigne, 2009). Orr et al. (2005) using ocean–carbon cycle models estimated that under the IS92a 'business-as-usual' scenario for future emissions of anthropogenic CO_2, the aragonite saturation horizon shoals dramatically from 2600m to 115m north of 50ºN in the North Atlantic during the 21st century. The greater shoaling in the North Atlantic is due to deeper penetration and higher concentrations of anthropogenic CO_2. It is projected that aragonite undersaturation will occur in Arctic surface waters within a decade and to become more widespread as atmospheric CO_2 continues to increase (Steinacher et al., 2009).

Calcification provides a structural base for marine organisms for support and protection and reduced calcification rates could affect the survival or fitness of certain species, with knock-on shifts in the ecosystem. A reduction in calcium carbonate saturation states makes it more difficult for marine calcifying organisms such as corals, molluscs, pteropods, echinoderms, foraminifera and calcareous algae, to form biogenic calcium carbonate, and at low levels could even result in $CaCO_3$ corrosion (e.g. Raven et al., 2005). Recent field and laboratory experiments have found that despite carbonate saturation greater than 1 (supersaturated), a decrease in saturation state resulted in reduced calcification rates of most calcifying organisms (Feely et al., 2004; Veron et al., 2009, and references within). Of particular concern in a more acidic ocean are cold water corals; deep water reef structures that support a rich biodiversity (Freiwald and Roberts, 2005; Orr et al., 2005). Guinotte et al. (2006) estimated that 70% of the known cold water coral ecosystems, most of which are in the North Atlantic, will

be in water that is undersaturated with aragonite by 2099, resulting in weaker coral structures with slower growth rates.

Increased rates of ocean acidification could also affect a range of physiological processes of marine life at all stages of their life cycle, such as growth, reproduction, recruitment, and photosynthesis. Doney et al. (2009a) has shown that different groups of marine biota respond in different ways to continued ocean acidification; generally there were negative affects on calcification and reproduction, while photosynthesis and nitrogen fixation showed a positive response. Sea grasses may actually benefit from increasing CO_2 since they use dissolved CO_2 rather than bicarbonate in photosynthesis (Palacios and Zimmerman, 2007). Decreasing seawater pH may lead to the speciation of chemical species that undergo acid-base reactions in seawater (Zeebe and Wolf-Gladrow, 2003) and include species required for ocean primary production such as phosphate, silicate, ammonium and iron (De Baar and Gerringa, 2009; Doney et al., 2009a). The extent of impact on marine ecosystems will depend on the ability of species to adapt to an unprecedented rapid change in ocean chemistry. Impacts experienced by any single species, and specifically keystone species (structurally important macroalgae, reef building oysters, sea urchins etc.) may have ramifications throughout all levels of the ecosystem so that a multidisciplinary ecosystem approach to future research in this area is required (Ní Longphuirt et al., 2010).

1.4 Oxygen in the ocean

Seawater is able to dissolve atmospheric gases, and oxygen concentrations in seawater are controlled by fluxes between the surface ocean and atmosphere and by biological activity through photosynthesis and remineralisation. Oxygen in seawater is less complex than the inorganic carbon system as it does not dissociate in seawater. The oxygen concentration of water in equilibrium with the atmosphere is governed by Henry's Law, where α is the Bunsen coefficient and p is the partial pressure of oxygen in the gas phase;

$$O_2 = \alpha \bullet p \qquad (15)$$

Lower temperature waters have higher oxygen solubility than warmer waters, while the salt content of seawater reduces the solubility of oxygen. For example at a salinity of 34.5 and temperature of 5ºC, the oxygen saturation is 308µmol kg^{-1}, while at a salinity and temperature of 36 and 15ºC respectively, the oxygen saturation is 246µmol kg^{-1}. In the North Atlantic, typical winter oxygen saturation values are 260-270µmol kg^{-1}. Apparent oxygen utilisation (AOU) is the difference between the theoretical 100% saturation value and the amount of oxygen measured in a sample, and can indicate both biological and physical processes influencing the concentration of oxygen in the sea (Broecker and Peng, 1982);

$$AOU = O_2 \text{ saturated} - O_2 \text{ observed} \quad (16)$$

1.5 Salinity

Salinity is the total amount of dissolved salts in one kilogram of sea water. The composition of sea salt, which itself occupies 35.17g in 1kg of seawater (i.e. 3.5%), is 30.7% sodium, 55.0% chloride, 7.7% sulphate, 3.6% magnesium, 1.2% calcium, 1.1% potassium and 0.7% minor constituents (Dickson, 2010; Millero et al., 2008). The variability of dissolved salt is very small with most of the ocean's water having salinity between 34.60 to 34.80; we therefore need definitions and instruments accurate to about one part per million (Stewart, 2008). The main interest in ocean salinity is to derive the density of a water parcel since its variability in time and space is important for understanding ocean circulation (Grasshoff et al., 1999).

Absolute Salinity (S_A) is the mass fraction of dissolved material in seawater, independent of temperature and pressure. It is however practically impossible to directly determine S_A. S_A is a multiple of chlorinity, which can be accurately measured using standard analytical techniques, which is still not possible for salinity (Millero et al., 2008). Salinity can also be measured by the electrical conductivity of a sample relative to that of a reference standard. Practical salinity (S) is related to absolute salinity (S_A) by a linear relationship (Grasshoff et al., 1999). It is defined in terms of the conductivity ratio of seawater to a reference material, where salinity is 35.000 when the conductivity ratio is 1.0000 at 15ºC

and 1 standard atmosphere. Due to inconsistencies between the chlorinity- and conductivity-based definitions, chlorinity is described as a separate, independent variable describing seawater properties (UNESCO, 1981). Millero et al. (2008), using the latest atomic weights and best estimates of major components of seawater, defined a new Reference-Composition Salinity (S_R) as a best approximation for the Absolute Salinity of Standard Seawater. S_R can be determined from practical salinity (ranging between 2 and 42) by the formula;

$$S_R = (35.16504/35)\ g\ kg^{-1} \times S \quad (17)$$

Millero et al. (2008) also suggests that at high degree of accuracies there are regional differences and proposed regional algorithms to covert S_R to S_A. The requirement for absolute salinities is driven by the need for ever more precise oceanographic models.

1.6 Long-term time series of carbon and nutrient biogeochemistry

Long term time series are vital to monitor changing biogeochemical parameters at different oceanic regions, particularly for parameters related to ocean acidification, where measurable changes occur over long timescales (Figure 1.6, Table 1.1). The Bermuda Atlantic Time Series (BATS) has been monitoring changes in hydrography, CO_2 and nutrient parameters in the Sargasso Sea since 1988. Bates (2011) observed an increase in C_T in subtropical mode water (STMW), which is the dominant upper-ocean water mass in the North Atlantic subtropical gyre, of $+1.51\pm0.08 \mu mol\ kg^{-1}yr^{-1}$, with a decrease in pH of $-0.0022\pm0.0002\ yr^{-1}$ and reduced carbonate saturation states between 1988 and 2011 at the BATS site. The Hawaii Ocean Time-Series (HOT) program has been monitoring physical and biogeochemical oceanographic parameters ~monthly at the station ALOHA in the subtropical North Pacific Ocean since 1988 and a decreasing trend in surface ocean pH of $-0.0019 \pm 0.0002\ yr^{-1}$ was observed between 1988 and 2009 (Dore et al., 2009). The European Station for Time Series in the Ocean (ESTOC) in the Canary Islands has been monitoring inorganic carbonate parameters in the surface and interior ocean since 1995.

Between 1995 and 2004 C_T, normalised to a constant salinity (NC_T), increased at a rate of 1μmol kg^{-1} yr^{-1}, with a decrease in pH of −0.0018±0.0003 units yr^{-1} in the upper 100m. Deeper in the water column the rate of increase in NC_T at 300, 600, and 1000m was of 0.69, 0.61 and 0.48μmol kg^{-1} yr^{-1}, respectively (González-Dávila et al., 2010). Olafsson et al. (2009) reported results of the Iceland Sea time series between 1985 and 2008 where a decrease in surface winter pH of 0.0024 yr^{-1} was measured. In the deeper waters, >1500m, the rate of reduction in pH was about one quarter that of the surface rate and the aragonite saturation horizon is shoaling ~4m yr^{-1} in the Iceland Sea due to decreasing aragonite saturation state. While the above time series have all measured nutrient concentrations alongside carbonate parameters, nutrient trends are generally not included in the publications. It is therefore assumed that concentrations did not change significantly with time, which may be true if time series sites are away from anthropogenic nutrient loading.

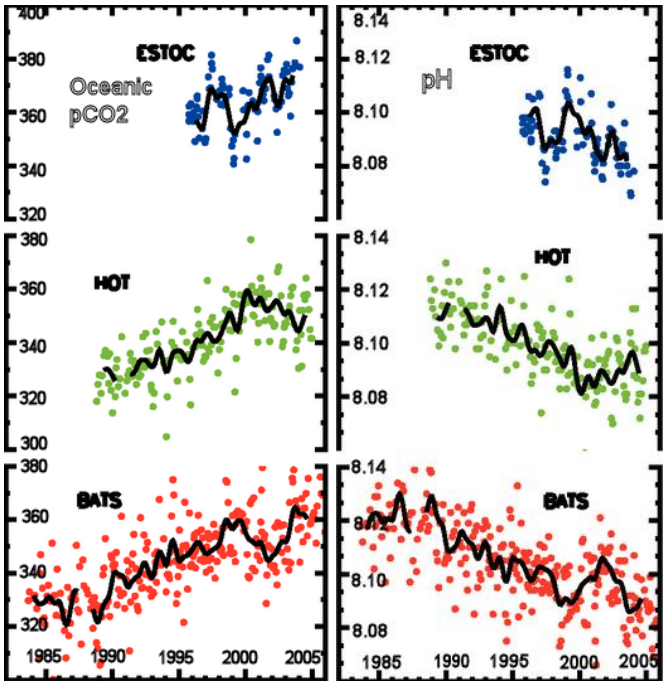

Figure 1.6. Changes in surface oceanic pCO_2 (left; in μatm) and pH (right) from three time series stations: Blue: European Station for Time-series in the Ocean, ESTOC, 29°N, 15°W; (González-Dávila et al., 2003); green: Hawaii Ocean Time-Series, HOT, 23°N, 158°W; (Dore et al., 2003); red: Bermuda Atlantic Time-series Study, BATS, 31/32°N, 64°W; (Bates, 2002; Gruber et al., 2002). Values of pCO_2 and pH were calculated from C_T and alkalinity at HOT and BATS; pH was directly measured at ESTOC and pCO_2 was calculated from pH and alkalinity. The mean seasonal cycle was removed from all data. The thick

black line is smoothed and does not contain variability less than 0.5 years period (from Solomon et al., 2007).

Table 1.1. Details of ocean carbon time series, with published annual rates of change of ocean acidification parameters in surface waters.

Location	Dates	C_T	pH	Calcite sat state	Aragonite sat state	Reference
BATS	1983-2011	+1.39 ± 0.06	−0.0017 ± 0.0001	−0.0141 ± 0.0009	−0.0091 ± 0.0006	Bates et al. (2012)
ALOHA	1988-2009	+0.85 ± 0.08	−0.0019 ± 0.0002			Dore et al. (2009)
ESTOC	1995-2004	+0.94 ± 0.5	−0.0018 ± 0.0003	−0.02	−0.015	González-Dávila et al. (2010)
Iceland	1985-2008	+1.44 ± 0.23	−0.0024 ± 0.0002	−0.012 ± 0.0011	−0.007 ± 0.0007	Olafsson et al. (2009)
Tatoosh, E.Pacific	2000-2007		−0.045			Wootton et al. (2008)

Coastal waters, however, are more susceptible to changes in nutrient concentrations due to human activities and nutrient and salinity data must therefore be assessed for trends. For example nitrate and phosphate concentrations increased in the Irish Sea in the 1960s through to the 1980s due to increased human-inputs (Allen et al., 1998; Evans et al., 2003), while concentrations started to decline in the 1990s likely due to a reduction in anthropogenic nutrient loads (Gowen et al., 2002; McGovern et al., 2002). The EEA (2011) also reported a decrease in oxidised nitrogen between 1985 and 2008 in 12% of the European estuarine, coastal and marine waters who reported to the EEA, while there was a decrease in phosphate in 15% of the reported water bodies. Monitoring acidification in coastal waters is highly complex due to seasonal biological activity, upwelling and riverine inputs of alkalinity and inorganic and organic carbon (Doney et al., 2009b). Borges et al. (2006) found that while continental shelves are significant sinks for atmospheric CO_2, estuaries are significant sources of CO_2 to the atmosphere.

1.7 The Study Area

1.7.1 The Rockall Trough

The Rockall Trough is a deep-sea channel west of the Irish continental shelf bounded to the west by the Porcupine Bank (Fig. 1.7). It is connected to the

Nordic Seas by the shallow (500m) Wyville-Thomson Ridge in the north. The southern entrance of the Trough ~51-54ºN is ~3500m deep and opens out onto the Porcupine Abyssal Plain (PAP) with depths over 4800m. The PAP is bounded to the west by the steep Irish continental slope, west of the Celtic Sea. Further north in the Trough the depth decreases to 1000-1500m with a complex topography of banks and seamounts that rise to ~500m deep, separated by channels approximately 1250m deep (Ellett and Martin, 1973).

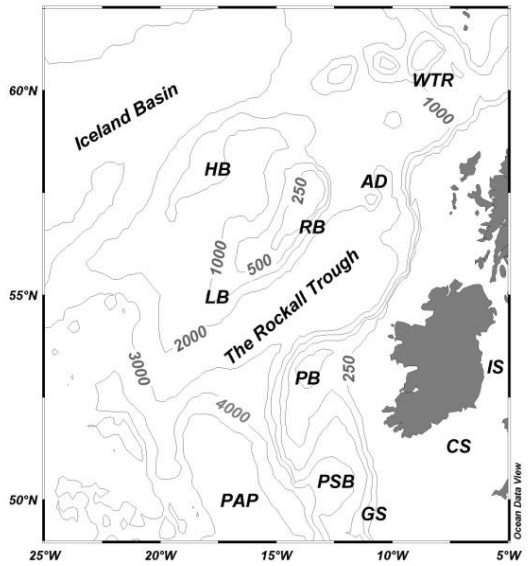

Figure 1.7. Bathymetry of the Irish shelf and Rockall Trough region. Irish Sea (IS), Celtic Sea (CS), Goban Spur (GS), Porcupine Seabight (PSB), Porcupine Abyssal Plain (PAP), Porcupine Bank (PB), Lorien Bank (LB), Rockall Bank (RB), Hatton Bank (HB), Anton Dohrn Seamount (AD) and Wyville-Thomson Ridge (WTR).

This region is an important part of the ocean-climate system, as it provides a pathway for warm and saline water of the upper North Atlantic to enter Nordic Seas, where it is converted into cold, dense overflow water as part of the thermohaline circulation (Ellet & Martin, 1973; Holliday et al., 2000). To the east of the Rockall Trough lies the boundary between the two counter-rotating gyres, the subpolar and subtropical gyres of the North Atlantic (Fig. 1.8). The relatively warm and saline North Atlantic Current (NAC) is an extension of the Gulf Stream that travels eastward across the North Atlantic and branches in two due to the topography of the Rockall Plateau. One branch circulates north and northwestwards to form the Irminger Current south of Iceland and the other

circulates northeastwards into the Rockall Trough and continues to the Norwegian Sea across the Wyville-Thomson Ridge (Ellett et al., 1983; Pollard et al., 1996). Winter mixing in the Rockall Trough generally extends down to depths of 500-700m (Ellett and Martin, 1973; Holliday et al., 2000; New and Smythe-Wright, 2001). This deep winter convection through strong temperature loss to the atmosphere helps to regulate the European climate.

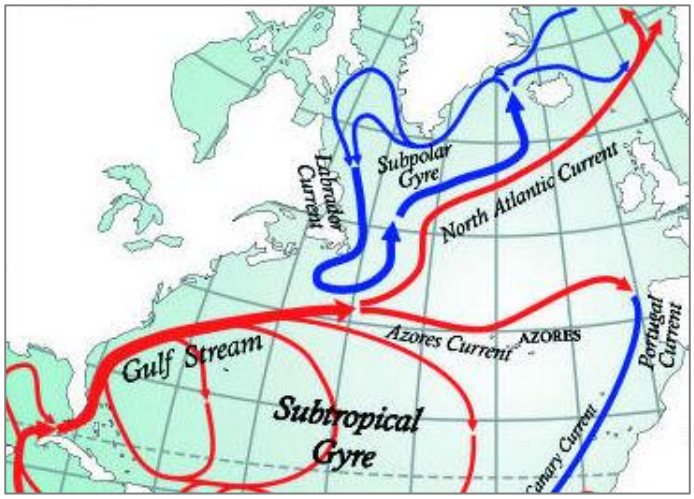

Figure 1.8. Surface currents of the North Atlantic Ocean (http://www.bigmarinefish.com/currents.html)

1.7.1.1 Water masses in the Rockall Trough

A water mass is a body of water with a common formation history, having its origin in a particular region of the ocean where it attains its characteristic properties (Tomczak, 1999). It is usually identified by temperature and salinity as they are conservative properties without any sources or sinks in the ocean interior. Non-conservative properties, such as nutrients or oxygen, change during the lifespan of a water mass and can therefore indicate different processes that have occurred along its path. Water masses can also form due to a mixture of two or more individual water masses and can therefore have a range of temperature and salinity values depending on the degree of mixing between them.

Figure 1.9 shows the main water masses in the Northeast Atlantic. Eastern North Atlantic Water (ENAW) is the dominating water mass in the upper 1000m of northeast Atlantic, with salinities lying within ±0.05 of a mixing line from potential temperature (θ) of 12ºC and salinity of 35.66, to θ of less that 4ºC and salinity <34.96, with a small inflexion point at 10ºC, salinity 35.40 (Harvey,

1982). This warm and saline water mass is formed in the Bay of Biscay (Pollard et al., 1996) and is progressively cooled and freshened as it moves north along the European margin by water moving in from the western North Atlantic with the NAC (Ellett, 1995). Subarctic Intermediate Water (SAIW) is a fresh, highly stratified water mass formed in the western boundary current of the subpolar gyre, with temperatures between 4 and 7ºC and salinity <34.9 (Harvey and Arhan, 1988). SAIW subducts and spreads westwards with a branch of the NAC to the southern entrance to the Rockall Trough (Arhan, 1990; Arhan et al., 1994) where it can result in a stable layer at intermediate depths restricting the maximum depth of winter mixing (Wade et al., 1997). It has been identified in the Rockall Trough with salinities between 35.1-35.2 and temperatures of 8-9ºC between 600 and 1000m (Ullgren and White, 2010). Mediterranean Water (MW), sometimes referred to as Mediterranean Overflow Water (MOW), is formed by density driven overflow of saline water from the Mediterranean Sea over a shallow sill near Gibraltar and subsequent entrainment of less dense water from the thermocline as is passes through the Gulf of Cadiz (Coste et al., 1988; Howe, 1982). This highly saline outflow has salinity of 36.5 and temperature of >11.5ºC in its source region (Pérez et al., 1993; Tomczak and Godfrey, 1994). MW is progressively diluted as it travels north along the Iberian Peninsula due to lateral mixing with adjacent water masses and is normally seen as an inflexion in the θ-S (potential temperature-salinity) plots at the southern entrance to the Rockall Trough (Ellett and Martin, 1973). Due to similar densities, MW and SAIW are found at similar depths in the southern Rockall Trough, and SAIW may act as a barrier for the northward transport of MW along the Porcupine Bank (Mohn et al., 2002). During high NAO (North Atlantic Oscillation) periods strong westerly winds expand the subpolar gyre and the NAC and SAIW can be found closer to the Irish continental shelf, restricting the northward flow of MW (Bersch et al., 1999; Lozier and Stewart, 2008; McCartney and Mauritzen, 2001). Wyville-Thomson Overflow Water (WTOW) is a southward flowing overflow water from the Nordic Seas across the Wyville-Thomson Ridge, found at intermediate depths in the northern Rockall Channel and is seen as an inflexion towards higher salinity in the θ-S diagrams (Sherwin et al., 2008). It has been found as far south as 55ºN in the Trough between 600-1200m, with θ-S properties along a mixing line of 0.5-8ºC and 34.85-35.25 (Johnson et al., 2010).

Below these intermediate water masses, Labrador Sea Water (LSW) is characterised by a marked salinity minimum between 1600-1900m (Ellett and Martin, 1973). LSW is formed from deep winter convection in the Labrador Sea and the θ-S properties vary annually due to changing convection regimes in the source region, ranging between 2.8-3.1ºC temperature and 34.84-34.90 salinity (Yashayaev, 2007). In the Trough, it is a relatively young water mass with a transit time from the Labrador Sea of ca. 10 years (Yashayaev et al., 2007). LSW recirculates with an anticyclonic circulation in the southern Rockall Trough and since there are no exit channels deeper than 1200m in the northern Trough, LSW inflow and outflow is through the southern entrance (New and Smythe-Wright, 2001).

Cold water from the Norwegian Sea flows south over the sills between Iceland and Scotland into the Iceland Basin, entraining warm, saline Sub-Polar Mode Water with cold and less saline LSW and Lower Deep Water (LDW), forming Iceland Scotland Overflow Water (ISOW) in the northern Iceland Basin (van Aken and De Boer, 1995). ISOW has salinity values >34.98 and potential temperature <3˚C (Harvey, 1982) but these characteristics are significantly altered due to diapycnal mixing when it travels south (van Aken, 2000a). Northeast Atlantic Deep Water (NEADW) is modified ISOW after it leaves the bottom layer in the Iceland Basin (Ellett and Martin, 1973; Lee and Ellett, 1965). In the Rockall Trough it is seen as a salinity maximum between the fresh LSW above it and LDW and Antarctic Bottom Water below it. NEADW has an upper limit of temperature and salinity of 2.5ºC and 34.94, and a lower limit of 2.03ºC and 34.89, respectively (Worthington et al., 1970).

Lower Deep Water (LDW) is characterised by a near-bottom salinity minimum, low oxygen and high silicate concentrations. The high silicate is due to the contribution of Antarctic Bottom Water flowing north into the eastern North Atlantic. Antarctic Bottom Water (AABW) is formed by deep convection associated with the freezing of sea ice in the Weddell and Ross Seas, and after mixing with the waters of the Circumpolar Current, it has a potential temperature of ~0.3ºC and salinity of 34.7 (Tomczak and Godfrey, 1994). AABW flows north, along the eastern side of the northeast Atlantic and then circulates into the Rockall Trough (Ellett and Martin, 1973; McCartney, 1992; New and Smythe-Wright, 2001; Tsuchiya et al., 1992). It is characterised by high silicate due to a

large component of re-cycled deep water during formation (Gnanadesikan, 1999).

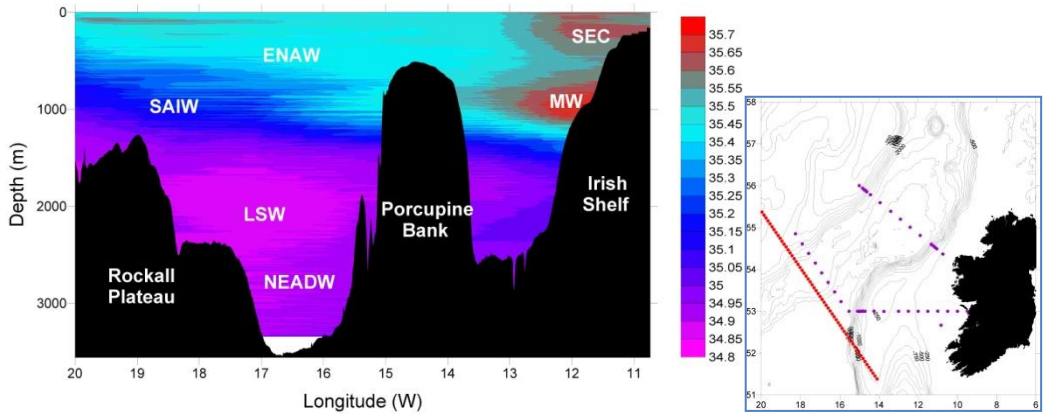

Figure 1.9. Cross section of salinity data taken from a 2010 Irish National Seabed Survey, the red line on the map outlines the transect position relative to the Rockall Trough surveys discussed in this thesis. Water masses outlined in the plot: Eastern North Atlantic Water (ENAW), Shelf Edge Current (SEC), Mediterranean Water (MW), Subarctic Intermediate Water (SAIW), Labrador Sea Water (LSW), Northeast Atlantic Deep Water (NEADW); Paper I (McGrath et al., 2012).

1.7.1.2 Nutrients in water masses in the Rockall Trough

The Gulf Stream transports large amounts of nutrients to the North Atlantic, and helps to replenish surface waters after the yearly spring bloom (Pelegri et al., 1996). Upwelling in the subpolar gyre results in surface waters being nutrient-rich relative to those of the subtropical gyre where downwelling occurs (Williams and Follows, 2003). Upon formation in the oligotrophic Mediterranean Sea, Mediterranean Water is relatively low in oxygen and nutrients (Cabecadas et al., 2002; Howe et al., 1974; Tsuchiya et al., 1992), however nutrient concentrations increase in MW as it moves away from source region due to mixing with the over-lying fresh, nutrient-rich Antarctic Intermediate Water, AAIW (van Aken, 2000b). Due to varying convection regimes in the Labrador Sea (Azetsu-Scott et al., 2005), chemical parameters may vary. Tsuchiya et al. (1992) observed a weak minima of silica, phosphate and nitrate in the low salinity (<34.9) LSW region along an eastern Atlantic section south of Iceland, however these nutrient minima were less clearly defined than the associated oxygen maximum. Nutrient concentrations increase suddenly in the deeper waters of the N. Atlantic and NEADW has >20µmol kg^{-1} nitrate, >24µmol kg^{-1}

silicate, >1.1µmol kg^{-1} PO_4 (Castro et al., 1998; New and Smythe-Wright, 2001; Tsuchiya et al., 1992; van Aken, 2000a). It acquires its nutrients from both the accumulation from sinking particulate matter and from mixing with the nutrient-rich AABW below it. Water masses from southern origin have high concentrations of nutrients due to exchanges with Pacific waters and as they move northwards they continually accumulate nutrients from sinking particles (Williams and Follows, 2003).

1.7.2 The Irish continental shelf and shelf edge

The Irish continental shelf is relatively broad to the west, north and south of Ireland, but narrows to only 30-60km to the northwest and southwest before reaching the steep continental slope. At the shelf edge, the depth sharply increases from ~200m to over 2000m in the Rockall Trough and over 4000m in the Porcupine Abyssal Plain (PAP). Measurements of temperature and salinity across the continental margin indicate a light, warm, saline boundary current along the upper continental slope between the 300 - 600m isobaths, called the Shelf Edge Current (SEC) (Hill and Mitchelson-Jacob, 1993; White and Bowyer, 1997). The direction of the SEC is predominantly poleward with a general northward increase in mean slope current speed and transport (Pingree et al., 1999; White and Bowyer, 1997). Surface temperature and salinity observations also show that the upper portion of the SEC in the Porcupine Sea Bight region can be topographically steered across the deeper part of the Irish Shelf to the east of the Porcupine Bank (White and Bowyer, 1997). The Irish Shelf Front (ISF) is a salinity front along the 35.3 salinity contour located between the 150-200m isobath separating coastal and oceanic waters (Huang et al., 1991; White and Bowyer, 1997). Prior to the onset of summer stratification, the isohalines of the ISF tend to slope downwards and onshore towards the seabed, while in summer they are typically ‘S’ shaped extending horizontally along the pycnocline (McMahon et al., 1995).

The shelf edge currents and fronts play an important role in physical exchange processes at the shelf break and cross-shelf fluxes of heat, salt, organic and inorganic materials between oceanic and Irish coastal waters (Huthnance, 1995; McMahon et al., 1995). While oceanic water is a potential source of nutrients to

the shelf in winter due to off shelf winter mixing (Hydes et al., 2004), strong winter winds act to enhance the northward flow of the shelf edge current rather than forcing surface water onto the shelf, thereby restricting cross-shelf fluxes (Pingree et al., 1999). The gradient of the shelf edge may also influence the cross-shelf transport of nutrients; Hydes et al. (2004) found sharp gradients in temperature, salinity and nutrients along the steep Malin shelf northwest of Ireland, while boundaries were less clear along the broad Celtic Sea shelf break, where vertical mixing of nutrient-rich oceanic water can occur (Huthnance et al., 2001). During positive NAO (North Atlantic Oscillation) phases, strong westerly winds and expansion of the subpolar gyre may result in the Irish shelf being more dominated by deeper Arctic waters, while during negative NAO phases it may be dominated by shallower water of southern origin. There has been a trend towards more positive phase NAO conditions over recent decades, which has been linked to an increased intensity of winter storms and shifts in temperature and salinity throughout the North Atlantic Ocean (Nolan et al., 2009). Denitrification occurs all along the shelf, increasing moving from the shelf break into the Irish Sea (Hydes et al., 2004), usually identified by a loss of nitrate relative to phosphate in the N:P ratios or by comparing the observed concentrations with the concentrations predicted by the salinity and the theoretical mixing line (Hydes et al., 1999).

Due to their important role in global biogeochemical cycles, shelf and coastal seas have a large influence on CO_2 storage and fluxes. The spatial and temporal variability of pCO_2 is controlled by a complex combination of primary production, degradation of organic matter, temperature change and freshwater inputs (Borges and Frankignoulle, 2003). Through a synthesis of global pCO_2 measurements, Chen and Borges (2009) found that most open shelves in the temperate and high latitude regions are undersaturated with respect to atmospheric CO2 during all seasons, while most inner estuaries, near-shore coastal waters and low latitude shelves seem to be oversaturated. European continental shelves are significant sinks for atmospheric CO_2 at an average rate of $-1.9 molCm^{-2}yr^{-1}$, while estuaries are significant sources of CO_2 to the atmosphere at an average rate of 49.9 $molCm^{-2}yr^{-1}$ (Borges et al., 2006).

1.8. Motivation and Aims

Changes in ocean circulation affect the transfer of carbon and nutrients between surface and deep waters of the oceans. Monitoring nutrient concentrations can highlight changes in physical and biological process that could in turn affect the carbon cycle and potentially affect the global climate (Solomon et al., 2007). The winter months are the most suitable for monitoring both nutrients and carbonate parameters due to a minimum in biological activity in surface waters and deep convective mixing setting preformed levels of biogeochemical parameters in the upper ocean. There is generally a lack of wintertime data in the North Atlantic due to adverse weather conditions (Holliday et al., 2006) and concentrations are often estimates rather than true measurements (Koeve, 2001; Körtzinger et al., 2001). One of the main aims of the thesis was to present winter biogeochemical data along the Irish shelf and across the Rockall Trough between 2008 and 2011. An investigation into the chemical characteristics of the water masses in the Trough should provide information on the physical and biological processes that have occurred along their path. The complex interaction of water masses in the Trough along with its important role in the global thermohaline circulation highlights the importance of monitoring changes in hydrography and biogeochemical parameters in this oceanic region.

ICES (2008) highlighted the urgent need for the development of highly resolved monitoring of carbonate chemistry at spatial and temporal scales over long periods of time (>10years) to investigate the extent of changing carbonate chemistry and the potential impacts of acidification on marine ecosystems. Particular requirements identified in the ICES report were the development of multidisciplinary carbonate monitoring systems, long-term time-series datasets and coastal to offshore transects to assess the penetration of terrestrial signals into shelf seas. One of the main aims of this project was to establish baseline data of inorganic carbon chemistry in Irish coastal, shelf and offshore waters against which future changes can be measured. Furthermore, through comparison with data measured in the Rockall Trough by the World Ocean Circulation Experiment (WOCE) in the 1990s, the project aimed to investigate changes in biogeochemistry in the region over the past two decades. This will be particularly

useful with regard to ocean acidification as there is currently a limited number of decadal repeat carbon data across the worlds oceans (Sabine and Tanhua, 2010). The Rockall Trough also hosts an array of cold water coral structures, interacting with a range of water masses along the continental margin, Rockall Bank and Porcupine Bank (De Mol et al., 2002; Roberts et al., 2003; Wheeler et al., 2011). Cold water corals are sensitive to any change in pH (Orr et al., 2005), and it is therefore critical to monitor the saturation state in the region to investigate the effects of ocean acidification on these deep water ecosystems.

On geological time scales, changes in magnitude of total and export production can strongly influence atmospheric CO_2 levels and hence climate (Fallowski et al., 1998). It is essential to measure seasonal nutrient inventories, net community production and biological CO_2 fluxes between the surface ocean and atmosphere to further understand the ocean carbon cycle. One of the aims of the thesis was to estimate the net community production along the Irish continental shelf edge, along with the net air-sea CO_2 exchange during the productive season.

In order to understand oceanic CO_2 uptake and to predict changes that may occur in the future, it is essential that we understand the factors governing the distribution of total alkalinity (A_T) of surface waters, which is the primary factor influencing the buffer capacity of the surface ocean. While the factors influencing the A_T of open ocean waters of the major ocean basins are well understood (Millero et al., 1998; Lee et al., 2006), processes governing A_T in shelf and coastal seas are far more complex due to biological activity, upwelling and riverine inputs (Doney et al., 2009b). Coastal and shelf waters are particularly susceptible to anthropogenic and climate influences and may respond faster than the open ocean (Andersson et al., 2005). Therefore research into the current status of inorganic chemistry in these regions will allow us to monitor future changes in the marine environment. One of the main aims of this thesis was therefore to establish the current status of total alkalinity in Irish coastal and shelf waters and investigate the processes governing its distribution. Lee et al. (2006) developed an algorithm to estimate A_T from surface temperature and salinity in the open ocean. One of the objectives of the study was to assess to what extent, this algorithm can be applied to Irish coastal and shelf waters.

2. Methods

Sample collection was carried out in conjunction with annual Marine Institute surveys and with NUI Galway research and training surveys. See Figure 2.1 for station positions of the surveys between 2008 and 2011 and details of chemistry samples are in Table 2.1. It should be noted that water samples for chemical analysis were not taken at every station on each survey.

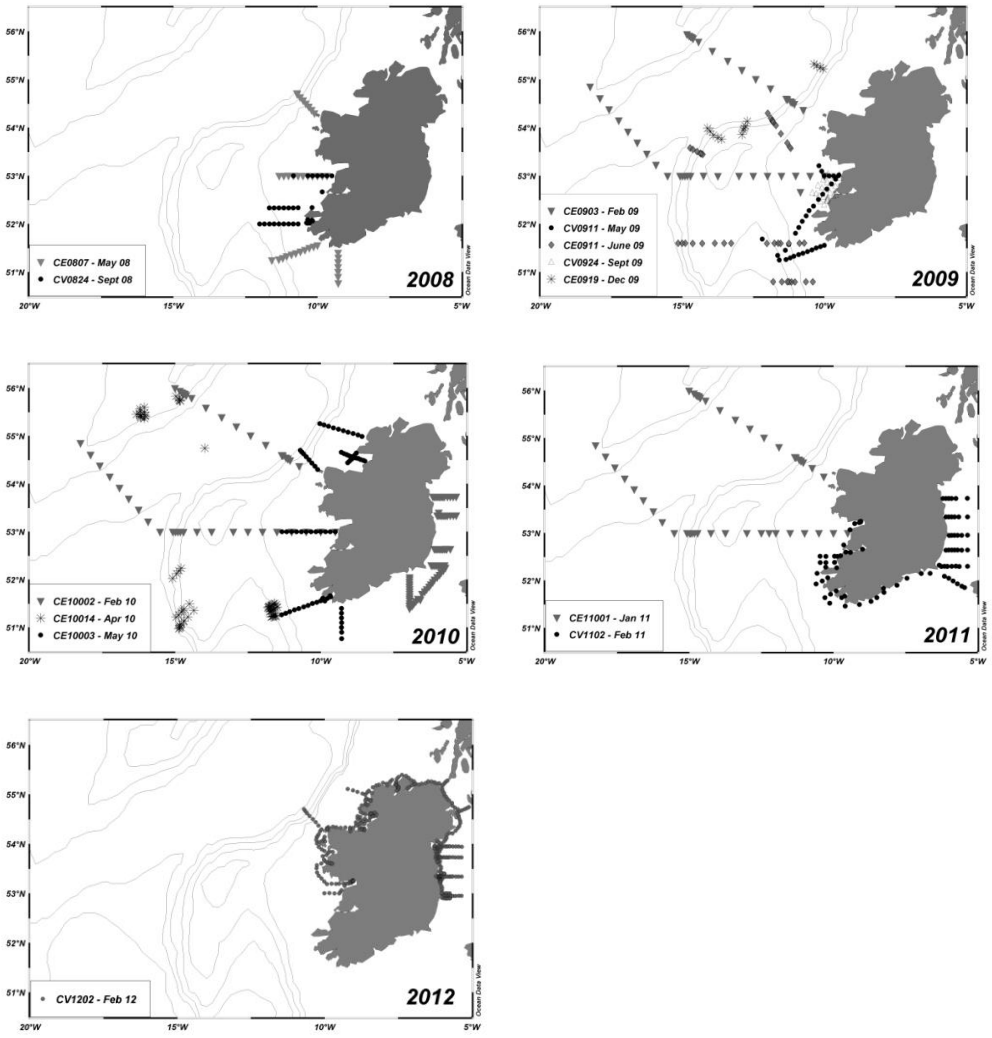

Figure 2.1. Station positions of the surveys described in this thesis, as listed in Table 2.1. While carbonate parameters were sampled on each of the surveys, they were not sampled at every CTD station marked on the map.

Table 2.1. Details of the surveys described in the thesis with the number of samples of each of the chemical parameters. Spaces in the table indicate no data of a particular parameter. Station positions are in Figure 2.1.

Survey	Date	C_T	A_T	O_2	NUT	SAL	DOC/ TOC
CE0807	26-29 May 08	55			70	70	
CV0824	4-7 Sept 08	35			38	38	
CE0903	5-15 Feb 09	64	64		144	133	
CV0911	3-7 May 09	23	23		73	45	
CE0911	14-22 June 09	172	172	249	250	229	87
CV0924	7-12 Sept 09	21	21		67	122	
CE0919	2-15 Dec 09	74	74		59	15	
CE10002	5-17 Feb 10	95	95	190	333	266	162
CE10014	20 Apr-5 May 10	89	89	89	92	15	
CE10003	17-22 May 10	38	38	134	157	158	92
CE11001	3-10 Jan 11	5	5	145	204	183	
CV1102	29 Jan-10 Feb 11	33	33	103	389	389	
CV1202	1-11 Feb 12	56	56	56	462	462	

2.1 Sample Collection

The primary variables required for this study were dissolved inorganic carbon (C_T), total alkalinity (A_T), dissolved oxygen, dissolved inorganic nutrients and salinity. Carbon samples were analysed by the author at NUI Galway in co-operation with Dr. Caroline Kivimäe, while nutrient and salinity samples were analysed by the author at the Marine Institute, Galway. The water samples were collected in Niskin bottles mounted on a large rosette frame with a CTD attached. This measures conductivity, temperature and pressure continuously, while the bottles were remotely triggered and closed at chosen depths. Sensitive samples were taken first from the Niskin bottles to avoid contamination with the atmosphere, first oxygen, followed by C_T/A_T, nutrients and salinity.

2.1.1 C_T and A_T

The Guide to Best Practices for Ocean CO_2 measurements (Dickson et al., 2007), which describes the standard methods now in use for determination of these parameters by researchers worldwide, was followed for the sampling of C_T and A_T. Generally C_T and A_T were analysed from the same bottle; a 500ml Schott Duran borosilicate glass bottle with ground glass stopper. After taking the oxygen sample, the silicone/tygon tubing was left attached to the tap of the

Niskin bottle. Sample water was allowed to flow through the tubing again to remove any air bubbles and the bottle was first rinsed before filling slowly from the bottom. The water was overflowed about 1 bottle volume. Using a plastic bulb pipette, a headspace (~2.5ml) was left in the top of the bottle to allow for water expansion, then 0.1ml of saturated mercuric chloride was added to poison the sample. The glass stopper was greased with Apiezon L Grease before arriving at the station. After the sample was poisoned, excess water was wiped from the neck of the bottle and the stopper was twisted slowly into place, squeezing the air out of the grease. Finally the stopper was clamped in place using 3 thick elastic bands. The bottle was inverted several times to disperse the mercuric chloride and the sample was stored in a cool, dark location.

Where there were insufficient borosilicate glass bottles, C_T and A_T were taken in separate containers using the same method described above. C_T was taken in 250ml amber glass bottles with ground glass stoppers and A_T was taken in 500ml high-density polyethylene (HDPE) bottles with screw caps. The individual A_T samples were not poisoned with mercuric chloride.

2.1.2 Oxygen

Oxygen samples were collected as soon as possible after each cast as per the SOP by Dickson (1995). Samples were collected in ~250ml iodine bottles with plastic stoppers. Deepest samples were drawn first, as it is generally the water furthest from equilibrium with surface temperature and pressure (Knapp et al., 1989). After checking the Niskin bottles for leaks, silicone/tygon tubing was attached to the tap of the Niskin bottle. The breather valve was then opened and a small volume of sample water was run through the tubing to remove any air bubbles. The tubing was placed to the end of the glass bottle, which was first rinsed before filling slowly from the bottom; care was taken to minimize bubbles when filling and the water was overflowed by 3 flask volumes. 2ml of the pickling reagents, $MnCl_2$ (no. 1) and NaOH/NaI (no. 2), were added immediately to the sample. The tips of the dispensers were submerged well below the surface before dispensing so that precipitate did not form in the excess sea water above the neck of the flask. The stopper was carefully inserted, avoiding any trapped air bubbles and twisted to make a seal. As the reagents are dense, they sink to the bottom,

and it is only seawater that is displaced after inserting the stopper. The flask was then inverted several times to mix the precipitate through the sample to ensure that all dissolved oxygen rapidly oxidizes an equivalent amount of manganous hydroxide. After the precipitate has settled at least half way, the bottle was shaken again. Samples were then stored in a cool dark location until titration.
An SBE oxygen sensor was deployed with the CTD on most surveys and where discrete samples were taken results were used to calibrate the sensor data. The sensors were calibrated annually with the manufacturers.

2.1.3 Nutrients

All equipment involved in the sampling and filtration of nutrient samples was acid-cleaned in 10% hydrochloric acid prior to sampling. A 1L HDPE bottle was first rinsed 3 times with sample water before filling. A 0.47µM polycarbonate filter was placed in the filtration unit and after homogenizing the sample water in the 1L bottle, ~100ml of sample was used to rinse the filtration unit, which was then discarded. Approx. 150ml of the sample water was then poured into the unit and filtered, and the filtrate was poured into two sterile 50ml falcon tubes. The tubes were immediately frozen upright at -20ºC.

2.1.4 Salinity

Salinity samples were collected in clear glass salinity bottles with plastic inserts and screw caps. The bottle was first rinsed three times with the sample water before filling up to the shoulder of the bottle. The neck of the bottles was dried well with clean kim wipes to prevent salt crystals forming on the top of the bottle. A plastic insert was then placed into the bottle to produce a tight seal to prevent evaporation, followed by closing the bottle with the screw cap. Samples were stored upright at room temperature.

2.2 Analytical Methods and Quality Assurance

2.2.1 Carbonate parameters

2.2.1.1 Dissolved inorganic carbon (C_T)

C_T is measured by acidification of the sample followed by coulometric titration (Johnson et al., 1987; Johnson et al., 1993) on a VINDTA-3C (Versatile Instrument for the Determination of Titration Alkalinity) system (Mintrop et al., 2000)) with UIC coulometer. A known volume of sample is acidified with phosphoric acid in order to transfer all dissolved inorganic carbon to CO_2. The resulting CO_2 is forced out of the sample by a continuous flow of pure nitrogen through the sample and the extracted CO_2 is passed into a titration cell in the coulometer. The CO_2 is titrated coulometrically with a dimethyl sulfoxide (DMSO) based absorbent containing ethanolamine. The CO_2 reacts quantitatively with the ethanolamine to produce hydroxyethylcarbonic acid. The pH of the titration is monitored by measuring the transmittance of the thymolphthalein indicator which shows when the titration is finished. The thymol blue indicator fades to the original colour due to generation of hydroxide ions at the cathode to maintain the transmittance of the solution at a constant value. The change in colour is monitored by the photodetector as a percentage of transmittance (%T). The amount of CO_2 extracted from the sample is determined by the time integrated current of the hydroxide ions generated. Once the endpoint is reached, the current stops and the VINDTA LabVIEW^{TM} software calculates the C_T concentrations. The relevant chemical equations that occur in the solution are;

$$CO_2 + HO(CH_2)_2NH_2 \rightarrow HO(CH_2)_2NHCOO^- + H^+ \quad (18)$$

$$H^+ + OH^- \rightarrow H_2O \quad (19)$$

2.2.1.2 Total Alkalinity (A_T)

A_T is analysed by potentiometric titration with 0.1M hydrochloric acid, also on the VINDTA 3C. During the titration the bases in the A_T definition are transferred to their acidic forms and the titration is monitored by a pH electrode that measures the electromotive force (emf). The process is controlled by the

LabVIEW^{TM} software and the endpoint is determined by the change in pH against the volume of acid added to the solution. The result of the titration is evaluated with a Gran function (Dickson et al., 2007).

2.2.1.3 Quality Assurance of C_T and A_T

The accuracy of both C_T and A_T analysis is ensured by analysing duplicate Certified Reference Materials (CRMs) before every batch of samples. CRMs were provided by A. Dickson, Scripps Institution of Oceanography, USA (Dickson, 2001). If many samples (>10) were run in a single batch, another duplicate CRM was run at the end of the day. The measured CRM results were used to calculate a CRM correction factor to adjust C_T and A_T sample results for any offset in the VINDTA.

CRM correction factor = assigned value / measured value

Sample results were then multiplied by the daily correction factors. The precision of the measurements is calculated as the standard deviation of the differences between duplicate samples.

Storage test

A storage test was carried out to investigate if storing samples for a prolonged length of time had an effect on the C_T / A_T concentration.

Sample collection: On May 21st 2010, twenty-six 500ml Schott Duran bottles were filled with water taken from 448m deep along the shelf edge (10.0322ºW, 55.2565ºN). All bottles were filled by the author, while a colleague poisoned, greased and sealed the bottles. Bottles were labelled A to Z. Six 250ml glass (not-borosilicate) bottles, used for C_T only, were also filled (labelled 1a to 1e) to ensure these bottles had the same storage capacity as the Schott Duran bottles.

Storage: All samples were stored at 4ºC in a dark fridge until they were analysed.

Analysis: the baseline set of samples (T = 0 months) was analysed on the 29th May 2010. A new set of samples was run approximately every month for the following 7 months. Subsequent sets were analysed every 2-3months. A duplicate of every bottle was run.

Results:

C_T

T=0 months; the average concentration of C_T was 2143µmol kg^{-1} (ranging between 2142-2144µmol kg^{-1}) in the 4 individual bottles (3 Duran bottles, 1 soft glass bottle). Both bottle types therefore yield similar concentrations.

Year 1 (May 2010 - May 2011); the monthly average over the entire year ranged between 2139 and 2144µmol kg^{-1}, with no increasing/decreasing trend (Figure 2.2). The average C_T over the full year was 2142µmol kg^{-1}, and variation around the mean is less than ±3µmol kg^{-1}. Both Schott Duran and soft glass bottles had similar concentrations after a year.

Year 2; C_T concentrations varied considerably, decreasing in July/Oct 2011, with higher concentrations in March 2012. The reason for this variability is uncertain. There are four more storage samples that will be run over the next few months to determine if there is a change in concentration with increasing time.

Conclusion; Storage of C_T samples in both types of bottles does not affect the C_T concentration for at least 12 months. Further testing is required to investigate the variability in concentration after a year of storage.

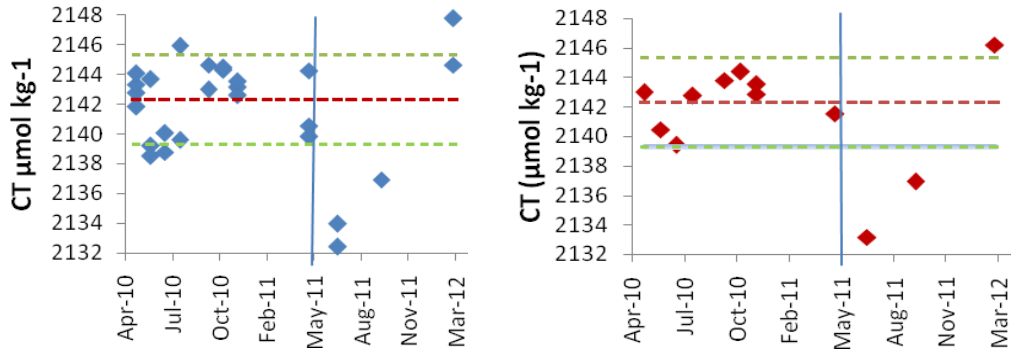

Figure 2.2. C_T concentration from each bottle analysed every month in blue (note every bottle value is an average of duplicate results from the same bottle), with average monthly C_T values in red. The red line is the mean concentration for the first year, and the green line indicates ±3µmol kg^{-1} around the mean. The vertical blue line indicates 1 year of storage.

A_T

T = 0 months; The average concentration of A_T in the three individual bottles is 2331µmol kg^{-1}, ranging between 2330-2332µmol kg^{-1}. A_T was not tested in the soft bottles as they leach silicate and therefore affect A_T concentrations.

May 2010- March 2012; With the exception of June 2010 results, A_T ranged from 2329 to 2333µmol kg^{-1}, less than ±2µmol kg^{-1} around the mean of 2331µmol kg^{-1} (Figure 2.3), indicating that storage of A_T samples does not affect the concentration for at least 20 months. It is unclear why the results from June 2010 were significantly higher than other months (average 2339µmol kg^{-1}); it appears to be a one-off error, despite running a duplicate CRM that day.

Conclusion; Storage of A_T samples for at least 20 months does not affect the A_T concentration.

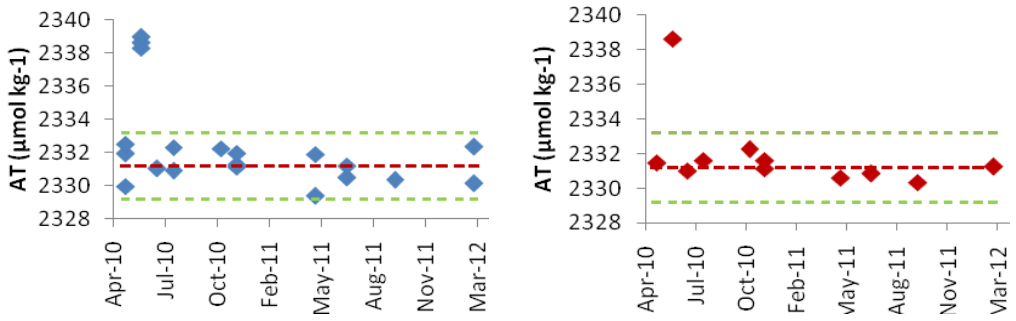

Figure 2.3. A_T concentration from each bottle analysed every month in blue (note every bottle value is an average of duplicate results from the same bottle), with average monthly A_T values in red. The red line is the mean concentration for the first year, and the green line indicates ±2µmol kg^{-1} around the mean.

Throughout this thesis, C_T and A_T samples were always analysed within 1 year of collection and therefore we are confident that storage of samples did not affect final results. Bates et al. (2012) indicated that samples from the BATS time series station were stored from a few months to several years.

Cross Validation with A. Dickson Laboratory, Scripps, USA.

In the survey CE11001 across the Rockall Trough in January 2011, a batch of surface C_T and A_T samples was sent to Scripps Institution of Oceanography, USA, for analysis. Five duplicates of these samples were analysed by the author

at NUIG. C_T and A_T results from NUIG were within ±3µmol kg^{-1} and ±1µmol kg^{-1}, respectively, of those analysed at Scripps (Figure 2.4).

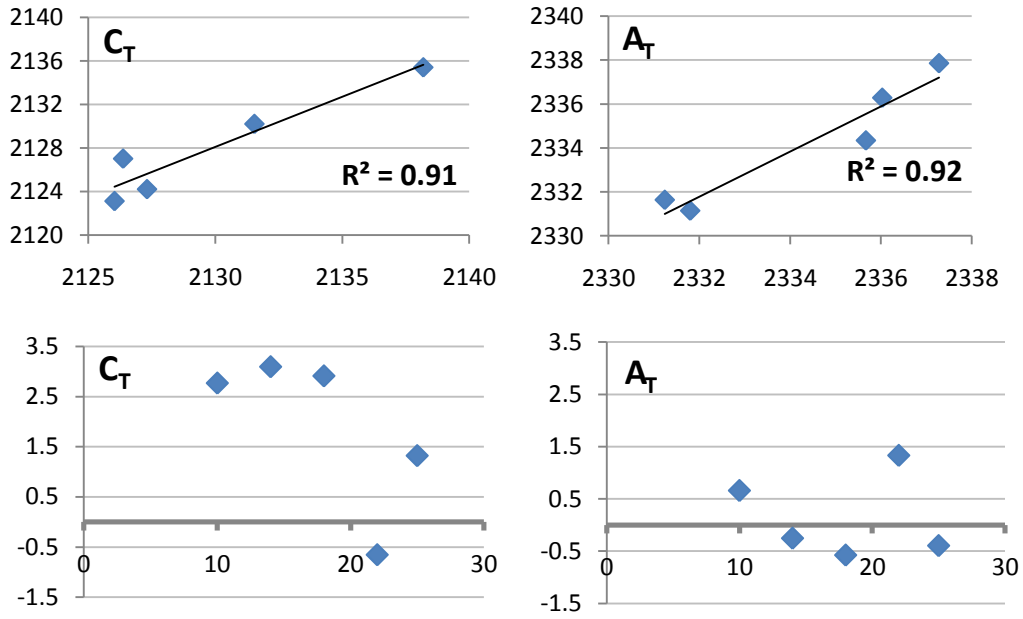

Figure 2.4 Top panel: linear regression of C_T and A_T results from Scripps and NUIG. Lower panel: Residuals (Scripps C_T/A_T minus NUIG C_T/A_T in µmol kg^{-1})

2.2.1.4 Calculation of pH and aragonite and calcite saturation

pH and the saturation of calcium carbonate minerals were calculated from the C_T and A_T results (along with salinity, potential temperature, pressure, phosphate and silicate) using CO2SYS (Lewis and Wallace, 1998). In the calculations, the total pH scale was used, along with constants K_1 & K_2 taken from Mehrback et al. (1973) refit by Dickson & Millero (1987), and Dickson's Kso_4. Note it is important that if comparisons are being made of pH data (and any other calculated parameters) from different sources, that they are calculated using the same methodology (i.e. pH scale and constants). pH was also calculated at 25ºC to allow for comparison with trends already published at this temperature. Calculating the uncertainty of the derived parameters is complicated as it includes the measurement uncertainties of each input parameter, along with the error in the equilibrium constants. Dickson and Riley (1978) calculated a combined uncertainty of 0.6 – 6.3% in pH and of 3.1% for the carbonate ion concentration, when calculated from A_T and C_T. The highest possible uncertainty is used with the results in the thesis.

2.2.2 Oxygen

2.2.2.1 Oxygen analysis

O_2 samples were analysed at sea following the SOP by Dickson (1995). The Winkler method is an iodometric titration; dissolved oxygen does not directly oxidise the iodide ion to iodine so manganese is used as a medium in a multistep oxidation (Grasshoff et al., 1983). Manganese (II) chloride and an alkaline sodium iodide are added to a known volume of seawater (pickling reagents). Manganese (II) is precipitated as a hydroxide and oxidised to Manganese (III) hydroxide in a heterogeneous reaction:

$$Mn^{2+} + 2OH^- \rightarrow Mn(OH)_2 \quad (20)$$

$$Mn(OH)_2 + {}^1/_2O_2 + H_2O = 2Mn(OH)_3 \quad (21)$$

Due to the instability of Mn(II) in an alkaline medium the fixation of oxygen is rapid and quantitative. For analysis, the sample is then acidified with sulphuric acid (H_2SO_4) to a pH between 1 and 2.5, which dissolves the hydroxide precipitates, and iodide ions added by reagent no.2 are oxidised to iodine by the manganese (III) ions, which are reduced to Mn(II) ions in the process:

$$2Mn(OH)_3 + 2I^- + 6H^+ \rightarrow 2Mn^{2+} + I_2 + 6H_2O \quad (22)$$

The iodine plus surplus iodide ions combine to give a complex of 3 iodine atoms with one negative charge.

$$I_2 + I \leftrightarrow I_3 \quad (23)$$

In the final step, the iodine is reduced to iodide by titration with thiosulfate, and the thiosulfate is oxidised to tetrathionate ion. It is crucial to know the concentration of thiosulfate precisely since the amount of iodine generated, which is equivalent to the amount of oxygen in the sample, is determined by the amount of thiosulfate required to reach the endpoint.

$$I_3 + 2S_2O_3^{2-} \rightarrow 3I^- + 3\ H_2O \quad (24)$$

In 2008 and 2009, a Metrohm Titrino 712 was used for analysis and the end point was determined visually, where the endpoint is considered complete when the pH of the sample came closer to neutral when the yellow colour of the tri-iodide

faded to clear. The visual cue was enhanced with the addition of a few drops of starch solution which turned the sample to dark blue which then changed to clear at the endpoint. One limitation of this method is that the sensitivity of the human eye varies from person to person. In 2010 and 2011, a Metrohm 848 Titrino Plus, with a Metrohm combined Pt electrode were used for analysis. The electrode was used for potentiometric endpoint determination, measuring the change in redox potential of the sample, which reaches a minimum at the endpoint (Furuya and Harada, 1995). This method of determination was also used effectively by numerous WOCE cruises in the Atlantic and Pacific Oceans, and also on the later Hawaii Ocean Time Series (HOT) cruises (http://www.soest.hawaii.edu/HOT_WOCE/).

2.2.2.2 Quality control of oxygen analysis

Before titration of the samples, duplicate reagent blanks were determined and duplicate standardization of the sodium thiosulfate titrant was carried out. The reagent blank should ideally be less than 0.01ml, while the duplicate thiosulfate standardization should typically fall within 0.002ml of each other (Dickson, 1996). Standardization of the thiosulfate is carried out in precisely the same conditions that the samples will be analysed under so that any iodine lost through the volatilization or gained by the oxidation of iodide while analysing the seawater samples will be compensated for with similar errors occurring during the standardization procedure (Knapp et al., 1989). Precision of the samples is estimated by running duplicate samples every 10-15 samples.

2.2.3 Nutrients and salinity

2.2.3.1. Analysis of dissolved inorganic nutrients

Seawater samples were analysed for total oxidised nitrogen (TOxN), nitrite, silicate and phosphate on a Skalar San ++ Continuous Flow Analyser at the Marine Institute (MI). The accredited MI methods for the analysis of nutrients in seawater and estuarine water were followed. The Skalar San++ System uses automatic segmented flow analysis where a stream of reagents and samples, segmented with air bubbles, is pumped through a manifold to undergo treatment

such as mixing and heating before entering a flow cell to be detected. The sample is pumped into the system and split into 4 channels where it is mixed with reagents. The reagents act to develop a colour, which is measured as an absorbance through a flow cell at a given wavelength.

Total oxidised nitrogen (TOxN)

For the determination of TOxN, the sample is first buffered at a pH of 8.2, with a buffer reagent made of ammonium chloride and ammonium hydroxide solution, and is then passed through a column containing granulated copper-cadmium to reduce nitrate to nitrite. The nitrite, originally present plus reduced nitrate, is determined by diazotizing with sulfanilamide and coupling with N-(1-naphthyl) ethylenediamine dihydrochloride to form a highly coloured azo dye which is measured at 540nm.

Nitrite

For the determination of nitrite the diazonium compounds formed by diazotizing of sulfanilamide by nitrite in water under acidic conditions (due to phosphoric acid in the reagent) is coupled with N-(1-naphthyl) ethylenediamine dihydrochloride to produce a reddish-purple colour which is measured at 540nm.

Silicate

For the determination of silicate the sample is acidified with sulphuric acid and mixed with an ammonium heptamolybdate solution forming molybdosilicic acid. This acid is reduced with L(+)ascorbic acid to a blue dye, which is measured at 810nm. Oxalic acid is added to avoid phosphate interference.

Phosphate

For the determination of phosphate ammonium heptamolybdate and potassium antimony(III) oxide tartrate react in an acidic medium (with sulphuric acid) with diluted solutions of phosphate to form an antimony-phospho-molybdate complex. This complex is reduced to an intensely blue-coloured complex by L(+)ascorbic acid and is measured at 880nm.

Based on the daily calibration standards, concentrations of nutrients can be quantified up to the maximum calibration standard concentration. If sample concentrations fall above this range (Table 2.2), they must be diluted with artificial seawater.

Table 2.2. Limit of detection (LOD), limit of quantification (LOQ), both in µmol l^{-1}, and uncertainty of measurement (UCM) for the nutrient analysis. The ranges given are the linear calibration ranges, concentrations that fall above these are diluted into the linear range.

	LOD	LOQ	UCM	Ranges
TOxN	0.02	0.26	2.3%	LOQ – 15
Nitrite	0.01	0.04	6.7%	LOQ – 1.5
Silicate	0.03	0.38	0.5%	LOQ – 15
Phosphate	0.01	0.16	1.3%	LOQ – 1.5

2.2.3.2 Salinity analysis

Salinity is analysed on an OSIL (Ocean Scientific International Ltd) Portasal Salinometer at the MI, where 4 electrode conductivity cells suspended in a temperature-controlled bath, measure the conductivity of the sample. The conductivity is related to salinity by calibration from a known standard. Two consecutive conductivity readings within 0.00002 units of each other must be taken before the salinity can be recorded. The temperature of the salinometer water bath must be set and stabilized to ~1-2ºC above ambient room temperature and samples must reach room temperature before analysis.

2.2.3.3 Quality control of nutrients and salinity analysis

The MI is accredited by the Irish National Accreditation Board (INAB) in compliance with ISO 17025 for nutrient and salinity analysis in seawater. The MI routinely participates in QUASIMEME proficiency testing scheme exercises for nutrients and salinity in the marine environment. A batch of QUASIMEME samples of unknown concentration are sent to the MI twice a year for analysis. The nutrient samples have a large range of concentrations from below the limit of quantification to high levels that require dilution. The final results submitted to QUASIMEME must have a z-score of ≤ 2 to be considered satisfactory. The author participated in 7 QUASIMEME rounds (44 samples) between Oct 2008 and Oct 2011 and the average z-score for all nutrients and salinity was <0.5, Figure 2.5.

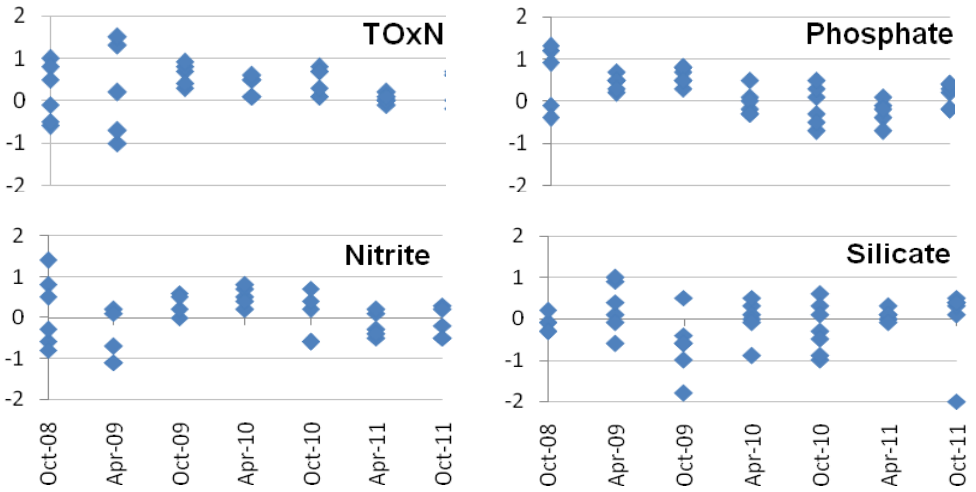

Figure 2.5. z-scores of 7 QUASIMEME rounds of nutrients in the marine environment analysed by the author between October 2008 and October 2011.

The accuracy of the nutrient analysis is ensured by running Eurofins Certified Reference Materials (CRMs) with every batch of samples, which must fall within specified limits; usually well within a standard deviation of 2. The system is also calibrated with every run using calibration standards made up daily in the laboratory; a regression coefficient of >0.990 is acceptable for at least 5 standards. A replicate of every sample is analysed and the relative percent difference (RPD: difference between the two values / mean * 100) of the results >LOQ (limit of quantification) should be ≤ 10.

The salinometer is calibrated daily with a P-series IAPSO seawater standard (sal~35) from OSIL and a standard is run every 4 hours during analysis. P-Series standards should fall within an allowable error of ± 0.003. DI water (sal~ 0), a 10L IAPSO standard (sal ~10) and a 38H IAPSO standard (sal ~38) are tested at the beginning of every batch of samples and must give a $|z|$ score <2.

3. Results and Discussion

The data that form the basis of this thesis were collected across twelve surveys between 2008 and 2011 in Irish coastal, shelf and offshore waters (Table 2.1, Figure 2.1). A range of chemical parameters including dissolved inorganic nutrients, dissolved oxygen, dissolved inorganic carbon and total alkalinity were measured alongside hydrographic parameters to describe the chemical characteristics of the water masses in the region.

One of the main aims of the thesis was to collect winter biogeochemical data across the Rockall Trough in order to determine the chemical signatures of the water masses in the area. Results from Paper I and II indicate that the use of nutrient, oxygen and inorganic carbon data as chemical tracers of regional water masses makes it possible to highlight physical and biological processes that could not be identified using temperature and salinity data alone.

The surface mixed layer across the Rockall Trough was approximately 97% oxygen saturated in late winter, with an increase in AOU below the mixed layer due to remineralisation of organic material, leading to an increase in dissolved inorganic nutrients and C_T. The influence of the physical and biological pumps are highlighted in Paper II, where the deepest MLDs (mixed layer depths) coincided with maximum nutrient and C_T concentrations due to vertical mixing. Increased surface temperatures and the onset of stratification during spring and summer surveys coincided with a decrease in nutrients and C_T due to uptake by phytoplankton during photosynthesis.

Nutrient and C_T data highlight the pathway of ENAW in the Rockall Trough; concentrations were elevated in the colder, fresher water coming from west of the Rockall Trough, relative to the warm saline water of the upper eastern North Atlantic of more southern origin along the shelf edge. Deep convective mixing and upwelling in the subpolar gyre generates nutrient- and carbon-rich surface waters which are transported to the Trough by the NAC, playing an important

role in the supply of nutrients to the surface layer in the region (Pelegrí et al., 2006; Williams and Follows, 2003). Mesoscale eddies have also been found to increase productivity across most of the North Atlantic through eddy-induced transport of nutrients into the euphotic zone (Garçon et al., 2001). This in turn has an influence on biological production and the drawdown of atmospheric CO_2 during spring and summer months, as seen in Paper III where winter conditions set the 'preformed' nutrient and C_T concentrations for the calculations of net community production and air-sea CO_2 exchange during the subsequent productive season. Cooler temperatures in the subpolar gyre may also result in more CO_2 absorption from the atmosphere relative to the warmer ENAW, and may be partly responsible for the elevated surface C_T in the western side of the Trough. Nutrient, oxygen and carbon data also proved useful in discriminating between SAIW and MW, which are often found at the same density level between 600-1100m at the southern entrance to the Trough (e.g. Mohn et al., 2002; Ullgren and White, 2010). SAIW had a high oxygen signature (average 244µmol kg^{-1}) in the Trough due to cold temperatures in its formation region in the western subpolar gyre (Wade et al., 1997). Preformed nutrient and C_T concentrations were also higher in SAIW than surrounding water masses, likely entrained from the subpolar gyre during formation. MW on the other hand, had a characteristically low oxygen signature (average 205µmol kg^{-1}) and low preformed nutrients due to the oligotrophic nature of the Mediterranean Sea (Cabecadas et al., 2002; Howe et al., 1974). The preformed molar N:P ratio in MW was high (18-19) at some depths and is likely due to increased N:P inputs, low levels of denitrification and/or fixation of atmospheric dinitrogen in the Mediterranean Sea (Bethoux et al., 1999; Ridame et al., 2003). MW could also be traced by a characteristic high-A_T signal along the shelf edge due to high evaporation and hence high salinity, coupled with high A_T inputs from freshwater sources (Schneider et al., 2007). Chemical data indicate an increased SAIW influence in 2010, with elevated preformed nutrients and C_T measured all the way across the Trough.

Between 1500-2000m there was a decrease in AOU and C_T due to the presence of LSW, a relatively young water mass in the Trough more recently in contact with the atmosphere relative to surrounding water masses (Yashayaev et al., 2007). Along with low salinity and temperature, LSW had a characteristically

high oxygen content due to cold temperatures (<3ºC) during formation (Yashayaev, 2007), allowing it to absorb more oxygen. LSW in the northern transect of the Trough was slightly warmer and more saline, with an increase in oxygen due to mixing with surrounding water masses with lower oxygen content. Nolan (in prep) found a freshening of LSW in the Trough between 2006 and 2009, with a return to higher salinity in 2010. This coincided with lower silicate, and to a lesser extent lower preformed nitrate, in 2009 relative to 2008 and 2010 (Paper I). There was a freshening and cooling of LSW between the late 1980s and mid 1990s due to severe winters in the Labrador Sea, resulting in increased winter convection which ended in 1994 with the start of a new phase of heat and salt accumulation (Yashayaev, 2007). If the low salinity signal in the Rockall Trough in 2009 was due to increased convection in the Labrador Sea, we would expect nutrient concentrations to be higher due to deeper vertical mixing. Therefore, the lower silicate in 2009 could indicate more of an influence from the Labrador Current during formation, which is relatively cool, fresh and low in nitrate and silicate (Clarke and Coote, 1988; Townsend et al., 2010). The lower salinity and silicate may however, also be due to convective entrainment with shallower, lower nutrient water during formation.

Nutrients and C_T increase steadily to the deepest parts of the Trough due to remineralisation, older water mass age and mixing with the nutrient-rich AABW. Nutrient concentrations, particularly silicate, are effective tracers of AABW in the Atlantic due to a large component of this water mass being recycled deep water with high silicate values (Gnanadesikan, 1999). While AABW is fractionally cooler with lower salinity than the NEADW above it, the nutrient concentrations sharply increase to 22µmol kg^{-1} nitrate, 42µmol kg^{-1} silicate and 1.5µmol kg^{-1} phosphate below 3000m in the Trough, indicative of water of southern origin.

Another aim of the research carried out in the Rockall Trough was to assess the current status of inorganic carbon chemistry in the region and to investigate changes that have occurred over 2 decades, through comparison of C_T and A_T from earlier WOCE surveys in the 1990s with results from 2009 and 2010. Results are presented in Paper II. A comparison of the pH, calculated from C_T and A_T, between surveys allows for an investigation into the rate of ocean

acidification in this part of the eastern North Atlantic. Since the anthropogenic carbon signal of surface waters in the North Atlantic can only be compared during winter months when biological activity is at a minimum and winter mixing has regenerated C_T to maximum concentrations, the 2009/10 dataset collected for this thesis provides baseline values of inorganic carbon and pH levels in surface waters of the Rockall Trough, as earlier WOCE surveys were carried out during spring/summer months or during the early stages of winter mixing.

Two independent methods to estimate the temporal evolution of anthropogenic carbon (ΔC_{ant}) between surveys were used in Paper II. The first method involved correcting C_T for the effects of remineralisation of organic matter and formation and dissolution of calcium carbonate, $\Delta C_{T\text{-}abio}$, as described by Tanhua et al. (2006). The ΔC_{ant} was also estimated using extended Multiple Linear Regression (ΔC_{ant}^{eMLR}) as described by Friis et al. (2005) and Tanhua et al. (2007). This eMLR technique accounts for the natural variations of carbon since both hydrographic (temperature and salinity) and biogeochemical (nutrients and oxygen) parameters are incorporated into the model to investigate the primary factors affecting the temporal evolution of C_T. There was an increase in $\Delta C_{T\text{-}abio}$ and ΔC_{ant}^{eMLR} of 18±4μmol kg^{-1} and 19±4μmol kg^{-1}, respectively, in the subsurface waters between 1991 and 2010, equivalent to a decrease of 0.040±0.003 pH units over the 19 year period. This is in line with a number of time series (HOT, BATS, ESTOC) who measured a decrease in pH of 0.02 pH units per decade over the last 20 years (Solomon et al., 2007). There was an increase in both $\Delta C_{T\text{-}abio}$ and ΔC_{ant}^{eMLR} of 8±4μmol kg^{-1} in LSW in the Trough between 1991 and 2010, which has acidified by 0.029±0.002 pH units over the same time period. This is similar to an increase of 9μmol kg^{-1} C_{ant} in LSW in the eastern North Atlantic between 1981 and 2006, measured by Perez et al. (2010), using the φC_T^o approach (Vázquez-Rodríguez et al., 2009).

In upper NEADW, between 2000 and 2500m deep, there was a trend of increase in C_T over the 19 years, ranging from 2150-2161μmol kg^{-1} in 1991 to 2170-2189μmol kg^{-1} in 2010, with a reduction in calculated pH of 0.029±0.002. While the ΔC_{ant}^{eMLR} could not be calculated across this depth range due to the small

number of data points, there was an increase in $C_{T\text{-}abio}$ of 3±3μmol kg^{-1}. We may therefore be seeing the effects of increasing atmospheric CO_2 at depths >2000m in the Trough. This is supported by Pérez et al. (2010) who measured an increase in C_{ant} of 4μmol kg^{-1} in the NADWu (upper North Atlantic Deep Water) between 1981 and 2006 off the Iberian Peninsula. The range in C_T also increases in lower NEADW (2500-3000m), from 2158-2185μmol kg^{-1} in 1991 to 2182-2206μmol kg^{-1} in 2010, with an increase in $C_{T\text{-}abio}$ of 2±3μmol kg^{-1} over the 19 years.

While surface and subsurface waters are still supersaturated with respect to aragonite and calcite, there was a gradual decrease in aragonite saturation from 2.17±0.07 to 1.88 ±0.06, and a reduction in calcite saturation from 3.40±0.11 to 2.94±0.09, in subsurface waters over the 19 years, which may result in reduced calcification rates in calcifying organisms in the region (Feely et al., 2004; Veron et al., 2009, and references within). LSW in the Rockall Trough is also still supersaturated with calcium carbonate minerals; however there was a slight decrease in both aragonite (0.08±0.01) and calcite (0.11±0.01) saturation between 1991 and 2010. Unfortunately we cannot draw conclusions on the changing saturation horizon in the Trough due to the small number of data points below 2300m in 2009/10. We do however expect a decrease in the depth of aragonite saturation horizon (ASH) in the North Atlantic due to increasing anthropogenic CO_2 penetration. In the eastern North Atlantic the ASH has shoaled by ~400m since the Industrial Revolution and is projected to decrease by ~700m by 2050 (Tanhua et al., 2007). The reduction in aragonite saturation measured down to at least 2000m will likely have implications for the cold water corals, found mainly between 500-1000m deep (White and Dorschel, 2010) interacting with a range of water masses along the continental margin, Rockall Bank and Porcupine Bank (De Mol et al., 2002; Roberts et al., 2003; Wheeler et al., 2011).

The transit time distribution (TTD) method (Tanhua et al., 2007; Waugh et al., 2004) was also attempted in order to calculate C_{ant} between the 1990s and 2010 using CFC data from the earlier WOCE surveys, (Toste Tanhua, personal communication; details not included in Paper II). Chemical tracers with time varying sources or sinks, such as CFCs, are called transient tracers. The surface

history of C_{ant} is reconstructed from the history of atmospheric CO_2 and the resulting equilibrium inorganic carbon system, and is then propagated into the ocean interior using the TTDs (Waugh et al., 2004). However, due to the non-linear input history of CFCs and therefore potential bias depending on input year, it was unrealistic to estimate CFC concentrations for 2009 and 2010, where no CFC measurements were made. Despite not being able to calculate C_{ant}^{TTD} over the 2 decades, it was possible to calculate the mean age (the time since the surface CFC concentration was equal to the interior concentration) of the water masses in the Trough from three WOCE surveys (A01E, A01 and A24). The main finding was a CFC mean age of LSW of ~50 years, longer than previous estimates of 5-10 years (e.g Sy et al., 1997; Yashayaev et al., 2007) for the transit time from the Labrador Sea to reach the eastern North Atlantic. However, unlike the TTD method which includes advective-diffusive flows, most other methods assume weak mixing with a single transit time rather than a distribution of transit times (Waugh et al., 2004). The lower estimates were probably the first pulse of LSW to the region, rather than the mean age and therefore 50 years is likely a better approximation. We may therefore expect a longer time lapse between changes in environmental conditions in the Labrador Sea and subsequent water mass signals in the Rockall Trough.

A further aim of the thesis was to calculate the net community production (NCP) and air-sea CO_2 exchange along the western shelf edge; results are presented in Paper III. From the June 2009 (CE0911) survey, NCP was calculated as the integrated deficit of nitrate and phosphate in the euphotic zone compared to their preformed concentrations. CE0911 sampled six transects along the shelf edge, which allowed for a north-south as well as cross-slope comparison of chemical parameters in the region. Results were similar to those of Paper I, where cooler temperatures and slightly lower salinity in the more northern transects resulted in slightly deeper MLDs and higher nutrient concentrations relative to more southerly transects. This again highlights the pathway of ENAW, which mixes with waters of western origin moving north through the Rockall Channel. Like in Paper II, there was also a clear MW signal in the southern transects of CE0911 with a high A_T, low oxygen signal at the salinity peak ~900-1100m deep. Out of the 43 stations, the NCP calculated from nitrate (C_N^{prod}) and phosphate (C_P^{prod})

were statistically similar in 33 of the stations. In five of the six transects, maximum C_N^{prod} was observed at stations above the ~500-750m contour; i.e. C_N^{prod} was slightly lower over the deeper waters off the shelf and lower over the shallow on-shelf waters. While the reason for this pattern is not clear, we suggest it may be related to the timing and degree of stratification along the shelf edge which influences the balance between nutrient supply and light limitation. Stratification may be too strong in shallow waters along the shelf limiting the nutrient supply, while offshore there may be adequate nutrients but phytoplankton may be mixed into light-limited deeper waters. Körtzinger et al. (2008) reported surface NCP values of 77±13 g C m^{-2} at the PAP site in the eastern North Atlantic. This is similar to the NCP of a nearby station from CE0911 of 72±7 g C m^{-2}. Out of the 24 stations where there are C_T data, 14 stations clearly indicate CO_2 uptake from the atmosphere. While most of the other stations also suggest CO_2 uptake, the uncertainties are larger than the final results. CO_2 uptake can be expected in this region due to the cooling of surface waters moving north and the influence of biological forcing during the productive season (Körtzinger et al., 2008; Takahashi et al., 2002). While this region may be a CO_2 sink during the production season, as blooms decay it may become a CO_2 source as the organic material becomes remineralised.

A final aim of the thesis was to establish the current status of A_T in Irish coastal and shelf waters and investigate the processes governing its distribution, since A_T influences the buffer capacity, and hence CO_2 uptake of the surface ocean. Results are presented in Paper IV. Along the western shelf west of 11ºW, A_T is generally governed by factors that affect salinity, mainly precipitation and evaporation, with higher A_T in the more saline waters towards the shelf edge and off-shelf waters relative to lower A_T-salinity water closer to the coast. Average A_T west of 11ºW was 2335µmol kg^{-1} at salinity of 35.50. Moving north through the centre of the Irish Sea, A_T is also mainly governed by physical processes, with slightly lower levels relative to the western shelf across the southern transect of St. George's Channel (2329µmol kg^{-1} at salinity 35.04), decreasing to 2314µmol kg^{-1} (salinity 34.61) at the seaward end of the Arklow transect to 2304µmol kg^{-1} (salinity of 34.16) at the seaward end of the Liffey transect. Salinity and A_T decreased to 34.12 and 2292 µmol kg^{-1}, respectively, across the

North Channel and highlights the predominantly northward flow through the Irish Sea, where Atlantic water is progressively freshened by riverine water from the Irish and UK coasts (Bowden, 1980).

This pattern is more complex in the outer estuarine and coastal waters, where there are marked differences in the A_T distribution depending on the location. Despite having similar salinity, the A_T along the Irish side of the southern St. George's Channel (2333µmol kg^{-1}) is higher than the UK side (2321µmol kg^{-1}), and is indicative of an A_T source from the Irish coast. Total alkalinity measured by the EPA (EPA, 2010) is very high in some of the rivers flowing into the Celtic Sea, with mean concentrations between 2007 and 2009 averaging over 5000µmol kg^{-1} in the lower Barrow and Nore, and over 4000µmol kg^{-1} in the Suir. These rivers likely acquired their high A_T from the limestone bedrock in their catchment and are therefore a significant A_T source to the Celtic and Irish Seas, with increased buffer capacity in the region as a result. The opposite is seen along the Arklow transect, further north in the Irish Sea, where A_T increases eastwards from the coast with increasing salinity, and coincides with relatively low A_T in the nearby Slaney and Avoca rivers which is transported northwards with the residual flow in the Irish Sea. The River Liffey on the other hand, is a high A_T source to the Irish Sea, with high concentrations measured at the mouth of the Liffey (2413µmol kg^{-1}, salinity 31.80), gradually decreasing outwards due to mixing with coastal waters. EPA A_T concentrations are also high in the River Liffey, with a mean of 4016µmol kg^{-1} between 2007 and 2009 at the seaward end of the river. The limestone bedrock catchment of the middle and lower Liffey and to a much lesser extent the high PO_4 concentrations may contribute to the excess A_T observed.

Relatively low A_T was measured around the North coast in February 2012, coinciding with relatively low salinity and a general lack of limestone bedrock. Despite the low salinity (<32) measured in the Foyle, A_T remained relatively low. A comparison of A_T-S regressions indicated that conditions in the Foyle were similar to those along the shelf edge in June, suggesting a more oceanic influence on A_T with minimal freshwater A_T sources.

The River Shannon on the west coast has a high buffering capacity with high A_T values measured in the low salinity water of the outer estuary in Feb 2011; 2864µmol kg^{-1} in surface waters at a salinity of 15.87 and 2821µmol kg^{-1} in

bottom waters at salinity of 17.61. Concentrations decrease to 2432µmol kg^{-1} at salinity 28.44, and to 2318µmol kg^{-1} at salinity of 34.98. The large annual discharge (long term average 209m^3s^{-1}) along with draining an extensive limestone region, results in this river having relatively high A_T. Also, the River Fergus which flows into the Shannon estuary also has a high A_T (4167µmol kg^{-1}) content at the seaward end of the river (EPA, 2010). The estuary therefore gains A_T from two rivers that drain extensive limestone catchments. Such high A_T values have also been measured in other rivers underlain by limestone bedrock, e.g. 3244µmol kg^{-1} in the river Vistula flowing into the Baltic (Hjalmarsson et al., 2008) and 4250µmol kg^{-1} in the Nahr-Ibrahim River flowing in the Mediterranean (Korfali and Davies, 2004). These results highlight the importance of measuring A_T in river systems and surrounding coastal waters when studying the affects of ocean acidification on marine ecosystems. Coastal waters with a high buffer capacity will be able to resist some of the pH change associated with ocean acidification, and therefore these regions may become more favourable for certain marine organisms as surface water pH continues to decline.

Seasonal alkalinity data show an increase in A_T of ~8µmol kg^{-1} along the 53ºN line between February and May 2010, likely due to photosynthesis in May resulting from the uptake of protons with nitrate by phytoplankton (Wolf-Gladrow et al., 2007). Silicate and A_T data indicate that there may have been a shift from diatoms to calcifying phytoplankton along the shelf edge in May 2009 and 2010. The buffer capacity may therefore be reduced along the shelf edge during the productive season, especially if conditions are favourable for coccolithophore blooms.

One of the objectives of the study was to assess to what extent the Lee et al. (2006) A_T algorithm for the N. Atlantic, which calculates A_T from temperature and salinity, can be applied to Irish coastal and shelf waters. The algorithm is said to fit a sea surface salinity between 31 and 37, and temperature between 0 and 20ºC in the open ocean surface waters of the North Atlantic. Results from Paper IV indicate that in Irish coastal waters A_T is underestimated in lower salinity (<35) water, while it is overestimated in more saline waters (>35.4). Specifically, it is only above a salinity of 35.2 where the calculated A_T was

within the given uncertainty for the North Atlantic of 6.4μmol kg^{-1}. Between sea surface salinity of 31 and 35, A_T was underestimated by between 243 and 8μmol kg^{-1}; results indicate this is due to varying but substantial A_T inputs from rivers in the region. Results indicate that while A_T should not be estimated using the L'06 algorithm in Irish coastal, it can be useful to determine the sources and magnitudes of the different freshwater inputs to the oceans.

Conclusions

Results from this thesis are beneficial to the scientific community as they provide a detailed account of the current status of the inorganic carbon and nutrient chemistry of the water bodies in Irish coastal, shelf and offshore waters for future comparison. Carbon, nutrient and oxygen results highlight that a water mass' chemical signatures can indicate both physical and biological processes that have occurred within that water mass which could not have been identified using hydrographic data alone. Furthermore, measurements of these parameters during winter months will fill some of the crucial gaps in North Atlantic oceanography data, which are often estimates rather than actual measurements. Subsurface waters of the Rockall Trough have acidified by 0.040±0.003 pH units between 1991 and 2010, similar to the decline of 0.02 pH units per decade measured by a number of ocean-carbon time series sites due to increasing atmospheric CO_2. There has been an increase in C_T and decrease in pH down to over 2000m in the Rockall Trough, and the reduced saturation state of calcite and aragonite observed may have implications for marine organisms in the region. The continental shelf edge fringing the west of Ireland is a net sink of atmospheric CO_2 during the productive season. The amount of NCP in the region is partly related to the euphotic depth and partly dependent on preformed nutrient concentrations, both of which are affected by the bottom topography and local and regional oceanography and climate. While the A_T of Irish shelf and outer coastal waters is largely governed by physical processes such as evaporation and precipitation, concentrations are variable in outer estuarine and coastal waters due to substantial inputs from Irish rivers. There may be certain coastal zones around Ireland that will be able to buffer some of the pH change associated with ocean acidification due to large A_T inputs from rivers with extensive limestone bedrock catchments. These areas may become favourable to marine organisms that will be more vulnerable in a more acidic ocean. Results from this thesis highlight the importance of continued monitoring of these chemical parameters in this critical region of the North Atlantic so as to better forecast the impacts of the changing environment on marine ecosystems.

Future Work

The north-east Atlantic margin is an important region for the study of the global thermohaline circulation (Paper I), as well as having an extensive and highly productive continental shelf area. Rising atmospheric CO_2 levels are expected to lead to major global, regional and local changes in the chemistry of seawater, with knock-on effects on marine organisms at all trophic levels. Due to the lack of ocean carbon data time series in this region, a long-term multidisciplinary ocean acidification monitoring programme should be initiated in Irish waters. This would provide information on the extent and rate of environmental change due to increasing atmospheric CO_2 concentrations. Furthermore, due to large natural variability in physical and biogeochemical parameters in the eastern North Atlantic, ongoing monitoring would allow for the discrimination between natural and anthropogenic factors influencing interannual variability in the region. Inclusion of carbonate parameter sampling and analysis with the Marine Institute's annual winter surveys across the Rockall Trough and in Irish coastal waters would ensure a cost-effective, multidisciplinary monitoring plan. This would require the expansion, or at least maintenance, of the pilot specialised research team capable of sampling and analysing inorganic carbon and nutrient samples in Ireland, which this thesis describes the work of. Such a monitoring programme would ensure Ireland meets the requirements of the Marine Strategy Framework Directive and the Joint Assessment and Monitoring Programme of the OSPAR Convention.

It is clear from Paper II that a greater number of samples must be taken below 2000m to investigate the perturbation of anthropogenic carbon (C_{ant}) in the deepest waters of the Trough. Higher vertical resolution between 1800 – 2500m would also allow for accurate determination of the aragonite and calcite saturation horizons for comparison with earlier WOCE surveys and for future comparison. Knowledge of the rate of shoaling saturation horizons associated with ocean acidification would support crucial research on the potential impacts of ocean acidification on deep water ecosystems, particularly the cold water corals in the region.

Measurements of CFCs alongside hydrographic and biogeochemical parameters across the Rockall Trough would allow for the calculation of water mass ages in the Trough, along with estimations of C_{ant} based on transit time distributions of CFCs (Tanhua et al., 2007; Waugh et al., 2004). The use of a number of independent methods of calculation of C_{ant} or ΔC_{ant} would support increased knowledge of processes and rates of environmental change, since different methods are sensitive to various assumptions. Collaboration with international research teams who have experience in measuring CFC samples, e.g. NOC, Southampton and Helmholtz Centre for Ocean Research, Kiel, would ensure generation of high quality data and expand Ireland's research capacity.

There is currently a limited amount of carbon data available in the Celtic Sea, and therefore future surveys should include sampling in this extensive region of the European continental shelf. Increased spatial and vertical resolution in the primary estuaries around Ireland, along with measurements from river water, would clarify what processes are controlling the carbonate system in estuarine and coastal waters, and sampling for carbonate parameters could be included in the EPA's existing sampling programme under the provisions of Water Framework Directive, keeping it cost-effective. Carbon and nutrient samples have already been collected in outer estuarine and coastal waters around the north and north-west coasts of Ireland. Analysis of these samples and the data generated would expand the results of Paper IV to give the current status of A_T distribution, and hence buffer capacity, in the primary marine areas around Ireland. Also, our 2009 and 2010 carbon data from the Rockall Trough is now available on the CDIAC database; data from the shelf edge and coastal waters will also be submitted to CDIAC over the coming months.

Another recommendation is to maximise the research potential of the Mace Head Atmospheric Research Station in Galway, through regular sampling of inorganic carbon and total alkalinity samples at the site. As discussed in Paper IV, it is possible to estimate total alkalinity in surface waters of the open ocean from temperature and salinity (Lee et al., 2006). While this is not as straight forward in coastal waters due to more complex processes and inputs, it may be possible to

describe a new algorithm for the Mace Head region to estimate A_T from the temperature and salinity. If this was feasible, the entire inorganic carbon system could be described from the continuous pCO_2 measurements alongside temperature and salinity data from the sensors at the site. This has to potential to generate an invaluable dataset which could indicate seasonal and interannual changes in air-sea CO_2 exchange, alongside changes in surface water carbon chemistry.

Finally, a multidisciplinary ecosystem approach is required to investigate the potential impacts of ocean acidification on Irish marine ecosystems. Research into ecologically vulnerable areas and keystone species would give an indication of how the ecosystem will respond to the changing environment (Ní Longphuirt et al., 2010).

The most important requirement however, for ensuring ocean acidification and its subsequent effects on marine ecosystems do not reach critical levels is to reduce CO_2 emissions to the atmosphere. It is hoped this thesis will help to highlight the importance of including ocean acidification research and monitoring in Ireland's future science budgets.

References

Allen, J.R., Slinn, D.J., Shammon, T.M., Hartnoll, R.G. and Hawkins, S.J., 1998. Evidence for eutrophication of the Irish Sea over four decades. Limnology and Oceanography, 43(8): 1970-1974.

Andersson, A.J., Mackenzie, F.T. and Lerman, A., 2005. Coastal ocean and carbonate systems in the high CO2 world of the Anthropocene. American Journal of Science, 305: 875-918.

Arhan, M., 1990. The North-Atlantic Current and Sub-Arctic Intermediate Water. Journal of Marine Research, 48(1): 109-144.

Arhan, M., Colin de Verdière, A. and Mémery, L., 1994. The Eastern Boundary of the Subtropical North Atlantic. Journal of Physical Oceanography, 24: 1295-1316.

Azetsu-Scott, K., Jones, E.P. and Gershey, R.M., 2005. Distribution and ventilation of water masses in the Labrador Sea inferred from CFCs and carbon tetrachloride. Marine Chemistry, 94(1-4): 55-66.

Bates, N.R., 2002. Interannual variability in the global uptake of CO2. Geophysical Research Letters, 29(5).

Bates, N.R., 2011. Multi-decadal uptake of carbon dioxide into subtropical mode water of the North Atlantic Ocean. Biogeosciences Discussions, 8: 12451–12476.

Bates, N.R. et al., 2012. Detecting anthropogenic carbon dioxide uptake and ocean acidification in the North Atlantic Ocean. Biogeosciences Discuss., 9(1): 989-1019.

Bersch, M., Meincke, J. and Sy, A., 1999. Interannual thermohaline changes in the northern North Atlantic 1991-1996. Deep Sea Research Part II: Topical Studies in Oceanography, 46(1-2): 55-75.

Bethoux, J.P. et al., 1999. The Mediterranean Sea: a miniature ocean for climatic and environmental studies and a key for the climatic functioning of the North Atlantic. Progress In Oceanography, 44(1-3): 131-146.

Borges, A.V. and Frankignoulle, M., 2003. Distribution of surface carbon dioxide and air-sea exchange in the English Channel and adjacent areas. J. Geophys. Res., 108(C5): 3140.

Borges, A.V., Schiettecatte, L.S., Abril, G., Delille, B. and Gazeau, F., 2006. Carbon dioxide in European coastal waters. Estuarine, Coastal and Shelf Science, 70(3): 375-387.

Bowden, K.F., 1980. Chapter 12 Physical and Dynamical Oceanography of the Irish Sea. In: F.T. Banner, M.B. Collins and K.S. Massie (Editors), The North-west European Shelf Seas: The Sea Bed and the Sea in Motion II. Physical and chemical oceanography, and physical resources. Elsevier Oceanography Series, pp. 391-413.

Broecker, W.S., 1997. Thermohaline Circulation, the Achilles Heel of Our Climate System: Will Man-Made CO2 Upset the Current Balance? Science, 278(5343): 1582-1588.

Broecker, W.S. and Peng, T.H., 1982. Tracers in the sea. Columbia University Press, Palisades, NY, 690 pp.

Burns, W.C.G., 2008. Anthropogenic carbon dioxide emissions and ocean acidification., Springer.
Cabecadas, G., Brogueira, M.J. and Goncalves, C., 2002. The chemistry of Mediterranean outflow and its interactions with surrounding waters. Deep-Sea Research Part II - Topical Studies in Oceanography, 49(19): 4263-4270.
Caldeira, K. and Wickett, M.E., 2003. Oceanography: Anthropogenic carbon and ocean pH. Nature, 425(6956): 365-365.
Cannaby, H. and Hüsrevoğlu, Y.S., 2009. The influence of low-frequency variability and long-term trends in North Atlantic sea surface temperature on Irish waters. ICES Journal of Marine Science: Journal du Conseil, 66(7): 1480-1489.
Castro, C.G., Perez, F.F., Holley, S.E. and Rios, A.F., 1998. Chemical characterisation and modelling of water masses in the Northeast Atlantic. Progress in Oceanography, 41(3): 249-279.
Cermeño, P. et al., 2008. The role of nutricline depth in regulating the ocean carbon cycle. Proceedings of the National Academy of Sciences, 105(51): 20344-20349.
Chen, C.-T.A. and Borges, A.V., 2009. Reconciling opposing views on carbon cycling in the coastal ocean: Continental shelves as sinks and near-shore ecosystems as sources of atmospheric CO2. Deep Sea Research Part II: Topical Studies in Oceanography, 56(8-10): 578-590.
Clarke, R.A. and Coote, A.R., 1988. The formation of Labrador Sea-Water. III: The evolution of oxygen and nutrient concentration. Journal of Physical Oceanography, 18(3): 469-480.
Coste, B., Corre, P.L. and Minas, H.J., 1988. Re-evaluation of the nutrient exchanges in the strait of gibraltar. Deep Sea Research Part A. Oceanographic Research Papers, 35(5): 767-775.
De Baar, H.J.W. and Gerringa, L.J.A., 2009. Effects of Ocean Acidification on the physical-chemical speciation of nutrients and trace metals.
De Mol, B. et al., 2002. Large deep-water coral banks in the Porcupine Basin, southwest of Ireland. Marine Geology, 188(1-2): 193-231.
Dickson, A.G., 1981. An exact definition of total alkalinity and a procedure for the estimation of alkalinity and total inorganic carbon from titration data. Deep Sea Research Part A. Oceanographic Research Papers, 28(6): 609-623.
Dickson, A.G., 1995. Determination of dissolved oxygen in sea water by Winkler titration. WOCE Operations Manual. Part 3.1.3 Operations & Methods, WHP Office Report WHPO 91-1.
Dickson, A.G., 2010. Guide to best practices for ocean acidifcation research and data reporting, Publications Office of the European Union, Luxembourg.
Dickson, A.G. and Millero, F.J., 1987. A comparison of the equilibrium constants for the dissociation of carbonic acid in seawater media. Deep Sea Research, 34: 1733-1743.
Dickson, A.G. and Riley, J.P., 1978. The effect of analytical error on the evaluation of the components of the aquatic carbon-dioxide system. Marine Chemistry, 6(1): 77-85.
Dickson, A.G., Sabine, C.L. and Christian, J.R., 2007. Guide to best practices for ocean CO2 measurements. PICES Special Publication 3: 1-191.

DOE, 1994. Handbook of methods for the analysis of the various parameters of the carbon dioxide system in sea water; version 2. ORNL/CDIAC-74.
Doney, S.C., 2006. Oceanography: Plankton in a warmer world. Nature, 444(7120): 695-696.
Doney, S.C., Fabry, V.J., Feely, R.A. and Kleypas, J.A., 2009a. Ocean Acidification: The Other CO2 Problem. Annual Review of Marine Science, 1(1): 169-192.
Doney, S.C. et al., 2009b. Surface-ocean CO2 variability and vulnerability. Deep Sea Research Part II: Topical Studies in Oceanography, 56(8-10): 504-511.
Dore, J.E., Lukas, R., Sadler, D.W., Church, M.J. and Karl, D.M., 2009. Physical and biogeochemical modulation of ocean acidification in the central North Pacific. Proceedings of the National Academy of Science of the USA, 106(30).
Dore, J.E., Lukas, R., Sadler, D.W. and Karl, D.M., 2003. Climate-driven changes to the atmospheric CO2 sink in the subtropical North Pacific Ocean. Nature, 424(6950): 754-757.
EEA, 2011. Nutrients in transitional, coastal and marine waters (CSI 021) - Assessment published July 2011.
Ellett, D.J., 1995. Physical Oceanography of the Rockall Trough. Ocean Challenge, 6: 18-23.
Ellett, D.J. et al., 1983. Water masses and mesoscale circulation of North Rockall Trough waters during Jasin 1978. Philosophical Transactions of the Royal Society of London Series a-Mathematical Physical and Engineering Sciences, 308(1503): 231-252.
Ellett, D.J. and Martin, J.H.A., 1973. Physical and Chemical Oceanography of Rockall Channel. Deep-Sea Research, 20(7): 585-625.
EPA, 2010. Water Quality in Ireland 2007-2009, Environmental Protection Agency, Wexford.
Evans, G.L., Williams, P.J.L. and Mitchelson-Jacob, E.G., 2003. Physical and anthropogenic effects on observed long-term nutrient changes in the Irish Sea. Estuarine Coastal and Shelf Science, 57(5-6): 1159-1168.
Feely, R.A. et al., 2004. Impact of anthropogenic CO2 on the CaCO3 system in the oceans. Science, 305(5682): 362-366.
Freiwald, A. and Roberts, J.M., 2005. Cold-water corals and ecosystems. Springer, 1243 pp.
Friis, K., Körtzinger, A., Pätsch, J. and Wallace, D.W.R., 2005. On the temporal increase of anthropogenic CO2 in the subpolar North Atlantic. Deep Sea Research Part I: Oceanographic Research Papers, 52(5): 681-698.
Furuya, K. and Harada, K., 1995. An Automated Precise Winkler Titration for Determining Dissolved Oxygen on Board Ship. Journal of Oceanography, 51: 375-383.
Garçon, V.C., Oschlies, A., Doney, S.C., McGillicuddy, D. and Waniek, J., 2001. The role of mesoscale variability on plankton dynamics in the North Atlantic. Deep Sea Research Part II: Topical Studies in Oceanography, 48(10): 2199-2226.
Gattuso, J.P., Frankignoulle, M. and Wollast, R., 1998. Carbon and carbonate metabolism in coastal aquatic ecosystems. Annual Review of Ecology and Systematics, 29: 405-434.

Gattuso, J.P. and Lavigne, H., 2009. Technical Note: Approaches and software tools to investigate the impact of ocean acidification. Biogeosciences, 6(10): 2121-2133.
Gnanadesikan, A., 1999. A global model of silicon cycling: Sensitivity to eddy parameterization and dissolution. Global Biogeochemical Cycles, 13(1): 199-220.
González-Dávila, M., Santana-Casiano, J.M., Rueda, M.-J., Llinás, O. and González-Dávila, E.-F., 2003. Seasonal and interannual variability of sea-surface carbon dioxide species at the European Station for Time Series in the Ocean at the Canary Islands (ESTOC) between 1996 and 2000. Global Biogeochem. Cycles, 17(3): 1076.
González-Dávila, M., Santana-Casiano, J.M., Rueda, M.J. and Llinás, O., 2010. The water column distribution of carbonate system variables at the ESTOC site from 1995 to 2004. Biogeosciences Discussions, 7: 1995–2032.
Gowen, R.J. et al., 2002. Assessing trends in nutrient concentrations in coastal shelf seas: a case study in the Irish Sea. Estuarine Coastal and Shelf Science, 54(6): 927-939.
Grasshoff, K., Ehrhardt, M., Kremling, K. and Almgren, T., 1983. Methods of seawater analysis. Verlag Chemie.
Grasshoff, K., Ehrhardt, M., Kremling, K. and Anderson, L.G., 1999. Methods of seawater analysis. Wiley-VCH.
Gruber, N., Keeling, C.D. and Bates, N.R., 2002. Interannual variability in the North Atlantic Ocean carbon sink. Science, 298(5602): 2374-2378.
Guinotte, J.M. and Fabry, V.J., 2008. Ocean Acidification and its potential effects on marine ecosystems. Annals of the New York Academy of Sciences 1134: 320-343.
Guinotte, J.M. et al., 2006. Will human-induced changes in seawater chemistry alter the distribution of deep-sea scleractinian corals? Frontiers in Ecology and the Environment, 4(3): 141-146.
Harvey, J., 1982. Theta-S relationships and water masses in the eastern North Atlantic. Deep-Sea Research Part a-Oceanographic Research Papers, 29(8): 1021-1033.
Harvey, J. and Arhan, M., 1988. The water masses of the Central North Atlantic in 1983-84. Journal of Physical Oceanography, 18: 1855-1875.
Hill, A.E. and Mitchelson-Jacob, E.G., 1993. Observations of a poleward-flowing saline core on the continental slope west of Scotland. Deep Sea Research Part I: Oceanographic Research Papers, 40(7): 1521-1527.
Hjalmarsson, S. et al., 2008. Distribution, long-term development and mass balance calculation of total alkalinity in the Baltic Sea. Continental Shelf Research, 28(4-5): 593-601.
Holliday, N.P., Pollard, R.T., Read, J.F. and Leach, H., 2000. Water mass properties and fluxes in the Rockall Trough 1975-1998. Deep Sea Research I, 47: 1303-1332.
Holliday, N.P. et al., 2006. Large-scale physical controls on phytoplankton growth in the Irminger Sea Part I: Hydrographic zones, mixing and stratification. Journal of Marine Systems, 59(3-4): 201-218.
Holt, J. et al., 2009. Modelling the global coastal ocean. Philosophical Transactions of the Royal Society A: Mathematical, Physical and Engineering Sciences, 367(1890): 939-951.

Howe, M.R., 1982. The Mediterranean Water Outflow in the Gulf of Cadiz. Oceanography and Marine Biology, 20: 37-64.
Howe, M.R., Abdullah, M.I. and Deetae, S., 1974. Interpretation of Double T-S Maxima in Mediterranean Outflow using Chemical Tracers. Journal of Marine Research, 32(3): 377-386.
Huang, W.G., Cracknell, A.P., Vaughan, R.A. and Davies, P.A., 1991. A Satellite and Field View of the Irish Shelf Front. Continental Shelf Research, 11(6): 543-562.
Huthnance, J.M., 1995. Circulation, exchange and water masses at the ocean margin: the role of physical processes at the shelf edge. Progress In Oceanography, 35(4): 353-431.
Huthnance, J.M. et al., 2001. Physical structures, advection and mixing in the region of Goban spur. Deep-Sea Research Part Ii-Topical Studies in Oceanography, 48(14-15): 2979-3021.
Hydes, D.J., Gowen, R.J., Holliday, N.P., Shammon, T. and Mills, D., 2004. External and internal control of winter concentrations of nutrients (N, P and Si) in north-west European shelf seas. Estuarine Coastal and Shelf Science, 59(1): 151-161.
Hydes, D.J., Kelly-Gerreyn, B.A., Le Gall, A.C. and Proctor, R., 1999. The balance of supply of nutrients and demands of biological production and denitrification in a temperate latitude shelf sea - a treatment of the southern North Sea as an extended estuary. Marine Chemistry, 68(1-2): 117-131.
ICES, 2008. Changes in surface CO2 and ocean pH in ICES shelf sea ecosystems, International Council for the Exploration of the Sea, Copenhagen.
Johnson, C., Sherwin, T., Smythe-Wright, D., Shimmield, T. and Turrell, W., 2010. Wyville Thomson Ridge Overflow Water: Spatial and temporal distribution in the Rockall Trough. Deep Sea Research Part I: Oceanographic Research Papers, 57(10): 1153-1162.
Johnson, K.M., Sieburth, J.M., Williams, P.J.l. and Brändström, L., 1987. Coulometric total carbon dioxide analysis for marine studies: Automation and calibration. Marine chemistry, 21: 117-133.
Johnson, K.M., Wills, K.D., Butler, D.B., Johnson, W.K. and Wong, C.S., 1993. Coulometric total carbon dioxide analysis for marine studies: maximizing the performance of an automated gas extraction system and coulometric detector. Marine chemistry, 44: 167-187.
Karcher, M., Gerdes, R., Kauker, F., Köberle, C. and Yashayaev, I., 2005. Arctic Ocean change heralds North Atlantic freshening. Geophys. Res. Lett., 32(21): L21606.
Knapp, G.P., Stalcup, M.C. and Stanley, R.J., 1989. Dissolved oxygen measurements in sea water at the Woods Hole Oceanographic Institution.
Koeve, W., 2001. Wintertime nutrients in the North Atlantic-new approaches and implications for new production estimates. Marine Chemistry, 74(4): 245-260.
Korfali, S.I. and Davies, B.E., 2004. Speciation of metals in sediment and water in a river underlain by limestone: role of carbonate species for purification capacity of rivers. Advances in Environmental Research, 8(3-4): 599-612.

Körtzinger, A., Koeve, W., Kähler, P. and Mintrop, L., 2001. C : N ratios in the mixed layer during the productive season in the northeast Atlantic Ocean. Deep Sea Research Part I: Oceanographic Research Papers, 48(3): 661-688.

Körtzinger, A. et al., 2008. The seasonal pCO2 cycle at 49°N/16.5°W in the northeastern Atlantic Ocean and what it tells us about biological productivity. Journal of Geophysical Research - Oceans, 113: C04020.

Lavelle, P. et al., 2001. Chapter 12: Nutrient Cycling, Ecosystems and human well-being: current status and trends. Island Press, pp. 331-353.

Lee, A. and Ellett, D., 1965. On the contribution of overflow water from the Norwegian Sea to the hydrographic structure of the North Atlantic Ocean. Deep Sea Research and Oceanographic Abstracts, 12(2): 129-142.

Lee, K. et al., 2006. Global relationships of total alkalinity with salinity and temperature in surface waters of the world's oceans. Geophysical Research Letters, 33(19).

Lewis, E. and Wallace, D.W.R., 1998. Program Developed for CO2 System Calculations. ORNL/CDIAC-105. Carbon Dioxide Information Analysis Center, Oak Ridge National Laboratory, U.S. Department of Energy, Oak Ridge, Tennessee.

Longhurst, A., Sathyendranath, S., Platt, T. and Caverhill, C., 1995. An estimate of global primary production in the ocean from satellite radiometer data. Journal of Plankton Research, 17: 1245–1271.

Lozier, M.S. and Stewart, N.M., 2008. On the temporally varying northward penetration of Mediterranean Overflow Water and eastward penetration of Labrador Sea water. Journal of Physical Oceanography, 38(9): 2097-2103.

Lüthi, D. et al., 2008. High-resolution carbon dioxide concentration record 650,000-800,000 years before present. Nature, 453(7193): 379-382.

McCartney, M.S., 1992. Recirculating components to the deep boundary current of the northern North Atlantic. Progress In Oceanography, 29(4): 283-383.

McCartney, M.S. and Mauritzen, C., 2001. On the origin of the warm inflow to the Nordic Seas. Progress in Oceanography, 51(1): 125-214.

McGovern, E. et al., 2002. Winter nutrient monitoring of the Western Irish Sea – 1990-2000, Marine Institute, Dublin.

McGrath, T., Nolan, G. and McGovern, E., 2012. Chemical characteristics of water masses in the Rockall Trough. Deep Sea Research Part I: Oceanographic Research Papers, 61(0): 57-73.

McMahon, T., Raine, R., Titov, O. and Boychuk, S., 1995. Some oceanographic features of northeastern Atlantic waters west of Ireland Ices Journal of Marine Science, 52(2): 221-232.

Mehrbach, C., Culberson, C.H., Hawley, J.E. and Pytkowicz, R.M., 1973. Measurement of the apparent dissociation constants of carbonic acid in seawater at atmospheric pressure. Limnology and Oceanography, 18: 897-907.

Millero, F.J., Feistel, R., Wright, D.G. and McDougall, T.J., 2008. The composition of Standard Seawater and the definition of the Reference-Composition Salinity Scale. Deep Sea Research Part I: Oceanographic Research Papers, 55(1): 50-72.

Mintrop, L., Pérez, F.F., Gonzalez-Dávila, M., Santana-Casiano, J.M. and Körtzinger, A., 2000. Alkalinity determination by potentiometry: intercalibration using three different methods. Ciencias Marinas, 26(1): 23-37.

Mohn, C., Bartsch, J. and Meincke, J., 2002. Observations of the mass and flow field at Porcupine Bank. Ices Journal of Marine Science, 59(2): 380-392.

New, A.L. and Smythe-Wright, D., 2001. Aspects of the circulation in the Rockall Trough. Continental Shelf Research, 21(8-10): 777-810.

Ní Longphuirt, S., Stengel, D., O'Dowd, C. and McGovern, E., 2010. Ocean Acidification: An Emerging Threat To Our Marine Environment., Marine Institute, Galway 2010.

Nolan, G., in prep. Variability of the intermediate and deep water masses in the Rockall Trough

Nolan, G., Gillooly, M. and Whelan, K., 2009. Irish Ocean, Climate and Ecosystem Status Report 2009, Marine Institute, Galway.

Olafsson, J. et al., 2009. Rate of Iceland Sea acidification from time series measurements. Biogeosciences Discussions, 6(3): 5251-5270.

Orr, J.C. et al., 2005. Anthropogenic ocean acidification over the twenty-first century and its impact on calcifying organisms. Nature, 437(7059): 681-686.

OSPAR, 2000. Quality Status Report 2000 Region III- Celtic Seas, OSPAR Commission, London, UK.

Palacios, S.L. and Zimmerman, R.C., 2007. Response of eelgrass Zostera marina to CO2 enrichment: possible impacts of climate change and potential for remediation of coastal habitats. Marine Ecology Progress Series, 344: 1-13.

Pelegri, J.L., Csanady, G.T. and Martins, A., 1996. The North Atlantic nutrient stream. Journal of Oceanography, 52(3): 275-299.

Pelegrí, J.L., Marrero-Díaz, A. and Ratsimandresy, A.W., 2006. Nutrient irrigation of the North Atlantic. Progress in Oceanography, 70(2-4): 366-406.

Pérez, F.F., Mouriño, C., Fraga, F. and Ríos, A.F., 1993. Displacement of water masses and remineralization rates off the Iberian Peninsula by nutrient anomalies. Journal of Marine Research, 51: 869-892.

Pérez, F.F. et al., 2010. Trends of anthropogenic CO2 storage in North Atlantic water masses. Biogeosciences, 7: 1789-1807.

Pingree, R.D., Sinha, B. and Griffiths, C.R., 1999. Seasonality of the European slope current (Goban Spur) and ocean margin exchange. Continental Shelf Research, 19(7): 929-975.

Pollard, R.T. et al., 1996. Vivaldi 1991-A study of the formation, circulation and ventilation of Eastern North Atlantic Central Water. Progress in Oceanography, 37(2): 167-192.

Raven, J. et al., 2005. Ocean Acidification due to Increasing Atmospheric Carbon Dioxide., The Royal Society, London.

Redfield, A.C., Ketchum, B.H. and Richards, F.A., 1963. The influence of organisms on the composition of sea-water. In: M.N. Hill (Editor), The Sea, pp. 26-77.

Revelle, R. and Suess, H.E., 1957. Carbon dioxide exchange between atmosphere and ocean and the question of an increase of atmospheric carbon dioxide during the past decades. Tellus, 9(18-27).

Ridame, C., Moutin, T. and Guieu, C., 2003. Does phosphate adsorption onto Saharan dust explain the unusual N/P ratio in the Mediterranean Sea? Oceanologica Acta, 26(5-6): 629-634.
Roberts, J.M., Long, D., Wilson, J.B., Mortensen, P.B. and Gage, J.D., 2003. The cold-water coral Lophelia pertusa (Scleractinia) and enigmatic seabed mounds along the north-east Atlantic margin: are they related? Marine Pollution Bulletin, 46(1): 7-20.
Sabine, C.L. et al., 2004. The oceanic sink for anthropogenic CO2. Science, 305(5682): 367-371.
Sabine, C.L. and Tanhua, T., 2010. Estimation of Anthropogenic CO(2) Inventories in the Ocean, Annual Review of Marine Science. Annual Review of Marine Science, pp. 175-198.
Sarmiento, J.L., Hughes, T.M.C., Stouffer, R.J. and Manabe, S., 1998. Simulated response of the ocean carbon cycle to anthropogenic climate warming. Nature, 393(6682): 245-249.
Schneider, A., Wallace, D.W.R. and Körtzinger, A., 2007. Alkalinity of the Mediterranean Sea. Geophysical Research Letters, 34(15): 1-5.
Sherwin, T.J., Griffiths, C.R., Inall, M.E. and Turrell, W.R., 2008. Quantifying the overflow across the Wyville Thomson Ridge into the Rockall Trough. Deep Sea Research Part I: Oceanographic Research Papers, 55(4): 396-404.
Smetacek, V., 2000. The giant diatom dump. Nature, 406: 574-575.
Solomon, S. et al., 2007. Climate Change 2007: The Physical Science Basis. Contribution of Working Group I to the Fourth Assessment Report of the Intergovernmental Panel on Climate Change, Cambridge University Press, Cambridge, United Kingdom and New York, NY, USA.
Steinacher, M., Joos, F., Frölicher, T.L., Plattner, G.-K. and Doney, S.C., 2009. Imminent ocean acidification in the Arctic projected with the NCAR global coupled carbon cycle-climate model. Biogeosciences, 6: 515–533.
Stewart, R.H., 2008. Introduction to physical oceanography, Texas, A & M University.
Sy, A. et al., 1997. Surprisingly rapid spreading of newly formed intermediate waters across the North Atlantic ocean. Nature, 386(6626): 675-679.
Takahashi, T., Olafsson, J., Goddard, J., Chipman, D.W. and Sutherland, S.C., 1993. Seasonal variation of CO_2 and nutrients in the high-latitude surface oceans: A comparative study. Global Biogeochemical Cycles, 7(4): 853-878.
Takahashi, T. et al., 2002. Global sea-air CO2 flux based on climatological surface ocean pCO(2), and seasonal biological and temperature effects. Deep-Sea Research Part Ii-Topical Studies in Oceanography, 49(9-10): 1601-1622.
Tanhua, T. et al., 2006. Changes of anthropogenic CO2 and CFCs in the North Atlantic between 1981 and 2004. Global Biogeochemical Cycles, 20(4): GB4017.
Tanhua, T., Körtzinger, A., Friis, K., Waugh, D.W. and Wallace, D., 2007. An estimate of anthropogenic CO2 inventory from decadal changes in oceanic carbon content. Proceedings of the National Academy of Science of the USA, 104.

Tomczak, M., 1999. Some historical, theoretical and applied aspects of quantitative water mass analysis. Journal of Marine Research, 57(2): 275-303.
Tomczak, M. and Godfrey, J.S., 1994. Regional oceanography: An Introduction. Oxford, Pergamon.
Townsend, D.W., Rebuck, N.D., Thomas, M.A., Karp-Boss, L. and Gettings, R.M., 2010. A changing nutrient regime in the Gulf of Maine. Continental Shelf Research, 30(7): 820-832.
Tsuchiya, M., Talley, L.D. and McCartney, M.S., 1992. An eastern Atlantic section from Iceland southward across the equator. Deep-Sea Research Part a-Oceanographic Research Papers, 39(11-12A): 1885-1917.
Ullgren, J.E. and White, M., 2010. Water mass interaction at intermediate depths in the southern Rockall Trough, northeastern North Atlantic. Deep Sea Research Part I: Oceanographic Research Papers, 57(2): 248-257.
UNESCO, 1981. The Practical Salinity Scale 1978 and the International Equation of State of Seawater 1980.
van Aken, H.M., 2000a. The hydrography of the mid-latitude northeast Atlantic Ocean I: The deep water masses. Deep-Sea Research Part I-Oceanographic Research Papers, 47(5): 757-788.
van Aken, H.M., 2000b. The hydrography of the mid-latitude Northeast Atlantic Ocean II: The intermediate water masses. Deep-Sea Research Part I-Oceanographic Research Papers, 47(5): 789-824.
van Aken, H.M. and De Boer, C.J., 1995. On the synoptic hydrography of intermediate and deep water masses in the Iceland Basin. Deep Sea Research Part I: Oceanographic Research Papers, 42(2): 165-189.
Vázquez-Rodríguez, M., Padin, X.A., Ríos, A.F., Bellerby, R.J.G. and Pérez, F.F., 2009. An upgraded carbon-based method to estimate the anthropogenic fraction of dissolved CO2 in the Atlantic Ocean. Biogeosciences Discuss, 6: 4527–4571.
Veron, J.E.N. et al., 2009. The coral reef crisis: The critical importance of <350 ppm CO2. Marine Pollution Bulletin, 58(10): 1428-1436.
Wade, I.P., Ellett, D.J. and Heywood, K.J., 1997. The influence of intermediate waters on the stability of the eastern North Atlantic. Deep-Sea Research Part I-Oceanographic Research Papers, 44(8): 1405-1426.
Walsh, J.J., Biscaye, P.E. and Csanady, G.T., 1988. The 1983–1984 shelf edge exchange processes (SEEP)-I experiment: hypotheses and highlights. Continental Shelf Research, 8: 435-456.
Walsh, J.J., Biscaye, P.E. and Csanady, G.T., 1991. Importance of continental margins in the marine biogeochemical cycling of carbon and nitrogen. Nature, 359: 53-59.
Waugh, D.W., Haine, T.W.N. and Hall, T.M., 2004. Transport times and anthropogenic carbon in the subpolar North Atlantic Ocean. Deep Sea Research Part I: Oceanographic Research Papers, 51(11): 1475-1491.
Wheeler, A.J. et al., 2011. The Moira Mounds, small cold-water coral banks in the Porcupine Seabight, NE Atlantic: Part A—an early stage growth phase for future coral carbonate mounds? Marine Geology, 282: 53-64.
White, M. and Bowyer, P., 1997. The shelf-edge current north-west of Ireland. Annales Geophysicae-Atmospheres Hydrospheres and Space Sciences, 15(8): 1076-1083.

White, M. and Dorschel, B., 2010. The importance of the permanent thermocline to the cold water coral carbonate mound distribution in the NE Atlantic. Earth and Planetary Science Letters, 296(3-4): 395-402.
Williams, R.J. and Follows, M.J., 2003. Physical Transport of Nutrients and the Maintenance of Biological Production. In: M. Fasham (Editor), Ocean Biogeochemistry: The role of the ocean carbon cycle in global change. Springer.
Wolf-Gladrow, D.A., Zeebe, R.E., Klaas, C., Körtzinger, A. and Dickson, A.G., 2007. Total alkalinity: The explicit conservative expression and its application to biogeochemical processes. Marine Chemistry, 106(1-2): 287-300.
Wootton, J.T., Pfister, C.A. and Forester, J.D., 2008. Dynamic patterns and ecological impacts of declining ocean pH in a high-resolution multi-year dataset. PNAS, 105(48): 18848–18853.
Worthington, L.V., Wright, W.R. and Erika, D., 1970. North Atlantic Ocean atlas: of potential temperature and salinity in the deep water including temperature, salinity and oxygen profiles from the Erika Dan cruise of 1962. Woods Hole Oceanographic Institution.
Yashayaev, I., 2007. Hydrographic changes in the Labrador Sea, 1960-2005. Progress in Oceanography, 73(3-4): 242-276.
Yashayaev, I., van Aken, H.M., Holliday, N.P. and Bersch, M., 2007. Transformation of the Labrador Sea Water in the subpolar North Atlantic. Geophys. Res. Lett., 34(22): L22605.
Zeebe, R.E. and Wolf-Gladrow, D., 2003. CO_2 in seawater: Equilibrium, kinetics, isotopes. Elsevier Oceanography Series, 65. Elsevier, 346 pp.

Paper I

Chemical characteristics of water masses in the Rockall Trough

2012. Deep Sea Research-Part I: Oceanographic Research Papers, 61 (0), 57-73.

Triona McGrath [a,b], Glenn Nolan[a], Evin McGovern [a]

[a] Marine Institute, Ireland
[b] National University of Ireland, Galway

Deep-Sea Research I 61 (2012) 57–73

Contents lists available at SciVerse ScienceDirect

Deep-Sea Research I

journal homepage: www.elsevier.com/locate/dsri

Chemical characteristics of water masses in the Rockall Trough

Triona McGrath [a,b,*], Glenn Nolan [a], Evin McGovern [a]

[a] The Marine Institute, Rinville, Oranmore, Galway, Ireland
[b] Department of Earth and Ocean Sciences, National University of Ireland, Galway, University Road, Galway, Ireland

ARTICLE INFO

Article history:
Received 23 June 2011
Received in revised form
14 November 2011
Accepted 22 November 2011
Available online 3 December 2011

Keywords:
Water masses
Nutrients
Oxygen
Salinity
Rockall Trough
North Atlantic

ABSTRACT

Direct observations of physical and chemical data in the Rockall Trough during February of 2008, 2009 and 2010 are presented. Results are compared to a similar WOCE transect, AR24, completed in November/December 1996. Temperature and salinity data have been used to identify the water masses present in the Trough, and have been combined with nutrient (nitrate, nitrite, phosphate, silicate) and oxygen data to produce a table outlining the chemical characteristics of each of the water masses. Eastern North Atlantic Water (ENAW) moving north through the Trough gains nutrients from a branch of the North Atlantic Current (NAC). Mediterranean Water (MW) was identified as a warm saline core, with characteristically low oxygen and low preformed nutrients along the Irish continental shelf break near 53°N. Found at a similar density level at the southern entrance to the Trough, Sub Arctic Intermediate Water (SAIW) has relatively high oxygen and preformed nutrients, likely entrained from the subpolar gyre when it was formed. LSW was identified as a prominent water mass between 1500 and 2000 m deep, with characteristically high oxygen content. Lower silicate, and to a lesser extent preformed nitrate, in 2009 coincide with a freshening of Labrador Sea Water (LSW) relative to other years, and could indicate a stronger influence from the Labrador Current when it was formed. Finally, traces of Antarctic Bottom Water (AABW) were found as far north as 53°N, indicated by a sharp increase in nutrient concentrations, particularly silicate in the deepest parts of the Trough.

1. Introduction

The Rockall Trough is a deep sea channel, west of the Irish continental shelf, bounded to the west by the Rockall Bank (Fig. 1). The southern entrance to the Trough is over 3000 m deep, and it is connected to Nordic Seas by the shallow (500 m) Wyville-Thomson Ridge in the north. To the west of the Rockall Trough lies the boundary between the two counter-rotating gyres, the subpolar and subtropical gyres of the North Atlantic. The North Atlantic Current (NAC) is an extension of the Gulf Stream that carries warm, salty water eastwards across the North Atlantic. Upon reaching the Rockall Plateau, one branch circulates northwest towards Iceland, while the other circulates through the Rockall Trough before reaching the Norwegian Sea (Ellett and Martin, 1973; Pollard et al., 1996). This region is therefore an important part of the ocean-climate system, as it provides a pathway for warm and saline water of the upper North Atlantic to enter the Nordic Seas, where it is converted into cold, dense overflow water as part of the warm-to-cold water transformation of the thermohaline circulation (Ellett and Martin, 1973; Holliday et al., 2000). Although the different water masses found in the Rockall Trough have been well documented (Johnson et al., 2010; New and Smythe-Wright, 2001; Read, 2001; Ullgren and White, 2010), the chemical make up of these water bodies is less well understood. Some of the water masses in the region have overlapping temperature-salinity properties, and so the chemical characteristics of each are examined here to help identify the water masses present.

Biogeochemical and physical processes determine the nutrient and oxygen distribution in the world's oceans. Although the ageing of a water mass results in a decrease in oxygen and increase in dissolved inorganic nutrients (due to respiration), vertical profiles broadly reflect water masses as defined by temperature and salinity, highlighting the important role of physical transport (Williams and Follows, 2003). Despite their non-conservative properties, chemical tracers like nutrients and oxygen can help us to more accurately define water masses and can indicate processes that have occurred along their path. They can also be combined in such a way as to make them conservative as their concentrations change in fixed proportions within the water mass.

Oxygen content in seawater is controlled by direct fluxes from the atmosphere when the water mass is formed, and by respiration and photosynthesis. The flux of atmospheric oxygen into seawater is temperature dependent, with colder water absorbing more oxygen than warm water. Apparent oxygen utilisation (AOU)

* Corresponding author at: The Marine Institute, Rinville, Oranmore, Galway, Ireland. Tel.: +353 91 387327; fax: +353 91 387201.
E-mail addresses: triona.mcgrath@marine.ie, triona_mcgrath@hotmail.com (T. McGrath), glenn.nolan@marine.ie (G. Nolan), evin.mcgovern@marine.ie (E. McGovern).

0967-0637/$ - see front matter © 2011 Elsevier Ltd. All rights reserved.
doi:10.1016/j.dsr.2011.11.007

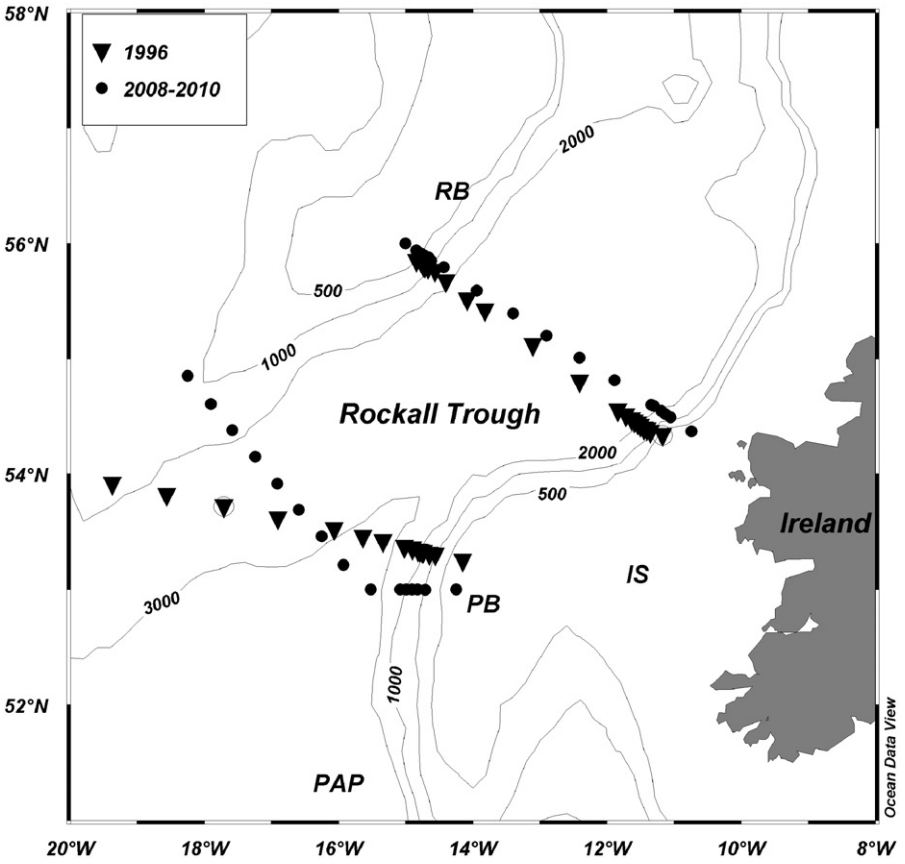

Fig. 1. Bathymetry of the Rockall Trough, with transect positions of the 2008, 2009 and 2010 surveys (dots) overlaying the 1996 WOCE AR24 survey (triangles). Labelled bathymetry: IS—Irish Shelf; PB—Porcupine Bank; RB—Rockall Bank; PAP—Porcupine Abyssal Plain.

is the oxygen saturation value minus the oxygen measured (Broecker and Peng, 1982). Positive AOU values are indicative of respiration in the water column, or in surface waters it could indicate upwelling or convection, with subsequent mixing of deeper oxygen-depleted water with surface water saturated with oxygen. Natural sources of nutrients to the open ocean are from atmospheric deposition, nitrogen fixation, land erosion and volcanic activity, while anthropogenic inputs from agriculture, industry and fossil fuel consumption may also reach the open ocean via rivers, rainfall and the atmosphere. Biological drawdown of nutrients through photosynthesis, remineralisation of organic material and physical mixing, largely determine the vertical profile of nutrients in the ocean (Williams and Follows, 2003). Due to the ageing of a water mass, it is not always possible to determine whether an increase of nutrients at a particular depth is due to remineralisation of organic matter or physical mixing with another water mass. We have therefore looked at both nutrient and preformed nutrient concentrations, to help identify the water masses present. Preformed nutrients are the sum of the total nutrients minus regenerated nutrients in a water mass, assuming that upon formation the oxygen concentration was in equilibrium with the atmosphere (Broecker and Peng, 1982). They are the nutrient concentrations initially present in seawater at the time of downwelling, before any remineralisation has occurred and are therefore characteristic of waters originating in different regions.

1.1. Water masses in the Rockall Trough

Much of the upper 1000 m in the northeast Atlantic is dominated by Eastern North Atlantic Water (ENAW), a water mass having salinities lying within ± 0.05 of a mixing line from θ (potential temperature) of 12 °C and salinity of 35.66, to θ of less than 4 °C and salinity < 34.96 (Harvey, 1982), with a small inflection point at 10 °C, salinity of 35.40. As ENAW travels north from its formation region in the Bay of Biscay (Pollard et al., 1996), it is progressively freshened by mixing with water masses moving in from the west (Ellett et al., 1986). Subarctic Intermediate Water (SAIW) is a highly stratified water mass, with temperatures between 4 and 7 °C and salinity < 34.9 in its formation region in the western boundary current of the subpolar gyre, in the Labrador Current (Harvey and Arhan, 1988). This cold, fresh water mass subducts and spreads westwards with a branch of the NAC to the southern entrance of the Rockall Trough (Arhan, 1990; Arhan et al., 1994), see Fig. 2. Ullgren and White (2010) identified SAIW in the Rockall Trough between 600 and 1000 m, with salinities of 35.1–35.2 and temperatures of 8–9 °C.

Found at a similar depth to SAIW at the southern entrance to the Rockall Trough, Mediterranean Water (MW) is a highly saline outflow from the Mediterranean Sea through the Straits of Gibraltar. Although MW has a temperature > 11.5 °C and salinity of 36.5 in the source region (Pérez et al., 1993; Tomczak and Godfrey, 1994), by the time it reaches the Rockall Trough these properties have been diluted due to lateral mixing with adjacent water masses and it is normally seen as an inflexion in the θ–S (potential temperature–salinity) plots in the Rockall Channel (Ellett and Martin, 1973). While earlier studies suggested the MW core continued through the northern end of the Rockall Channel (Reid, 1979), recent studies have found that the warm waters of the NAC set the inflow characteristics to the Nordic Seas and MW is only a dilute constituent of the inflow, but indirectly through its contribution to the interior subtropical gyre, from

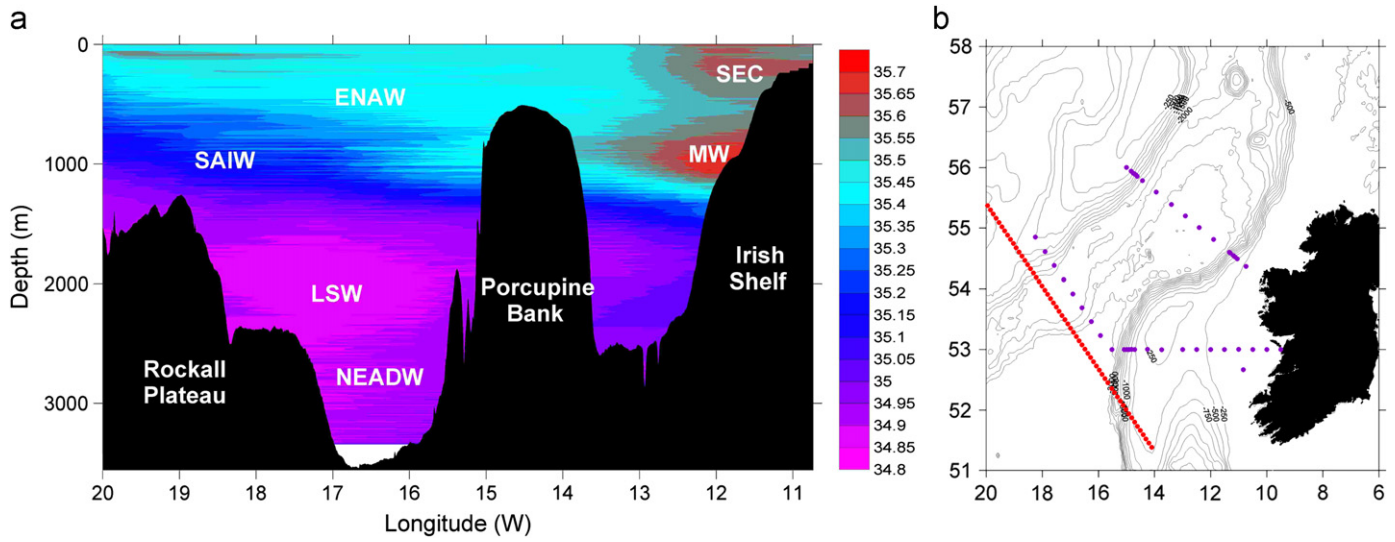

Fig. 2. Cross section of salinity along a transect extending from the Irish shelf about 52 °N across the southern Rockall Trough. Salinity data were taken from a 2010 National Seabed Survey, the red line on the overlay map outlines the transect position relative to surveys discussed in this paper. Water masses outlined in the plot; Eastern North Atlantic Water (ENAW); Shelf Edge Current (SEC); Mediterranean Water (MW); SAIW (Sub Arctic Intermediate Water); Labrador Sea Water (LSW); North East Atlantic Deep Water (NEADW).

Table 1
Hydrographic characteristics of water masses in the North Atlantic discussed in this paper, taken from the literature, (a) Cabecadas et al., 2010; (b) Castro et al., 1998; (c) Johnson et al., 2010; (d) New and Smythe-Wright, 2001; (e) Pérez et al., 1993; (f) Stoll et al., 1996; (g) Thomas, 2002; (h) Tsuchiya et al., 1992; (i) Ullgren and White, 2010. Preformed nutrients are estimated at 100% oxygen saturation using stoichiometric ratios given by Pérez et al. (1993). All chemistry parameters are in μmol kg^{-1}.

Water Mass	Depth	*S*	*T*	O_2	AOU	NO_3	Si	PO_4	NO_3°	PO_4°	Ref
ENAW	0–600	35.4–35.58	9–11	200	84	18–19	8	1.1	10.3	0.58	b, e
MW	400–1000	36.5	11.74	145–166	96–117	15–17	10–11	0.9–1	5.4	0.32	b, e
SAIW	600–1000	35.1–35.2	8–9		60	< 13		< 0.9			a, b, e, i
WTOW	600–1200	34.85–35.25	0.5–8								c
LSW	1600–1900	34.9	3.4	260–270	45–50	17–19	12.3–14.7	1–1.2	12–14	0.76–0.87	b, e, f
NEADW	> 2500	34.8–34.92	2.5	250–270	80–90	20–22	37	1.4–1.6	13–14	0.8–1	a, b, e, g
ISOW	1800–2000	34.96–35	< 3	286	46	14.8	9–10		10.2		f, h
LDW	> 2500	34.94	2.5	246	82	20.4	35.3		12.2		f
AABW	> 3000	34.7	1	< 250	90	> 23	> 40	> 1.5	26	0.94	g, d

which the NAC draws its water (McCartney and Mauritzen, 2001; New et al., 2001).

Wyville-Thomson Overflow Water (WTOW), a southward-flowing overflow water from the Nordic Seas, is found at intermediate depths in the northern Rockall Channel and is also seen as an inflexion towards higher salinity in θ–S diagrams (Sherwin et al., 2008). It has only recently been placed as an intermediate water mass found as far south as 55 °N in the Trough, with θ–S properties along a mixing line of 0.5–8 °C and 34.85–35.25 (Johnson et al., 2010).

Labrador Sea Water (LSW) is formed from deep winter convection in the Labrador Basin and θ–S properties of LSW can vary between years depending on local climate factors that influence the convection regimes in the Labrador Sea. Yashayaev (2007) reported potential temperatures (θ) < 2.8 °C and salinities < 34.84 in LSW during an extremely cold and fresh phase in 1994, while θ was 2.9–3.1 °C and salinity 34.88–34.90 during a warmer, saltier state in 2005. It has been clearly identified in the Rockall Trough between 1600 and 1900 m (Ellett et al., 1986; Ellett and Martin, 1973). LSW is a relatively young water mass in the Trough, and has a transit time from the Labrador Sea to Rockall Trough of ca. 10 years (Yashayaev et al., 2007).

Iceland-Scotland Overflow Water (ISOW) has salinity values > 34.98 and potential temperature < 3 °C (Harvey, 1982). It is formed in the northern Iceland Basin and characteristics of this water mass are significantly altered due to diapycnal mixing when it travels south (van Aken, 2000a). In the Rockall Trough, it is strongly modified by mixing with ENAW, and creates a deep salinity maximum about 1800–2000 m found on the western side of the Rockall Channel (Castro et al., 1998).

Northeast Atlantic Deep Water (NEADW) is seen as a salinity maximum between the fresh LSW above it and LDW (Lower Deep Water) and/or AABW (Antarctic Bottom Water) below it (Ellett and Martin, 1973). The upper limit of NEADW has a temperature and salinity of 2.5 °C and 34.94 respectively, and a lower limit of 2.03 °C and 34.89, and represents one of the largest water mass volumes of the European Basin (Worthington et al., 1970). AABW is formed by deep convection associated with the freezing of sea ice in the Weddell and Ross Seas, and after mixing with the waters of the Circumpolar Current, it has a potential temperature of ~0.3 °C and salinity of 34.7 (Tomczak and Godfrey, 1994). AABW flows north, along the eastern side of the northeast Atlantic, and mixes up into NEADW, which then circulates into the Rockall Trough (Ellett and Martin, 1973; McCartney, 1992; New and Smythe-Wright, 2001; Tsuchiya et al., 1992).

Fig. 2 illustrates the position of the major water masses across the region extending from the Irish shelf about 52 °N across the Rockall Trough. Salinity data was taken from a National Seabed Survey in 2010. Table 1 summarizes the hydrographic characteristics of the above water masses in the northeast Atlantic.

2. Method

The main data sets presented here were collected during three surveys to the Rockall Trough (Fig. 3); two on the *RV Celtic Explorer* in February 2009 (CE0903) and 2010 (CE10002), and one on the *RV Thalassa* in February 2008 (TH08). Data from a similar survey, WOCE-AR24 completed in November/December 1996 has also been examined to identify any differences over a longer timescale. WOCE AR24 data was extracted from the CDIAC database (https://cdiac.ornl.gov/oceans/).

2.1. CTD data

On all recent cruises a Seabird SBE 9/11 CTD rosette system was employed. Temperature calibration for the Seabird CTD was carried out using an independent Seabird SBE-35 electronic digital thermometer while salinity was calibrated by analysing discrete water samples on a Guildline Portasal salinometer (Model 8410A). An SB43 oxygen sensor was deployed with the CTD, which was calibrated annually with the manufacturer.

2.2. Sample collection

Seawater samples were collected in Niskin bottles for the analysis of dissolved oxygen (O_2), dissolved nutrients (silicate (Si), total oxidised nitrogen (TOxN), phosphate (PO_4), nitrite (NO_2^-)) and salinity. The natural level of NO_2^- in seawater is very low, since in the presence of oxygen, NO_2^- should be oxidised to NO_3. (Grasshoff et al., 1983). NO_2^- results were generally below the limit of quantification ($<0.04\ \mu mol\ kg^{-1}$), therefore TOxN and nitrate (NO_3) can be considered equivalent. NO_2 data is therefore not included here. O_2 samples, collected in 2010 only, were analysed on board ship following the Winkler method (Winkler, 1988), modified with potentiometric endpoint determination. A Metrohm 848 Titrino Plus was used for O_2 analysis, with a Metrohm combined Pt electrode; precision is estimated to be $\pm 1.45\ \mu mol\ kg^{-1}$. There was a constant offset of $\sim 15\ \mu mol\ kg^{-1}$ between the oxygen sensor data and Winkler results in 2010; sensor data was corrected for this offset. See supplementary information.

The apparent oxygen utilization (AOU) (Broecker and Peng, 1982) was calculated as

$$AOU = O_2 sat - O_2 observed \quad (1)$$

and assumes that seawater downwelling from the surface is 100% saturated with respect to the atmosphere. Discrete oxygen samples were only collected in 2010, and the resulting AOU in the surface mixed layer was $7.67\ \mu mol\ kg^{-1}$ (i.e., 97% saturated). While 2008 oxygen sensor data gave similar values (98% saturated in the surface mixed layer), there appeared to be an offset of $\sim 28\ \mu mol\ kg^{-1}$ in the 2009 oxygen sensor data (see supplementary information). While other studies have adopted an air saturation of 98% as a best estimate for late winter in the northeast Atlantic (Koeve, 2001; Körtzinger et al., 2001), the 2009 oxygen sensor data was re-calculated based on the assumption that the surface mixed layer is approximately 97% saturated each winter, since the Winkler data from 1996 and 2010, which are more accurate than sensor data, resulted in 97% saturation in the surface mixed layer in the Trough.

For the above calculations of AOU, and also for preformed nutrients in the following section, it is assumed that upon formation a water mass is 100% saturated with oxygen with respect to the atmosphere. There may be times however, when this assumption is questionable, particularly with any water mass formed by convection. Surface cooling results in the rapid sinking of surface water in a convection cell, which is replaced by water that rises to the surface on the perimeter of the cell, mixing partially with the water in the core. The resulting water mass may therefore be undersaturated with respect to the atmosphere and its oxygen concentration is determined by the oxygen

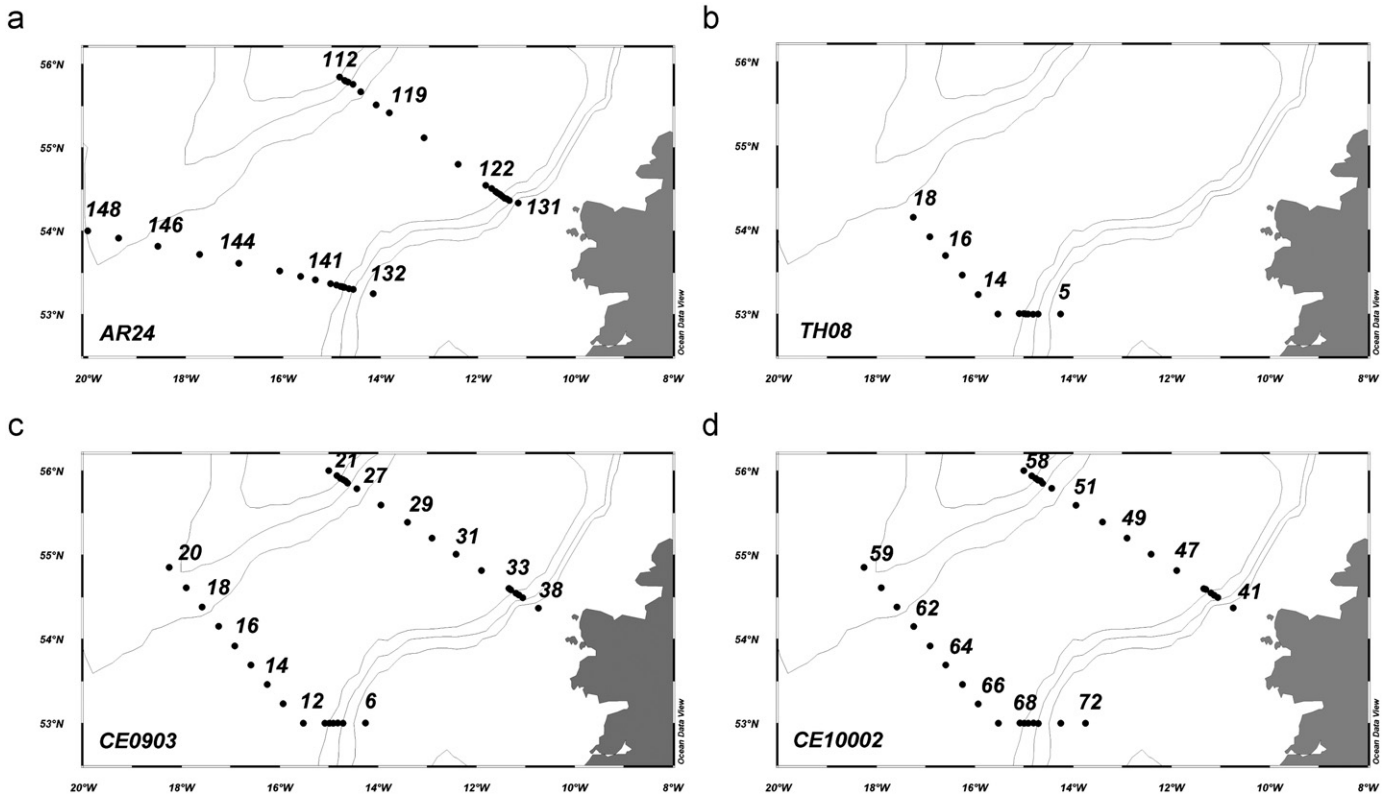

Fig. 3. Cruise track and station numbers of WOCE AR24 (Nov/Dec 1996), TH08 (Feb 2008), CE0903 (Feb 2009) and CE10002 (Feb 2010).

Table 2a
Chemical properties of regional water masses after entering the Rockall Trough in 1996 (AR24), 2008 (TH08), 2009 (CE0903) and 2010 (CE10002) for (a) the upper and intermediate water masses, and (b) the deeper masses. Standard deviations are in brackets beside average values. SROCK=southern transect of the Rockall Trough; NROCK=northern transect of the Rockall Trough; SW=Surface Water; SAIW=Subarctic Intermediate Water; MW=Mediterranean Water; WTOW=Wyville-Thomson Overflow Water; LSW=Labrador Sea Water; NEADW=North East Atlantic Deep Water; AABW=Antarctic Bottom Water; S=salinity; T=temperature (°C); DO=dissolved oxygen (μmol kg^{-1}); NO_3=nitrate; Si=silicate; PO_4=phosphate; NO_3°=preformed nitrate; PO_4°=preformed phosphate; *n*=number of chemistry samples. All nutrients are in μmol kg^{-1}.

Water bodies	Section	Year	Depth	Stations	S	T	DO	% sat	AOU	NO_3	Si	PO_4	NO_3°	PO_4°	*n*
SW	SROCK	2010	0–300	All	35.47 (0.1)	10.78 (0.3)	261 (4.2)		7.67 (4)	10.1 (0.5)	3.37 (0.3)	0.60 (0.1)			38
		2009	0–300	7–14	35.53 (0.01)	11.17 (0.1)	259 (0.5)		7.79 (0.6)	10 (0.4)	3.45 (0.1)	0.54 (0.04)			20
				15–20	35.44 (0.02)	10.52 (0.2)	259 (1.3)		11.3 (1.3)	11.4 (1)	4.38 (0.9)	0.66 (0.1)			13
		2008	0–300	6–15	35.52 (0.02)	11.35 (0.1)	261 (2.2)		5.3 (2.4)	9.67 (0.9)	3.25 (0.5)	0.57 (0.1)			38
				16–18	35.41 (0.02)	10.57 (0.1)	262 (1.5)		7.9 (1.5)	11 (0.4)	4.06 (0.1)	0.67 (0.03)			13
		1996	0–150	All	35.45 (0.1)	11.26 (0.2)	259 (1.7)		6.99 (1.4)	7.1 (0.4)	2.03 (0.3)	0.52 (0.02)			52
SW	NROCK	2010	0–300	All	35.46 (0.03)	10.39 (0.2)	261 (3.5)		10.5 (3.7)	10.7 (0.6)	3.44 (0.4)	0.65 (0.1)			45
		2009	0–300	All	35.47 (0.02)	10.45 (0.3)	261 (1.7)		9.5 (1.8)	11.2 (0.8)	4.18 (0.9)	0.62 (0.1)			33
		1996	0–150	All	35.4 (0.1)	10.96 (0.3)	260 (2.5)		8.48 (0.9)	7.87 (0.3)	2.82 (0.2)	0.55 (0.02)			77
ENAW	SROCK	2010	0–700	67–73	35.08–35.53	7.53–11.06	202–269		2.32–82.2	9.37–20.6	3.07–10.1	0.45–1.21			59
				59–66	34.98–35.52	6.41–11.01									
		2009	0–700	7–14	35.23–35.55	8.94–11.34	209–262		6.52–75.4	9.41–19.1	3.29–10.3	0.47–1.23			44
				15–20	35.10–35.47	6.93–10.91									
		2008	0–700	6–15	35.19–35.55	8.89–11.5	202–264		2.1–85.6	8.89–21.1	2.98–10.9	0.5–1.24			71
				16–18	35.04–35.42	6.93–10.73									
		1996	0–700	132–143	35.1–35.55	8.9–11.58	206–263		5.58–82.9	6.23–18.72	1.56–11.43	0.48–1.24			163
				144–148	35.08–35.55	6.37–11.84									
ENAW	NROCK	2010	0–700	All	35.21–35.5	7.58–10.68	210–269		1.47–76.2	9.65–18.0	2.61–6.71	0.55–0.96			64
		2009	0–700	All	35.19–35.5	8.18–10.92	214–266		5.76–70.3	7.73–18.6	3.54–9.35	0.48–1.1			48
		1996	0–700	All	35.25–35.55	8.44–11.27	224–267		7.52–53.0	7.42–14.8	2.44–7.91	0.52–0.98			210
SAIW	SROCK	2010	700–1000	64–66	35.08 (0.1)	5.93 (0.8)	248 (2.2)	100%	57.3	19.0 (0.9)	10.5 (0.2)	1.12 (0.03)	13.2	0.77	6
								85%	11.5 (1.5)				17.7 (1)	1.07 (0.05)	
		2009	700–1000	17–20	35.12 (0.1)	6.05 (0.6)	250 (3.1)	100%	57.1	17.3 (0.3)	10.7 (0.4)	1.12 (0.1)	11.6	0.77	2
								85%	11.1 (2)				16.2 (0.05)	1.05 (0.1)	
		2008	800–1000	16–18	35.11 (0.04)	5.79 (0.5)	243 (8.9)	100%	62.5	18.1 (0.3)	10.8 (0.1)	1.05 (0.2)	11.9	0.67	3
								85%	16.6 (6.1)				16.5 (0.9)	0.95 (0.2)	
		1996	800–1000	144–148	35.08 (0.04)	5.73 (0.5)	234 (8.1)	100%	70.1	18.5 (0.1)	11.5 (0.1)	1.22 (0.01)	11.5	0.80	10
								85%	24.5 (5.2)				16.1 (0.4)	1.07 (0.03)	
MW	SROCK	2010	700–800	70–71	35.36 (0.03)	9.18 (0.3)	203 (2.9)		75.6 (5.4)	18.3 (0.4)	8.6 (0.4)	1.09 (0.1)	10.7 (0.8)	0.63 (0.06)	2
		2009	1000	9–13	35.32 (0.04)	9.28 (0.4)	211 (1.1)		76.8 (1)	17.3 (1.1)	9.6 (1.7)	1.10 (0.1)	9.59 (1.2)	0.63 (0.1)	4
		2008	700–800	7–9	35.35 (0.1)	9.26 (0.5)	200 (4.5)		76.2 (5.8)	17.9 (0.2)	8.5 (0.7)	1.05 (0.03)	10.3 (0.3)	0.65 (0.01)	2
		1996	700–900	134–140	35.38 (0.03)	9.12 (0.2)	205 (3.9)		74.6 (4.3)	16.9 (0.4)	9.3 (0.5)	1.09 (0.02)	9.39 (0.1)	0.63 (0.01)	14
WTOW	NROCK	2010	800–1100	50–51	35.03–35.26	5.02–7.81	237		66.6	17.9	10.7	1.12	11.4	0.71	1
		2009	800–1100	27–28	35.12–35.35	5.99–9.48	214		73.7	17.4	9.8	0.99	10.1	0.54	1

Table 2b
Chemical properties of regional water masses after entering the Rockall Trough in 1996 (AR24), 2008 (TH08), 2009 (CE0903) and 2010 (CE10002) for (a) the upper and intermediate water masses, and (b) the deeper masses. Standard deviations are in brackets beside average values. SROCK=southern transect of the Rockall Trough; NROCK=northern transect of the Rockall Trough; SW=Surface Water; SAIW=Subarctic Intermediate Water; MW=Mediterranean Water; WTOW=Wyville-Thomson Overflow Water; LSW=Labrador Sea Water; NEADW=North East Atlantic Deep Water; AABW=Antarctic Bottom Water; S=salinity; T=temperature (°C); DO=dissolved oxygen (μmol kg^{-1}); NO_3=nitrate; Si=silicate; PO_4=phosphate; NO_3°=preformed nitrate; PO_4°=preformed phosphate; *n*=number of chemistry samples. All nutrients are in μmol kg^{-1}.

Water bodies	Section	Year	Depth	Stations	S	T	DO	% sat	AOU	NO_3	Si	PO_4	NO_3°	PO_4°	*n*
LSW	SROCK	2010	1500–2000	All	34.92 (0.01)	3.67 (0.2)	273 (4)	100 %	44	18.0 (0.7)	12.3 (1.1)	1.09 (0.03)	13.3	0.81	9
								90%	12.2 (2.2)				16.5 (0.3)	1.01 (0.02)	
		2009	1500–2000	All	34.91 (0.01)	3.65 (0.2)	271 (4.9)	100 %	46.4	17.4 (1)	11.5 (1.1)	1.11 (0.1)	12.8	0.82	10
								90%	14.7 (2.3)				16.0 (1)	1.02 (0.1)	
		2008	1500–2000	All	34.92 (0.02)	3.7 (0.26)	271 (3.4)	100 %	46.9	17.8 (0.6)	12.2 (1.5)	1.01 (0.1)	13.1	0.73	12
								90%	15.1 (1.7)				16.3 (0.7)	0.92 (0.1)	
		1996	1500–2000	All	34.92 (0.02)	3.69 (0.3)	272 (4.9)	100 %	45.5	17.4 (0.2)	12 (0.7)	1.16 (0.01)	12.8	0.88	34
								90%	13.8 (3.5)				16.0 (0.2)	1.08 (0.01)	
LSW	NROCK	2010	1500–2000	All	34.93 (0.01)	3.78 (0.3)	268 (2.7)	100 %	47.6	17.9 (0.2)	11.9 (1.6)	1.13 (1.64)	13.2–	0.86–	8
								90%	16 (2.7)				16.4 (0.2)	1.04 (0.02)	
		2009	1500–2000	All	34.93 (0.02)	3.92 (0.3)	265 (7)	100 %	49.3	17.4 (0.4)	11.2 (1)	1.05 (0.1)	12.6–	0.75–	7
								90%	17.9 (3.8)				15.7 (0.6)	0.94 (0.1)	
		1996	1500–2000	All	34.94 (0.02)	3.88 (0.3)	267 (3.4)	100 %	49.1–	17.3 (0.4)	13.04 (1.2)	1.16 (0.03)	12.4–	0.86	40
								90%	17.5 (2.9)				15.6 (0.3)	1.05 (0.02)	
NEADW	SROCK	2010	2500–2600	All	34.93 (0)	3.03 (0.1)	273 (4)		50.1 (3.5)	18.3 (0.6)	18.2 (0.4)	1.16 (0.03)	13.9	0.81–0.87	3
-upper		2009	2500–2600	All	34.93 (0)	3.03 (0.1)	267 (3.3)		55 (4)	18.6	15.5–19.1	1.20 (0.1)	12.8	0.86 (0.03)	2
		2008	2500–2600	All	34.93 (0)	3 (0.1)	250–270		51.8–73.5	18–21.7	16.4–29	1.02–1.31	11.8–14.4	0.66–0.86	6
		1996	2500–2600	All	34.95 (0)	3.12 (0.1)	262 (2.6)		60.7 (3)	18.5 (0.2)	22.4 (1.2)	1.26 (0.02)	12.4 (0.2)	0.89 (0.01)	6
NEADW	NROCK	2010	2500–2600	All	34.93 (0)	2.96 (0.1)	249–267		54.7–75.4	17.8–21.5	18.5–32.8	1.16–1.35	12.3–13.9	0.82–0.88	1
-upper		2009	2500–2600	All	34.92 (0)	3.04 (0.1)	255–267		54.1–69.5	17.8–18.9	17.8–27.9	1.06–1.13	12.0–12.4	0.7 - 0.93	2
		1996	2500–2600	All	34.94 (0)	3.02 (0.1)	248–261		60.3–76.5	18.2–20.3	21.2–33.5	1.26–1.39	12.1–12.7	0.86–0.92	6
NEADW	SROCK	2010	2900–3000	All	34.92 (0.01)	2.56 (0.1)	260		72.1		30.9	1.29	18.5	0.85	1
-lower		2009	2900–3000	All	34.92 (0.01)	2.67 (0.1)	252 (2)		73.3 (2.5)	20.8 (0.8)	30.9 (2.5)	1.31 (0.1)	13.5 (0.5)	0.86 (0.1)	2
		2008	2900–3000	All	34.92 (0.01)	2.65 (0.2)	246 (2.6)		79.8 (3.3)	21 (0.04)	34 (2)	1.07 (0.01)	13.0 (0.4)	0.58 (0.01)	3
		1996	2900–3000	All	34.94 (0)	2.76 (0.1)	247 (3.4)		78.6 (4.4)	20.8 (0.6)	31.9–40	1.43 (0.1)	12.9 (0.2)	0.94 (0.02)	4
NEADW	NROCK	2010	>2800	All	34.92 (0)	2.68 (0.1)	250 (2.1)		75.1 (2.1)	20.8 (0.2)	33.3 (1.2)	1.38 (0.03)	13.3 (0)	0.92 (0.04)	2
-lower		2009	>2800	All	34.92 (0)	2.71 (0.04)	250 (2)		74.8 (2.3)	19.8 (0.5)	32.7 (0.5)	1.33 (0.08)	12.3 (0.7)	0.88 (0.1)	2
		1996	>2800	All	34.94 (0)	2.77 (0.1)	247 (1.2)		78 (1.4)	20.5 (0.2)	34.8 (1.3)	1.4 (0.02)	12.7 (0.1)	0.92 (0.01)	6
AABW	SROCK	2010	>2990	65–67	34.92 (0.01)	2.55 (0.1)	243 (0.7)		84.2 (0.8)	22 (0.2)	41.3 (0.5)	1.46 (0.02)	13.7	0.93	3
		2009	>2990	12	34.91 (0.01)	2.51 (0.03)	245		82.1	21.6	40.5	1.43	13.4	0.93	1
		2008	>2990	15	34.91 (0.01)	2.52 (0.1)	237		90.4	22.7	41.7	1.25	13.6	0.70	1
		1996	>3000	142–143	34.93 (0.01)	2.6 (0.1)	241 (0.1)		85.9 (0.1)	22 (0.1)	42 (0.4)	1.51 (0.01)	13.4 (0.1)	0.98 (0.01)	2

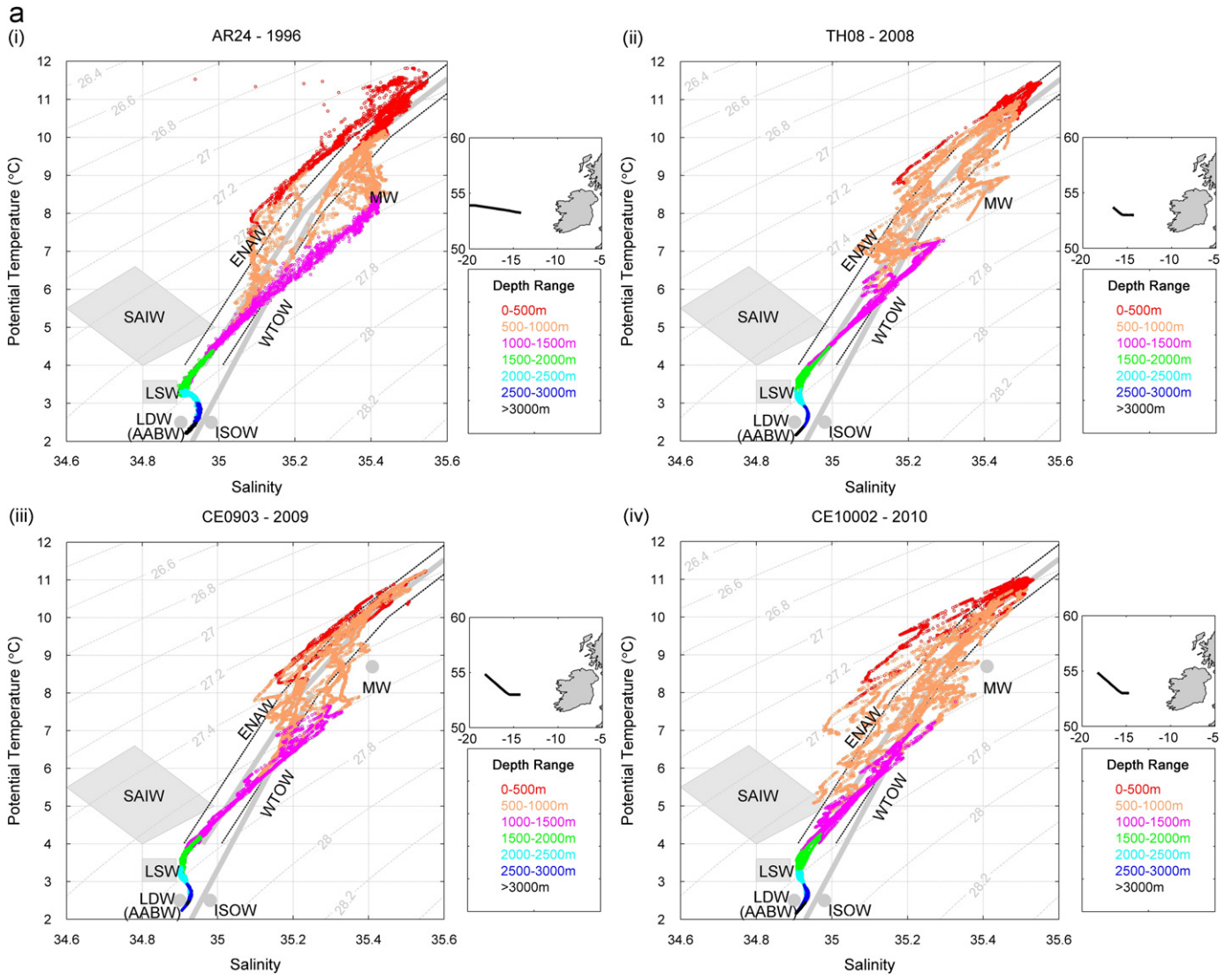

Fig. 4. (a) θ–S plots with density contours, using CTD data of the southern transect from (i) AR24, (ii) TH08, (iii) CE0903 and (iv) CE10002. A subplot outlining the transect position is beside each θ–S plot. Water mass properties were taken from the literature: ENAW, MW, LSW and AABW (Harvey, 1982); SAIW (Bubnov, 1968; Harvey and Arhan, 1988); WTOW (Johnson et al., 2010); LDW (Holliday et al., 2000); ISOW (Harvey, 1982; van Aken and Becker, 1996). Note the temperature and salinity of MW is much higher in the source region, properties plotted here are typical of MW in the eastern North Atlantic. (b) θ–S plots of the northern transect from (i) AR24, (ii) CE0903 and (iii) CE10002. References of water masses described in Fig. 4(a).

content of the sinking water, which is saturated in oxygen, and by the oxygen content of the rising water, which mixes with it (Tomczak, 1999). This is particularly the case for LSW, where saturation levels between 60% and 100% have been reported in the Labrador Sea, with significant horizontal and vertical variability (Azetsu-Scott et al., 2005; Wallace and Lazier, 1988). Therefore, both AOU and preformed nutrients have been calculated for a range of saturation states between 60 and 100% for this water mass. On the other hand, the saturation state of a subducted water mass, e.g. SAIW, is generally saturated with oxygen due to the slow downward motion of the surface water (Tomczak, 1999). To ensure this is true for SAIW, AOU and preformed nutrients were therefore also calculated for a range of initial saturation levels.

Samples for dissolved nutrients were filtered through acid-cleaned 0.45 μM polycarbonate filters and filtration units, and frozen on board in 50 ml falcon tubes. The nutrients were analysed with a Skalar San^{++} continuous flow analyser at the Marine Institute by standard colorimetric methods (Skalar methods M461-031e for TOxN, M467-033 for NO_2, M503-010wlr for PO_4 and M563-051 for Si). The Marine Institute routinely participates in QUASIMEME proficiency testing scheme exercises for nutrients and salinity in the marine environment. Results from 7 QUASIMEME rounds (42 samples) between July 2008 and May 2011 gave an average z-score of ≤ 0.5 for all parameters, putting confidence in the nutrient and salinity data. It is very clear from Fig. 6b that the TH08 (2008) PO_4 is lower from below 1000 m to the deepest part of the Trough. This has not been explained but all the CRMs and calibration curves were checked, and there does not appear to be a problem with the analysis.

WOCE AR24 O_2 samples were also determined with a modified Winkler technique using a Metrohm Model 665 Dosimat Buret and PC controller. Aliquots of the prepared sample were titrated similar to Strickland and Parsons (1972) and the endpoint was determined amperometrically using a dual plate electrode. Nutrient samples were collected in acid-cleaned HDPE bottles, and were refrigerated and analysed on an ODF-modified 4-channel Technicon Auto Analyser II within 4 h of sampling.

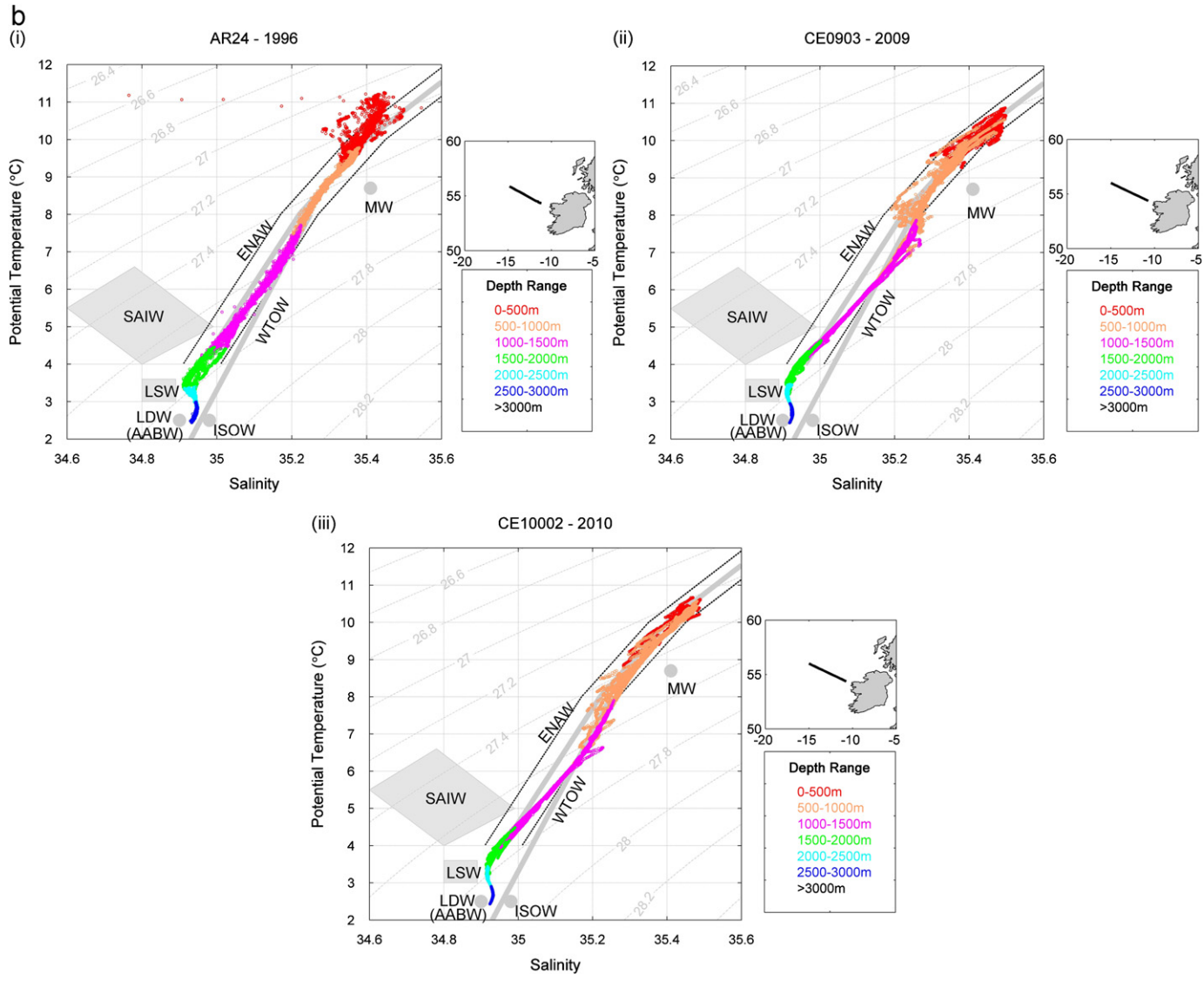

Fig. 4. (*continued*)

Preformed nutrients are calculated by combining O_2 and NO_3 or O_2 and PO_4 in such a way that respiration can be cancelled;

$$NO_3^\circ = NO_3 - AOU/a \quad (2)$$

$$PO_4^\circ = PO_4 - AOU/b \quad (3)$$

where a and b are equivalence factors between moles of oxygen consumed and nitrate/phosphate released by oxidation of organic material (Broecker and Peng, 1982). Here we have used stoichiometric ratios of $a=10$ and $b=163$, calculated for the northeast Atlantic and European margins by Pérez et al. (1993). There is no accepted stoichiometric ratio for silica with oxygen because the dissolution of biogenic silica in diatom frustules occurs differently than remineralisation of organic material (Pérez et al., 1993). Fig. 7e clearly illustrates the conservative nature of preformed nutrients with salinity, with a straight mixing line between the relatively low-nutrient ENAW, and a mixture of LSW, NEADW and AABW. While PO_4° is not shown here, the profile is very similar to that of NO_3°. This supports the idea that the distribution of preformed nutrients is largely determined by physical mixing and the water masses present.

The innovative aspect of this paper is Table 2, outlining the chemical characteristics of regional water masses after entering the Rockall Trough. Water masses were first identified using temperature and salinity data, then the average of the chemical parameters within each water mass were calculated to produce the table of results (Table 2).

3. Results

In order to identify the different water masses present in the Rockall Trough during the winter months of 1996, 2008, 2009 and 2010, we first examine and compare the θ–S (potential temperature-salinity) profiles of the southern (Fig. 4a) and northern (Fig. 4b) transects of the Trough. We then combine the nutrient and oxygen results with the physical data to determine the chemical make up of each of the water masses present, and note the significant differences, if any, between each year.

3.1. Physics

In the upper 1000 m, there is a clear signal of the warm and salty ENAW for all years, across both transects. There is much more variability in water properties in the upper 1000 m of the southern transects (Fig. 4a) relative to the northern transects

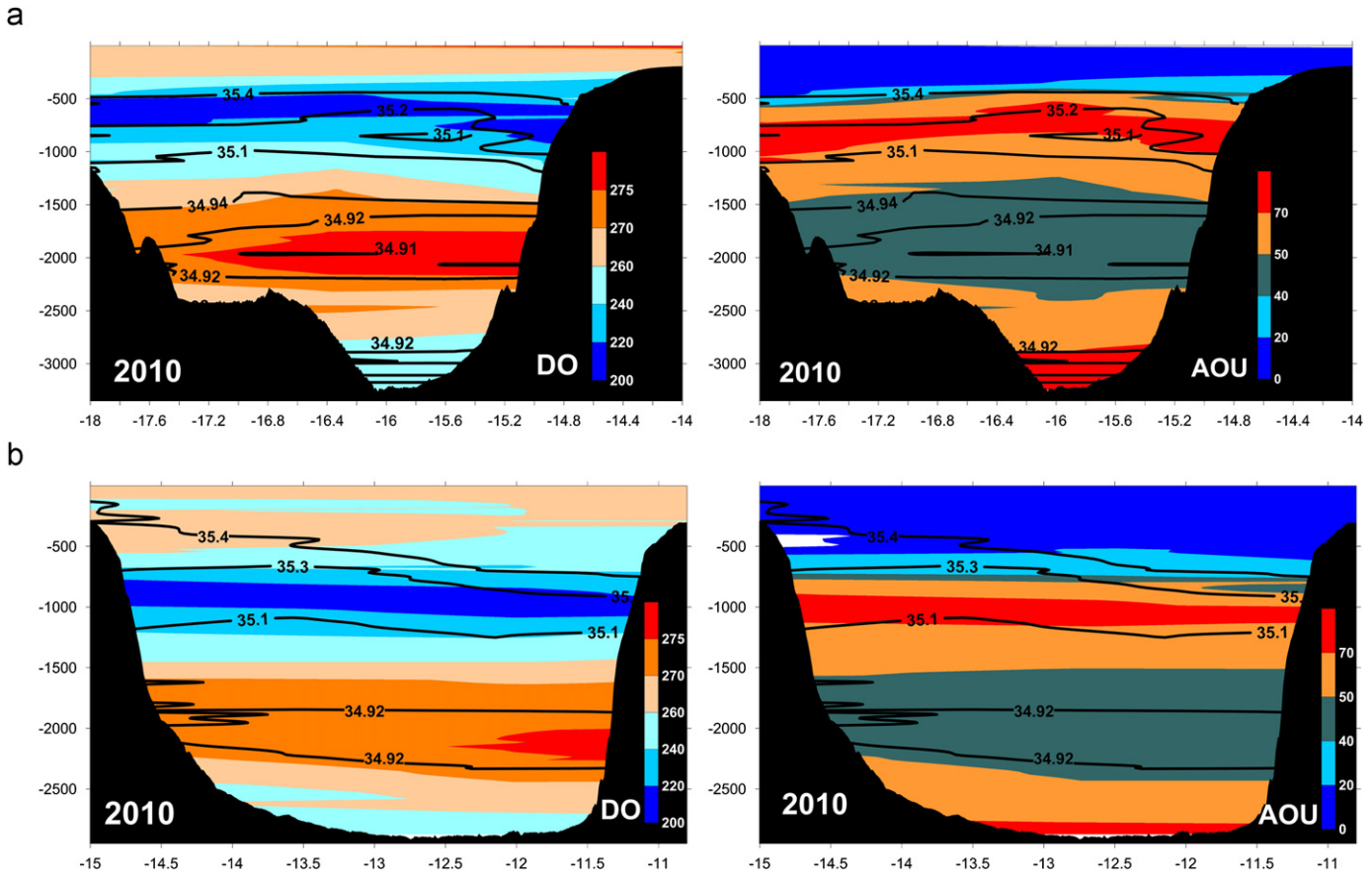

Fig. 5. 2010 section plots of dissolved oxygen (DO) and apparent oxygen utilisation (AOU), both in μmol kg^{-1}, for (a) southern Rockall transect and (b) northern Rockall transect (note plots are from sensor data that have been corrected using Winkler results).

(Fig. 4b). Between 500 and 1000 m in the southern transects, on the eastern side of the section the θ–S tend towards MW, while on the western side of the Trough, tend towards SAIW. The SAIW is most prominent in 2010, see Fig. 4a (iv). MW and SAIW signatures are not present in the northern transects, where properties in the upper 1000 m appear more uniform (Fig. 4b). There is a slight inflexion towards higher salinity in the θ–S profile in the northern transect of 2009 and 2010 close to the WTOW mixing line about 1000 m (Fig. 4b(ii)). While the salinity inflexion falls slightly above the WTOW line as described by Johnson et al. (2010), that line is based on measurements along a transect north of 57°N in the Trough so the salinity may have increased due to mixing with the more saline ENAW. There is no WTOW inflexion apparent in the 1996 data (Fig. 4b(i)), with a straight mixing line between ENAW and LSW. Below these intermediate water masses, θ–S profiles join together outlining a clear LSW signal in both transects. LSW has been observed to freshen in this region between 2006 and 2009 with a return to higher salinities observed in 2010 (Nolan, in preparation). LDW or AABW are found in the deepest parts of the Trough.

3.2. Oxygen

The average oxygen concentration in the surface mixed layer (~300 m) across both transects in 2010 is 261 μmol kg^{-1}, with AOU values close to 8 μmol kg^{-1}, i.e. surface waters are 97% saturated (Fig. 5). The surface mixed layer of both transects in 1996 was similarly 97% saturated, also calculated using O_2 Winkler data. Below the winter mixed layer, oxygen concentrations decrease rapidly coinciding with a large increase in AOU. This low oxygen and high AOU zone closely mirrors the base of the winter mixed layer as seen in the temperature and salinity contours, and is seen slightly deeper in the northern transect (Fig. 5). Although this low oxygen zone extends across the Trough, concentrations are lowest between 700 and 1000 m along the continental shelf of the southern transect, for example in 2010 oxygen values average 203 μmol kg^{-1} between 700 and 800 m (AOU 76 μmol kg^{-1}, 73% saturated). Between 1500 and 2000 m, the oxygen concentration markedly increases, to concentrations the same as or above surface concentrations, and AOU is approximately 40 μmol kg^{-1} (86% saturated). Below this oxygen rich layer, the dissolved oxygen gradually decreases with depth from a maximum of 277 μmol kg^{-1} at 2000 m, to less than 245 μmol kg^{-1} at 3000 m, while AOU concentrations increase to almost 85 μmol kg^{-1} in the deepest part of Trough (74% saturated). Oxygen concentrations and AOU for the northern and southern sections in 2010 are plotted in Fig. 5. Similar section profiles were also seen in the oxygen sensor data of 2008 and 2009.

3.3. Nutrients

Nutrients in the Trough are low in surface waters (SW) each year, with a sharp increase in concentrations below the winter mixed layer, coinciding with the increase in AOU (Fig. 6). The increase in Si is less pronounced that of NO_3 and PO_4. NO_3 in surface waters of AR24 (1996) is lower than recent years, and coincides with a shallower surface mixed layer (~150 m). The average NP ratio in the 1996 data is also much lower (13.7) in the surface mixed layer than the average over 2008–2010 (~17). Between 1500 and 2000 m there is a slight decrease in NO_3 and

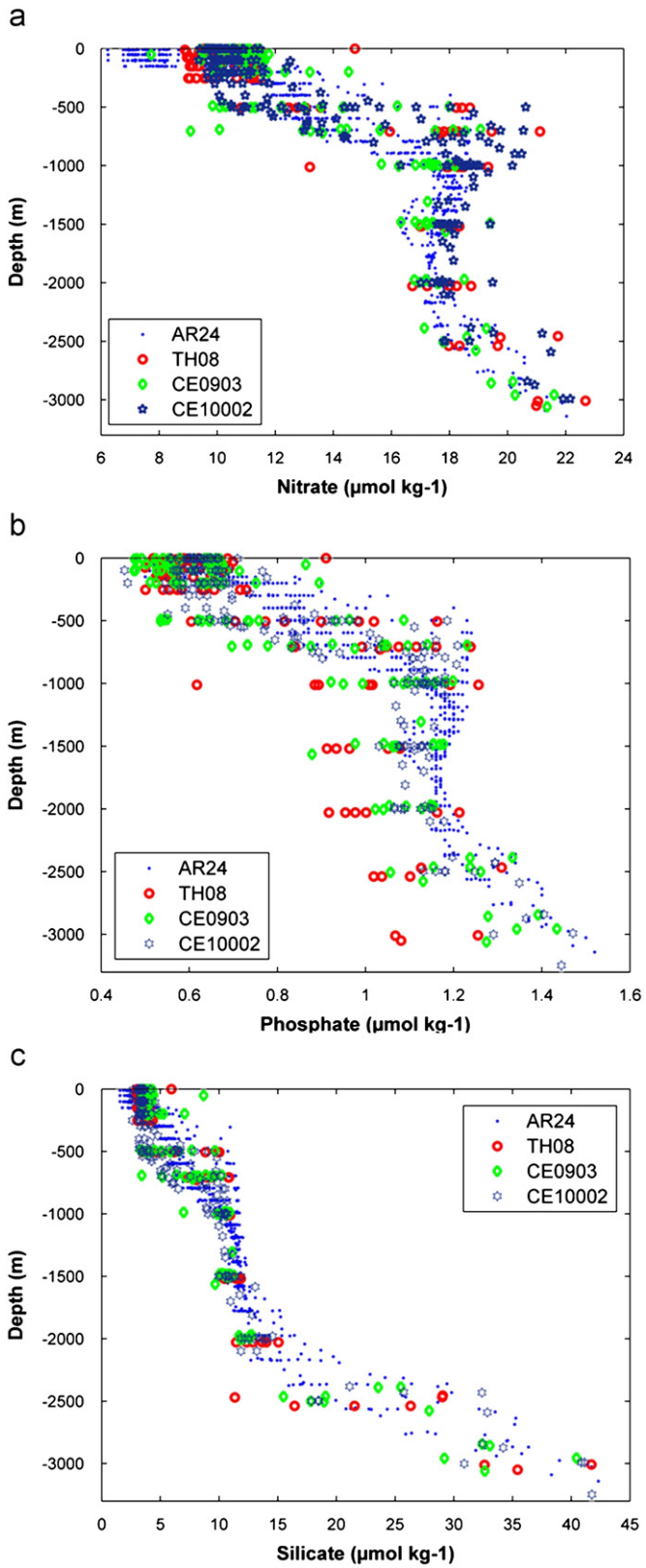

Fig. 6. Vertical profiles of (a) nitrate, (b) phosphate and (c) silicate (in μmol kg^{-1}) across the both transects in 1996 (AR24), 2008 (TH08), 2009 (CE0903) and 2010 (CE10002).

PO_4, with little change in Si concentrations. Below 2000 m there is a steady increase in all nutrients down to the deepest parts of the Trough, particularly seen in the Si profiles.

3.4. Spatial distribution

In 2008 and 2009, stations at the western end of the southern transect have lower surface (<300 m) temperatures and salinities than stations along the eastern side of the Trough (see Fig. 8, temperature not shown here). This colder, fresher surface water has higher concentrations of nutrients than the water near the shelf edge (see results in Table 2a and Fig. 7). This pattern is not as obvious in 1996 and 2010, where surface waters appear slightly more mixed across the channel.

Section plots of the southern transect of 1996, 2008 and 2009 indicate water below the winter mixed layer at the western side of the Trough has lower salinity and temperature relative to water towards the continental shelf (Fig. 8). In 2010, this cooler, fresher water is seen in the middle of the Trough (stations 64–66). This pattern is seen in all years down to below 1000 m (Fig. 8). Between 500 and 600 m, the colder, fresher water has lower oxygen, and higher nutrients and AOU than surrounding water at the same depth. Although the preformed nutrients are also relatively high in this water, the higher AOU suggests remineralisation has also contributed to the elevated nutrients seen at these stations.

Between 700 and 1000 m, the colder, fresher waters found at western-most stations in 2008 and 2009 and in the centre of the Trough in 2010, have average temperature and salinity values of 6.02 °C and 35.11 over the three years, typical of SAIW in the Rockall Trough (Ullgren and White, 2010). This is supported by the θ–S diagrams, which illustrate that some data points from the southern transect tend towards SAIW properties (Fig. 4a). SAIW is also clearly identified in 1996 with average salinity and temperature of 35.08 and 5.83 °C, at stations 144–148 at the western end of the transect. AOU and preformed nutrients were calculated for a range of initial saturation states and results indicated that the SAIW measured in the Trough in 2008, 2009 and 2010 was between 85 and 100% saturated when it was formed, while the SAIW that was measured in the Trough in 1996 was initially 80–100% saturated. Any initial saturation level below these values resulted in SAIW having positive AOU values and preformed nutrients higher than the actual nutrient concentrations measured in the Trough. This could not be the case since SAIW has been away from the surface for a number of years, therefore oxygen levels should gradually decrease. In any year, an initial saturation of 80% when SAIW was formed yields lower AOU and higher preformed nutrients than an initial saturation of 100% (see Table 2a). Therefore, in all years, regardless of the initial saturation value used between 80 and 100%, SAIW measured in the Trough has higher nutrients and calculated preformed nutrients than surrounding water, along with higher oxygen concentrations and relatively lower levels of AOU. This suggests that remineralisation does not contribute to the elevated nutrient levels, and that source water properties are higher in oxygen and nutrients than surrounding water masses (Table 2a). Fig. 7e clearly illustrates that between 500 and 1000 m, water with salinity between 35.1 and 35.2 has higher preformed nutrients than the same depth further east in the Trough.

In all years, apart from surface waters, highest salinity and temperature are found at stations closest to the shelf between 700 and 1000 m deep at the southern transect (Fig. 8). The width of this warm, saline core varies between years; in 2008 and 2010 it was confined to 1 or 2 stations on the shelf edge ($\sim$30 km from shelf edge), while in 1996 and 2009 this core spread further out to $\sim$130 km from shelf break. Lowest oxygen values measured in the Trough were also measured in this warm, saline core. Temperature, salinity and O_2 concentrations average 35.35, 9.23 °C and 204 μmol kg^{-1}, respectively, in this core over 2008, 2009 and 2010; indicative of MW in the southern Rockall Trough region.

While NO_3 and PO_4 concentrations are similar at these stations to surrounding water at that depth, preformed nutrients are lower, suggesting source water has lower nutrient concentrations. The N°:P° ratio (preformed NP ratio) is however higher here than water further west in the Trough, reaching 19 at station 70 (900 m) and 71 (720 m) in 2010, 18 at station 12 (1000 m) in 2009 and 17.5 at stations 7–9 (700 m) in 2008, suggesting source water has a high NP ratio. This high NP signal was however not measured at all depths within this water mass each year, and was not measured in the 1996 data. Si concentrations at these stations are lower than similar depths across the rest of the Trough (Table 2a). In 1996, highest salinities and temperatures were also found at the stations closest to the shelf (station 134–140) at ~900 m. Low oxygen (205 μmol kg^{-1}) and high AOU (75.6 μmol kg^{-1}) values were also measured here, along with lower preformed nutrients than stations further west in the Trough.

The top 1000 m of the northern transects in 1996, 2009 and 2010 are somewhat similar to that seen further south, however there is little east–west gradient in water properties across the Trough (Fig. 8). The decrease in oxygen and increase in nutrients also occurs slightly deeper in the water column than the southern transects, and SAIW and MW signals are absent in the northern transects each year.

θ–S diagrams of the 2009 and 2010 northern transects indicate the presence of WTOW between 800 and 1100 m at stations close to the Rockall Bank. Like MW in the southern transect, WTOW is seen as an inflexion in the θ–S diagrams (see Fig. 4b). However, oxygen is much higher in WTOW than in MW, agreeing with Johnson et al. (2010) that the salinity inflexion is not a continuation of the MW signal. In relation to the rest of the northern transect at that depth, oxygen and nutrient concentrations do not appear significantly different than surrounding water; however there are very few data points to accurately determine the chemical characteristics of this water mass in the region. There does not appear to be any clear WTOW signature in the northern transect of the 1996 AR24 survey.

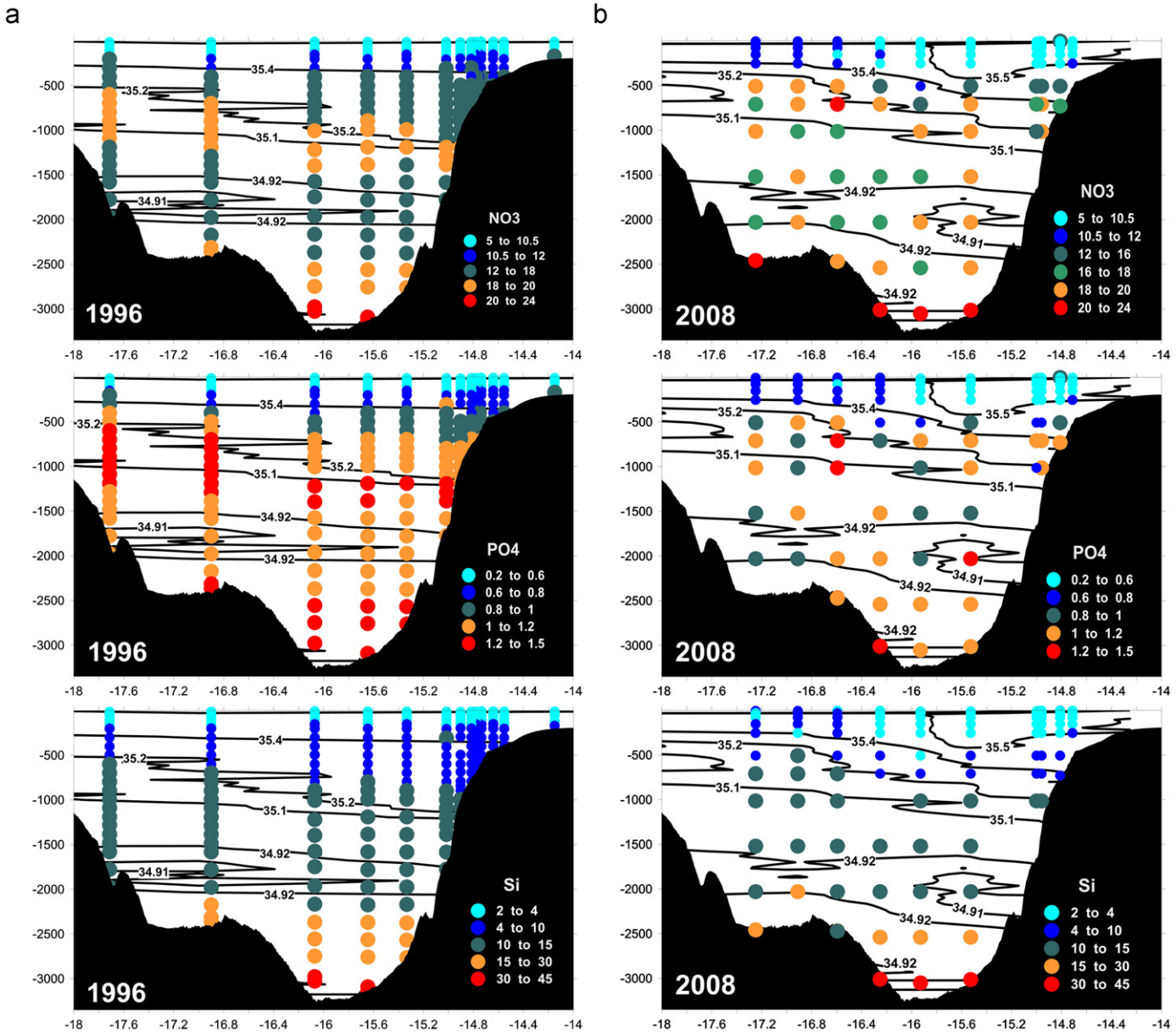

Fig. 7. Section plots of nutrient concentrations overlaying salinity contours for the southern transects of (a) 1996, (b) 2008, (c) 2009 and (d) 2010 surveys. The section plot of NO_3° with salinity contours in (e) is from 1996, however a similar profile is seen in recent years (not shown here). NO_3° is almost conservative with salinity in all surveys, with a straight mixing line between ENAW and a mixture of LSW, NEADW and AABW.

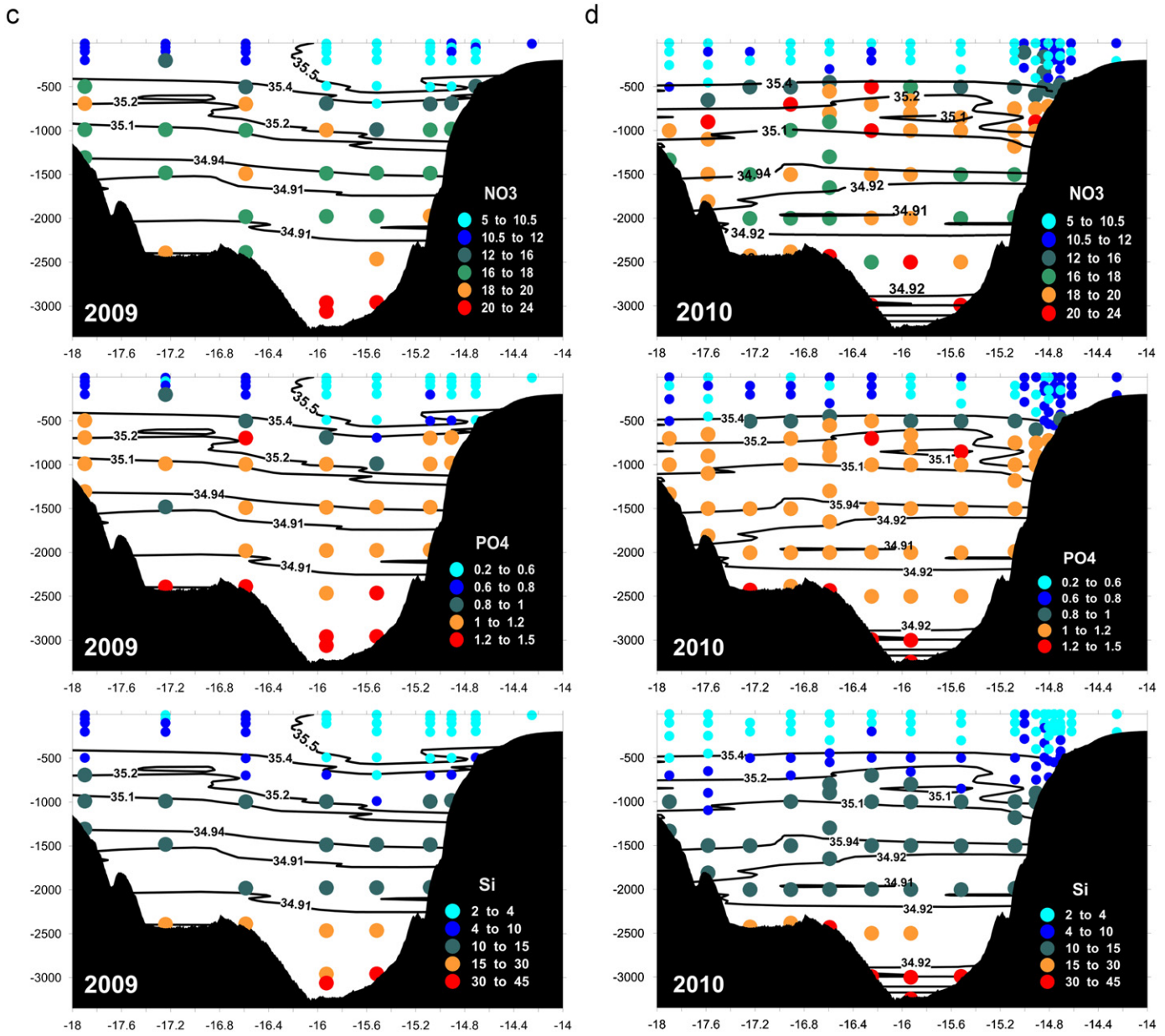

Fig. 7. (*continued*)

Unlike the water depths above it, there is no east–west gradient in temperature, salinity, oxygen or nutrients across the transects between 1500 and 2000 m deep. The average salinity, temperature and oxygen over 2008, 2009 and 2010 was 34.92, 3.72 °C and 278 μmol kg^{-1}, respectively. The low salinity and temperature, and high oxygen values measured between 1500 and 2000 m are typical of LSW properties in the Rockall Channel (Stoll et al., 1996). The temperature and salinity of this water mass is marginally higher in the northern transect in 1996, 2009 and 2010. As mentioned previously, between 60 and 100% saturation states have been reported in the Labrador Sea (Azetsu-Scott et al., 2005). AOU and preformed nutrients were therefore calculated for LSW at 60%, 70%, 80%, 85%, 90% and 100% saturation states. For all years, AOU calculated at any initial saturation less than 85%, indicated that LSW in the Rockall Trough was supersaturated with oxygen, and preformed nutrient values were higher than the actual nutrient concentrations measured. This is obviously not the case, as the water mass has been away from the surface for a number of years so we would expect oxygen concentrations to decrease gradually to due ageing. Therefore the LSW that reached the Rockall Trough in 1996, 2008, 2009 and 2010 was likely between 90 and 100% saturated when it was formed (Table 2).

Vertical nutrient profiles (Fig. 6) indicate a weak minimum for NO_3 and PO_4 in LSW, however these minima are not as clearly defined as the salinity or oxygen extremes. The NO_3° (calculated at 100% saturation) for LSW in 2009 is marginally lower than 2008 and 2010, which may be due to a difference in oxygen saturation when the water mass was formed, or may also be related to the lower salinity and lower silicate measured in LSW that year (Table 2). The PO_4 across the southern transect is lower in 2008 than in 2009/10, and this low-PO_4 signal is seen in the northern transect in 2009. AR24 Si data in the northern transect is slightly higher than recent years, coincident with a higher salinity (34.94). While NP ratios are ~16 in LSW in 2009/10, they are generally lower through the water column in 1996 data, with an average NP of 15 in LSW.

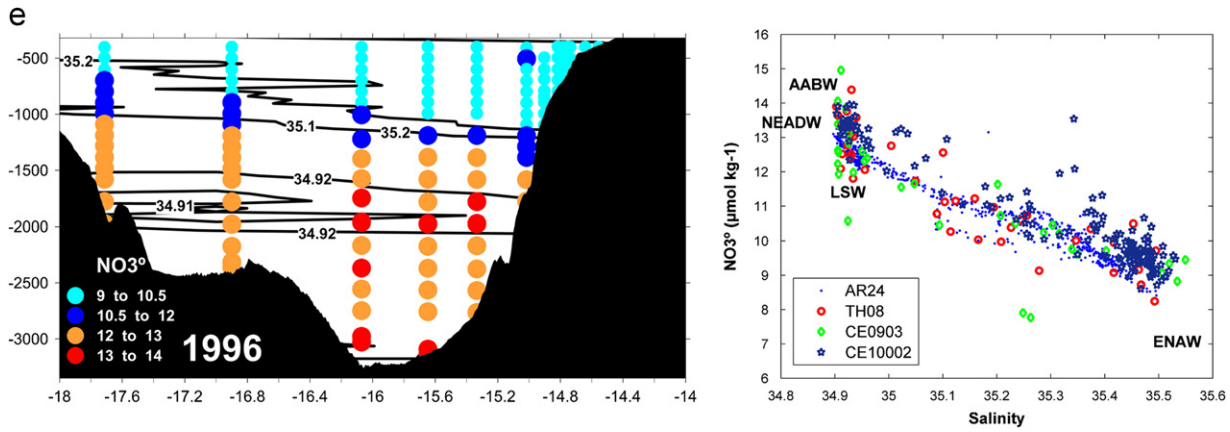

Fig. 7. (*continued*)

In the deepest waters in the Trough, there is a slight increase in salinity and decrease in temperature below LSW; typical of NEADW. The gradual increase in AOU below 2000 m (Fig. 5) suggests ageing of this water mass, as oxygen gets used up by remineralisation and dissolved inorganic nutrients are released into the water column. Nutrient concentrations consequently increase with depth, ranging from 18 to 24 µmol kg^{-1} NO_3, 17 to 42 µmol kg^{-1} Si and 1.1 to 1.4 µmol kg^{-1} PO_4 between 2500 m and 3000 m (Figs. 6 and 7). Maximum values are found at the southern transect generally below 3000 m, reaching 22 µmol kg^{-1} NO_3, 42 µmol kg^{-1} Si and 1.5 µmol kg^{-1} PO_4. Such high values are seen in all deep waters (> 3000 m) of the Trough in 1996 and 2010, on the western side in 2008 and on the eastern side in 2009 (Table 2). Lowest NP ratios were measured in the deepest part of the Trough in all years (~15).

4. Discussion

Low nutrient levels were measured in the surface mixed layer each year; surface waters of the N. Atlantic are generally depleted in nutrients during spring and summer months due to biological activity (photosynthesis), and while entrainment of deeper waters due to deep winter convection increases nutrient concentrations, levels remain lower than the rest of the water column (Fig. 6). Nutrient concentrations are lower in the surface mixed layer in 1996 relative to 2008, 2009 and 2010, particularly seen for NO_3. A first glance would suggest that lower NO_3 is due to some biological activity in surface waters of the 1996 survey; however a positive AOU suggests photosynthesis is not occurring in the surface layer. Sampling of WOCE-AR24 occurred at the end of November 1996 in the southern Rockall region, while it occurred in February in 2008, 2009 and 2010. Warmer surface waters and a shallower winter mixed layer in 1996 suggests winter mixing had only begun to break down the seasonal thermocline and deep winter convection may not have fully replenished surface waters with subsurface nutrients. This highlights the important role of physical mixing in replenishing nutrients to the surface waters of the Trough.

In 1996, 2008 and 2009, upper ENAW on the eastern side of the Trough is slightly warmer, more saline, with fewer nutrients relative to the western side (Figs. 7 and 8). This supports previous studies that suggested ENAW is cooled and freshened as it moves north from its formation region in the Bay of Biscay (Pollard et al., 1996) by cooler, fresher water moving in from the western North Atlantic with the NAC (Ellett, 1995). Read (2001) also identified the NAC by a slight freshness in the warm saline water of the upper eastern North Atlantic. The NAC transports nutrients to the northern North Atlantic (Pelegri et al., 1996), which can be seen in the elevated nutrient levels in the colder, less saline water moving in from the west. Also, upwelling in the subpolar gyre results in nutrient-rich surface water (Williams and Follows, 2003) which is being mixed with the upper ENAW as it is moving north through the Rockall Trough. Surface plots of the entire WOCE-AR24 survey (not shown here), indicate surface nutrient values increase steadily from a minimum along the transect in the Porcupine Sea Bight, to a surface maximum along the northern transect of the Rockall Trough. This can be seen in 1996, 2008 and 2009 right down to 1000 m. In 2010, this nutrient-rich, fresher water is found further east into the Trough closer to the continental shelf and is possibly indicative of an elevated NAC/subpolar gyre influence that year (Fig. 8). There are clearly higher remineralisation rates between 500 and 600 m at the western side of the Trough, indicated by elevated AOU and nutrient levels relative to the eastern side. This may be due to higher flux of particulate matter from the subpolar gyre, an area of high primary productivity (Williams and Follows, 2003).

Below the winter mixed layer, oxygen concentration decreases rapidly (Fig. 5), which could be in part due to remineralisation of sinking organic material below the thermocline, and/or the mixing with a water mass with lower oxygen content. The increase in AOU in this region (Fig. 5) suggests biologically induced consumption of oxygen and subsequent release of inorganic nutrients has occurred in the water column, typical of water below the permanent thermocline. The increase in Si with depth (Fig. 6c) is much smaller than that seen for NO_3 and PO_4 due to the relatively slower remineralisation of silica from sinking particles (Gnanadesikan, 1999). This allows for Si to be used as an effective tracer of water masses since concentrations are not as quickly altered by biological activity.

The high salinity, low oxygen core along the continental shelf-break of the southern transect is indicative of a MW signal, which is restricted to a few stations near the shelf in 2008 and 2010, but has a wider spread in 1996 and 2009 (Fig. 8). Upon formation in the oligotrophic Mediterranean Sea, MW is relatively low in oxygen and nutrients (Cabecadas et al., 2002; Howe et al., 1974; Tsuchiya et al., 1992). Cabaecadas et al. (2002) found that NO_3 and PO_4 concentrations increased slightly in MW between the Gulf of Cadiz and a transect north of its origin due to mixing with overlying nutrient-rich Antarctic Intermediate Water (AAIW), however there was no increase in Si. The lower Si, NO_3° and PO_4° values measured in this core each year agrees with van Aken (2000b), who stated that despite mixing with AAIW after formation, MW is characterised by relatively low preformed nutrients.

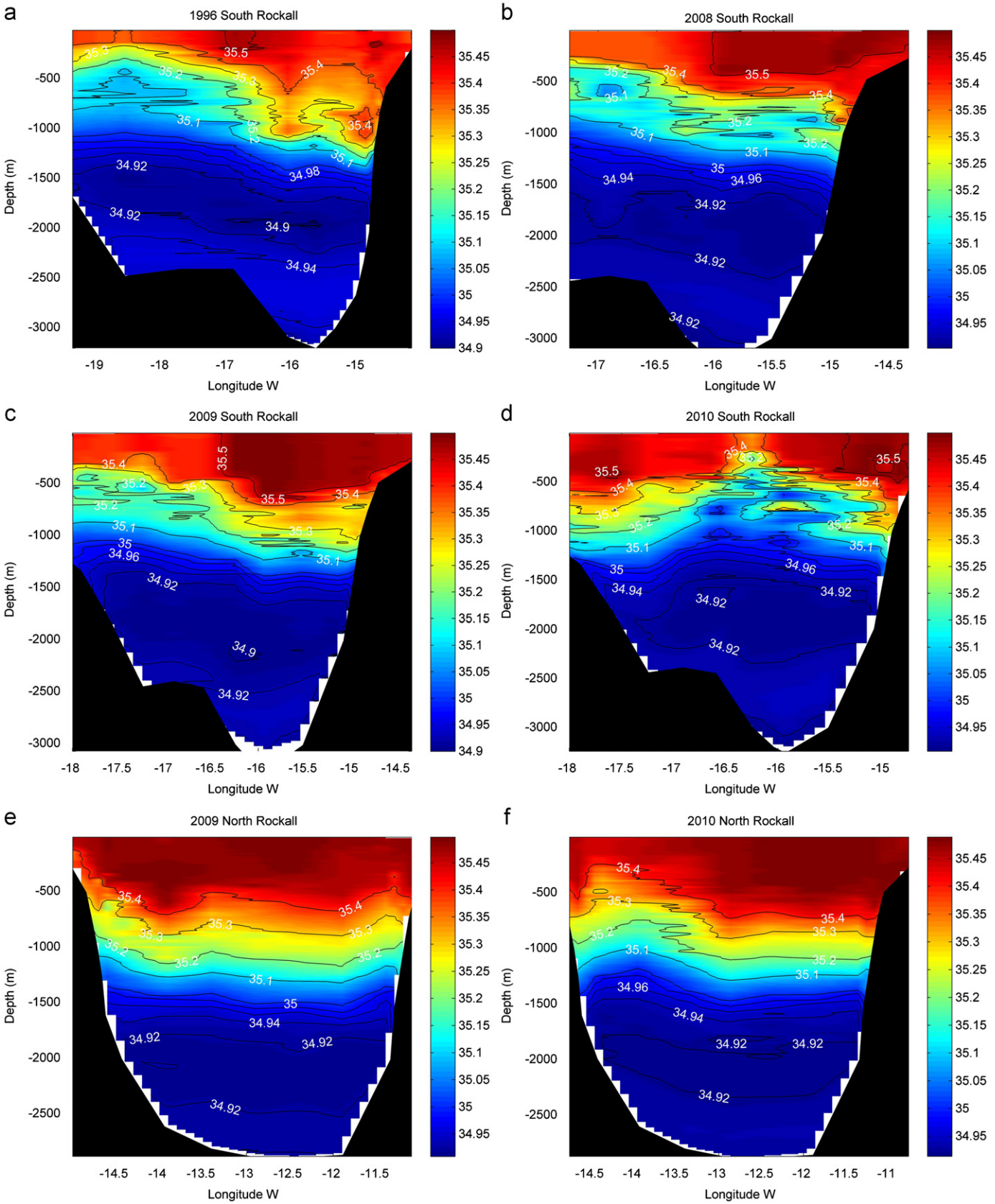

Fig. 8. Salinity across the southern Rockall Trough over (a) 1996 (AR24), (b) 2008 (TH08), (c) 2009 (CE0903) and (d) 2010 (CE10002) and across the northern transect in (e) CE0903 and (f) CE10002.

van Aken (2000b) also suggested MW is characterised by low AOU, however the ageing of this water mass along its pathway to the Rockall Trough has increased the AOU and dissolved inorganic nutrients to the higher levels measured here. In 2008–2010, the $N^{\circ}:P^{\circ}$ ratio was relatively high at a few stations in the MW core. This also supports a MW origin, since the Mediterranean Sea has a high NP ratio (22) (Bethoux et al., 1999) due to increased N:P inputs, low levels of denitrification and possibly fixation of atmospheric dinitrogen (Ridame et al., 2003). Pérez et al., 1993 also measured elevated $N^{\circ}P^{\circ}$ ratios in the MW core along the Iberian Peninsula.

Between 700 and 1000 m stations along western side of the southern transect in 2008 and 2009, and stations at the centre of the Trough in 2010, have salinity and temperature values typical of SAIW in the Rockall Trough (Ullgren and White, 2010). This water has higher oxygen, lower AOU, and higher nutrients than the rest of the Trough at that depth. Low salinity and high oxygen content is due to the influence from the Labrador Current during formation in the western subpolar gyre (Wade et al., 1997). AOU and preformed nutrients were calculated at a range of initial saturation states, to account for the possibility of this water mass being undersaturated with oxygen depending on the rate of subduction when it was formed. As the saturation state may vary between years, comparison of AOU and preformed nutrients over a number of years should be studied with caution. Preformed nutrients and AOU, can however be used to distinguish between SAIW and surrounding water masses. Regardless of the initial saturation level, SAIW has higher preformed nutrients and lower AOU than the surrounding water at that depth, indicating that the elevated nutrients are not due to biological activity, and it is likely that these nutrients have been entrained from the subpolar gyre when SAIW was formed. θ–S profiles indicate that the SAIW signal is stronger in 2010 than the previous 2 years, which would explain why it is found closer to the continental shelf than 2008/09. This could be the reason why MW was more confined to the shelf edge in 2010, since these two water masses have similar density and so have been found to 'compete' for space at the same depth in the water column. Mohn et al. (2002) suggested SAIW could be a barrier for the northward transport of MW along the Porcupine Bank. Preformed nutrient levels and oxygen are higher in SAIW than in MW and therefore concentrations can also be used to distinguish between the two water masses in the region.

The decrease in oxygen and increase in nutrients below the permanent thermocline occurs slightly deeper in the water column in the northern transects. This reflects both increased levels of mixing of intermediate water masses moving north in the Trough, and also the absence of SAIW, which is a highly stratified water mass that can result in a stable layer at intermediate depths, restricting the maximum depth of winter mixing (Wade et al., 1997). In the northern transects some of the data points between 800 and 1100 m near the Rockall Bank tend towards higher salinity along the WTOW mixing line (Fig. 4b). If the θ–S plots of northern and southern transects were plotted together, this θ–S signal could be mistaken for MW, which is also seen as an inflexion in the θ–S plots towards higher salinity. However, WTOW has higher oxygen content than that of MW seen in the south. While McCartney and Mauritzen (2001) measured lower nutrients and higher oxygen in the slightly more saline WTOW, few data points in 2009/10 make it difficult to accurately describe the chemical characteristics of this water mass in the region.

LSW occupies most of water column between 1500 and 2000 m deep and properties are typical of LSW in the Rockall Channel (Stoll et al., 1996). The high oxygen content seen at that depth is characteristic of LSW as it is a young water mass relatively recently in contact with the atmosphere. Oxygen levels are even higher than surface waters in the Trough, since LSW is also much colder and therefore capable of absorbing more oxygen during formation. LSW in the northern transects is slightly warmer and more saline and with lower oxygen than the LSW in the southern transects. This supports New and Smythe-Wright (2001) who also reported an increase in salinity in LSW exiting the Trough due to mixing with surrounding water masses.

Due to varying convection regimes in the Labrador Sea, the oxygen concentration may vary to due the level of mixing between the sinking, oxygen-rich surface water with the rising deeper water which is lower in oxygen. Azetsu-Scott et al. (2005) measured average saturation levels of 77% for CFC-12 for the entire Labrador Sea in May/June 1997, with significant horizontal and vertical variability. For each year, at saturation states less than 85%, the average AOU was negative, and preformed nutrient values higher than actual values measured. Therefore the LSW that reached the Trough in 1996, 2008, 2009 and 2010, was likely 90–100% saturated during formation, since LSW has been away from surface waters for a number of years the dissolved oxygen is likely to decrease slightly, with an increase in dissolved nutrients due to remineralisation.. The weak minima of PO_4 and NO_3 seen in the LSW region is similar to that seen along an eastern Atlantic section south of Iceland by Tsuchiya et al. (1992), however these nutrient minima were less clearly defined than the associated oxygen maximum. LSW properties measured in the Rockall Trough (averaged over 2008, 2009 and 2010) have been altered slightly with respect to source water properties as defined by BATs (Henry-Edwards and Tomczak, 2005), from 305 to 270 $\mu mol\ kg^{-1}$ O_2; 16.4 to 17.6 $\mu mol\ kg^{-1}$ NO_3; 9.1 to 12.1 $\mu mol\ kg^{-1}$ Si and 1.09 to 1.10 $\mu mol\ kg^{-1}$ PO_4. The increase in nutrients is relatively small between source water and the Rockall Trough due to the short length of time, $\sim$10 years (Yashayaev et al., 2007), LSW has been subjected to remineralisation. Calculated preformed nutrient values (at 100% oxygen saturation) are similar to those from previous studies for LSW in the Eastern North Atlantic (Castro et al., 1998; Pérez et al., 1993; Stoll et al., 1996), however it is difficult to directly compare preformed values between years since the saturation state may have varied depending on convection regimes (Azetsu-Scott et al., 2005). Severe winters can create mixed layer depths over 1500 m deep of colder, less saline LSW, while mild winters cause LSW at intermediate depths to become isolated from the upper mixed layer, becoming warmer and more saline due to mixing with surrounding intermediate water masses (Yashayaev, 2007). Nolan (in preparation) recorded a freshening of LSW in the Trough between 2006 and 2009, with a return to higher salinities in 2010. Perhaps this is a delayed response to the shift towards a higher salinity phase of the Labrador Sea from 1994 through to subsequent years reported by Yashayaev (2007). The lower Si measured in LSW in 2009 relative to other years, could be associated with the freshening of LSW that year. The main process responsible for the cooling and freshening of LSW between 1987 and 1994 was the recurrence of severe winters during these years which resulted in increased winter convection (Yashayaev, 2007). If this was to have any effect on the nutrient concentrations in LSW, it should tend to increase concentrations, with increased convection entraining nutrients from deeper waters. The lower Si in 2009 could therefore indicate more of an influence of the Labrador Current, which is relatively cool, fresh and low in NO_3 and Si (Clarke and Coote, 1988; Townsend et al., 2010). This is supported by marginally lower NO_3° measured in LSW in 2009. While the lower NO_3° may also be due to a different saturation state during formation, the PO_4° of LSW is the same in 2009 as in 2010, which may suggest the saturation states were similar each year. The opposite is seen in the 1996 LSW signal in the northern transect, where a higher salinity coincides with slightly elevated Si results.

This could indicate a reduced influence from the Labrador Current, or increased mixing with the slightly more saline NEADW, with higher Si concentrations. The lower PO_4 in 2008 is difficult to explain. It could be due to unknown local factors or could also indicate mixing with another water mass with lower PO_4, e.g. ISOW, however there is little change in salinity or in the other nutrient concentrations to support this statement. The lower PO_4 signal of LSW reached the southern entrance to the Rockall Channel in 2008 and can be seen in the northern section of the Trough in 2009, but is not seen again in 2010. While this signal may outline the northward flow of LSW into the Trough the lower PO_4 and elevated NP ratios were measured in all deeper waters of 2008, and therefore should be studied with caution.

The decrease in oxygen below LSW (Fig. 5) is due to the presence of NEADW and AABW, both older water masses with a large amount of the oxygen depleted by respiration and remineralisation. This is also illustrated in the higher AOU in these deeper waters. Between 2500 and 3000 m the nutrient values are typical of NEADW, with pronounced vertical gradients (Fig. 6) due to the degree of mixing with the nutrient-rich AABW below it (New and Smythe-Wright, 2001). The NP ratios in NEADW and AABW are similar to those reported by Pérez et al. (1993) for the same water masses off the Iberian Peninsula. While the temperature and salinity results alone could not distinguish between NEADW and AABW, the high nutrient values seen below 3000 m, particularly for Si, clearly indicate this water has a southern origin, i.e. AABW influence. The silicate concentration is particularly high as a large component of AABW is re-cycled deep water with high silicate values (Gnanadesikan, 1999). Highest silicate concentrations are found in different parts of the Trough each year, suggesting that the strength and position of the AABW signal varies between years.

5. Conclusion

Temperature and salinity data have been used to identify the water masses present in the Rockall Trough during the winter months of 1996, 2008, 2009 and 2010, and the chemical make up of these water masses has been described. ENAW is progressively cooled and freshened as it moves north through the Rockall Channel, by water masses moving in from the west with the NAC. The NAC tends to elevate nutrient levels in ENAW, with nutrient concentrations increasing moving west and north in the Trough. SAIW and MW, found at a similar density level at the southern entrance to the Trough, can also be identified with their chemical properties; SAIW has relatively high oxygen and high preformed nutrient concentrations, while MW has characteristically low oxygen and low preformed nutrients. While oxygen data can successfully identify LSW in the Trough, nutrient data is less clearly defined. Oxygen and nutrient data, through the calculations of AOU and preformed nutrients, indicate that LSW reaching the Trough in 1996, 2008, 2009 and 2010 was 90–100% saturated with oxygen when it was formed. Lower silicate, and to a lesser extent preformed nitrate, coincided with a freshening of LSW in 2009, possibly linked to a stronger influence from the Labrador Current when it was formed. Nutrient concentrations, in particular silicate, have proved to be effective tracers for AABW, with traces of this water mass found at the southern entrance to the Trough each year.

Acknowledgements

This study was in part funded by the Irish Government funded project "Impacts of Increased Atmospheric CO_2 on Ocean Chemistry and Ecosystems", carried out under the Sea Change strategy with the support of the Marine Institute and the Marine Research Sub-Programme of the National Development Plan 2007–2013. Surveys were funded by the Irish government's National Development Plan 2007–2013. We are grateful to the officers, crew and scientists on the cruises referred to in this paper. We thank Rachel Cave for her comments on the manuscript, Eileen Joyce for her training and help with the nutrient analysis and Kieran Lyons for his help in Matlab. We acknowledge the significant contribution of each of the reviewers to manuscript.

Appendix A. Supplementary material

Supplementary data associated with this article can be found in the online version at doi:10.1016/j.dsr.2011.11.007.

References

Arhan, M., 1990. The North-Atlantic current and sub-arctic intermediate water. J. Mar. Res. 48 (1), 109–144.
Arhan, M., Colin de Verdière, A., Mémery, L., 1994. The eastern boundary of the subtropical North Atlantic. J. Phys. Oceanogr. 24, 1295–1316.
Azetsu-Scott, K., Jones, E.P., Gershey, R.M., 2005. Distribution and ventilation of water masses in the Labrador Sea inferred from CFCs and carbon tetrachloride. Mar. Chem. 94 (1–4), 55–66.
Bethoux, J.P., Gentili, B., Morin, P., Nicolas, E., Pierre, C., Ruiz-Pino, D., 1999. The Mediterranean Sea: a miniature ocean for climatic and environmental studies and a key for the climatic functioning of the North Atlantic. Prog. Oceanogr. 44 (1–3), 131–146.
Broecker, W.S., Peng, T.H., 1982. Tracers in the sea. Columbia University Press, Palisades, NY.
Bubnov, V.A., 1968. Intermediate subarctic waters in the northern part of the Atlantic Ocean. Okeanologia 19, 136–153.
Cabecadas, G., Brogueira, M.J., Cavaco, M.H., Goncalves, C., 2010. Chemical signature of intermediate water masses along Western Portuguese Margin. J. Oceanogr. 66 (2), 201–210.
Cabecadas, G., Brogueira, M.J., Goncalves, C., 2002. The chemistry of Mediterranean outflow and its interactions with surrounding waters. Deep-Sea Res. Part II – Top. Stud. Oceanogr. 49 (19), 4263–4270.
Castro, C.G., Perez, F.F., Holley, S.E., Rios, A.F., 1998. Chemical characterisation and modelling of water masses in the Northeast Atlantic. Prog. Oceanogr. 41 (3), 249–279.
Clarke, R.A., Coote, A.R., 1988. The formation of Labrador Sea-Water. III: The evolution of oxygen and nutrient concentration. J. Phys. Oceanogr. 18 (3), 469–480.
Ellett, D.J., 1995. Physical oceanography of the Rockall Trough. Ocean Challenge 6, 18–23.
Ellett, D.J., Edwards, A., Bowers, R., 1986. The hydrography of the Rockall Channel – an overview. Proc. R. Soc. Edinburgh 88B, 61–68.
Ellett, D.J., Martin, J.H.A., 1973. Physical and chemical oceanography of Rockall Channel. Deep-Sea Res. 20 (7), 585–625.
Gnanadesikan, A., 1999. A global model of silicon cycling: sensitivity to eddy parameterization and dissolution. Global Biogeochem. Cycles 13 (1), 199–220.
Grasshoff, K., Ehrhardt, M., Kremling, K., Almgren, T., 1983. Methods of seawater analysis. Verlag Chem.
Harvey, J., 1982. Theta–*S* relationships and water masses in the eastern North Atlantic. Deep-Sea Res. Part a-Oceanogr. Res. Pap. 29 (8), 1021–1033.
Harvey, J., Arhan, M., 1988. The water masses of the Central North Atlantic in 1983–84. J. Phys. Oceanogr. 18, 1855–1875.
Henry-Edwards, A., Tomczak, M., 2005. Detecting changes in Labrador Sea water through water mass analysis of BATS data. Ocean Sci. Discuss. 2, 417–435.
Holliday, N.P., Pollard, R.T., Read, J.F., Leach, H., 2000. Water mass properties and fluxes in the Rockall Trough 1975–1998. Deep Sea Res. I 47, 1303–1332.
Howe, M.R., Abdullah, M.I., Deetae, S., 1974. Interpretation of double T-S maxima in mediterranean outflow using chemical tracers. J. Mar. Res. 32 (3), 377–386.
Johnson, C., Sherwin, T., Smythe-Wright, D., Shimmield, T., Turrell, W., 2010. Wyville Thomson Ridge overflow water: Spatial and temporal distribution in the Rockall Trough. Deep Sea Res. Part I: Oceanogr. Res. Pap. 57 (10), 1153–1162.
Koeve, W., 2001. Wintertime nutrients in the North Atlantic – new approaches and implications for new production estimates. Mar. Chem. 74 (4), 245–260.
Körtzinger, A., Koeve, W., Kähler, P., Mintrop, L., 2001. C:N ratios in the mixed layer during the productive season in the northeast Atlantic Ocean. Deep Sea Res. Part I: Oceanogr. Res. Pap. 48 (3), 661–688.
McCartney, M.S., 1992. Recirculating components to the deep boundary current of the northern North Atlantic. Prog. Oceanogr. 29 (4), 283–383.

McCartney, M.S., Mauritzen, C., 2001. On the origin of the warm inflow to the Nordic Seas. Prog. Oceanogr. 51 (1), 125–214.
Mohn, C., Bartsch, J., Meincke, J., 2002. Observations of the mass and flow field at Porcupine Bank. Ices J. Mar. Sci. 59 (2), 380–392.
New, A.L., Barnard, S., Herrmann, P., Molines, J.M., 2001. On the origin and pathway of the saline inflow to the Nordic Seas: insights from models. Progr. Oceanogr. 48 (2–3), 255–287.
New, A.L., Smythe-Wright, D., 2001. Aspects of the circulation in the Rockall Trough. Continental Shelf Res. 21 (8–10), 777–810.
Nolan, G., in preparation. Variability of the intermediate and deep water masses in the Rockall Trough.
Pelegri, J.L., Csanady, G.T., Martins, A., 1996. The North Atlantic nutrient stream. J. Oceanogr. 52 (3), 275–299.
Pérez, F.F., Mouriño, C., Fraga, F., Ríos, A.F., 1993. Displacement of water masses and remineralization rates off the Iberian Peninsula by nutrient anomalies. J. Mar. Res. 51, 869–892.
Pollard, R.T., Griffiths, M.J., Cunningham, S.A., Read, J.F., Perez, F.F., Rios, A.F., 1996. Vivaldi 1991 – a study of the formation, circulation and ventilation of Eastern North Atlantic Central Water. Prog. Oceanogr. 37 (2), 167–192.
Read, J.F., 2001. CONVEX-91: water masses and circulation of the Northeast Atlantic subpolar gyre. Progr. Oceanogr. 48, 461–510.
Reid, J.L., 1979. Contribution of the Mediterranean Sea outflow to the Norwegian Greenland Sea. Deep-Sea Res. Part a – Oceanogr. Res. Pap. 26 (11), 1199–1223.
Ridame, C., Moutin, T., Guieu, C., 2003. Does phosphate adsorption onto Saharan dust explain the unusual N/P ratio in the Mediterranean Sea? Oceanol. Acta 26 (5–6), 629–634.
Sherwin, T.J., Griffiths, C.R., Inall, M.E., Turrell, W.R., 2008. Quantifying the overflow across the Wyville Thomson Ridge into the Rockall Trough. Deep Sea Res. Part I: Oceanogr. Res. Pap. 55 (4), 396–404.
Stoll, M.H.C., van Aken, H.M., de Baar, H.J.W., Kraak, M., 1996. Carbon dioxide characteristics of water masses in the northern North Atlantic Ocean. Mar. Chem. 55, 217–232.
Strickland, J.D.H., Parsons, T.R., 1972. A Practical Handbook of Seawater Analysis. Fisheries Research Board of Canada.
Thomas, H., 2002. Remineralization ratios of carbon, nutrients, and oxygen in the North Atlantic Ocean: a field databased assessment. Global Biogeochem. Cycles 16, 3.
Tomczak, M., 1999. Some historical, theoretical and applied aspects of quantitative water mass analysis. J. Mar. Res. 57 (2), 275–303.
Tomczak, M., Godfrey, J.S., 1994. Regional Oceanography: An Introduction. Pergamon, Oxford.
Townsend, D.W., Rebuck, N.D., Thomas, M.A., Karp-Boss, L., Gettings, R.M., 2010. A changing nutrient regime in the Gulf of Maine. Continental Shelf Res. 30 (7), 820–832.
Tsuchiya, M., Talley, L.D., McCartney, M.S., 1992. An eastern atlantic section from Iceland southward across the equator. Deep-Sea Res. Part a – Oceanogr. Res. Pap. 39 (11–12A), 1885–1917.
Ullgren, J.E., White, M., 2010. Water mass interaction at intermediate depths in the southern Rockall Trough, northeastern North Atlantic. Deep Sea Res. Part I: Oceanogr. Res. Pap. 57 (2), 248–257.
van Aken, H.M., 2000a. The hydrography of the mid-latitude northeast Atlantic Ocean I: The deep water masses. Deep-Sea Res. Part I – Oceanogr. Res. Pap. 47 (5), 757–788.
van Aken, H.M., 2000b. The hydrography of the mid-latitude Northeast Atlantic Ocean II: The intermediate water masses. Deep-Sea Res. Part I – Oceanogra Res. Pap. 47 (5), 789–824.
van Aken, H.M., Becker, G., 1996. Hydrography and through-flow in the north-eastern North Atlantic Ocean: the NANSEN project. Prog. Oceanogr. 38 (4), 297–346.
Wade, I.P., Ellett, D.J., Heywood, K.J., 1997. The influence of intermediate waters on the stability of the eastern North Atlantic. Deep-Sea Res. Part I – Oceanogr. Res. Pap. 44 (8), 1405–1426.
Wallace, D.W.R., Lazier, J.R.N., 1988. Anthropogenic chlorofluoromethanes in newly formed Labrador Sea water. Nature 332 (6159), 61–63.
Williams, R.J., Follows, M.J., 2003. Physical transport of nutrients and the maintenance of biological production. In: Fasham, M. (Ed.), Ocean Biogeochemistry: The Role of the Ocean Carbon Cycle in Global Change, Springer.
Winkler, L.W., 1988. Die Bestimmung des im Wasser gelösten Sauerstoffen. Ber. Dtsch. Chem. Ges. 21 (2), 2843–2855.
Worthington, L.V., Wright, W.R., Erika, D., 1970. North Atlantic Ocean Atlas: Of Potential Temperature and Salinity in the Deep Water including Temperature, Salinity and Oxygen Profiles from the Erika Dan Cruise of 1962. Woods Hole Oceanographic Institution.
Yashayaev, I., 2007. Hydrographic changes in the Labrador Sea, 1960–2005. Progr. Oceanogr. 73 (3–4), 242–276.
Yashayaev, I., van Aken, H.M., Holliday, N.P., Bersch, M., 2007. Transformation of the Labrador Sea water in the subpolar North Atlantic. Geophys. Res. Lett. 34 (22), L22605.

Supplementary Information

Chemical characteristics of water masses in the Rockall Trough
McGrath, T., Nolan, G. and McGovern, E., 2012. Deep Sea Research Part I: Oceanographic Research Papers, 61(0): 57-73.

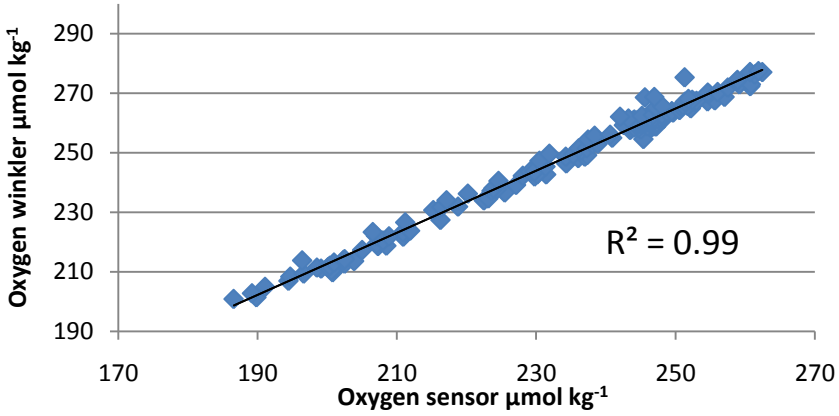

(a)

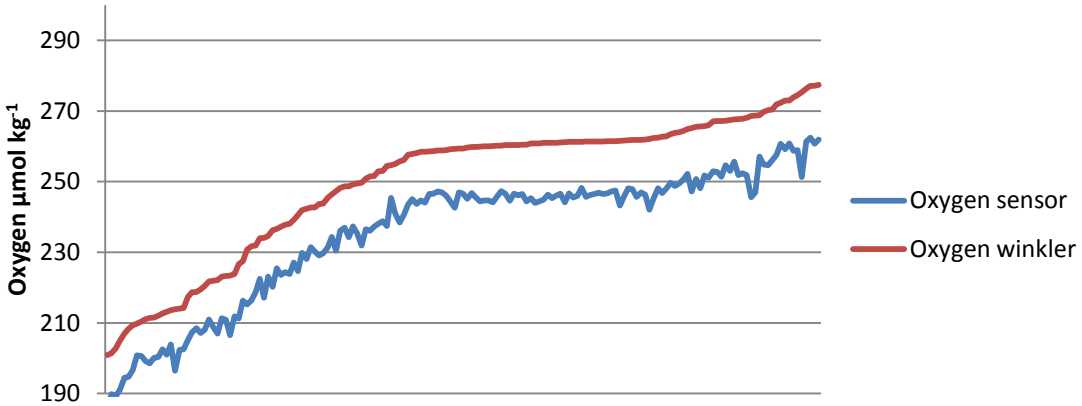

(b)

Figure 1. Oxygen (Winkler) data plotted against CTD sensor data for CE10002. While there is good correlation (a) between data sets (r^2=0.99), there is an almost constant offset of 15µmol kg^{-1} between results (b). CTD sensor data have been corrected for this offset.

Paper II

Inorganic carbon and pH levels in the Rockall Trough 1991-2010

2012. Deep Sea Research Part I: Oceanographic Research Papers, 68(0): 79-91.

Triona McGrath [a,b], Caroline Kivimäe [b], Toste Tanhua[c], Rachel R. Cave[b], Evin McGovern [a]

[a] Marine Institute, Ireland
[b] National University of Ireland, Galway
[c] Helmholtz-Zentrum für Ozeanforschung Kiel (GEOMAR)

Deep-Sea Research I 68 (2012) 79–91

Contents lists available at SciVerse ScienceDirect

Deep-Sea Research I

journal homepage: www.elsevier.com/locate/dsri

Inorganic carbon and pH levels in the Rockall Trough 1991–2010

Triona McGrath [a,b,*], Caroline Kivimäe [b], Toste Tanhua [c], Rachel R. Cave [b], Evin McGovern [a]

[a] The Marine Institute, Rinville, Oranmore, Galway, Ireland
[b] Department of Earth and Ocean Sciences, National University of Ireland, Galway, University Road, Galway, Ireland
[c] Helmholtz-Zentrum für Ozeanforschung Kiel (GEOMAR), Marine Biogeochemistry, Duesternbrooker Weg 20, D-24105 Kiel, Germany

ARTICLE INFO

Article history:
Received 12 December 2011
Received in revised form
14 May 2012
Accepted 20 May 2012
Available online 15 June 2012

Keywords:
Anthropogenic carbon
Acidification
Inorganic carbon
Water masses
Rockall Trough
North Atlantic

ABSTRACT

The accumulation of anthropogenic CO_2 in the oceans is altering seawater carbonate chemistry. Investigation and monitoring of the carbonate parameters is therefore necessary to understand potential impacts on ocean ecosystems. Total alkalinity (AT) and dissolved inorganic carbon (CT) were sampled across the Rockall Trough in Feb 2009 (CE0903) and Feb 2010 (CE10002) as part of a baseline study of inorganic carbon chemistry in Irish shelf waters. The results have been compared with data from WOCE surveys A01E (Sept 1991), A01 (Dec 1994), AR24 (Nov 1996) and A24 (June 1997). The 2009 and 2010 datasets provide a snapshot of the biogeochemical parameters which can act as a baseline of inorganic carbon and acidity levels in surface waters of the Rockall Trough in late winter for future comparison since previous surveys in the area have been affected by biological activity. The dataset also offers the possibility to compare decadal changes in subsurface waters. The temporal evolution of anthropogenic carbon (ΔC_{ant}) between the 1990s and 2010 was evaluated using two separate methods; (i) a comparison of the concentrations of C_T between surveys, after correcting it for remineralisation of organic material and formation and dissolution of calcium carbonate ($\Delta C_{T\text{-abio}}$) and (ii) an extended Multiple Linear Regression was used to calculate the ΔC_{ant} (ΔC_{ant}^{eMLR}). There was an increase in $\Delta C_{T\text{-abio}}$ and ΔC_{ant}^{eMLR} of 18 ± 4 μmol kg^{-1} and 19 ± 4 μmol kg^{-1}, respectively, in the subsurface waters between 1991 and 2010, equivalent to a decrease of 0.040 ± 0.003 pH units over the 19 year period. There was an increase in both $\Delta C_{T\text{-abio}}$ and ΔC_{ant}^{eMLR} of 8 ± 4 μmol kg^{-1} in Labrador Sea Water (LSW) in the Trough between 1991 and 2010, and LSW has acidified by 0.029 ± 0.002 pH units over the same time period. A reduction in calcite and aragonite saturation states was observed, which may have implications for calcifying organisms in the region.

1. Introduction

The world's oceans have taken up close to half of the accumulated anthropogenic fossil fuel emissions since the Industrial Revolution, buffering even more serious climate change (Sabine et al., 2004). When CO_2 reacts with seawater, chemical changes occur that result in a decrease in ocean pH, a process referred to as ocean acidification. Research into oceanic carbon uptake and storage is necessary to understand impacts on ocean ecosystems, along with the need to predict future storage capacity and subsequent effects on global climate. The North Atlantic is an important sink of atmospheric CO_2 (Takahashi et al., 2002). While a number of papers have described the carbonate signature of the water masses in the North Atlantic (e.g. Olafsson et al., 2009; Pérez et al., 2010; Ríos et al., 2001; Stoll et al., 1996; Tanhua et al., 2006), an extensive study had yet to be carried out in the Rockall Trough. This oceanic region is an important area in climate research as it provides a pathway for warm saline waters of the upper North Atlantic to reach the Nordic Seas, where they are continually cooled resulting in deep water formation as part of the global thermohaline circulation (Ellett and Martin, 1973; Holliday et al., 2000). The water column in the Trough has a complex structure due to the presence of several water masses with different origins and histories and is therefore well suited for the study of carbonate chemistry. This area also hosts a vast array of cold water coral structures, interacting with a range of water masses along the continental margin, Rockall Bank and Porcupine Bank (De Mol et al., 2002; Roberts et al., 2003; Wheeler et al., 2011). These organisms are sensitive to any change in pH (Orr et al., 2005), and therefore this region provides a natural laboratory to study the effects of ocean acidification on deep water ecosystems.

Carbon in the ocean is present in both inorganic and organic forms, either dissolved or particulate. The focus of this paper is on the inorganic part of the oceanic carbon cycle, which is quantitatively the dominant form of carbon present in seawater. Zeebe and Wolf-Gladrow (2003) described the processes that affect the carbon chemistry of a water mass; dissolved inorganic carbon (C_T) levels change due to air–sea interaction between the atmosphere and

* Corresponding author at: The Marine Institute, Rinville, Oranmore, Galway, Ireland. Tel.: +353 91 387327; fax: +353 91 387201.
E-mail addresses: triona.mcgrath@marine.ie, triona_mcgrath@hotmail.com (T. McGrath), caroline.kivimae@gmail.com (C. Kivimäe), ttanhua@ifm-geomar.de (T. Tanhua), rachel.cave@nuigalway.ie (R.R. Cave), evin.mcgovern@marine.ie (E. McGovern).

0967-0637/$ - see front matter © 2012 Elsevier Ltd. All rights reserved.
http://dx.doi.org/10.1016/j.dsr.2012.05.011

surface waters, where C_T distribution is temperature-dependent with increased CO_2 solubility in colder waters, and also decreasing solubility with increasing salinity. Respiration of organic matter and dissolution of $CaCO_3$ in the water column tend to increase C_T concentrations, while photosynthesis and formation of calcium carbonate ($CaCO_3$) in surface layers reduces C_T levels. Total alkalinity decreases with $CaCO_3$ formation, while it increases with the dissolution of $CaCO_3$, with a slight increase with photosynthesis. A_T is not affected by CO_2 exchange with the atmosphere, concentrations are generally governed by factors that affect salinity (Broecker and Peng, 1982; Lee et al., 2006) and it is found to behave conservatively in surface waters of the major oceans (Lee et al., 2006; Millero et al., 1998a).

An important link to the global carbon cycle is the formation and dissolution of $CaCO_3$ which effectively neutralizes the acidification effect of CO_2 absorbed by the oceans (Zeebe and Wolf-Gladrow, 2003); such that $CaCO_3$ formation in surface waters, its sinking and re-dissolution at depth, effectively transfers CO_2 from the surface to deep waters (Millero, 2007). Many organisms in the ocean depend on $CaCO_3$ to lay down their shells or skeletons, made of either calcite or aragonite depending on the species. $CaCO_3$ solubility tends to increase with depth and the saturation horizon refers to the depth below which calcite or aragonite is under-saturated ($\Omega < 1$). A number of studies have found that dissolution of $CaCO_3$ can occur above the saturation horizon (e.g. Chen, 2002; Feely et al., 2004; Milliman et al., 1999); however it may not be a significant process in the North Atlantic (Friis et al., 2006a, 2006b). Aragonite is more soluble than calcite and the aragonite saturation horizon (ASH) occurs at shallower depths, ~3500 m deep in the North Atlantic (Feely et al., 2004). A shoaling of the saturation horizons is expected in the oceans due to increasing C_T, which may have detrimental effects on marine ecosystems (Feely et al., 2004; Orr et al., 2005).

C_T and A_T were measured in water samples collected across the Rockall Trough in February of 2009 and 2010, close to the end of the winter mixing period. Körtzinger et al. (2008) reported maximum C_T in March marking the end of winter mixing. Since biological activity is at a minimum during winter, it is possible to describe 'preformed' carbonate conditions in the upper water column, useful when trying to detect any changes due to increasing atmospheric CO_2. Results were compared to similar WOCE transects across the Trough in Sept 1991 (A01E), Dec 1994 (A01), Nov 1996 (AR24) and June 1997 (A24), (Fig. 1). Our goal here is to characterise the carbonate parameters in the different water masses in the Rockall Trough region, and to identify any changes over the 19 year period since the WOCE transects were made. The recent paper by McGrath et al. (2012), which describes the nutrient and oxygen characteristics of the water masses in the 2009/10 surveys and compares them with those encountered in the WOCE 1996 survey, sets the background for the chemical properties of the water masses in the Trough.

2. Method

The main data sets presented here were collected during two surveys on the RV Celtic Explorer to the Rockall Trough, one in February 2009 and one in February 2010. WOCE data were extracted from the CDIAC database (https://cdiac.ornl.gov/oceans/). See Fig. 1 and Table 1 for details on all surveys discussed.

2.1. Ancillary data

Details of temperature, salinity and oxygen sensors used in the 2009 and 2010 surveys, along with sampling, analysis and quality control of dissolved inorganic nutrients and oxygen are supplied in McGrath et al. (2012). Details of WOCE survey methods can be

Table 1
Information on surveys discussed in the paper with details on the chemistry data available. Data sources: WOCE—World Ocean Circulation Experiment (https://cdiac.ornl.gov/oceans/); NUIG—National University of Ireland, Galway; MI—Marine Institute, Ireland. Chemistry samples: C_T; dissolved inorganic carbon; A_T; total alkalinity; NUT; dissolved inorganic nutrients; O_2; dissolved oxygen. Note while there were A_T data taken in 1991 and 2009, there was a large offset in the data, and while there were no oxygen bottle samples taken in 2009, oxygen sensor data is available.

Survey	Date	Source	C_T	A_T	NUT	O_2
A01E	17–21 Sept 1991	WOCE	√	×	√	√
A01	13–15 Dec 1994	WOCE	√	×	√	√
AR24	22–27 Nov 1996	WOCE	√	√	√	√
A24	8–10 June 1997	WOCE	√	√	√	√
CE0903	6–10 Feb 2009	NUIG, MI	√	×	√	×
CE10002	11–14 Feb 2010	NUIG, MI	√	√	√	√

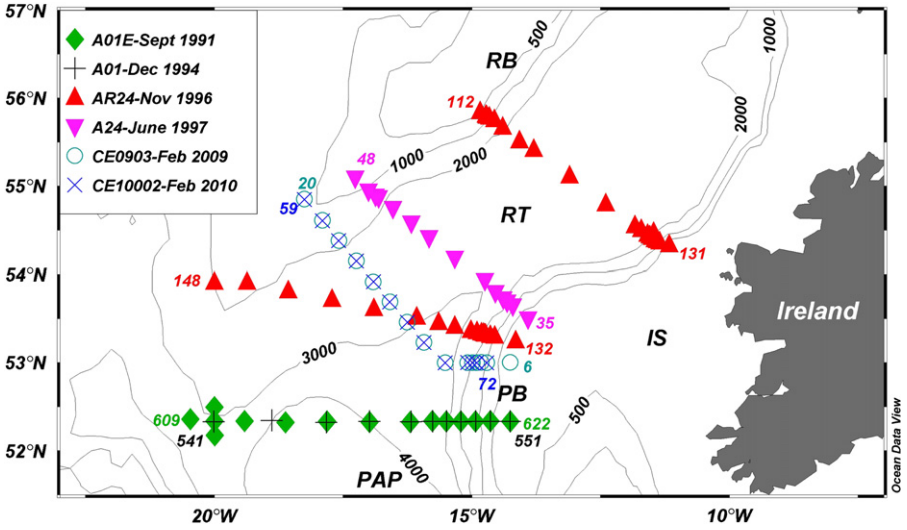

Fig. 1. Bathymetry of the Rockall Trough. Labelled bathymetry: RT—Rockall Trough; IS—Irish Shelf; PB—Porcupine Bank; RB—Rockall Bank; PAP—Porcupine Abyssal Plain; with overlying transect positions of WOCE A01E (Sept 1991), A01 (Dec 1994), AR24 (Nov 1996), A24 (June 1997), CE0903 (Feb 2009) and CE10002 (Feb 2010). Station numbers of the surveys are at the end of each transect.

found on the CDIAC website and in CDIAC (2003). It should be noted that there were no oxygen bottle samples analysed in 2009, and therefore the sensor data were calibrated based on the assumption that the surface mixed layer is 97% saturated in winter, as was measured in the 1994, 1996 and 2010 winter surveys. Since there was a variability of $\pm 2\%$ in the oxygen saturation in surface waters of these surveys, this increases the uncertainty of oxygen results from ± 1.5 μmol kg^{-1} in Winkler data to ± 5.6 μmol kg^{-1} in the 2009 sensor data.

2.2. Dissolved inorganic carbon (C_T) and total alkalinity (A_T)

2009 and 2010 C_T and A_T were sampled and analysed as per Dickson et al. (2007). C_T was analysed by coulometric titration and A_T by potentiometric titration (Dickson et al., 2007) at NUI, Galway, both on a VINDTA-3C (Versatile INstrument for the Determination of Total inorganic carbon and titration Alkalinity), manufactured by Marianda (Mintrop et al., 2000). The system was calibrated by running duplicate Certified Reference Materials with every batch of samples (CRMs provided by A. Dickson, Scripps Institute of Oceanography, USA). The precision of both CRMs and samples was calculated as the standard deviation of the difference between duplicate samples; precision was ± 2 μmol kg^{-1} for C_T and ± 1 μmol kg^{-1} for A_T. There appears to be a negative offset of 7–8 μmol kg^{-1} down through the water column in the 2009 A_T data relative to all other data sets. If this uncorrected data was included in the study, the lower A_T would result in anthropogenic carbon estimates over 20% higher than those presented for the 19 years. Such a large difference in A_T between 2009 and the other datasets is unlikely; A_T cannot be expected to vary that much through the entire water column in the open ocean, especially since the 2009 salinity is similar to the other surveys. The only process that could reduce A_T would be a large increase in $CaCO_3$ formation through the water column, which is very unlikely. At present the reason for the offset is unknown, and therefore the 2009 A_T data have not been included in the present study.

WOCE C_T samples were analysed by coulometric detection on the SOMMA system (Johnson et al., 1987) and precision was ± 2 μmol kg^{-1} for all surveys. WOCE AR24 and A24 A_T was determined by potentiometric titration on a MATS system (Millero et al., 1993); precision was ± 1 μmol kg^{-1}. While there is a small number of A_T samples in the Trough from A01E, results are at least 40 μmol kg^{-1} higher than other datasets and have therefore not been included here. Wanninkhof et al. (2003) also found A01E A_T values significantly different from neighbouring cruises and recommended that it not be used. There are no A_T data from the 1994 A01 survey.

Where A_T data was not available (1991, 1994, 2009), a multiple linear regression (MLR) approach was applied to the available A_T datasets to derive an equation that could calculate A_T from temperature, salinity, C_T, phosphate and silicate. A separate MLR was derived for the depths above and below 2000 m due to the large difference in A_T profiles. Details of the MLRs of the combined dataset of 1996, 1997 and 2010 surveys are in the SI. Residuals are normally distributed and centred at zero, and the r-squared of the calculated versus measured A_T is 0.91 in the top 2000 m and 0.97 below 2000 m. The uncertainty of the estimated A_T, calculated as the standard deviation of residuals, is ± 3 μmol kg^{-1}.

To investigate the vertical distribution of A_T in the water column without the effect of salinity, it was normalised to a salinity of 35 as described by Friis et al. (2003);

$$NA_T = \left(A_T^{meas} - A_T{}^{S=0}\right) \Big/ S^{meas} S^{ref} + A_T^{S=0}$$

where NA_T is the normalised A_T, A_T^{meas} is the measured A_T, S^{meas} is the measured salinity of the sample and S^{ref} is 35. $A_T^{S=0}$ is the salinity adjustment based on the constant term of salinity=0. Friis et al. (2003) calculated $A_T^{S=0}$ as 728.3 μmol kg^{-1} from combined North Atlantic surface data, with an uncertainty for NA_T of ± 7 μmol kg^{-1}. Although this calculation is based on surface waters of the North Atlantic, we have applied it here to the entire water column to give a broad idea of the normalised A_T distribution. The exact NA_T values are therefore not discussed since the calculation does not apply to waters at depth or from waters originating outside of the North Atlantic.

2.3. Calculation of pH and aragonite/calcite saturation

pH and aragonite/calcite saturation were calculated from the C_T and A_T data (along with potential temperature, salinity, pressure, silicate and phosphate data) using CO2SYS (Lewis and Wallace, 1998). The total pH scale was used, K_1 and K_2 were taken from Mehrbach et al. (1973), refit by Dickson and Millero (1987) and Dickson's K_{HSO_4} was selected. pH was also calculated at 25 °C to investigate temporal changes between 1991 and 2010 and to allow for comparison with trends already published at this temperature. Calculating the uncertainty of the derived parameters is complicated as it includes the measurement uncertainties of each input parameter, along with the error in the equilibrium constants. Dickson and Riley (1978) calculated a combined uncertainty of 0.6–6.3% in pH and of 3.1% for the carbonate ion concentration, when calculated from A_T and C_T. The highest possible uncertainty is used with the results in this paper.

2.4. Estimation of anthropogenic carbon (ΔC_{ant})

C_T was corrected for changes in remineralisation of organic matter and dissolution of calcium carbonate ($\Delta C_{T\text{-abio}}$) using the equation from Tanhua et al., (2006);

$$\Delta C_{T\text{-abio}} = \Delta C_T - 0.746 \times \Delta AOU - 0.5 \times (\Delta A_T + \Delta NO_3)$$

where Δ is the change in properties between the earlier WOCE surveys and the recent 2009/10 surveys, AOU is the apparent oxygen utilisation, 0.746 is the stoichiometric ratio relating inorganic carbon to oxygen, calculated for the Northeast Atlantic by Körtzinger et al. (2001) and 0.5 is the effect on C_T by change in A_T due to dissolution of calcium carbonate. The combined analytical uncertainty in determining $\Delta C_{T\text{-abio}}$ is estimated to be ± 3 μmol kg^{-1}, based on the 2010 dataset. When A_T is estimated from MLR the uncertainty of $\Delta C_{T\text{-abio}}$ increases to ± 4 μmol kg^{-1}, and in 2009, when both A_T and O_2 are estimated it increases to ± 5 μmol kg^{-1}. Since $\Delta C_{T\text{-abio}}$ is independent of the effects of the biological pump, it can therefore be assumed that any changes in $\Delta C_{T\text{-abio}}$ within a water mass are due to increasing levels of anthropogenic CO_2.

The change in anthropogenic carbon between the 1991 and 2010 surveys was also calculated using extended Multiple Linear Regression, eMLR, as described by Friis et al. (2005) and Tanhua et al. (2007). Here, C_T was fit with an MLR as a function of common hydrochemical parameters that influence its distribution

$$C_T = a_0 + a_1 p_1 + a_2 p_2, \ldots, + a_n p_n + R,$$

where p_1 to p_n are the set of parameters used in the regression, a_0 to a_n are the corresponding coefficients and R is the residual. Separate MLRs were used for the depth range 200–1000 m and 1000–2200 m due to different water masses present. The separate coefficients determined from the regressions of the 2 surveys (a_0 to a_n and b_0 to b_n) are subtracted to create a new equation that relates only the temporal difference in C_T to the hydrochemical parameters. This is interpreted as the change in C_T due to increasing levels of anthropogenic CO_2, $\Delta C_{ant}{}^{eMLR}$

Table 2
Derived multiple linear regression equations for C_T prediction of 1991 (WOCE-A01E) and 2010 (CE10002) for two separate depth intervals, with the average residual (R); the predicted C_T minus measured C_T, the regression coefficient (R^2) and the number of samples (n) for each regression.

		a_0	a_1 (θ)	a_2 (S)	a_3 (O_2)	a_4 (NO_3)	a_5 (Si)	R	R^2	n
200–1000 m	1991	1427.62	−6.32	24.60	−0.47	0.09	1.59	−0.7	0.99	43
200–1000 m	2010	2025	2.50	0.10	0.13	3.34	3.69	−0.6	0.96	27
1000–2200 m	1991	4203.55	11.18	−61.25	−0.03	1.40	2.55	−0.3	0.98	27
1000–2200 m	2010	3926.82	−13.33	−43.39	−1.05	6.35	−2.41	−1.0	0.87	13

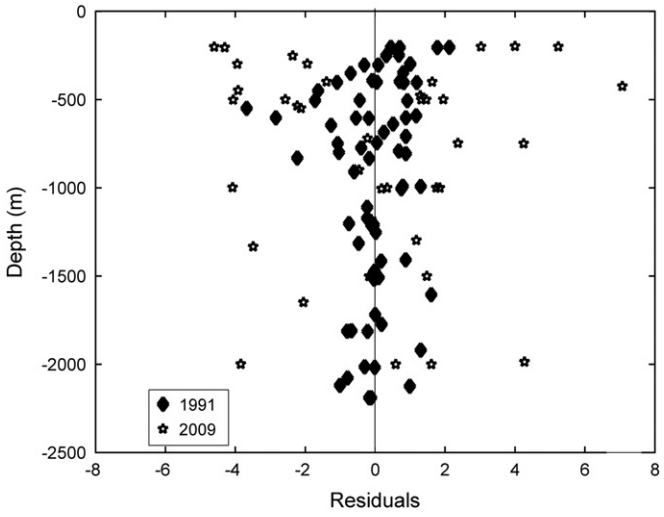

Fig. 2. C_T MLR residuals (C_T predicted minus C_T measured) for both the 1991 and 2010 datasets.

(Tanhua et al., 2007).

$$\Delta C_{ant}{}^{eMLR} = (a_0 - b_0) + (a_1 - b_1)p_1 + (a_2 - b_2)p_2, \ldots, (a_n - b_n)p_n + R$$

Details of the MLRs that were used to calculate $\Delta C_{ant}{}^{eMLR}$ are in Table 2. The eMLR was applied to the 1991 dataset as there were more data points and the residuals were closer to zero (Fig. 2). The two main assumptions of the eMLR method are (1) that the linear multiple-parameter model is able to describe a regions spatially varying hydrographic C_T distribution and (2) that the underlying natural correlations of C_T with the selected independent parameters do not change over the period of interest. A number of studies have highlighted that natural variability in oceanic C_T can be comparable to or larger than the anthropogenic signal sought by the decadal repeat occupations due to the influence of ocean circulation on annual variations in C_T (Doney et al., 2009; Levine et al., 2008; Rodgers et al., 2009). This eMLR technique accounts for the natural variations of carbon due to both hydrographic (temperature and salinity) and biogeochemical (nutrients and oxygen) parameters incorporated into the model. It should therefore account for changes in water mass movement between the surveys.

It is difficult to directly assess the accuracy and precision of the eMLR based estimate of ΔC_{ant}, see Tanhua et al. (2007) and Wanninkhof et al. (2010) for a discussion on the robustness of the eMLR method. The independent variables in the eMLR are not fully uncorrelated which can potentially lead to biases in the method. Even though the eMLR technique tends to cancel out the residual in the individual MLRs, the residual of the MLR fit for the two cruises can give an idea of the uncertainty in the eMLR based ΔC_{ant} estimate (see Fig. 2). Assuming that the residual of the individual MLRs are independent suggest that the precision of the eMLR is $\pm 4\ \mu mol\ kg^{-1}$, even though this does not account for potential biases in the eMLR approach.

3. Results and discussion

3.1. Carbonate parameters of water masses in the Rockall Trough

3.1.1. Physical oceanography

A full description of the CE0903, CE10002 and AR24 temperature, salinity, oxygen and nutrient data is given in McGrath et al. (2012). Potential temperature–salinity plots and salinity sections for each of the surveys listed in Table 1 are in Figs. 1 and 2 of the Supplementary Information (SI). To summarize, ENAW (Eastern North Atlantic Water) as described by Harvey (1982), occupies much of the water column in the top 1000 m in all surveys. As the relatively saline ENAW travels north from its formation region in the Bay of Biscay (Pollard et al., 1996), it is progressively freshened by mixing with water masses moving in from the west (Ellett et al., 1986). Between 500 and 1000 m along the southern transects in the Rockall Trough, temperature and salinity tend towards MW (Mediterranean Water) on the eastern side of the Trough, while on the western side some of the data points tend towards SAIW (Sub Arctic Intermediate Water). SAIW forms in the western boundary current of the subpolar gyre; this cold, fresh water mass spreads westwards with a branch of the North Atlantic Current (NAC) to the southern entrance of the Trough (Arhan, 1990; Arhan et al., 1994; Harvey and Arhan, 1988). MW, also called Mediterranean Overflow Water (MOW), is a highly saline outflow from the Mediterranean Sea (Pérez et al., 1993; Tomczak and Godfrey, 1994) that is normally seen as an inflexion towards higher salinity in the θ–S (potential temperature–salinity) plots in the Rockall Channel (Ellett and Martin, 1973). The strength of these water mass signals varies between years; strongest MW signal is apparent in 1996, while strongest SAIW signal is apparent in 2010 (Fig. 1 in SI). While there is a weak inflexion towards MW signal in A24, the signal is less than that seen in other years, and is likely due to a more northerly position than the other southern Rockall transects.

θ–S profiles are similar across all years below 1500 m, and indicate a clear LSW (Labrador Sea Water) signal between 1500 and 2000 m deep. LSW is formed from deep winter convection in the Labrador Basin, and water properties of LSW can vary between years depending on local climate factors that influence the convection regimes in the Labrador Sea (Azetsu-Scott et al., 2005; Yashayaev, 2007). Northeast Atlantic Deep Water (NEADW) is seen as a salinity maximum about 2600 m between the fresh LSW above it and LDW (Lower Deep Water) below it. (Ellett and Martin, 1973; van Aken, 2000), with some Antarctic Bottom Water (AABW) in the deepest parts of the Trough. AABW is formed by deep convection associated with the freezing of sea ice in the Weddell and Ross Seas, (Tomczak and Godfrey, 1994), it flows north along the eastern side of the North Atlantic and mixes up into NEADW, which then circulates into the Rockall Trough

(Ellett and Martin, 1973; McCartney, 1992; New and Smythe-Wright, 2001; Tsuchiya et al., 1992).

For the AR24 northern transect, once again much of the top 1000 m falls along the ENAW line. While there are no MW or SAIW signals apparent in this transect, there is a clear LSW signal, with LDW in the deepest parts of the transect. Due to the shallower depth of the northern transect, there is no AABW signal.

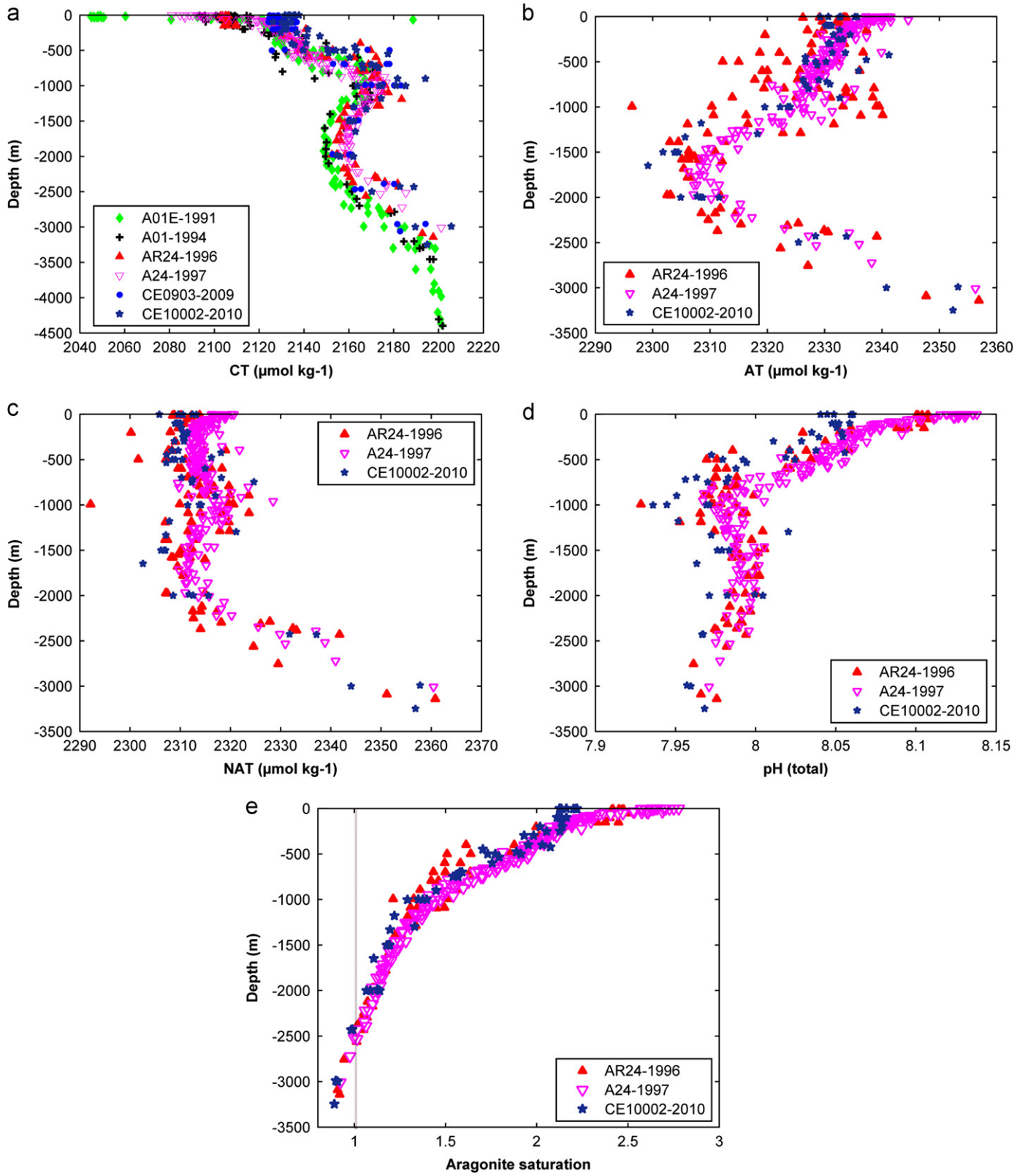

Fig. 3. Vertical profiles of the carbonate parameters with depth (m) for A01E (Sept 1991), A01 (Dec 1991), AR24 (Nov 1996), A24 (June 1997), CE0903 (Feb 2009) and CE10002 (Feb 2010); (a) C_T (b) A_T (c) NA_T (d) pH (total scale) and (e) aragonite saturation, with the sample potential temperature as the reference temperature. Note the longer depth scale for C_T is due a greater depth in A01E and A01.

3.1.2. Vertical profiles

Vertical profiles of C_T broadly reflect the influence of the 'biological pump' in the ocean. C_T concentrations are lower in summer surveys than in winter and concentrations increase in all surveys below the surface mixed layer down to 1000 m (Fig. 3a). Carbon is taken up in the surface ocean where organic matter and $CaCO_3$ are produced; this material is then transported to deeper waters where remineralisation releases inorganic carbon back into the water column. There is a slight decrease in C_T between 1500 and 2000 m due to the presence of LSW, a relatively young water mass in the Northeast Atlantic (Yashayaev et al., 2007). Concentrations increase again to maximum levels in the deepest parts of the Trough due to high levels of remineralisation in the older NEADW and AABW. Apart from a few high-A_T points about 1000 m (Fig. 3b), A_T profiles illustrates a steady decrease from surface waters down to a minimum between 1500 and 2000 m, before gradually increasing towards a maximum in the deepest waters. A comparison of A_T with NA_T profiles (Fig. 3c) indicates that above 2000 m, A_T is largely governed by salinity. Below 2000 m the dissolution of $CaCO_3$ influences the A_T distribution since NA_T increases steadily to the deepest parts of the Trough. These profiles are similar to those measured off the Iberian Peninsula by Ríos et al. (1995), who found a sharp increase in A_T below 2300 m due to the dissolution of $CaCO_3$. The high A_T signal (Fig. 3b) measured at ~1000 m along the Irish shelf edge is due to the presence of MW, which is characteristically high in A_T due to high evaporation and hence salinity, coupled with high freshwater A_T inputs (Schneider et al., 2007).

3.1.3. Surface mixed layer

The surface mixed layer is a region in the upper ocean where there is little variation in water properties with depth. Here we have defined the mixed layer depth (MLD) as the depth where the temperature is less than the surface value by 0.5 °C (Monterey and Levitus, 1997). The average MLD for each survey is given in Table 3. To calculate the averages of water parameters within the mixed layer, the minimum MLD from each survey was used as the depth limit to ensure the given parameters are representative of the entire mixed layer across each transect.

The surface C_T across the various surveys highlights the effects of the biological and physical forcing on chemical parameters in the water column. Deepest MLDs were measured in 2009/10 surveys due to late-winter sampling, close to the end of winter mixing. Nutrient and C_T concentrations are higher than other surveys through regeneration from subsurface waters from deep vertical mixing. The average C_T concentration in the surface mixed layer of 2010 (2133 ± 2 μmol kg^{-1}) is similar to concentrations in the surface mixed layer along the western side of the Trough in 2009 (2133 ± 2 μmol kg^{-1}), and represent ENAW of western origin with slightly cooler temperatures, lower salinity and higher nutrients. Average C_T levels are slightly lower (2128 ± 2 μmol kg^{-1}) in the top 200 m at stations closer to the shelf in 2009 relative to the western side of the Trough, coinciding with higher temperature and salinity and lower nutrients (Fig. 4, Table 3). This east–west gradient was also seen in the surface layer of the June 1997 survey and in both cases is likely related to the pathway of ENAW from the Bay of Biscay. Upwelling in the subpolar gyre regenerates surface waters with nutrients and C_T from below the permanent thermocline (Williams and Follows, 2003) which are mixed from the west across the Rockall Trough. Lower C_T (2105 ± 2 μmol kg^{-1}) in the Dec 1994 and Nov 1996 surveys coincides with a slightly shallower mixed layer and lower nutrient concentrations. This is largely due to sampling in early winter where mixing had not fully replenished C_T and nutrients to surface waters in the Trough. The average mixed layer depth is

Table 3
Average concentration of the chemical parameters of the surface mixed layer from A01E, A01, AR24, A24, CE0903 and CE10002. Standard deviations are in *italics* beside the average concentrations. MLD; average mixed layer depth across the transects and *n*; number of carbon samples from each survey. pH (total), aragonite ($Ar\Omega$) and calcite ($Ca\Omega$) saturation were calculated using CO2SYS, details described in Methods section. pH was calculated at potential temperature (θ). The * indicates where A_T or O_2 are estimated.

Year	MLD	Depth	ST	*S*	*T*	DO	AOU	NO_3	Si	PO_4	C_T	A_T	pH (t) $T=\theta$	$Ar\Omega$	$Ca\Omega$	*n*
Sept 1991	**51**	**0–40**	**All**	**35.32** (*0.09*)	**15.41** (*0.47*)	**246.3** (*3.0*)	**−1.3** (*1.5*)	**0.45** (*0.30*)	**0.68** (*0.15*)	**0.15** (*0.03*)	**2049** (*4*)	**2337*** (*6*)	**8.161*** (*0.004*)	**3.11*** (*0.06*)	**4.83*** (*0.09*)	**12**
Dec 1994	**211**	**0–135**	**All**	**35.45** (*0.08*)	**11.31** (*0.25*)	**256.7** (*2.3*)	**9.4** (*1.4*)	**8.38** (*0.70*)	**2.50** (*0.29*)	**0.54** (*0.03*)	**2106** (*6*)	**2334*** (*5*)	**8.108*** (*0.008*)	**2.44*** (*0.04*)	**3.81*** (*0.07*)	**29**
Nov 1996	**180**	**0–135**	**132–148**	**35.45** (*0.07*)	**11.40** (*0.17*)	**258.8** (*1.6*)	**6.9** (*1.3*)	**7.08** (*0.33*)	**2.29** (*0.29*)	**0.52** (*0.02*)	**2105** (*1*)	**2332** (*3*)	**8.105** (*0.003*)	**2.44** (*0.03*)	**3.82** (*0.05*)	**12**
			112–131	**35.40** (*0.10*)	**10.96** (*0.25*)	**259.8** (*1.7*)	**8.5** (*0.8*)	**7.82** (*0.33*)	**2.81** (*0.23*)	**0.55** (*0.02*)	**2115** (*8*)	**2329** (*3*)	**8.087** (*0.017*)	**2.31** (*0.08*)	**3.62** (*0.13*)	**11**
June 1997	**45**	**0–25**	**35–41**	**35.47** (*0.05*)	**12.73** (*0.56*)	**269.9** (*1.6*)	**−12.4** (*1.6*)	**4.27** (*0.56*)	**0.48** (*0.07*)	**0.30** (*0.03*)	**2088** (*5*)	**2339** (*1*)	**8.128** (*0.008*)	**2.71** (*0.05*)	**4.23** (*0.08*)	**7**
		0–25	**42–47**	**35.46** (*0.04*)	**11.97** (*0.32*)	**270.1** (*4.0*)	**−7.6** (*4.1*)	**5.41** (*0.52*)	**1.00** (*0.45*)	**0.37** (*0.04*)	**2097** (*4*)	**2339** (*2*)	**8.127** (*0.006*)	**2.61** (*0.03*)	**4.08** (*0.05*)	**7**
Feb 2009	**470**	**0–200**	**7–14**	**35.53** (*0.01*)	**11.16** (*0.06*)	**259.2***(*0.5*)	**7.8*** (*0.6*)	**10.03** (*0.38*)	**3.45** (*0.11*)	**0.54** (*0.04*)	**2128** (*3*)	**2338*** (*0*)	**8.070*** (*0.008*)	**2.25*** (*0.05*)	**3.53*** (*0.07*)	**17**
			15–20	**35.45** (*0.01*)	**10.56** (*0.17*)	**259.0***(*1.3*)	**11.3*** (*1.3*)	**11.44** (*1.03*)	**4.38** (*0.87*)	**0.66** (*0.08*)	**2133** (*3*)	**2333*** (*1*)	**8.059*** (*0.007*)	**2.16*** (*0.05*)	**3.38*** (*0.08*)	**11**
Feb 2010	**450**	**0–200**	**All**	**35.47** (*0.04*)	**10.75** (*0.27*)	**262.4** (*2.9*)	**7.0** (*1.9*)	**10.06** (*0.44*)	**3.33** (*0.24*)	**0.59** (*0.05*)	**2133** (*2*)	**2332** (*2*)	**8.052** (*0.007*)	**2.16** (*0.04*)	**3.38** (*0.06*)	**12**

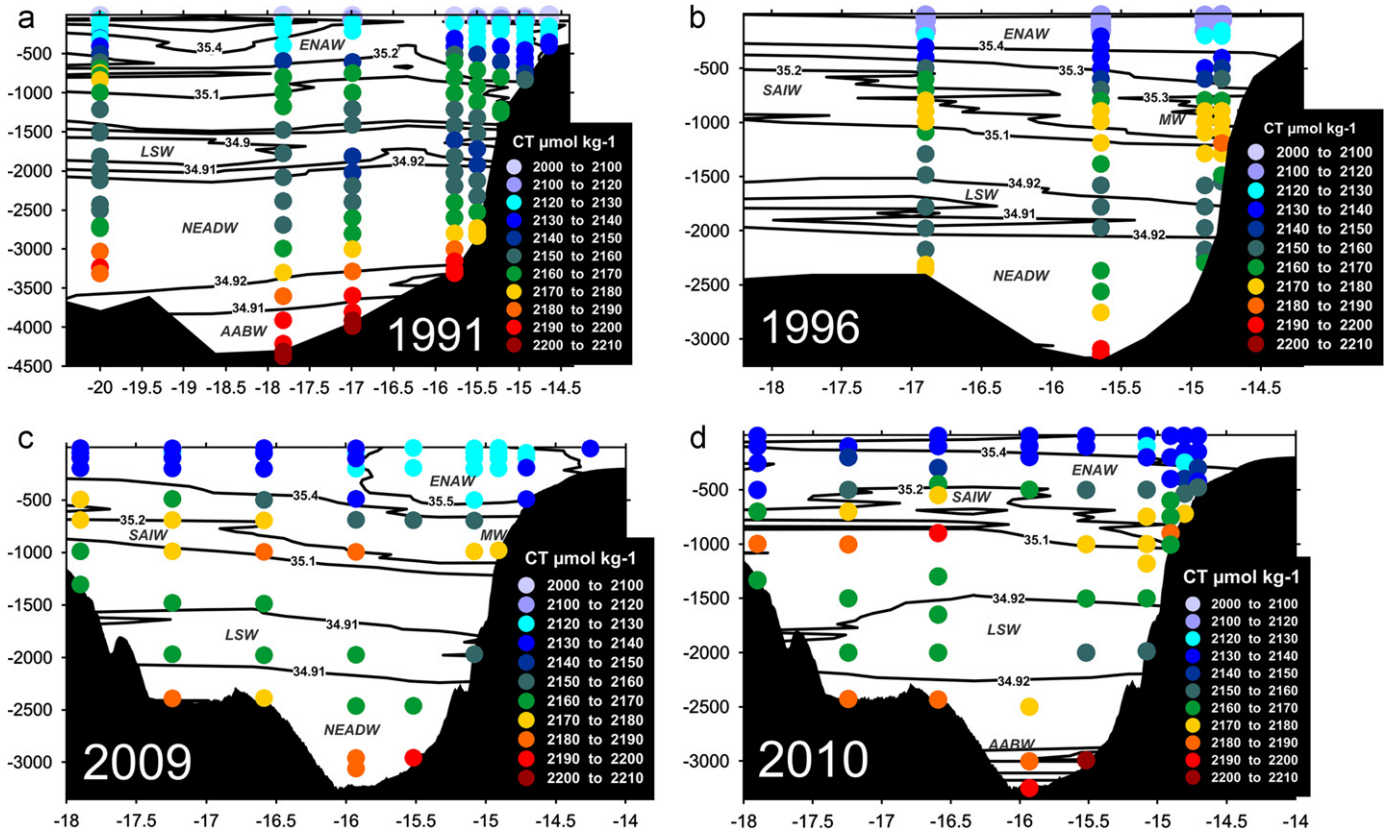

Fig. 4. Section profiles of C_T (µmol kg^{-1}) with salinity contours and water masses across the southern Rockall Trough in 1991, 1996, 2009 and 2010.

slightly deeper in the northern transect of AR24 (224 m) relative to the southern transect (180 m), and coincides with elevated nutrient and C_T concentrations due to increased mixing in the surface layer moving north in the Trough.

In A01E (Sept 1991) and A24 (June, 1997), higher surface temperature and a seasonal thermocline less than 45 m deep, are both typical N. Atlantic features during the summer months. Results from the June survey indicate the progression of the spring–summer bloom as the water column stratifies, and photosynthesis in the surface waters results in a decrease in nutrients and C_T, with negative AOU values as oxygen is produced in the process. In September 1991, nutrients are almost depleted, with lowest surface nutrient and C_T values, likely marking the end of the spring–summer bloom (Table 3). Elevated A_T in the surface waters during the June and September surveys relative to the winter surveys, is likely related to photosynthesis in surface waters, which slightly increases A_T due to the uptake of protons with nitrate by phytoplankton (Millero et al., 1998b; Wolf-Gladrow et al., 2007).

3.1.4. *Intermediate waters (500–1100 m)*

The east–west gradient in carbonate parameters across the southern entrance to the Trough observed between 500 and 1100 m is likely due to the pathway of ENAW and also the presence of SAIW and MW, two water masses with differing chemical properties. Highest levels of A_T at these intermediate depths were generally found at stations close to the shelf, coinciding with higher salinities (Fig. 3) and low oxygen, particularly seen in AR24. For example in AR24 average A_T was 2335 ± 1 µmol kg^{-1} (2333–2338 µmol kg^{-1}) near the continental shelf (stations 137–139), while it averaged 2316 ± 1 µmol kg^{-1} (2296–2331 µmol kg^{-1}) further west in the Trough (station 144–146). This gradient was not observed in the NA_T data and is therefore related to salinity distribution. The high A_T along the shelf edge must therefore be related to the more saline ENAW in the upper 1000 m along the eastern side of the Trough, and also due to the presence of MW between 700 and 1000 m, a highly saline core, characteristically low in oxygen and high in A_T (Cabecadas et al., 2002; Howe et al., 1974; Santana-Casiano et al., 2002). Like oxygen, A_T can therefore be used as an effective tracer of MW in the Rockall Trough. There is also an east–west gradient in C_T between 500 and 1100 m, particularly seen in AR24 and CE0903 (Fig. 4). For example in CE0903 the average C_T between 500 and 1100 m is 2155 ± 2 µmol kg^{-1} (2126–2183 µmol kg^{-1}) at stations 7–13 near the shelf, while the average is 2171 ± 2 µmol kg^{-1} (2153–2180 µmol kg^{-1}) at stations 15–19 at the western side of the Trough. Like in surface waters, the gradient in C_T and nutrients is likely related to water from the subpolar gyre which has been subjected to high levels of winter mixing and upwelling (Pelegrí et al., 2006; Williams and Follows, 2003). Upwelling transports nutrient- and carbon-rich deeper waters back up the water column. In 2010, the higher C_T from the western side of the Trough was measured all the way across the intermediate depths (average C_T 2168 ± 2 µmol kg^{-1}) and is likely related to an elevated SAIW influence that year (McGrath et al., 2012). SAIW likely acquired its high C_T signal from mixing and upwelling in the subpolar gyre when it was formed, and due to low temperatures in its formation region which increases the capability of absorbing more CO_2. The east–west gradient in water parameters is less marked in the northern transect of AR24 relative to the southern transect, due to increased mixing and the absence of SAIW and MW signals.

3.1.5. *Deep waters (> 1500 m)*

There is a strong LSW signal both in the northern and southern transects of the Trough, with characteristically low salinity and high oxygen concentrations. The isopycnals used to describe LSW

in a number of studies range between 27.68 and 27.80 kg m^{-3} (Dengler et al., 2006; Kieke et al., 2006), however this range would suggest that LSW occupies between 900 and 2500 m deep in the Trough. We have however looked at the core of LSW at depths between 1500 and 2000 m, which each year has an average density of 27.75–27.76 kg m^{-3} (ranging between 27.71 and 27.80 kg m^{-3}), and coincides with the characteristic salinity minimum and oxygen maximum values.

In the vertical profiles (Fig. 3a), there is a clear decrease in C_T between 1500 and 2000 m in all datasets relative to the rest of the water column which coincides with the relatively young age of LSW in the Trough, as inferred from CFC data (not shown). The minimum A_T measured at this depth range is due to the low salinity of LSW; as it is absent in the NA_T profiles. Average A_T ranges from 2305–2309 μmol kg^{-1} in LSW in all datasets, similar to A_T values reported for LSW near the Iberian Peninsula by Pérez et al. (1993). Below LSW there is a slight increase in salinity, and decrease in temperature, typical of NEADW. Within this water mass, oxygen concentrations decrease downwards, with a steady increase in nutrients and C_T below 2000 m due to remineralisation of organic matter (Fig. 4a). There is also a steady increase in both A_T and NA_T from below 2000 m to the deepest parts of the Trough due to the dissolution of $CaCO_3$ (Fig. 3b and c). Traces of AABW were found in the deepest water (>3000 m) at the southern entrance to the Rockall Trough, identified using silicate data (McGrath et al., 2012). Highest concentrations of C_T and A_T (and NA_T) are also found at these depths; however there are too few data points to accurately describe the carbonate characteristics of this water mass in the Trough.

3.2. Temporal trends in carbonate parameters between 1991 and 2010

The effects of increasing atmospheric CO_2 on surface water pH can only be compared over the winter months, when biological activity is at a minimum. It is not possible to investigate the change in anthropogenic carbon signal in the surface waters of the Trough due to varying times of sampling between surveys. The WOCE winter surveys were completed in early winter and therefore inorganic carbonate parameters had not reached preformed conditions like in 2009 and 2010. Data from the Mace Head Atmospheric Research Station along the west coast of Ireland show an increase in pCO_2 from 355.4 ppm at the end of winter in 1991 to 393.5 ppm at the end of winter in 2010 (Michele Ramonet, personal communication). Assuming that the air–sea disequilibrium of CO_2 remained constant, along with constant salinity, temperature and alkalinity, this increase of 38.1 ppm pCO_2 is equivalent to an increase in C_T of 18 μmol kg^{-1} and a reduction in pH of 0.038 units (calculated using CO2SYS; Lewis and Wallace, 1998) in surface waters of the Trough over the 19 years.

Sub-surface water, i.e. water at the bottom of the mixed layer in winter surveys and below the thermocline in summer surveys, nutrient and carbon concentrations were examined to identify changes in the 'preformed' carbon conditions between all surveys, without direct seasonal influences (Table 4). Due to varying nutrient and AOU concentrations between the surveys, direct comparisons of C_T and subsequent pH cannot differentiate between anthropogenic and natural factors affecting the C_T distribution. After correcting C_T for remineralisation and dissolution of calcium carbonate, the increase in $C_{T\text{-abio}}$ is 18 ± 3 μmol kg^{-1} in the subsurface layer between 1991 and 2010 (Fig. 5). This is insignificantly less than the increase of 19 ± 4 μmol kg^{-1} in the calculated ΔC_{ant}^{eMLR} in subsurface waters over the same period. Both estimates suggest an increase in ΔC_{ant} of ~1 μmol kg^{-1} yr^{-1} in the Trough between 1991 and 2010.

Table 4
Average concentration of the chemical parameters of the subsurface waters from A01E, A01, AR24, A24, CE0903 and CE10002. Standard deviations are in *italics* beside the average concentrations and *n* is the number of carbon samples from each survey. pH (total), aragonite (Arℿ) and calcite (Caℿ) saturation were calculated using CO2SYS, details described in Methods section. pH was calculated at both potential temperature (θ) and 25 °C. The * indicates where A_T or O_2 are estimated.

Year	Depth	*S*	*T*	DO	AOU	NO_3	Si	PO_4	C_T	A_T	pH (θ) $T=\theta$	pH (t) $T=25$ °C	$C_{T\text{-abio}}$	Arℿ	Caℿ	*n*
1991	**150–250**	**35.44** (*0.08*)	**10.56** (*0.57*)	**248.0** (*3.3*)	**22.9** (*1.5*)	**11.74** (*0.56*)	**4.99** (*0.45*)	**0.77** (*0.05*)	**2125** (*2*)	**2337*** (*3*)	**8.077*** (*0.004*)	**7.861*** (*0.009*)	**934*** (*2*)	**2.21*** (*0.05*)	3.47* (*0.08*)	**11**
1994	**200–300**	**35.43** (*0.07*)	**10.52** (*0.59*)	**246.9** (*3.4*)	**23.7** (*4.5*)	**12.16** (*1.17*)	**4.37** (*0.68*)	**0.74** (*0.06*)	**2125** (*7*)	**2333*** (*3*)	**8.072*** (*0.012*)	**7.855*** (*0.017*)	**935*** (*5*)	**2.17*** (*0.09*)	3.40* (*0.13*)	**11**
1996	**200–300**	**35.42** (*0.07*)	**10.51** (*0.47*)	**242.3** (*2.7*)	**28.1** (*3.4*)	**11.82** (*0.71*)	**4.96** (*0.50*)	**0.77** (*0.05*)	**2132** (*5*)	**2329** (*7*)	**8.047** (*0.013*)	**7.832** (*0.015*)	**941** (*6*)	**2.06** (*0.07*)	3.23 (*0.11*)	**4**
1997	**150–250**	**35.43** (*0.03*)	**10.31** (*0.26*)	**255.7** (*4.2*)	**16.0** (*4.5*)	**10.95** (*0.70*)	**4.79** (*0.62*)	**0.72** (*0.04*)	**2129** (*4*)	**2334** (*2*)	**8.069** (*0.009*)	**7.850** (*0.010*)	**945** (*3*)	**2.15** (*0.05*)	3.38 (*0.08*)	**16**
2009	**400–500**	**35.42** (*0.13*)	**10.36** (*0.97*)	**242.0*** (*19.4*)	**30.8*** (*27.0*)	**12.15** (*3.04*)	**4.97** (*2.36*)	**0.70** (*0.22*)	**2149** (*21*)	**2332*** (*6*)	**8.020*** (*0.042*)	**7.798*** (*0.057*)	**949*** (*3*)	**1.88*** (*0.24*)	2.94* (*0.36*)	**6**
2010	**400–500**	**35.42** (*0.11*)	**10.32** (*0.70*)	**235.4** (*17.7*)	**35.8** (*20.5*)	**13.80** (*2.96*)	**5.61** (*1.86*)	**0.82** (*0.18*)	**2150** (*11*)	**2332** (*5*)	**8.014** (*0.029*)	**7.797** (*0.030*)	**952** (*6*)	**1.88** (*0.14*)	2.94 (*0.21*)	**8**

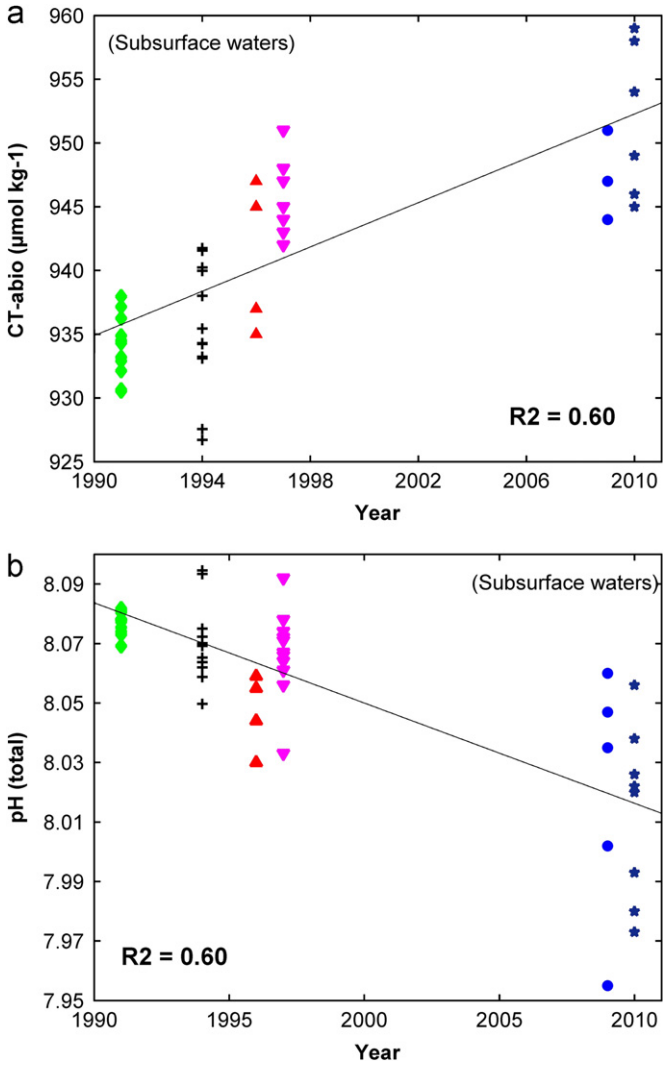

Fig. 5. (a) $\Delta C_{T\text{-abio}}$ concentration (μmol kg^{-1}) and (b) pH (total scale, calculated using in situ C_T, A_T, θ, salinity, pressure, Si and PO_4) in the subsurface waters across all transects of the southern Rockall Trough between 1991 and 2010.

Direct comparison of calculated pH at these depths indicates that pH in subsurface waters has decreased by 0.055 ± 0.004 units since 1991; however the increase in C_T of 25 ± 2 μmol kg^{-1} may be in part due to the higher AOU and nutrient levels, and hence biological activity, in 2010 relative to 1991. Therefore, 18 μmol kg^{-1} and 19 μmol kg^{-1} C_T was added to the 1991 dataset to investigate the change in pH due to the $\Delta C_{T\text{-abio}}$ and ΔC_{ant}^{eMLR}. The increase in $C_{T\text{-abio}}$ is equivalent to a decrease in pH of 0.039 ± 0.002, while the increase in C_{ant}^{eMLR} is equivalent to a pH reduction of 0.041 ± 0.003. Both indicate that subsurface waters in the Trough have acidified by $\sim$0.020 pH units per decade. This is in line with observations from a number of time series (Hawaii Ocean Time-series, the Bermuda Atlantic Time-Series Study, and European Station for Time-Series in the Ocean in the eastern Atlantic) who measured a decrease of 0.02 pH units per decade over the last 20 years (IPCC, 2007). Results are also supported by atmospheric CO_2 data from Mace Head which indicated a reduction in pH in surface waters of 0.02 pH units per decade, assuming constant air–sea disequilibrium. Finally, while surface and subsurface waters are still supersaturated with respect to aragonite and calcite, there is a gradual decrease in saturation states between 1991 and 2010, with a reduction in aragonite saturation from 2.17 ± 0.07 to 1.88 ± 0.06, and a reduction in calcite saturation from 3.40 ± 0.11 to 2.94 ± 0.09, in subsurface waters over the 19 years. Recent field and laboratory experiments have found that despite carbonate saturation greater than 1 (supersaturated), a decrease in saturation state resulted in a decrease in calcification rate of most calcifying organisms (Feely et al., 2004; Veron et al., 2009, and references within).

At intermediate depths (500–1100 m), it is difficult to directly compare the inorganic carbonate parameters due to varying thermohaline profiles and water mass signals between surveys. Despite the large range in inorganic carbon, the span in C_T each year did progressively increase from 2133–2172 μmol kg^{-1} in 1991 to 2151–2194 μmol kg^{-1} in 2010, and a comparison of the upper and lower pH limits indicates a decrease in pH of 0.026–0.043 ± 0.003 units over the 19 years. The increase in C_{ant}^{eMLR} over the same period averaged 15 ± 4 μmol kg^{-1}, ranging from 8 to 22 μmol kg^{-1} between 500 and 1000 m. The increasing C_T and decreasing pH observed in both the subsurface and intermediate depths may therefore have implications for the cold water corals living in the Trough, which are found mainly between 500 and 1000 m deep (White and Dorschel, 2010).

While there is no overall trend in nutrient concentrations, C_T levels increased from 2150 to 2160 μmol kg^{-1} in LSW between 1991 and 2010 (Table 5). Out of this increase of 10 μmol kg^{-1} C_T, 8 μmol kg^{-1} can be attributed to anthropogenic carbon signal since both $\Delta C_{T\text{-abio}}$ and ΔC_{ant}^{eMLR} estimated an increase of 8 ± 4 μmol kg^{-1} in LSW between 1991 and 2010 (Fig. 6). This indicates an increase in anthropogenic carbon of 0.4 μmol kg^{-1} yr^{-1} in LSW in the Trough. Due to changing convection regimes in the Labrador Sea, the air saturation of LSW may vary and rates between 70 and 100% have been reported (Azetsu-Scott et al., 2005). While $\Delta C_{T\text{-abio}}$ is affected by time-varying CO_2 air–sea disequilibrium due to the assumption of constant air saturation during formation, the eMLR method should incorporate such effects through the use of salinity and potential temperature in the regression. Pérez et al. (2010) measured a similar increase in C_{ant} of $\sim$9 μmol kg^{-1} in LSW in the eastern North Atlantic between 1981 and 2006.

There is a decrease in the calculated pH in this water mass of 0.029 ± 0.002 pH units (at in situ temperature) and 0.027 ± 0.002 at 25 °C over the 19 years (Fig. 6, Table 5). Regardless of the initial saturation state or temperature used to calculate pH, there has been a reduction in pH in LSW in the Trough at a rate of 0.015 units per decade. LSW in the Rockall Trough is still supersaturated with calcite and aragonite, with a slight decrease in both aragonite (0.08 ± 0.01) and calcite (0.11 ± 0.01) saturation between 1991 and 2010 (Table 5). Due to the gradual increase in C_T in LSW, without corresponding increase in nutrients or AOU, we assume that this increase in $C_{T\text{-abio}}$ and C_{ant}^{eMLR}, and decrease in pH, is due to increasing levels of anthropogenic carbon in its source water in the Labrador Sea. The rate of increase in C_T in LSW is slower than the observed increase in subsurface waters in the Trough. This may be because surface waters in the Labrador Sea cannot keep pace with increasing atmospheric pCO_2 due to fast transport times away from the surface during deep convection (Tanhua et al., 2007; Terenzi et al., 2007). Also, LSW has not been subjected to as high atmospheric pCO_2 as the subsurface waters that were more recently in contact with the atmosphere. See section of ΔC_{ant}^{eMLR} at the southern entrance to Rockall between 1991 and 2010 (Fig. 7).

In upper NEADW, between 2000 and 2500 m deep, there is an increasing trend in C_T ($R^2 = 0.61$) over the 19 years, ranging from 2150–2161 μmol kg^{-1} in 1991 to 2170–2189 μmol kg^{-1} in 2010. There is a reduction in calculated pH of 0.029 ± 0.002 between 1991 and 2009/10 ($R^2 = 0.68$) in this depth range and an increase in $C_{T\text{-abio}}$ of 3 ± 3 μmol kg^{-1}. The increasing maximum value of C_T in NEADW may indicate that we are seeing the effects of increasing atmospheric CO_2 at depths >2000 m in the Trough. This is supported by Pérez et al. (2010) who measured an increase

Table 5
Average concentration of the chemical parameters in Labrador Sea Water between 1500 and 2000 m across the southern Rockall Trough from A01E, A01, AR24, A24, CE0903 and CE10002. Standard deviations are in *italics* beside the average concentrations and *n* is the number of carbon samples from each survey. pH (total), aragonite ($Ar\Omega$) and calcite ($Ca\Omega$) saturation were calculated using CO2SYS, details described in Methods section. pH was calculated at both potential temperature (θ) and 25 °C. The * indicates where A_T or O_2 are estimated.

Year	*S*	*T*	DO	AOU	NO_3	Si	PO_4	C_T	A_T	pH (t) $T=\theta$	pH (t) $T=25$ °C	$C_{T\text{-abio}}$	$Ar\Omega$	$Ca\Omega$	*n*
1991	**34.90** *(0.01)*	**3.59** *(0.10)*	**277.1*** *(2.1)*	**41.4** *(1.8)*	**17.17** *(0.23)*	**11.62** *(0.57)*	**1.17** *(0.01)*	**2150** *(1)*	**2306*** *(1)*	**8.014*** *(0.004)*	**7.697*** *(0.004)*	**958*** *(2)*	**1.21*** *(0.03)*	**1.87*** *(0.05)*	**11**
1994	**34.91** *(0.02)*	**3.76** *(0.34)*	**270.8** *(8.5)*	**46.0** *(5.7)*	**18.21** *(0.39)*	**10.93** *(0.51)*	**1.16** *(0.02)*	**2151** *(4)*	**2306*** *(2)*	**8.008*** *(0.010)*	**7.691*** *(0.005)*	**955*** *(3)*	**1.19*** *(0.06)*	**1.84*** *(0.03)*	**5**
1996	**34.92** *(0.02)*	**3.69** *(0.27)*	**272.2** *(4.9)*	**45.6** *(3.3)*	17.4 *(0.19)*	**12.01** *(0.73)*	**1.16** *(0.01)*	**2156** *(2)*	**2306** *(3)*	**7.996** *(0.007)*	**7.680** *(0.005)*	**961** *(2)*	**1.16** *(0.04)*	**1.80** *(0.06)*	**14**
1997	**34.93** *(0.01)*	**3.72** *(0.23)*	**267.4** *(5.5)*	**49.3** *(4.8)*	**17.33** *(0.11)*	**13.03** *(0.83)*	**1.16** *(0.01)*	**2160** *(2)*	**2309** *(2)*	**7.995** *(0.006)*	**7.680** *(0.009)*	**961** *(2)*	**1.17** *(0.04)*	**1.82** *(0.06)*	**18**
2009	**34.91** *(0.01)*	**3.65** *(0.21)*	**267.8*** *(6.7)*	**46.4*** *(2.3)*	**17.53** *(0.69)*	**11.49** *(0.98)*	**1.09** *(0.08)*	**2160** *(4)*	**2307*** *(1)*	**7.989*** *(0.015)*	**7.671*** *(0.013)*	**962*** *(5)*	**1.10*** *(0.03)*	**1.70*** *(0.05)*	**5**
2010	**34.92** *(0.01)*	**3.67** *(0.20)*	**273.3** *(4.3)*	**44.0** *(2.1)*	**18.00** *(0.65)*	**11.97** *(1.26)*	**1.09** *(0.03)*	**2160** *(3)*	**2305** *(4)*	**7.985** *(0.014)*	**7.669** *(0.012)*	**966** *(4)*	**1.13** *(0.05)*	**1.76** *(0.08)*	**9**

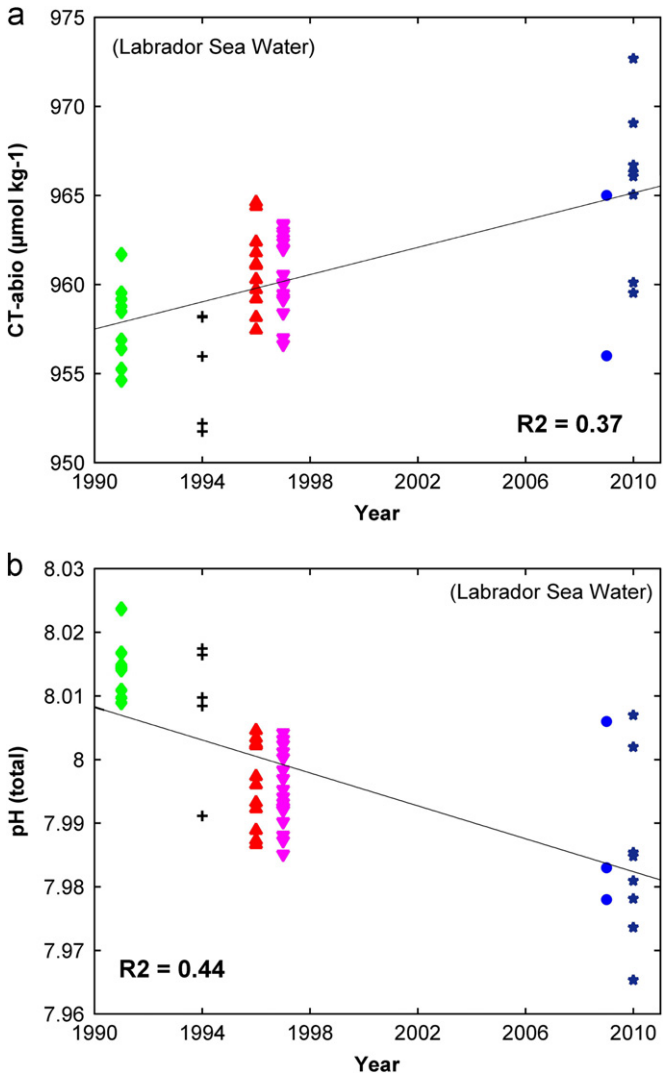

Fig. 6. (a) $\Delta C_{T\text{-abio}}$ concentration ($\mu mol\ kg^{-1}$) (b) pH (total scale, calculated using in situ C_T, A_T, θ, salinity, pressure, Si and PO_4) between 1500 and 2000 m across all transects of the southern Rockall Trough between 1991 and 2010.

in Cant of 4 $\mu mol\ kg^{-1}$ in the NADWu (upper North Atlantic Deep Water) between 1981 and 2006 off the Iberian Peninsula.

Between 2500 and 3000 m, C_T also gradually increases ($R^2=0.45$), ranging from 2158–2185 $\mu mol\ kg^{-1}$ in 1991 to 2182–2206 $\mu mol\ kg^{-1}$ in 2010, with a subsequent decrease in pH of 0.019 ($R^2=0.47$). $\Delta C_{T\text{-abio}}$ however only increases 2 ± 3 $\mu mol\ kg^{-1}$ over the 19 years. Due to only a few data points in the 2009/10 surveys below 2000m, ΔC_{ant}^{eMLR} could not be calculated. Unfortunately we cannot draw conclusions on the changing saturation horizon in the Trough due to a small number of data points below 2300 m in 2009/10. We do however expect a decrease in the depth of aragonite saturation horizon (ASH) in the North Atlantic due to increasing anthropogenic CO_2 penetration. There has already been a 20% reduction in calcium carbonate saturation between 1766 and 2007 (Caldeira and Wickett, 2003; Gattuso and Lavigne, 2009). In the eastern North Atlantic the ASH has shoaled by ~400 m since the Industrial Revolution and is projected to decrease by ~700 m by 2050 (Tanhua et al., 2007). It is expected that the Arctic will be undersaturated with respect to aragonite within a decade (Steinacher et al., 2009). The ASH in the nearby Iceland Sea is shoaling at a rate of 4 m yr^{-1} (Olafsson et al., 2009).

C_T ranges between 2180 and 2205 $\mu mol\ kg^{-1}$ across all surveys below 3000 m, however there is only 1 data point in 2009

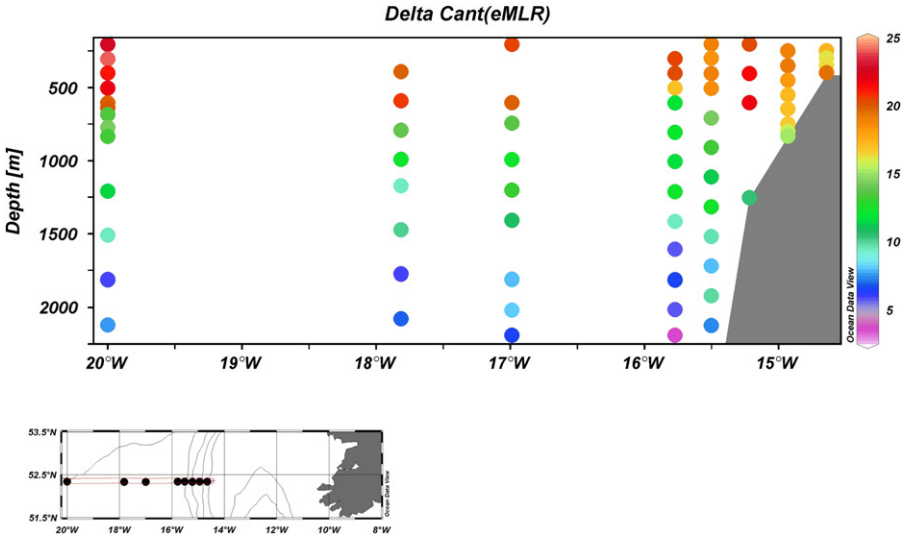

Fig. 7. ΔC_{ant}^{eMLR} (μmol kg^{-1}) between 200 and 2200 m across the southern Rockall Trough between 1991 and 2010.

and 1 in 2010, so we cannot draw conclusions about decadal changes in carbonate chemistry in AABW between surveys. Pérez et al. (2010) reported C_{ant} in lower NADW off the Iberian Peninsula between 4 and 9 μmol kg^{-1}, with no overall increasing/decreasing trend between 1981 and 2006. It is expected that AABW should have only a small anthropogenic signal due to its high age.

The storage of anthropogenic carbon between 1991 and 2010 was calculated by integrating the vertical profiles of ΔC_{ant}^{eMLR}. We provide an estimate of the carbon storage rate between 1991 and 2010 of 0.70 ± 0.08 mol m^{-2} yr^{-1} between 200 and 1000 m, and 0.50 ± 0.04 mol m^{-2} yr^{-1} between 1000 and 2000 m. If we assume a constant air–sea CO_2 disequilibrium, the storage rate for the top 200 m is 0.17 ± 0.01 mol m^{-2} yr^{-1}, resulting in a total storage rate for the upper 2000 m in the Trough of 1.37 ± 0.13 mol m^{-2} yr^{-1}. The higher storage rates of the upper water column are likely associated with the warmer, saltier waters of the eastern North Atlantic with a large buffer capacity (Sabine and Tanhua, 2010).

4. Conclusion

We have described a comprehensive dataset of inorganic carbon and associated parameters from a range of water masses in the Rockall Trough, against which future changes can be measured. The 2009 and 2010 datasets provide a baseline of late winter or 'preformed' inorganic carbon and acidity levels in the surface waters of the Trough. Comparisons with data from WOCE surveys in the 1990s show that the pH in subsurface waters in the Trough has decreased by 0.040 ± 0.003 units due to a gradual increase in $C_{T\text{-abio}}$ and C_{ant}^{eMLR} of $18–19 \pm 4$ μmol kg^{-1} between 1991 and 2010. This is in line with a number of other time series who also measured a decrease in pH of 0.02 units per decade. It appears that rising C_T in subsurface waters in the Trough is keeping pace with changes in atmospheric CO_2 concentrations since the increase in pCO_2 measured at Mace Head is equivalent to a similar increase in C_T and decrease in pH. ΔC_{ant} has increased in LSW by 8 ± 4 μmol kg^{-1}, with a reduction in pH of 0.029 ± 0.002 over the 19 years. There has been a gradual reduction in aragonite and calcite saturation states which may have implications for calcifying organisms in the region, particularly the cold water corals along the Irish continental shelf. The total water column storage rate of 1.37 ± 0.13 mol m^{-2} yr^{-1} is significantly larger than the global average of 0.55 mol m^{-2} yr^{-1} (Sabine et al., 2008). In general we think that this observed increase in anthropogenic carbon is robust as two independent methods for calculating ΔC_{ant} give consistent results and show high level of agreement with other studies in the North Atlantic.

Acknowledgements

This study was funded by the Irish Government funded project "Impacts of Increased Atmospheric CO_2 on Ocean Chemistry and Ecosystems", with Colin O'Dowd as PI and carried out under the Sea Change strategy with the support of the Marine Institute and the Marine Research Sub-Programme of the National Development Plan 2007–2013. Surveys were funded by the Irish government's National Development Plan 2007–2013. We are grateful to the officers, crew and scientists on the cruises referred to in this paper. We thank Kieran Lyons and Glenn Nolan for their help in Matlab, and Jonathan White for his help with R. We would like to extend our gratitude to two anonymous reviewers for their constructive and careful comments.

Appendix A. Supplementary material

Supplementary data associated with this article can be found in the online version at http://dx.doi.org/10.1016/j.dsr.2012.05.011.

References

Arhan, M., 1990. The North-Atlantic Current and Sub-Arctic Intermediate Water. J. Mar. Res. 48 (1), 109–144.
Arhan, M., Colin de Verdière, A., Mémery, L., 1994. The eastern boundary of the subtropical North Atlantic. J. Phys. Oceanogr. 24, 1295–1316.
Azetsu-Scott, K., Jones, E.P., Gershey, R.M., 2005. Distribution and ventilation of water masses in the Labrador Sea inferred from CFCs and carbon tetrachloride. Mar. Chem. 94 (1–4), 55–66.
Broecker, W.S., Peng, T.H., 1982. Tracers in the Sea. Columbia University Press, Palisades, NY.
Cabecadas, G., Brogueira, M.J., Goncalves, C., 2002. The chemistry of Mediterranean outflow and its interactions with surrounding waters. Deep-Sea Res. Part II—Top. Stud. Oceanogr. 49 (19), 4263–4270.
Caldeira, K., Wickett, M.E., 2003. Oceanography: anthropogenic carbon and ocean pH. Nature 425 (6956) (365–365).
CDIAC, 2003. Carbon Dioxide, Hydrographic, and Chemical Data Obtained During the R/V Knorr Cruises in the North Atlantic Ocean on WOCE Sections AR24

(November 2–December 5, 1996) and A24, A20, and A22 (May 30–September 3, 1997). Carbon Dioxide Information Analysis Center, ORNL/CDIAC-143, NDP-082.

Chen, C.-T., 2002. Shelf-vs. dissolution-generated alkalinity above the chemical lysocline. Deep-Sea Res. II 49, 5365–5375.

De Mol, B., Van Rensbergen, P., Pillen, S., Van Herreweghe, K., Van Rooij, D., McDonnell, A., Huvenne, V., Ivanov, M., Swennen, R., Henriet, J.P., 2002. Large deep-water coral banks in the Porcupine Basin, southwest of Ireland. Mar. Geol. 188 (1–2), 193–231.

Dengler, M., Fischer, J.r., Schott, F.A., Zantopp, R., 2006. Deep Labrador Current and its variability in 1996–2005. Geophys. Res. Lett., 33.

Dickson, A.G., Millero, F.J., 1987. A comparison of the equilibrium constants for the dissociation of carbonic acid in seawater media. Deep Sea Res. 34, 1733–1743.

Dickson, A.G., Riley, J.P, 1978. The effect of analytical error on the evaluation of the components of the aquatic carbon-dioxide system. Mar. Chem. 6 (1), 77–85.

Dickson, A.G., Sabine, C.L., Christian, J.R., 2007. Guide to Best Practices for Ocean CO_2 Measurements. PICES Special Publication 3, 1–191.

Doney, S.C., Lima, I., Feely, R.A., Glover, D.M., Lindsay, K., Mahowald, N., Moore, J.K., Wanninkhof, R., 2009. Mechanisms governing interannual variability in upper-ocean inorganic carbon system and air–sea CO_2 fluxes: physical climate and atmospheric dust. Deep Sea Res. Part II: Top. Stud. Oceanogr. 56 (8–10), 640–655.

Ellett, D.J., Edwards, A., Bowers, R., 1986. The hydrography of the Rockall Channel—an overview. Proc. R. Soc. Edinburgh 88B, 61–68.

Ellett, D.J., Martin, J.H.A., 1973. Physical and chemical oceanography of Rockall Channel. Deep-Sea Res. 20 (7), 585–625.

Feely, R.A., Sabine, C.L., Lee, K., Berelson, W., Kleypas, J., Fabry, V.J., Millero, F.J., 2004. Impact of anthropogenic CO_2 on the $CaCO_3$ system in the oceans. Science 305 (5682), 362–366.

Friis, K., Körtzinger, A., Pätsch, J., Wallace, D.W.R., 2005. On the temporal increase of anthropogenic CO_2 in the subpolar North Atlantic. Deep Sea Res. Part I: Oceanogr. Res. Pap. 52 (5), 681–698.

Friis, K., Körtzinger, A., Wallace, D.W.R., 2003. The salinity normalization of marine inorganic carbon chemistry data. Geophys. Res. Lett. 30 (2), 1085.

Friis, K., Najjar, R.G., Follows, M.J., Dutkiewicz, S., 2006a. Possible overestimation of shallow-depth calcium carbonate dissolution in the ocean. Global Biogeochem. Cycles 20 (4), GB4019.

Friis, K., Najjar, R.G., Follows, M.J., Dutkiewicz, S., Körtzinger, A., Johnson, K.M., 2006b. Dissolution of calcium carbonate: observations and model results in the North Atlantic. Biogeosci. Discuss. 3 (5), 1715–1738.

Gattuso, J.P., Lavigne, H., 2009. Technical note: approaches and software tools to investigate the impact of ocean acidification. Biogeosciences 6 (10), 2121–2133.

Harvey, J., 1982. Theta-S relationships and water masses in the eastern North Atlantic. Deep-Sea Res. Part a—Oceanogr. Res. Pap. 29 (8), 1021–1033.

Harvey, J., Arhan, M., 1988. The water masses of the Central North Atlantic in 1983–84. J. Phys. Oceanogr. 18, 1855–1875.

Holliday, N.P., Pollard, R.T., Read, J.F., Leach, H., 2000. Water mass properties and fluxes in the Rockall Trough 1975–1998. Deep Sea Res. I 47, 1303–1332.

Howe, M.R., Abdullah, M.I., Deetae, S., 1974. Interpretation of double T-S Maxima in Mediterranean outflow using chemical tracers. J. Mar. Res. 32 (3), 377–386.

IPCC, 2007. Climate Change 2007: The Physical Science Basis. Contribution of Working Group I to the Fourth Assessment Report of the Intergovernmental Panel on Climate Change. Solomon S., Qin D., Manning M., Chen Z., Marquis M., Averyt K.B., et al. (Eds.), Cambridge, UK, Cambridge Univ. Press.

Johnson, K.M., Sieburth, J.M., Williams, P.J.l., Brändström, L., 1987. Coulometric total carbon dioxide analysis for marine studies: automation and calibration. Mar. Chem. 21 (2), 117–133.

Kieke, D., Rhein, M., Stramma, L., Smethie, W.M., LeBel, D.A., Zenk, W., 2006. Changes in the CFC inventories and formation rates of Upper Labrador Sea Water, 1997–2001. J. Phys. Oceanogr. 36, 64–86.

Körtzinger, A., Koeve, W., Kähler, P., Mintrop, L., 2001. C:N ratios in the mixed layer during the productive season in the northeast Atlantic Ocean. Deep Sea Res. Part I: Oceanogr. Res. Pap. 48 (3), 661–688.

Körtzinger, A., Send, U., Lampitt, R., Hartman, S., Wallace, D.W.R., Karstensen, J., Villagarcia, M.G., Llinas, O., DeGrandpre, M.D., 2008. The seasonal pCO_2 cycle at 49°N/16.5°W in the northeastern Atlantic Ocean and what it tells us about biological productivity. J. Geophys. Res.—Oceans 113, C04020.

Lee, K., Tong, L.T., Millero, F.J., Sabine, C.L., Dickson, A.G., Goyet, C., Park, G.H., Wanninkhof, R., Feely, R.A., Key, R.M., 2006. Global relationships of total alkalinity with salinity and temperature in surface waters of the world's oceans. Geophys. Res. Lett. 33, 19.

Levine, N.M., Doney, S.C., Wanninkhof, R., Lindsay, K., Fung, I.Y., 2008. Impact of ocean carbon system variability on the detection of temporal increases in anthropogenic CO_2. J. Geophys. Res.—Oceans 113 (C3).

Lewis, E., Wallace, D.W.R., 1998. Program Developed for CO_2 System Calculations. ORNL/CDIAC-105. Carbon Dioxide Information Analysis Center, Oak Ridge National Laboratory, U.S. Department of Energy, Oak Ridge, Tennessee.

McCartney, M.S., 1992. Recirculating components to the deep boundary current of the northern North Atlantic. Prog. Oceanogr. 29 (4), 283–383.

McGrath, T., Nolan, G., McGovern, E., 2012. Chemical characteristics of water masses in the Rockall Trough. Deep Sea Res. Part I: Oceanogr. Res. Pap. 61 (0), 57–73.

Mehrbach, C., Culberson, C.H., Hawley, J.E., Pytkowicz, R.M., 1973. Measurement of the apparent dissociation constants of carbonic acid in seawater at atmospheric pressure. Limnol. Oceanogr. 18, 897–907.

Millero, F.J., 2007. The marine inorganic carbon cycle. Chem. Rev. 107, 308–341.

Millero, F.J., Dickson, A.G., Eischeid, G., Goyet, C., Guenther, P.R., Johnson, K.M., Key, R.M., Lee, K., Purkerson, D., Sabine, C.L., Schottle, R.G., Wallace, D.W.R., Lewis, E., Winn, C.D., 1998a. Assessment of the quality of the shipboard measurements of total alkalinity on the WOCE Hydrographic Program Indian Ocean CO_2 survey cruises 1994–1996. Mar. Chem. 63, 9–20.

Millero, F.J., Lee, K., Roche, M., 1998b. Distribution of alkalinity in the surface waters of the major oceans. Mar. Chem. 60 (1–2), 111–130.

Millero, F.J., Zhang, J.-Z., Lee, K., Campbell, D.M., 1993. Titration alkalinity of seawater. Mar. Chem. 44 (2–4), 153–165.

Milliman, J.D., Troy, P.J., Balch, W.M., Adams, A.K., Li, Y.H., Mackenzie, F.T., 1999. Biologically mediated dissolution of calcium carbonate above the chemical lysocline? Deep Sea Res. Part I: Oceanogr. Res. Pap. 46 (10), 1653–1669.

Mintrop, L., Pérez, F.F., Gonzalez-Dávila, M., Santana-Casiano, J.M., Körtzinger, A., 2000. Alkalinity determination by potentiometry: intercalibration using three different methods. Cienc. Mar. 26 (1), 23–37.

Monterey, G., Levitus, S., 1997. Seasonal Variability of Mixed Layer Depth for the World Ocean. NOAA Atlas NESDIS 14. U.S. Government Printing Office, Washington D.C..

New, A.L., Smythe-Wright, D., 2001. Aspects of the circulation in the Rockall Trough. Cont. Shelf Res. 21 (8–10), 777–810.

Olafsson, J., Olafsdottir, S.R., Benoit-Cattin, A., Danielsen, M., Arnarson, T.S., Takahashi, T., 2009. Rate of Iceland Sea acidification from time series measurements. Biogeosci. Discuss. 6 (3), 5251–5270.

Orr, J.C., Fabry, V.J., Aumont, O., Bopp, L., Doney, S.C., Feely, R.A., Gnanadesikan, A., Gruber, N., Ishida, A., Joos, F., Key, R.M., Lindsay, K., Maier-Reimer, E., Matear, R., Monfray, P., Mouchet, A., Najjar, R.G., Plattner, G.K., Rodgers, K.B., Sabine, C.L., Sarmiento, J.L., Schlitzer, R., Slater, R.D., Totterdell, I.J., Weirig, M.F., Yamanaka, Y., Yool, A., 2005. Anthropogenic ocean acidification over the twenty-first century and its impact on calcifying organisms. Nature 437 (7059), 681–686.

Pelegrí, J.L., Marrero-Díaz, A., Ratsimandresey, A.W., 2006. Nutrient irrigation of the North Atlantic. Prog. Oceanogr. 70 (2–4), 366–406.

Pérez, F.F., Mouriño, C., Fraga, F., Ríos, A.F., 1993. Displacement of water masses and remineralization rates off the Iberian Peninsula by nutrient anomalies. J. Mar. Res. 51, 869–892.

Pérez, F.F., Vázquez-Rodríguez, M., Mercier, H., Velo, A., Lherminier, P., Ríos, A.F., 2010. Trends of anthropogenic CO_2 storage in North Atlantic water masses. Biogeosciences 7, 1789–1807.

Pollard, R.T., Griffiths, M.J., Cunningham, S.A., Read, J.F., Perez, F.F., Rios, A.F., 1996. Vivaldi 1991—a study of the formation, circulation and ventilation of Eastern North Atlantic Central Water. Prog. Oceanogr. 37 (2), 167–192.

Ríos, A.F., Anderson, T.R., Pérez, F.F., 1995. The carbonic system distribution and fluxes in the NE Atlantic during Spring 1991. Prog. Oceanogr. 35 (4), 295–314.

Ríos, A.F., Pérez, F.F., Fraga, F., 2001. Long-term (1977–1997) measurements of carbon dioxide in the Eastern North Atlantic: evaluation of anthropogenic input. Deep Sea Res. Part II: Top. Stud. Oceanogr. 48 (10), 2227–2239.

Roberts, J.M., Long, D., Wilson, J.B., Mortensen, P.B., Gage, J.D., 2003. The cold-water coral *Lophelia pertusa* (Scleractinia) and enigmatic seabed mounds along the north–east Atlantic margin: are they related? Mar. Pollut. Bull. 46 (1), 7–20.

Rodgers, K.B., Key, R.M., Gnanadesikan, A., Sarmiento, J.L., Aumont, O., Bopp, L., Doney, S.C., Dunne, J.P., Glover, D.M., Ishida, A., Ishii, M., Jacobson, A.R., Monaco, C.L., Maier-Reimer, E., Mercier, H., Metzl, N., Pérez, F.F., Rios, A.F., Wanninkhof, R., Wetzel, P., Winn, C.D., Yamanaka, Y., 2009. Using altimetry to help explain patchy changes in hydrographic carbon measurements. J. Geophys. Res. 114 (C09013).

Sabine, C.L., Feely, R., Millero, F.J., Dickson, A.G., Langdon, C., 2008. Decadal changes in Pacific carbon. J. Geophys. Res.—Oceans 113 (C07021).

Sabine, C.L., Feely, R.A., Gruber, N., Key, R.M., Lee, K., Bullister, J.L., Wanninkhof, R., Wong, C.S., Wallace, D.W.R., Tilbrook, B., Millero, F.J., Peng, T.H., Kozyr, A., Ono, T., Rios, A.F., 2004. The oceanic sink for anthropogenic CO_2. Science 305 (5682), 367–371.

Sabine, C.L., Tanhua, T., 2010. Estimation of anthropogenic $CO_{(2)}$ inventories in the ocean. Annu. Rev. Mar. Sci., 175–198.

Santana-Casiano, J.M., Gonzalez-Davila, M., Laglera, L.M., 2002. The carbon dioxide system in the Strait of Gibraltar. Deep Sea Res. Part II: Top. Stud. Oceanogr. 49 (19), 4145–4161.

Schneider, A., Wallace, D.W.R., Körtzinger, A., 2007. Alkalinity of the Mediterranean Sea. Geophys. Res. Lett. 34 (15), 1–5.

Steinacher, M., Joos, F., Frölicher, T.L., Plattner, G.-K., Doney, S.C., 2009. Imminent ocean acidification in the Arctic projected with the NCAR global coupled carbon cycle-climate model. Biogeosciences 6, 515–533.

Stoll, M.H.C., van Aken, H.M., de Baar, H.J.W., Kraak, M., 1996. Carbon dioxide characteristics of water masses in the northern North Atlantic Ocean. Mar. Chem. 55, 217–232.

Takahashi, T., Sutherland, S.C., Sweeney, C., Poisson, A., Metzl, N., Tilbrook, B., Bates, N., Wanninkhof, R., Feely, R.A., Sabine, C., Olafsson, J., Nojiri, Y., 2002. Global sea–air CO_2 flux based on climatological surface ocean $pCO_{(2)}$, and seasonal biological and temperature effects. Deep-Sea Res. Part II—Top. Stud. Oceanogr. 49 (9–10), 1601–1622.

Tanhua, T., Biastoch, A., Körtzinger, A., Lüger, H., Böning, C., Wallace, D.W.R., 2006. Changes of anthropogenic CO_2 and CFCs in the North Atlantic between 1981 and 2004. Global Biogeochem. Cycles 20 (4), GB4017.

Tanhua, T., Körtzinger, A., Friis, K., Waugh, D.W., Wallace, D., 2007. An estimate of anthropogenic CO_2 inventory from decadal changes in oceanic carbon content. In: Proceedings of the National Academy of Science of the USA, vol. 104.

Terenzi, F., Hall, T.M., Khatiwala, S., Rodehacke, C.B., LeBel, D.A., 2007. Uptake of natural and anthropogenic carbon by the Labrador Sea. Geophys. Res. Lett. 34 (6), L06608.

Tomczak, M., Godfrey, J.S., 1994. Regional Oceanography: An Introduction. Pergamon, Oxford.

Tsuchiya, M., Talley, L.D., McCartney, M.S., 1992. An eastern Atlantic section from Iceland southward across the equator. Deep-Sea Res. Part a—Oceanogr. Res. Pap. 39 (11–12A), 1885–1917.

van Aken, H.M., 2000. The hydrography of the mid-latitude northeast Atlantic Ocean I: the deep water masses. Deep-Sea Res. Part I—Oceanogr. Res. Pap. 47 (5), 757–788.

Veron, J.E.N., Hoegh-Guldberg, O., Lenton, T.M., Lough, J.M., Obura, D.O., Pearce-Kelly, P., Sheppard, C.R.C., Spalding, M., Stafford-Smith, M.G., Rogers, A.D., 2009. The coral reef crisis: the critical importance of <350 ppm CO_2. Mar. Pollut. Bull. 58 (10), 1428–1436.

Wanninkhof, R., Doney, S.C., Bullister, J.L., Levine, N.M., Warner, M., Gruber, N., 2010. Detecting anthropogenic CO_2 changes in the interior Atlantic Ocean between 1989 and 2005. J. Geophys. Res.—Oceans, 115.

Wanninkhof, R., Peng, T.H., Huss, B., Sabine, C.L., Lee, K., et al., 2003. Comparison of Inorganic Carbon System Parameters Measured in the Atlantic Ocean from 1990 to 1998 and Recommended Adjustments. ORNL/CDIAC-140.

Wheeler, A.J., Kozachenko, M., Henry, L.A., Foubert, A., de Haas, H., Huvenne, V.A.I., Masson, D.G., Olu, K., 2011. The Moira Mounds, small cold-water coral banks in the Porcupine Seabight, NE Atlantic: part A—an early stage growth phase for future coral carbonate mounds? Mar. Geol. 282, 53–64.

White, M., Dorschel, B., 2010. The importance of the permanent thermocline to the cold water coral carbonate mound distribution in the NE Atlantic. Earth Planet. Sci. Lett. 296 (3–4), 395–402.

Williams, R.J., Follows, M.J., 2003. Physical transport of nutrients and the maintenance of biological production. In: Fasham, M. (Ed.), Ocean Biogeochemistry: The Role of the Ocean Carbon Cycle in Global Change. Springer.

Wolf-Gladrow, D.A., Zeebe, R.E., Klaas, C., Körtzinger, A., Dickson, A.G., 2007. Total alkalinity: the explicit conservative expression and its application to biogeochemical processes. Mar. Chem. 106 (1–2), 287–300.

Yashayaev, I., 2007. Hydrographic changes in the Labrador Sea, 1960–2005. Prog. Oceanogr. 73 (3–4), 242–276.

Yashayaev, I., van Aken, H.M., Holliday, N.P., Bersch, M., 2007. Transformation of the Labrador Sea Water in the subpolar North Atlantic. Geophys. Res. Lett. 34 (22), L22605.

Zeebe, R.E., Wolf-Gladrow, D., 2003. CO_2 in Seawater: Equilibrium, Kinetics, Isotopes. Elsevier.

Supplementary Information
Inorganic carbon and pH levels in the Rockall Trough
McGrath, T., Kivimae, C., Tanhua, T., Cave, R.R., McGovern, E.

Potential Temperature-Salinity Plots

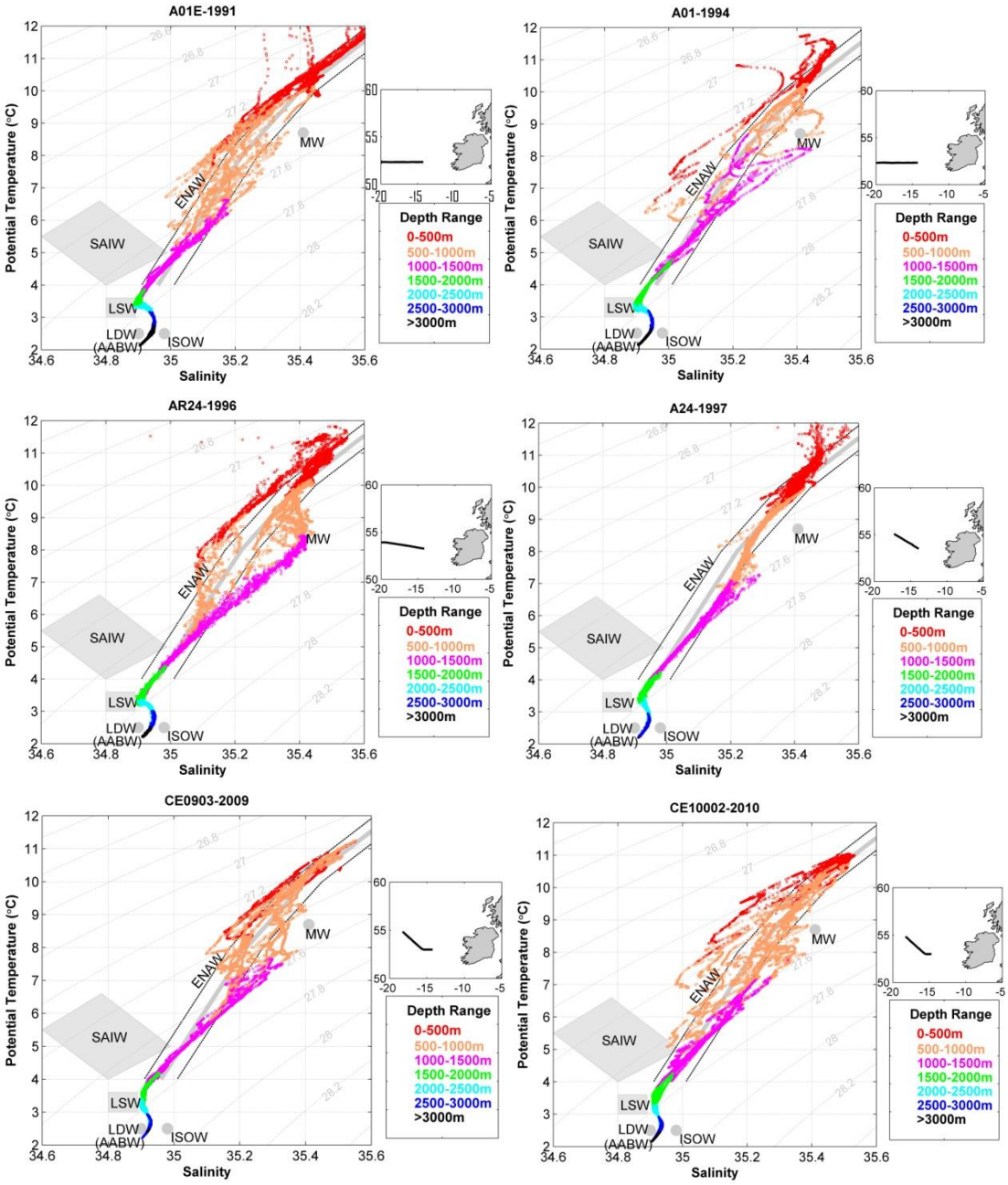

Figure 1. θ-S plots with density contours, using CTD data of the southern transect from (i) A01E, (ii) A01 (iii) AR24, (iv) A24, (v) CE0903 and (vi) CE10002. A subplot outlining the transect position is beside each θ-S plot. Water mass properties were taken from the literature: ENAW, MW, LSW and AABW (Harvey, 1982); SAIW (Bubnov, 1968; Harvey and Arhan, 1988); LDW (Holliday et al., 2000); ISOW

(Harvey, 1982; van Aken and Becker, 1996). Note the temperature and salinity of MW is much higher in the source region, properties plotted here are typical of MW in the eastern North Atlantic.

Salinity contour sections

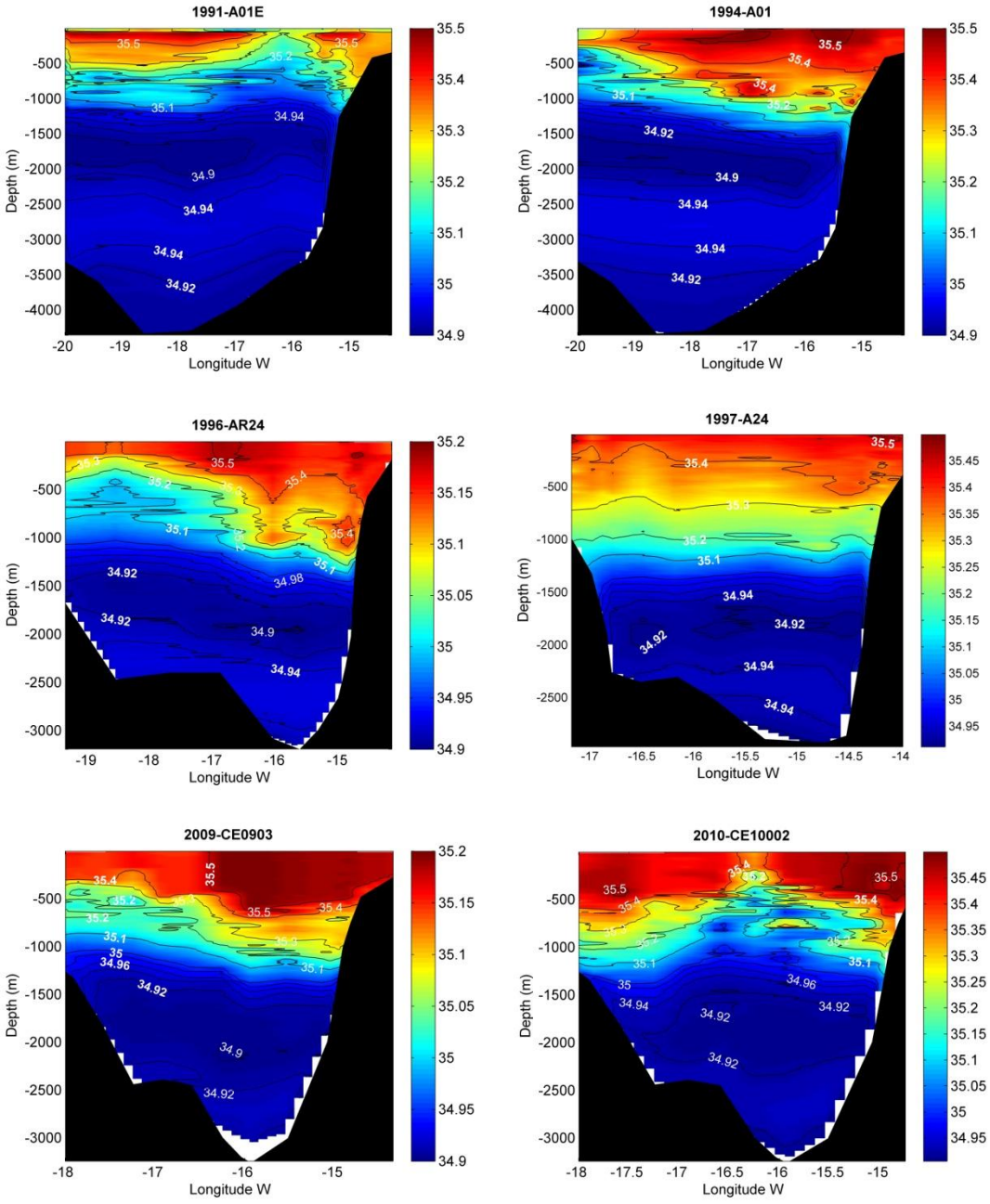

Figure 2. Salinity contour sections across the Rockall Trough for each of the surveys.

Calculation of A_T using multiple linear regression, where A_T is a function of temperature, salinity, C_T, PO_4 and Si.

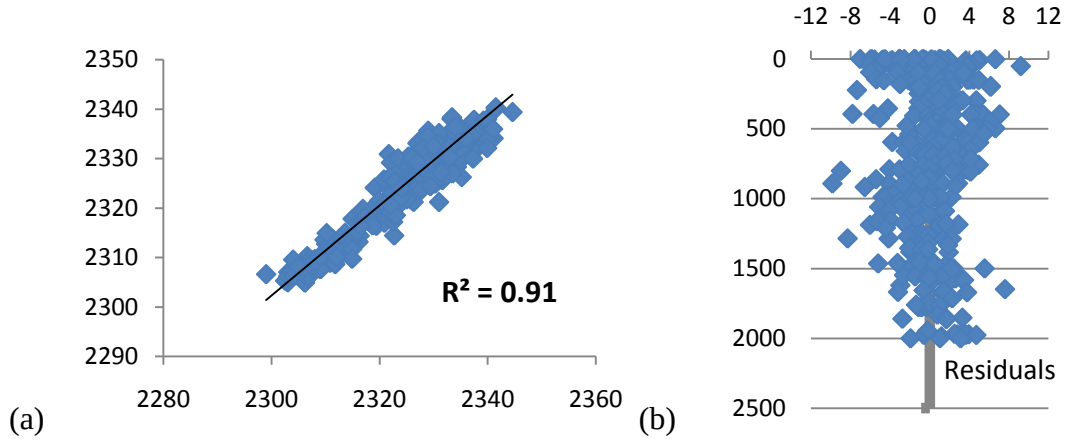

Figure 2. (a) Measured A_T plotted against the calculated A_T using multiple linear regression (MLR) in the top 2000m. (b) The residuals, measured A_T minus the calculated A_T, with depth (m).

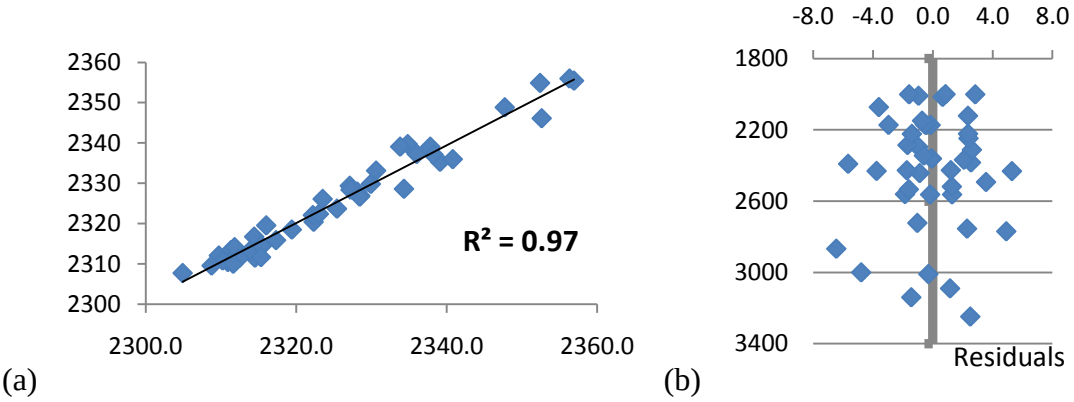

Figure 3. (a) Measured A_T plotted against the calculated A_T using multiple linear regression (MLR) below 2000m. (b) The residuals, measured A_T minus the calculated A_T, with depth (m).

Table 1. Derived multiple linear regression equation for A_T prediction of the combined 1996, 1997 and 2010 datasets for the top 2000m and below 2000m; a_0 is the intercept, R is the average residual (the predicted A_T minus measured A_T), R^2 is the regression coefficient and *n* is the number of samples in the regression.

	a_0	$a_1(T)$	$a_2(S)$	$a_3(C_T)$	$a_4(PO_4)$	$a_5(Si)$	R	R^2	*n*
< 2000m	721.15	1.61	50.07	-0.09	-2.74	1.89	0	0.91	382
> 2000m	2124.82	7.79	10.33	-0.10	-10.54	2.15	-0.1	0.97	50

References

Bubnov, V.A., 1968. Intermediate subarctic waters in the northern part of the Atlantic Ocean. Okeanologia, 19: 136-153.

Harvey, J., 1982. Theta-S relationships and water masses in the eastern North Atlantic. Deep-Sea Research Part a-Oceanographic Research Papers, 29(8): 1021-1033.

Harvey, J. and Arhan, M., 1988. The water masses of the Central North Atlantic in 1983-84. Journal of Physical Oceanography, 18: 1855-1875.

Holliday, N.P., Pollard, R.T., Read, J.F. and Leach, H., 2000. Water mass properties and fluxes in the Rockall Trough 1975-1998. Deep Sea Research I, 47: 1303-1332.

van Aken, H.M. and Becker, G., 1996. Hydrography and through-flow in the north-eastern North Atlantic Ocean: the NANSEN project. Progress In Oceanography, 38(4): 297-346.

Paper III

Net community production from biogeochemical parameters along the Irish continental slope from 49.8 – 55.4ºN

Submitted to Marine Chemistry

Caroline Kivimäe [a] , Triona McGrath [a,b], Rachel R. Cave [a], and Martin White [a]

[a] National University of Ireland, Galway
[b] Marine Institute, Ireland

Abstract

Marine primary production is a major driver of the transfer of carbon from the atmosphere to the deep ocean, partially controlling both the concentration of inorganic carbon in surface waters and the export of organic carbon from surface to deeper waters. Primary production in turn is controlled by the availability of light and dissolved inorganic nutrients. This paper presents the net community production (NCP), based on measurements of nitrate, phosphate and dissolved oxygen, from six transects across the shelf edge (49.8-55.4°N) in June 2009, the first NCP estimates for this part of the Irish shelf. Separate estimates of NCP derived from nitrate and phosphate were in good agreement, and combined with measured dissolved inorganic carbon allowed the calculation of air-sea exchange of CO_2. NCP estimates based on nitrate ranged from 37 (±3) – 114 (±11) g C m^{-2}, with local maxima above the 500-1000 m isobaths, indicating enhanced NCP above the mid-upper continental slope. Air-sea exchange of CO_2 ranged between -5.5 (±3.7) and -34.7 (±6.3) g C m^{-2} (uptake by surface waters), except at one station on top of the Porcupine Bank where outgassing had taken place.

Introduction

The global oceans' primary productivity (PP) estimated by models to be 35-78 GtC yr^{-1} (Carr et al., 2006), is an enormous resource, being the 'motor' driving almost all life in the oceans. The amount of PP varies depending on location but also shows a large year to year variability. PP is an essential link in the global carbon cycle, transforming inorganic carbon into organic carbon. During this process inorganic carbon concentrations in the surface seawater decrease, enhancing uptake of atmospheric CO_2. The organic carbon created during PP can either be recycled in the mixed layer or exported to greater depths; when exported, the carbon can be effectively sequestered from the atmosphere for up to hundreds of years.

The increasing atmospheric CO_2, from 280 μatm prior to the industrial revolution to 394 μatm in February 2012 (www.esrl.noaa.gov/gmd/ccgg/trends/), has an effect on the surface ocean where the PP takes place, by increasing the concentrations of dissolved inorganic carbon (C_T), leading to lower pH and by trapping radiation which increases the temperature at the sea surface (WBGU, 2006). While it still is not clear how high pCO_2 levels will affect the amount of net community production, especially since it may affect various plankton species differently (Crawfurd et al., 2011; Delille et al., 2005; Engel et al., 2005), decreasing pH is likely to have a direct effect on calcification. Mesocosm experiments with coccolithophorids (e.g. *Emiliania huxleyi*) have shown that at high pCO_2/low pH the plankton struggle to produce their $CaCO_3$ skeletons (Riebesell et al., 2000; Zondervan et al., 2001) and this in turn may influence the amount of export production giving a positive feed-back on climate change. Knowledge of the amount of PP taking place in the different parts of the ocean, what controls it and how it varies both spatially and temporally is thus of great importance for both biogeochemical cycling and climate change research.

Biological production can be quantified in several ways with different relationships to gross primary production (the total amount of carbon fixed during PP). One quantitative measure of PP is net community production (NCP), which is the gross PP less community respiration (Platt et al., 1989). NCP thus represents the amount of organic material available for the heterotrophs further up the food chain. The integrated drawdown of dissolved inorganic carbon (C_T) and nutrients seen in the

water column as a result of biological activity can be used for estimating NCP. Export production is the part of the NCP that falls down below the mixed layer. Considering the increase of dissolved organic carbon and recycling of organic material that occurs within the mixed layer during the productive season, export production is always smaller than the NCP.

The continental slope is a dynamic region of the ocean and a natural boundary between contrasting continental shelf and deep ocean water masses. Transects across the slope will show this transition of waters and water properties. The steep topography of the NW European continental slope (with a gradient up to 11% between 750-1000 m in this study) gives the conditions for a topographically steered current along the slope. White and Bowyer (1997) and Burrows and Thorpe (1999) have shown such a current exists along the slope west of Ireland and Scotland; it is possible that this current persists along the entire NW European continental margin. The shelf edge current (SEC) is characterised by a warm saline core found between the 300-1000 m isobaths northwest of Malin Head, Ireland (Hill and Mitchelson-Jacob, 1993; White and Bowyer, 1997), and is important for cross-slope exchange and fluxes.

The physical and biogeochemical properties of the waters in the Rockall Trough (53-56°N) during winter have recently been described in McGrath et al. (2012) and McGrath et al. (in press). The OMEX project looked at primary production across the Celtic Sea shelf break from 47-50ºN (Joint et al. (2001) and references therein). However this paper presents what we believe are the first NCP estimates to be published from along the Irish continental slope between 49.8-55.4°N (the Porcupine Sea-bight, Porcupine Bank and the eastern flank of the Rockall Trough), together with water properties in the area and their evolution along and across the shelf edge, and from winter to summer.

Material and methods

Sample collection and analysis

The data presented here are mainly from a summer survey CE0911 (14-22 June 2009) but other data are included from 3 winter and 2 spring surveys (see Table 1). The surveys were conducted onboard R/V Celtic Explorer between May 2008 and February 2010 (Figure 1 and Table 1). Seawater was sampled with a Seabird 911 CTD with a carousel of 12 or 24 Niskin bottles. Parameters sampled on CE0911 were total dissolved inorganic carbon (C_T), total alkalinity (A_T), dissolved inorganic nutrients (silicate (Si), total oxidised nitrogen (TOxN), nitrite (NO_2), phosphate (P)) and salinity. Nitrate (NO_3) was calculated as TOxN minus NO_2. Discrete dissolved oxygen (DO) samples were also collected and used to calibrate the CTD oxygen sensor (SBE 43), according to Sea-Bird Electronics application note 64-2 (http://www.seabird.com/application_notes/AN64-2.htm).

DO samples were analysed at sea following the SOP by Dickson (1995), using a Metrohm Titrino 712, with visual endpoint determination. Precision, estimated by running duplicate samples, was ±1μmol kg^{-1}.

Samples for dissolved nutrients were filtered through acid-cleaned 0.45μM polycarbonate filters and filtration units, and frozen on board. The nutrients were analysed with a Skalar San^{++} continuous flow analyser at the Marine Institute (MI) by accredited standard colorimetric methods. Salinity samples were analysed on an OSIL (Ocean Scientific International Ltd) Portasal Salinometer at the MI. The MI participates in QUASIMEME proficiency testing scheme exercises for nutrients and salinity in the marine environment (www.quasimeme.org) and the methods are accredited to ISO17025 by the Irish National Accreditation Board. Results from 7 QUASIMEME rounds (42 samples) between July 2008 and May 2011 gave an average z-score of ≤0.5 for TOxN, PO_4, Si and salinity.

C_T and A_T were sampled and analysed as per Dickson et al. (2007). A_T was analysed by potentiometric titration at sea and C_T by coulometric titration at NUI, Galway, both on a VINDTA-3C (Mintrop et al., 2000). The system was calibrated by running duplicate Certified Reference Materials with every batch of samples (CRMs provided by A. Dickson, Scripps Institute of Oceanography, USA). The precision of the measurements was calculated as the standard deviation of duplicate samples; precision was ±2μmol kg^{-1} for C_T and ±1μmol kg^{-1} for A_T. pCO_2 was calculated using

CO2SYS (Lewis and Wallace, 1998) with the constants of Mehrbach et al. (1973) as refit by Dickson and Millero (1987).

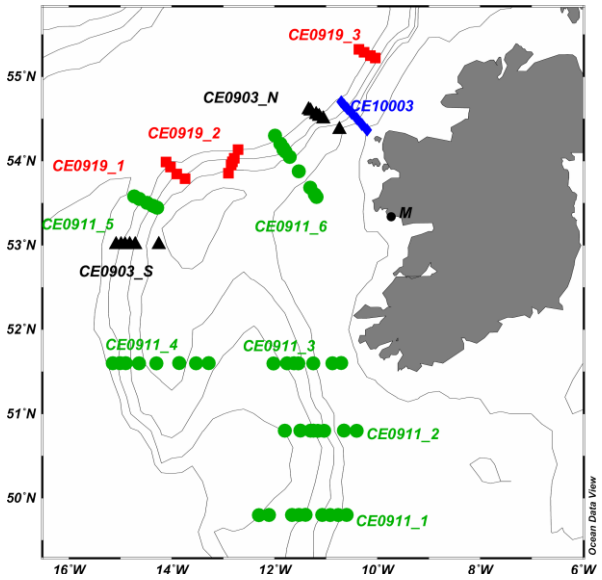

Figure 1: Survey and transect numbers for stations used in this paper. Please note that survey CE10002 covered the same two transects as CE0903, the same applies for survey CE0807 and CE10003. M denotes the position of the Mace Head Atmospheric Research Station.

Table 1 Details of surveys discussed in this paper. CE refers to R/V Celtic Explorer.

Survey	Year	Month	# Stations	# Transects
CE0807	2008	May	2	
CE0903	2009	Feb	12	2
CE0911	2009	June	48	6
CE0919	2009	Dec	25	3
CE10002	2010	Feb	12	2
CE10003	2010	May	6	

Euphotic depth and summer mixed layer estimates

The euphotic depth (ED, the depth down to which production has taken place) was calculated following the O_2-step method from Koeve (2001) using calibrated CTD oxygen sensor data.. The resulting oxygen profiles were analysed to find the depth of 99.5% saturation, which was set as the ED. The summer mixed layer depth (sML) is created by heating of the surface water and at the time of the CE0911 survey the sML, calculated as the depth of $\Delta\sigma_T \geq 0.125$ from the surface (Brainerd and Gregg, 1995),

was between 16 and 34 m. The importance of light availability for the North Atlantic spring bloom has been recognised for a long time (Sverdrup, 1953) although direct quantification of the relationship is difficult (Siegel et al., 2002). Due to the shallowness of the sML in comparison to the ED (see results and discussion) the ED was used for integration of production.

Net community production and air-sea exchange calculations

NCP was calculated as the integrated deficit of nitrate and phosphate through the water column down to the ED compared to the 'preformed' concentration (i.e. the surface concentration at the end of winter mixing). The preformed concentrations were taken from the integrated concentration below the ED (from ED down to the bottom or a maximum of 500 m) at each station.

$$N_{prod} = \int_0^{ED} (NO_3^{pre} - NO_3)\,\mathrm{dz} + K_z \cdot (\Delta NO_3 / \Delta z) \cdot t \quad (1a)$$

$$P_{prod} = \int_0^{ED} (P^{pre} - P)\,\mathrm{dz} + K_z \cdot (\Delta P / \Delta z) \cdot t \quad (1b)$$

where N_{prod} and P_{prod} are the NCP calculated from nitrate and phosphate deficit respectively, NO_3 and P are the nitrate and phosphate concentrations at depth z and NO_3^{pre} and P^{pre} are the preformed concentrations. K_z is the eddy (vertical) diffusivity, ΔNO_3 and ΔP the difference in concentration between the water in and below the ED. It is assumed that the gradient has developed linearly since the end of winter mixing and thus the value used is half of the measured difference. K_z was taken from Sharples et al. (2007), who reported mean daily K_z during neap and spring tides at a site on the shelf edge of the Celtic Sea. Here the mean value of 3.85×10^{-4} m s^{-2} was used. t is the time since the start of production. In this area of the ocean production starts around the beginning of April (Mohn and White, 2007), so here t was set to 75 days. In order to compare the productivity estimates from nitrate and phosphate, the corresponding drawdown in C_T was calculated using the C:N and C:P ratios from Körtzinger et al. (2001), where C:N = 7.2 and C:P = 123

$$C_N^{prod} = N_{prod} \cdot (C:N) \quad (2a)$$

$$C_P^{prod} = P_{prod} \cdot (C:P) \quad (2b)$$

where C_N^{prod} and C_P^{prod} are the NCP calculated from the nitrate and phosphate deficits respectively, expressed in terms of C_T. The change in C_T concentration from the end of winter mixing (ΔC_T) is however due both to biological production and air-sea exchange,

$$\Delta C_T = C_T^{prod} + C_T^{air\text{-}sea} \quad (3)$$

where C_T^{prod} is the NCP and $C_T^{air\text{-}sea}$ is the air-sea exchange. To calculate the uptake of CO_2 from the atmosphere, the drawdown in C_T was calculated in the same way as for nitrate and phosphate using measured C_T concentrations,

$$\Delta C_T = \int_0^{ED} (C_T^{pre} - C_T)\, dz + K_z \cdot (\Delta C_T / \Delta z) \cdot t \quad (4)$$

Finally, the air-sea exchange was calculated by setting C_T^{prod} equal to C_N^{prod} or C_P^{prod}

$$C_{T\text{-}N}^{air\text{-}sea} = \Delta C_T - C_N^{prod} \quad (5a)$$

$$C_{T\text{-}P}^{air\text{-}sea} = \Delta C_T - C_P^{prod} \quad (5b)$$

where negative results will denote uptake from the atmosphere.

The NCP and air-sea exchange uncertainties were calculated by error propagation based on the measurement uncertainties and a 50% uncertainty of K_z (Jonathan Sharples pers. comm.).

Results and discussion

Surface water

Most of the upper 1000 m in the NE Atlantic is dominated by Eastern North Atlantic Water (ENAW; Harvey, 1982) as can be seen for CE0911 in Figure 2. As the ENAW flows north from its formation region in the Bay of Biscay (Pollard et al., 1996) it is gradually freshened by mixing with waters flowing in from the west (Ellett et al., 1986). This evolution was seen as slightly higher salinity in the southern transects compared to northern during all three winter surveys. The south-to-north decrease in salinity was also seen during June in the remaining winter mixed layer (wML, below ~100 m), i.e. in the mode water (McCartney and Talley, 1982).

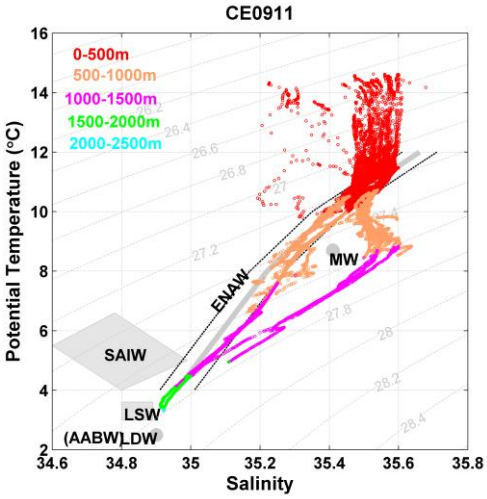

Figure 2. Potential temperature-salinity plot from CE0911 with water mass abbreviations. ENAW, Eastern North Atlantic Water; MW, Mediterranean Water; SAIW, Subarctic Intermediate Water; LSW, Labrador Sea Water; LDW, Lower Deep Water; AABW, Antarctic Bottom Water. The temperature and salinity of MW are much higher in the source region, properties are typical of MW in the southern Rockall Trough region (McGrath et al., 2012).

Comparison between transects CE0903_S, CE0911_5, CE0919_1 and CE10002_S (Figure 1) showed similar temperature and salinity of the wML (i.e. mode water) with variability between surveys being no greater than variability between stations on a given transect. Variability in T-S properties is expected along the shelf edge due to filaments of the SEC at different depths. Nutrient concentrations (in the wML) are somewhat higher in transect CE0911_6 compared to CE0911_1.

The sea surface (~3 m) salinity, temperature and nitrate concentrations are presented in Figure 3, minimum and maximum values of sea surface characteristics are shown in Table 2 where comparisons also can be made with the situation in December (CE0919) and January (CE0903 and CE10002). The surface water had been heated during spring and early summer as it was around 3°C warmer than in January. Temperatures in December were slightly higher than in January indicating the ongoing cooling and deep mixing during winter. The ED calculated from oxygen saturation was between 46 and 206 m while the heating of the surface water formed a shallower sML (16-34 m), as can be seen in Figure 4. During the OMEX project, Joint et al (2001) found mean summer mixed layer depths of 35-45 m at OMEX I, just to the south of our study area. The temperature and salinity were fairly uniform across the six summer transects (Figure 3) although there was a tendency for decreasing

values northwards. There was also a clear decrease in salinity and increase in temperature towards the shallower stations on CE0911_6.

All biologically active substances (e.g. NO_3, C_T and DO, Figure 5) showed a clear change from winter values in the upper ~100 m, especially NO_3 and P which were almost, or sometimes entirely, depleted in summer. On the deeper stations surface nitrate concentrations were slightly higher across the two northernmost transects, coinciding with higher preformed values. There was also a tendency for decreasing nitrate concentrations towards the inner shelf. There was no south-north trend in surface CE0911 phosphate or silicate (not shown). C_T values were higher in the north (by ~10 μmol/kg) but not across the board. The seasonal progression in biologically active substances can be observed with December concentrations being somewhat lower than in January due to the continuation of deep mixing (Table 2). Figure 6 shows profiles of nitrate and C_T for selected stations in the same area for February (CE10002), May (CE0807 and CE10003) and June (CE0911). Since oxygen is produced instead of consumed during PP, concentrations have increased compared to winter values which, together with increasing temperatures, result in supersaturation reaching a maximum of 114% during CE0911. Below the ED the concentrations of biologically active substances increase towards winter concentrations as illustrated in Figure 6.

Intermediate/deep waters

Below 500m there is a clear south-north differentiation in water masses between CE0911_4 and CE0911_5, (Figure 4). The difference is most obvious between 900-1100m due to the presence of Mediterranean Water (MW) and Sub Arctic Intermediate Water (SAIW), two water masses with contrasting temperature-salinity properties, yet found at a similar density level at the southern entrance to the Rockall Trough. In CE0911, the salinity peak along the shelf edge, south of 52°N (CE0911 transect 1-4) is characteristic of MW. There is also a trace of MW seen in CE10002_S (McGrath et al., 2012). The intermediate peak in salinity due to MW is supported by the high A_T and low DO of the water (McGrath et al., in press), due to the

oligotrophic nature of the Mediterranean Sea, high evaporation and high freshwater A_T inputs (Cabecadas et al., 2002; Howe, 1982; Schneider et al., 2007). Conversely, SAIW is a cool, fresh highly stratified water mass (Harvey and Arhan, 1988), observed at ~800m north of 52°N on CE0919_1 and CE10002_S, which gets diluted further north in the Trough. No such signal is seen during CE0903. During CE10002_S the higher C_T and nutrients in this layer are probably due to the larger influence of SAIW, which has higher 'preformed' nutrients and C_T due to cooler temperatures and mixing in the subpolar gyre (McGrath et al., in press). CE0919_3 has lower nitrate at this depth than the other two transects from that survey, again due to the stronger influence from SAIW further south. Below 1200 m in the water column the biogeochemical parameters are similar for all transects during CE0903, CE0919 and CE10002. Considering that no 2000 m stations were sampled south of 52°N, no south-to-north deep water comparisons could be made.

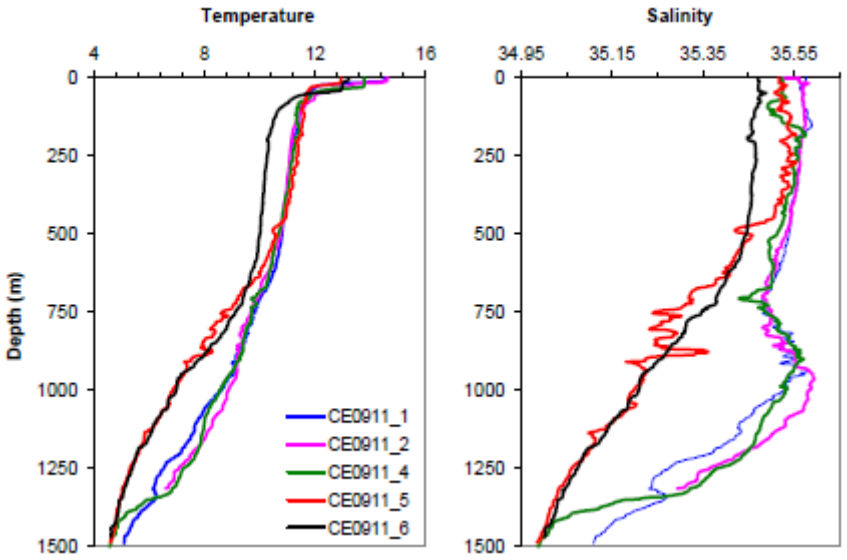

Figure 4: Temperature and salinity versus depth (m) at the CE0911 1500 m stations. Legend numbers refer to which transect the station was occupied on.

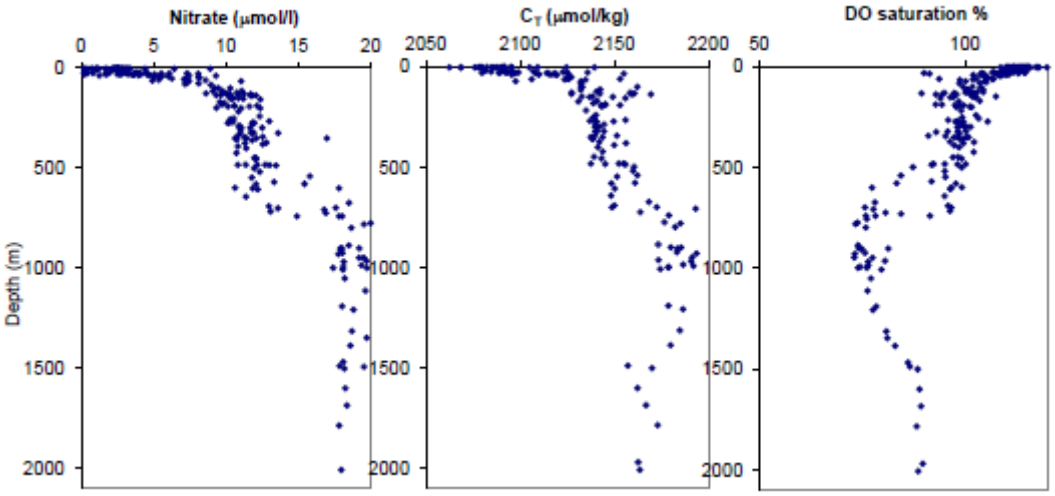

Figure 5: CE0911 nitrate, C_T and oxygen saturation versus depth (m) for all stations.

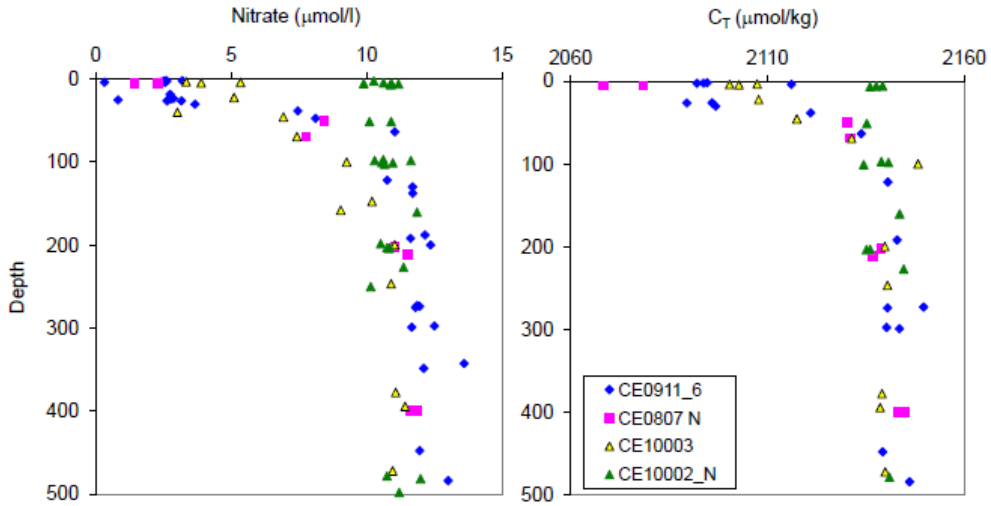

Figure 6: Nitrate and C_T concentrations in the top 500 m for selected transects from CE0807, CE0911, CE10002 and CE10003 (see Figure 1).

Net community production

NCP was calculated based on ED deficit of nitrate and phosphate and the results are shown in Figure 7 and Table 3. The drawdown in C_T (ΔC_T) is also included. The results show C_N^{prod} ranging from 37 (±3) to 114 (±11) g C m^{-2} while C_P^{prod} ranged from 26 (±2) to 104 (±11) g C m^{-2}. There are statistical differences between C_N^{prod} and C_P^{prod} at only 10 stations (#9, 15, 21, 24, 32-35, 43 and 44) out of 43 in total, where they range 7 to 30 g C m^{-2}, and out of these 8 stations have higher C_N^{prod}. Due to the general similarity of the estimates the following discussion will be based on the C_N^{prod} values.

The south-to-north and west-to-east evolution of several water properties in the surveyed region raises the question of spatial trends in NCP. The observed amounts of NCP show no definite such trends however; variability within a transect can be as large as between transects (Figure 7). This is particularly apparent on transect six (CE0911_6) which has the stations with the highest and the second lowest NCPs (#42 and 43 respectively). There are however some tendencies in the variability that will be discussed here but it should be emphasised that considering the uncertainties these are not statistically significant trends. Across the transects there is a local maximum of NCP above a bottom depth of 500-750 m, except on transect 1 where it occurs at 1000 m. On the three southern transects the local minimum NCP occurs at the 200 m stations, and while there are no 200 m stations to compare to on transect 4 and 5, minimum NCP occurs at 500 m on transect 6. There is a tendency for higher production on transect 5 & 6 compared to 2 & 3. Mean values of NCP at stations with similar bottom depth show an increase from shallow waters out to 750 m, followed by a decrease in deeper waters.

While the reason for this pattern is not clear, it may be related to the timing and degree of stratification across the shelf edge which influences the balance between nutrient supply and light limitation (Siegel et al., 2002). Stratification may be too strong in shallow waters on the shelf limiting the nutrient supply, while offshore there may be adequate nutrients but phytoplankton may be mixed into light-limited deeper waters, especially early during the season. The differences in NCP are to some degree due to the gradient in nitrate between the concentrations within the ED compared to the preformed concentrations below. Overlain on this is the ED; a station with a shallow ED will have a smaller integrated deficit than a station with a deeper ED if the gradient is the same, but if the gradient is larger, as is the case of some of the shallower stations, the vertical flux will be larger. The tendency for a local maximum in NCP over the 500-1000 m depth range is accompanied by an increase in ED at the 750 m stations. The reason for this deeper ED is not clear but may be a slope effect. The EDs do tend to increase from shallow waters out to 750 m, after which they decrease somewhat.

To our knowledge no estimates of NCP has been done in the region discussed here, but comparisons can be made with some other areas of the NE Atlantic. Bargeron et al. (2006) present new production estimates along the route of the SOO 'The pride of Bilbao' based on surface water oxygen budgets and nitrogen assimilation. They calculate a new production of 31-40 g C m^{-2} based on oxygen for the shelf break (200-2000 m) west of France at about 47°N, 5.5°W. This is somewhat lower than the majority of our estimates. At the PAP site (49°N, 16.5°W) in the open NE Atlantic, Körtzinger et al. (2008) estimated a seasonal (March-early August 2004) mixed layer NCP of 6.4 ± 1.1 mol C m^{-2} (77 ± 13 g C m^{-2}) from surface water pCO_2, an estimate similar to the 72 ± 7 g C m^{-2} at station #9 (49.8°N, 12.3°W). Hartman et al. (2010) used changes in nitrate to estimate new production at the PAP site for 2003-2005 and found decreasing production from 85.4 to 40.3 ± 4.3 g C m^{-2} yr^{-1} over the three years. Further north (~61.2ºN, 26.5ºW) in open ocean waters, Alkire et al. (2012) found an NCP of 13 g C m^{-2} over a 12 day bloom, if extended over 75 days this would give a value of 81 g C m^{-2}.

By using ED instead of sML we avoid the question of how much of the production occurs during the pre-stratification period, something that can otherwise create a significant error as shown by Körtzinger et al. (2008). Of the total 77 ± 13 g C m^{-2} NCP they estimated, 53 ± 11 g C m^{-2} occurred in the pre-stratification period. By integrating over the entire ED, all the NCP is captured no matter when it occurred in relation to the development of thermal stratification.

pCO_2 and air-sea exchange of CO_2

The atmospheric pCO_2 at Mace Head, Ireland, varied around a mean of ~390 μatm (Keane-Brennan, 2011) from January to July 2009. During CE10002 the surface pCO_2 west of 10º W was on average 389 μatm (varying between 337 and 408 μatm). Surface water (~3 m) pCO_2 during the CE0911 survey was between 305-413 μatm with a mean of 340 μatm. Keane-Brennan (2011) reports a mean June pCO_2 of 320 ± 18 μatm in the water off the coast of Ireland. All stations on CE0911, except station #25, have surface pCO_2 below the atmospheric mean, which is as expected in this

region in June. The high pCO_2 at station # 25 (413 μatm) is due to the second highest surface C_T (2124 μmol/kg) measured during the survey.

The change in C_T since the end of winter mixing, ΔC_T, spans 11 (±4) - 94 (±10) g C m^{-2} (Table 3). Air-sea exchange calculated from C_N^{prod} and C_P^{prod} is shown in Table 4. Of the 24 stations where there are C_T data, 15 have air-sea exchange statistically different from 0 when based on nitrate and 10 when based on phosphate (see Table 4). At the other stations the uncertainty was similar to or larger than the calculated air-sea exchange. Of the 15 stations that have a significant air-sea exchange based on nitrate all have uptake from the atmosphere, except station #28 on top of Porcupine Bank where there has been outgassing. Retention of water and organic matter above the Porcupine Bank (Mohn and White, 2007; White et al., 2005) allowing remineralisation of the retained organic material, may be the cause for the observed outgassing. Even without this station the air-sea exchange varies considerably, the uptake at station #25 being six times larger than at station #15. There is a cross-slope tendency with no CO_2 uptake observed in shallow waters and clear uptake observed in deeper waters. All stations over bottom depths of 1000 m or more, except station #7, have significant uptake from the atmosphere - between 9-35 g C m^{-2} - while stations with bottom depths of 200 m or less do not have any significant uptake, except at station #15 (6 g C m^{-2}). Stations with bottom depths of 350 and 500 m show no consistent uptake, and the maximum uptake over this bottom depth is 13 g C m^{-2}. Due to the limited number of stations it is not possible to evaluate any south-to-north trend.

The air-sea exchange estimates here are for the season March - mid June, other estimates on the same time scale are scarce. Frankignoulle and Borges (2001) present monthly CO_2 fluxes in the Gulf of Biscay and environs based on underway pCO_2 or measurements of pH and alkalinity. Adding together their values for March, April, May and half of June results in an uptake of 10.8 g C m^{-2}, somewhat lower than the majority of our stations (Table 4).

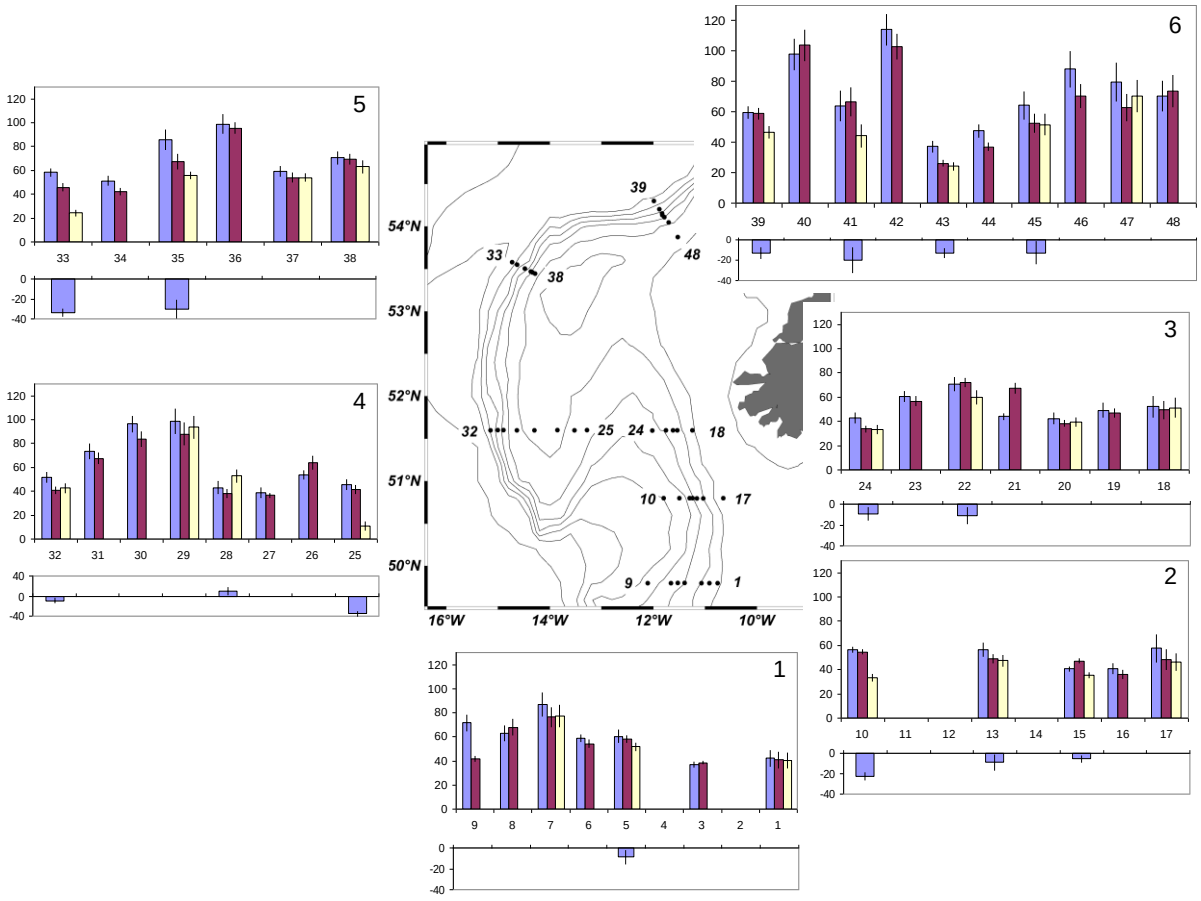

Figure 7: Net community production, C_N^{prod} (left), C_P^{prod} (middle) and ΔC_T (right) in g C m^{-2} with uncertainty estimates vs. station number Numbers in the corner of each graph denote the transect. Lower bar shows the air-sea exchange calculated from ΔC_T and C_N^{prod}, note the different scale for station #25-32. There was no statistically significant air-sea exchange on transect 3.

Conclusions

The June 2009 survey onboard R/V Celtic Explorer collected detailed hydrographical and biogeochemical information on six transects along the western Irish continental shelf edge from 49.8-55.4°N. Temperature and salinity at the sea surface showed a decrease from south to north, there was also some differences across-slope, especially on the northernmost transect. Nitrate showed an increase northwards on the deeper stations, coinciding with higher preformed values, but was also almost, or completely depleted on the shallowest stations. The spatial trends in temperature, salinity and nitrate raised the question of spatial trends in NCP. NCP was calculated as the seasonal integrated deficit of nitrate, C_N^{prod}, and phosphate, C_P^{prod}. C_N^{prod} and C_P^{prod} were statistically similar for the majority of stations, and C_N^{prod} ranged 37 (±3) - 114

(±11) g C m^{-2}. While the amount of NCP is partly due to the euphotic depth, no clear and consistent spatial trends are evident, however there is a tendency for a local maximum of NCP over bottom depths between 500-1000 m, partly due to the deeper ED at 750 m. Air-sea exchange of CO_2 ranged between -5.5 (±3.7) and -34.7 (±6.3) g C m^{-2}, except at a station on top of the Porcupine Bank where outgassing had taken place. There was a tendency for more uptake in deeper waters. These results highlight the enhanced productivity along the shelf edge compared to adjacent on and off-shelf waters, something which should be considered in global models of primary production.

Acknowledgements

This study was part of the Irish Government funded project "Impacts of Increased Atmospheric CO_2 on Ocean Chemistry and Ecosystems" (PI Colin O'Dowd), under the Rapid Climate Change Programme and carried out under the Sea Change strategy with the support of the Marine Institute and the Marine Research Sub-Programme of the National Development Plan 2007-2013. All surveys were funded by the Irish government's National Development Plan 2007-2013. We are grateful to the master, crew and scientists on the research surveys referred to in this paper. We thank Heather Cannaby for the processing of the CTD data.

References

Alkire, M.B. et al., 2012. Estimates of net community production and export using high-resolution, Lagrangian measurements of O2, NO3âˆ’, and POC through the evolution of a spring diatom bloom in the North Atlantic. Deep Sea Research Part I: Oceanographic Research Papers, 64(0): 157-174.

Bargeron, C.P., Hydes, D.J., Woolf, D.K., Kelly-Gerreyn, B.A. and Qurban, M.A., 2006. A regional analysis of new production on the northwest European shelf using oxygen fluxes and a ship-of-opportunity. Estuarine Coastal and Shelf Science, 69(3-4): 478-490.

Brainerd, K.E. and Gregg, M.C., 1995. Surface mixed and mixing layer depths. Deep Sea Research Part I: Oceanographic Research Papers, 42(9): 1521-1543.

Burrows, M. and Thorpe, S.A., 1999. Drifter observations of the Hebrides slope current and nearby circulation patterns. Annales Geophysicae-Atmospheres Hydrospheres and Space Sciences, 17(2): 280-302.

Cabecadas, G., Brogueira, M.J. and Goncalves, C., 2002. The chemistry of Mediterranean outflow and its interactions with surrounding waters. Deep-Sea Research Part II - Topical Studies in Oceanography, 49(19): 4263-4270.

Carr, M.-E. et al., 2006. A comparison of global estimates of marine primary production from ocean color. Deep Sea Research Part II: Topical Studies in Oceanography, 53(5â€“7): 741-770.

Crawfurd, K.J., Raven, J.A., Wheeler, G.L., Baxter, E.J. and Joint, I., 2011. The Response of Thalassiosira pseudonana to Long-Term Exposure to Increased CO2 and Decreased pH. Plos One, 6(10): 9.

Delille, B. et al., 2005. Response of primary production and calcification to changes of pCO(2) during experimental blooms of the coccolithophorid Emiliania huxleyi. Global Biogeochemical Cycles, 19(2).

Dickson, A.G., 1995. Determination of dissolved oxygen in sea water by Winkler titration. WOCE Operations Manual. Part 3.1.3 Operations & Methods, WHP Office Report WHPO 91-1.

Dickson, A.G. and Millero, F.J., 1987. A comparison of the equilibrium constants for the dissociation of carbonic acid in seawater media. Deep Sea Research, 34: 1733-1743.

Dickson, A.G., Sabine, C.L. and Christian, J.R., 2007. Guide to best practices for ocean CO2 measurements. PICES Special Publication 3: 1-191.

Ellett, D.J., Edwards, A. and Bowers, R., 1986. The hydrography of the Rockall Channel - an overview. Proceedings of the Royal Society of Edinburgh, 88B: 61-68.

Engel, A. et al., 2005. Testing the direct effect of CO2 concentration on a bloom of the coccolithophorid Emiliania huxleyi in mesocosm experiments. Limnology and Oceanography, 50(2): 493-507.

Frankignoulle, M. and Borges, A.V., 2001. European continental shelf as a significant sink for atmospheric carbon dioxide. Global Biogeochemical Cycles, 15(3): 569-576.

Hartman, S.E., Larkin, K.E., Lampitt, R.S., Lankhorst, M. and Hydes, D.J., 2010. Seasonal and inter-annual biogeochemical variations in the Porcupine Abyssal Plain 2003-2005 associated with winter mixing and surface circulation. Deep Sea Research Part II: Topical Studies in Oceanography, 57(15): 1303-1312.

Harvey, J., 1982. Theta-S relationships and water masses in the eastern North Atlantic. Deep-Sea Research Part a-Oceanographic Research Papers, 29(8): 1021-1033.
Harvey, J. and Arhan, M., 1988. The water masses of the Central North Atlantic in 1983-84. Journal of Physical Oceanography, 18: 1855-1875.
Hill, A.E. and Mitchelson-Jacob, E.G., 1993. Observations of a poleward-flowing saline core on the continental slope west of Scotland. Deep Sea Research Part I: Oceanographic Research Papers, 40(7): 1521-1527.
Howe, M.R., 1982. The Mediterranean Water Outflow in the Gulf of Cadiz. Oceanography and Marine Biology, 20: 37-64.
Joint, I. et al., 2001. Pelagic production at the Celtic Sea shelf break. Deep Sea Research Part II: Topical Studies in Oceanography, 48(14-15): 3049-3081.
Keane-Brennan, J., 2011. Air to Sea Gas Exchange of CO_2 in the north-east Atlantic Ocean, National University of Ireland, Galway, Galway, 208 pp.
Koeve, W., 2001. Wintertime nutrients in the North Atlantic-new approaches and implications for new production estimates. Marine Chemistry, 74(4): 245-260.
Körtzinger, A., Koeve, W., Kähler, P. and Mintrop, L., 2001. C : N ratios in the mixed layer during the productive season in the northeast Atlantic Ocean. Deep Sea Research Part I: Oceanographic Research Papers, 48(3): 661-688.
Körtzinger, A. et al., 2008. The seasonal pCO2 cycle at 49°N/16.5°W in the northeastern Atlantic Ocean and what it tells us about biological productivity. Journal of Geophysical Research - Oceans, 113: C04020.
Lewis, E. and Wallace, D.W.R., 1998. Program Developed for CO2 System Calculations. ORNL/CDIAC-105. Carbon Dioxide Information Analysis Center, Oak Ridge National Laboratory, U.S. Department of Energy, Oak Ridge, Tennessee.
McCartney, M.S. and Talley, L.D., 1982. THE SUB-POLAR MODE WATER OF THE NORTH-ATLANTIC OCEAN. Journal of Physical Oceanography, 12(11): 1169-1188.
McGrath, T., Kivimäe, C., Tanhua, T., Cave, R.R. and McGovern, E., in press. Inorganic carbon and pH levels in the Rockall Trough 1991-2010. Deep-Sea Research Part I.
McGrath, T., Nolan, G. and McGovern, E., 2012. Chemical characteristics of water masses in the Rockall Trough. Deep Sea Research Part I: Oceanographic Research Papers, 61(0): 57-73.
Mehrbach, C., Culberson, C.H., Hawley, J.E. and Pytkowicz, R.M., 1973. Measurement of the apparent dissociation constants of carbonic acid in seawater at atmospheric pressure. Limnology and Oceanography, 18: 897-907.
Mintrop, L., Pérez, F.F., Gonzalez-Dávila, M., Santana-Casiano, J.M. and Körtzinger, A., 2000. Alkalinity determination by potentiometry: intercalibration using three different methods. Ciencias Marinas, 26(1): 23-37.
Mohn, C. and White, M., 2007. Remote sensing and modelling of bio-physical distribution patterns at Porcupine and Rockall Bank, Northeast Atlantic. Continental Shelf Research, 27(14): 1875-1892.
Platt, T. et al., 1989. Biological production of the oceans: the case for a consensus. Marine ecology progress series, 52: 77-88.
Pollard, R.T. et al., 1996. Vivaldi 1991-A study of the formation, circulation and ventilation of Eastern North Atlantic Central Water. Progress in Oceanography, 37(2): 167-192.

Riebesell, U. et al., 2000. Reduced calcification of marine plankton in response to increased atmospheric CO2. Nature, 407(6802): 364-367.
Schneider, A., Wallace, D.W.R. and Körtzinger, A., 2007. Alkalinity of the Mediterranean Sea. Geophysical Research Letters, 34(15): 1-5.
Sharples, J. et al., 2007. Spring-neap modulation of internal tide mixing and vertical nitrate fluxes at a shelf edge in summer. Limnology and Oceanography, 52(5): 1735-1747.
Siegel, D.A., Doney, S.C. and Yoder, J.A., 2002. The North Atlantic spring phytoplankton bloom and Sverdrup's critical depth hypothesis. Science, 296(5568): 730-733.
Sverdrup, H.U., 1953. On conditions for the vernal blooming of phytoplankton. Journal du Conseil International pour l'Exploration de la Mer, 18: 287-295.
WBGU, 2006. The Future Oceans - Warming up, Rising High, Turning Sour, GERMAN ADVISORY COUNCIL ON GLOBAL CHANGE, Berlin.
White, M. and Bowyer, P., 1997. The shelf-edge current north-west of Ireland. Annales Geophysicae-Atmospheres Hydrospheres and Space Sciences, 15(8): 1076-1083.
White, M., Mohn, C., de Stigter, H. and Mottram, G., 2005. Deep-water coral development as a function of hydrodynamics and surface productivity around the submarine banks of the Rockall Trough, NE Atlantic. In: A. Freiwald, Roberts, JM. (Editor), Cold-water Corals and Ecosystems. Springer-Verlag, Berlin Heidelberg, pp. 503-514.
Zondervan, I., Zeebe, R.E., Rost, B. and Riebesell, U., 2001. A time series study of silica production and flux in an eastern boundary region: Santa Barbara Basin, California. Global Biogeochem. Cycles, 15(2): 507-516.

Table 2 Surface water characteristics from winter and summer surveys.

Survey	Transect	Temperature		Salinity		Nitrate		Silicate		Phosphate		C_T		A_T		Winkler DO	
						µmol/l		µmol/l		µmol/l		µmol/kg		µmol/kg		umol/kg	
		min	max	min	max	min	max	min	max	min	max	min	max	min	max	min	max
CE0903	S	10.32	11.08	35.483	35.525	9.99	11.72	3.43	4.12	0.49	0.66	2126.4	2132.9	2323.2	2326.2		
CE0911	1	14.02	14.65	35.567	*35.595*	<0.26	3.23	0.37	0.87	<0.01	<0.16	2081.0	*2089.9*	2333.8	2339.8	270.9	290.5
CE0911	2	14.30	14.61	35.468	35.549	<0.01	2.30	0.23	2.49	<0.16	0.55	2078.1	2083.7	2329.9	2336.9	264.1	285.5
CE0911	3	13.87	14.36	35.231	35.514	<0.01	4.42	0.23	0.77	<0.16	0.32	2078.8	2114.2	2330.7	2337.5	270.0	286.0
CE0911	4	13.25	13.99	35.474	35.532	2.36	6.43	0.40	0.79	<0.01	0.45	2075.9	2122.5	2337.0	2338.8	279.0	292.4
CE0911	5	12.90	13.13	35.512	35.525	2.40	3.12	0.38	0.67	<0.16	0.24	2088.1	2094.9	2337.5	2338.7	275.8	284.4
CE0911	6	12.81	14.15	35.276	35.477	<0.01	3.19	0.60	1.01	<0.01	0.23	2065.5	2116.1	2334.1	2337.5	277.0	283.4
CE10002	N	10.09	10.59	35.455	35.487	9.89	11.17	2.75	3.47	0.61	0.66	2136.1	2139.3	2332.9	2335.9	261.0	267.8
CE10002	S	10.50	11.10	35.497	35.512	9.65	10.88	3.14	3.53	0.59	0.63	2133.1	2139.3	2329.2	2335.7	259.9	262.9
CE0919	1	11.12	11.39	35.422	35.468	8.65	8.72	2.00	2.41	0.40	0.42	2124.6	2122.3	2338.6	2331.9		
CE0919	2	11.28	11.56	35.463	35.509	8.81	9.18	2.12	2.41	0.40	0.43	2129.9	2126.6	2336.2			
CE0919	3	11.65	11.82	35.525	35.554	8.83	9.05	2.25	2.29	0.40	0.41	2132.4	2126.6	2337.8	2334.8		

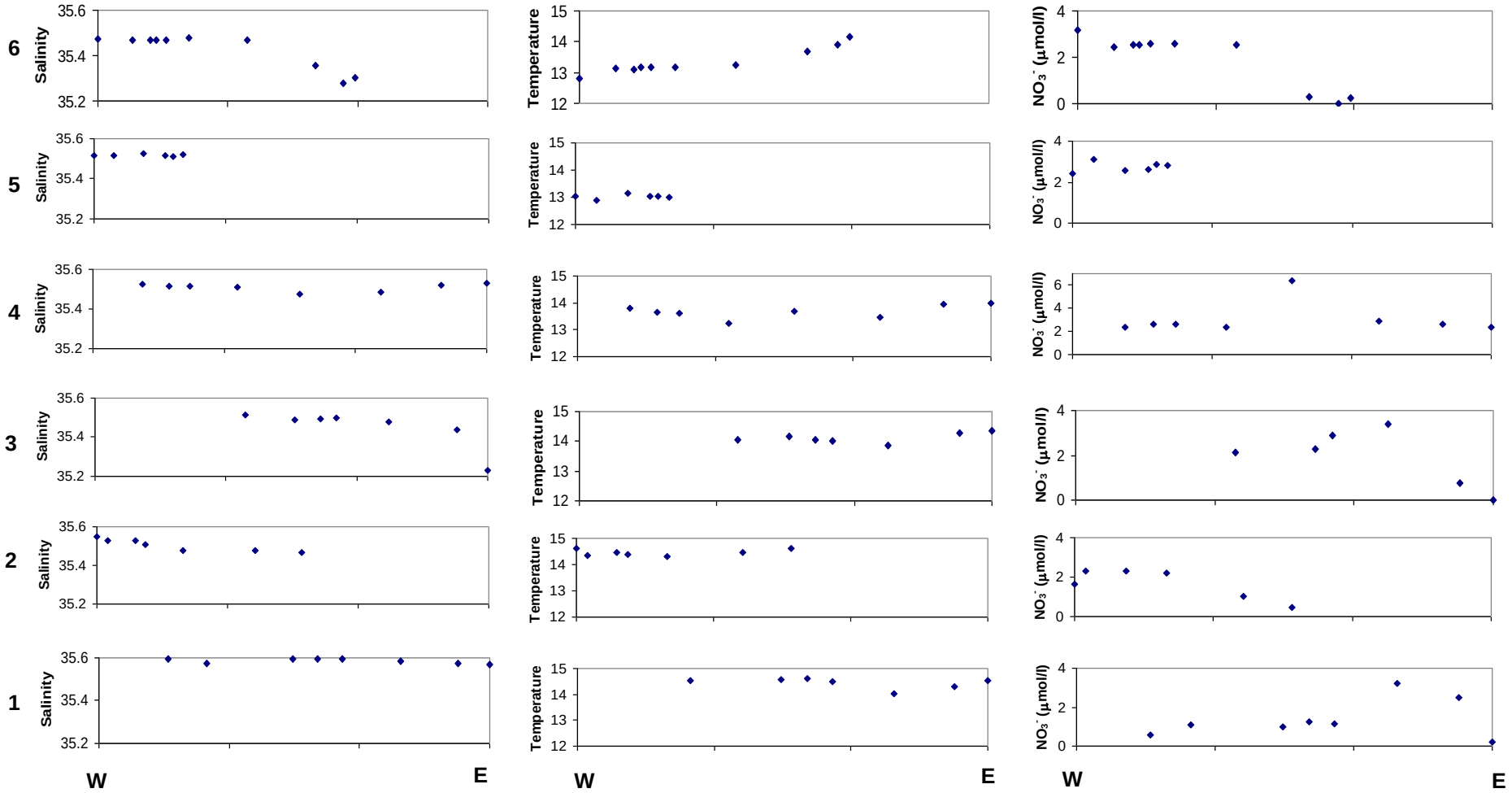

Figure 3: Cross slope transects from CE0911 of sea surface salinity (a), temperature (b) and nitrate (c) vs. transect distance (where the x-axis is 150 km in length) in order to show the scale of variability. Bold numbers 1-6 denote CE0911 transect from Figure 1. Note the difference in scale of nitrate on transect 4. E and W denotes east and west respectively

Table 3 NCP calculated from nitrate (C_N^{prod}), phosphate (C_P^{prod}) and C_T drawdown (ΔC_T).

Stn #	Euphotic depth	Bottom depth	C_N^{prod} g C m^{-2}		C_P^{prod} g C m^{-2}		ΔC_T g C m^{-2}	
1	66	140	42.1	±7.4	40.7	±6.9	40.3	±7.1
3	104	200	36.6	±2.7	38.6	±1.7		
5	117	500	60.5	±5.7	58.1	±3.6	51.7	±4.0
6	132	750	58.7	±3.5	54.2	±3.9		
7	116	1000	86.8	±10.2	76.5	±8.6	77.3	±9.4
8	117	1500	63.0	±7.1	67.9	±7.2		
9	142	2000	71.8	±7.2	41.9	±2.9		
10	150	1500	56.2	±2.7	54.8	±2.5	33.4	±3.1
13	134	500	56.4	±6.2	49.0	±4.3	47.3	±5.1
15	106	200	40.8	±2.4	47.2	±2.4	35.3	±2.8
16	69	160	41.0	±4.8	36.0	±4.1		
17	61	140	57.7	±11.7	48.2	±8.9	46.5	±7.6
18	46	140	52.1	±9.1	49.4	±8.1	51.3	±8.4
19	77	160	49.1	±6.5	46.9	±4.1		
20	112	200	42.4	±5.2	38.3	±2.9	39.3	±4.0
21	153	350	44.1	±3.2	67.3	±4.7		
22	194	500	70.8	±5.9	72.4	±4.1	59.8	±6.0
23	171	750	60.6	±5.0	56.7	±4.3		
24	149	1000	43.0	±4.9	33.7	±3.3	33.6	±4.2
25	155	1000	45.7	±4.9	41.8	±4.2	11.0	±3.9
26	152	750	54.1	±4.1	64.1	±6.2		
27	111	500	38.9	±4.6	36.4	±2.5		
28	129	350	43.2	±6.1	38.1	±4.1	52.9	±5.6
29	130	500	98.8	±11.1	88.0	±9.9	93.7	±9.7
30	206	750	96.3	±7.0	83.7	±6.5		
31	138	1000	73.4	±6.9	67.6	±5.1		
32	149	1500	51.5	±4.8	41.1	±3.4	42.6	±4.5
33	118	2000	58.3	±3.6	45.7	±3.7	24.4	±3.1
34	129	1500	51.3	±4.6	42.2	±3.6		
35	115	1000	85.8	±8.9	67.3	±7.0	55.7	±3.5
36	158	750	98.7	±8.5	95.6	±5.0		
37	139	500	59.4	±4.6	54.1	±4.6	54.1	±4.0
38	149	350	70.6	±5.7	69.4	±4.6	63.1	±6.0
39	147	2000	59.5	±4.2	58.8	±4.3	46.5	±4.3
40	133	1500	97.8	±10.8	103.8	±10.7		
41	74	1000	63.9	±10.3	66.7	±9.9	44.2	±7.9
42	183	750	114.2	±10.6	103.0	±8.8		
43	59	500	37.1	±4.2	26.2	±2.3	24.1	±3.1
44	78	350	47.5	±4.5	37.0	±2.9		
45	91	300	64.3	±9.4	52.7	±6.6	51.6	±7.4
46	100	200	88.0	±12.0	70.4	±8.2		
47	93	160	79.7	±13.0	62.7	±9.3	70.3	±10.9
48	98	140	70.3	±10.4	73.5	±10.8		

Table 4 Air-sea exchange calculated from ΔC_T and nitrate ($C_{T\text{-}N}^{air\text{-}sea}$) or phosphate ($C_{T\text{-}P}^{air\text{-}sea}$). Bold represent stations where the value is larger than the uncertainty. Negative values indicate uptake from the atmosphere, positive values indicate outgassing.

Stn #	$C_{T\text{-}N}^{air\text{-}sea}$ g C m^{-2}		$C_{T\text{-}P}^{air\text{-}sea}$ g C m^{-2}	
1	-1.8	±10.3	-0.4	±9.9
5	**-8.8**	**±7.0**	**-6.4**	**±5.4**
7	-9.5	±13.8	0.8	±12.7
10	**-22.8**	**±4.1**	**-21.4**	**±4.0**
13	**-9.1**	**±8.0**	-1.6	±6.7
15	**-5.5**	**±3.7**	**-12.0**	**±3.7**
17	-11.2	±14.0	-1.7	±11.7
18	-0.8	±12.4	1.9	±11.7
20	-3.1	±6.5	1.0	±5.0
22	**-11.0**	**±8.4**	**-12.6**	**±7.3**
24	**-9.4**	**±6.4**	-0.2	±5.3
25	**-34.7**	**±6.3**	**-30.7**	**±5.7**
28	**9.7**	**±8.3**	**14.8**	**±7.0**
29	-5.1	±14.7	5.7	±13.8
32	**-8.9**	**±6.6**	1.5	±5.7
33	**-33.9**	**±4.8**	**-21.3**	**±4.8**
35	**-30.0**	**±9.5**	**-11.6**	**±7.9**
37	-5.3	±6.1	-0.02	±6.1
38	-7.6	±8.3	-6.4	±7.5
39	**-13.0**	**±6.0**	**-12.3**	**±6.1**
41	**-19.7**	**±12.9**	**-22.4**	**±12.7**
43	**-13.0**	**±5.3**	-2.0	±3.9
45	**-12.7**	**±12.0**	-1.1	±9.9
47	-9.4	±17.0	7.5	±14.3

Paper IV

Total alkalinity in Irish coastal and shelf waters

Submitted to Estuarine Coastal and Shelf Science

Triona McGrath [a,b], Rachel R. Cave [a], Caroline Kivimäe [a] and Evin McGovern [b]

[a] National University of Ireland, Galway
[b] Marine Institute, Ireland

Abstract

Alkalinity is a measure of the buffer capacity of the ocean and it is essential that we understand the factors governing total alkalinity (A_T) in surface waters in order to understand oceanic CO_2 uptake and predict changes that may occur in the future. The distribution of A_T in coastal and shelf waters is more complex than in the open ocean due to the addition of freshwater and a range of processes that either remove or generate A_T in the water column. The A_T distribution in outer estuarine, coastal and shelf waters around Ireland is presented from data generated from a number of surveys between May 2008 and February 2012. Generally A_T is governed by factors affecting salinity along the western shelf and through the centre of the Irish Sea. The Shannon and Liffey rivers have high buffer capacity and add high concentrations of A_T to surrounding coastal waters, largely due to the limestone-rich bedrock of their catchments. In comparison, Lough Foyle on the North coast and coastal waters near Arklow in the East have low A_T due to their surrounding river drainage basins having non-limestone lithology. Results illustrate the highly variable and region-specific A_T distribution around Ireland. Photosynthesis resulted in higher A_T (~8μmol kg^{-1}) along the 53ºN transect in May relative to February, while in the summer months A_T and nutrient concentrations indicate a cross-shelf shift in phytoplankton community. The algorithm published by Lee et al. (2006), Global relationships of total alkalinity with salinity and temperature in surface waters of the world's oceans. Geophysical Research Letters, 33(19), which calculates A_T from sea surface salinity and temperature, was tested to investigate to what extent it can be applied in Irish shelf, coastal and open ocean waters. Generally the algorithm can be applied to shelf waters but should not be used in coastal waters due to riverine discharges which have variable impacts depending on composition. The algorithm overestimates A_T along the shelf edge and across the Rockall Trough, likely due to deep winter mixing. Results highlight the importance of monitoring A_T in all areas around the Irish coast to understand future CO_2 uptake and pH change, and to predict subsequent impacts on local ecosystems.

1. Introduction

Despite its relatively small surface area, coastal and shelf waters play a crucial role in the global climate through their influence on major biogeochemical cycles. Shelf and coastal seas are regions of exceptionally high biological productivity with high rates of biogeochemical cycling and are of immense socio-economic importance (Doney et al., 2009; Holt et al., 2009). The marine environment is undergoing changes due to both natural climate cycles and human activities. Coastal and shelf waters are particularly susceptible to both anthropogenic and climate influences and may respond faster than the open ocean (Andersson et al., 2005).

There is growing concern over the effects of increasing atmospheric CO_2 on marine chemistry and ecosystems. Ocean acidification is the process whereby increased atmospheric CO_2 is resulting in a decrease in ocean pH and carbonate ion (CO_3^{2-}) concentrations, while at the same time increasing concentrations of dissolved inorganic carbon (C_T) and bicarbonate ions (HCO_3^-). Measurements of total alkalinity (A_T), dissolved inorganic carbon (C_T), pH and pCO_2 have been made in ocean waters with increasing regularity since the GEOSECS expeditions of the 1970s (Takahashi et al., 1980), as part of programmes such as the Joint Global Ocean Flux Study, the Ocean Atmosphere Carbon Exchange Study, and the World Ocean Circulation Experiment. The knowledge of any two of these parameters, along with temperature, salinity, pressure, phosphate, silicate and the equilibrium constants, allows the determination of the other two parameters. Monitoring acidification in coastal and shelf waters is crucial to increase our understanding of the global carbon cycle. The marine inorganic carbon system in coastal waters, is however highly complex due to biological activity, upwelling and riverine inputs of alkalinity and inorganic and organic carbon (Doney et al., 2009).

Total alkalinity (A_T) is a measure of the acid/base balance of seawater and is largely responsible for the buffering capacity of the ocean. The presence of carbonate ions in seawater means that it is able to accept some of the excess hydrogen ions that are produced when CO_2 reacts with seawater, without changing pH. Therefore by buffering the pH change A_T plays a crucial role in controlling the rate of change in pH with increasing atmospheric pCO_2. A_T is a conservative property; it stays constant with varying pressure and temperature. It is not affected by CO_2 exchange with the

atmosphere and concentrations are generally governed by factors that affect salinity such as evaporation and precipitation, since concentrations of the key chemical species (i.e. HCO_3^-, CO_3^{2-} and $B(OH)_4^-$) that contribute to A_T proportionally increase with increasing salinity (Broecker and Peng, 1982; Lee et al., 2006; Millero et al., 2008). A_T concentrations are also affected by $CaCO_3$ formation (A_T decreases) and dissolution (A_T increases), with a smaller influence from photosynthesis (A_T increases) and remineralisation (A_T decreases) (Zeebe and Wolf-Gladrow, 2003). There has been growing research into marine processes that could potentially affect A_T concentrations, and therefore the drawdown of atmospheric CO_2. Hjalmarsson et al. (2008) highlighted the importance of the mineralogy of a river's drainage basin on the A_T signal of riverine water, where rivers flowing over limestone bedrock have higher A_T relative to those with a granite bedrock. Riverine inputs of A_T are known to be highly variable (Beldowski et al., 2010; Cai et al., 2010; Howland et al., 2000; Raymond and Cole, 2003) which can result in marked regional differences in pH and CO_2 uptake in near-shore waters. Estuaries and coastal waters have high rates of biology activity, with large amounts of organic material that can affect A_T through the addition of organic bases or the protonation of organic acids (Hernández-Ayón et al., 1999; Muller and Bleie, 2008). Phytoplankton and bacterial cells may also contribute to measured alkalinity in seawater and in regions of high organic material, alkalinity measurements may need to be made on filtered seawater (Kim et al., 2006). Anaerobic processes in the sediment, such as denitrification or sulphate reduction on the continental shelves, generate alkalinity (Chen, 2002; Chen and Wang, 1999; Thomas et al., 2009). Denitrification leads to an increase in A_T by 1 mole per mole of nitrate converted (Wolf-Gladrow et al., 2007) since bacterial cells, to ensure electroneutrality, exchange OH^- or alternatively H^+ ions with surrounding water, therefore influencing the total alkalinity (Paulmier et al., 2009). Benthic anaerobic degradation of organic material has been found to increase CO_2 uptake by up to 25% in the North Sea through A_T generation (Thomas et al., 2009). This process may not be ubiquitous in all shelf seas; despite denitrification occurring in Liverpool Bay, it did not increase concentrations of A_T relative to those of C_T (Hydes and Hartman, 2012). Hu and Cai (2011) also suggest that denitrification-generated alkalinity may be valid only on regional scales, with low global significance.

A_T has been found to behave conservatively in surface waters of the major oceans (Lee et al., 2006; Millero et al., 1998). Lee et al. (2006), later referred to as L'06, designed an algorithm to calculate A_T from sea surface salinity and temperature within a global area-weighted uncertainty of ±8.1μmol kg^{-1}. If A_T can be accurately calculated from sea surface salinity and temperature, then only one of the other carbonate parameters is required to monitor open ocean acidification. The correct use of this algorithm has the potential to generate substantial amounts of marine inorganic carbon data through the use of underway pCO_2, temperature and salinity instruments with predicted A_T values, and subsequent calculation of C_T and pH. Coastal and shelf zones have however, far more complicated processes influencing A_T concentrations than the open ocean, and therefore an investigation into where the algorithm can be applied is required.

1.1 The Study Area

Ireland is surrounded by the Irish Sea to the east, the Celtic Sea to the south and the eastern North Atlantic along the north and western side of the country (Figure 1). The Irish Sea is a semi-enclosed body of water connected to the North Atlantic through the North Channel, and to the Celtic Sea through St. George's Channel. The flow through the Irish Sea is predominantly northwards, however a southerly flow has been identified along the Irish coast during the summer months (Bowden, 1980). The Irish Sea is well mixed and vertically uniform during the winter months, and throughout the entire year in most places due to strong tidal currents (Brown and Gmitrowicz, 1995). N. Atlantic waters entering through St. George's Channel set the background salinity and nutrient concentrations and deviations reflect internal cycling, river inputs and anthropogenic nutrient sources (Gillooly et al., 1992). The largest freshwater sources discharging directly to the western Irish Sea are the Slaney to the south and the Boyne in the north, each with a long term average (up to 2010) of $39m^3\ s^{-1}$, with a smaller contribution from the Avoca and Liffey rivers (EPA, personal communication).

The Celtic Sea is connected to the Irish Sea through St. George's Channel and to the Atlantic Ocean along the 200m isobath at the continental shelf edge. Residual surface currents in the centre of the Celtic Sea are usually weak (Pingree and Griffiths, 1980; Pingree and Le Cann, 1989) and stratification often occurs during the summer months

(Pingree et al., 1978). Horsburgh et al. (1998) using satellite imagery, observed a distinct tidal-mixing front at the boundary between the stratified Celtic Sea and the mixed waters of the southern Irish Sea. The Celtic Sea is a productive shelf region due to both thermal fronts which help to keep phytoplankton in the surface sunlit waters and periodic upwelling which regenerates nutrients from deeper waters (Raine et al., 1990 and references within). Upwelling has the potential to transfer high-A_T deep waters to the surface, where it can buffer more atmospheric CO_2. The River Blackwater has the largest freshwater discharge into the Celtic Sea, followed by the River Suir. Other rivers flowing into the Celtic Sea include the Bandon, Lee, Nore and Barrow.

The Irish continental shelf is relatively broad to the west, north and south of Ireland, but narrows to only 30-60km to the northwest and southwest before reaching the steep continental slope. At the shelf edge, the depth sharply increases from ~200m to over 2000m in the Rockall Trough and over 4000m in the Porcupine Abyssal Plain (PAP) (Figure 1). The Shelf Edge Current (SEC) is a light, warm, saline current along the upper continental slope between the 300 - 600m isobaths, (Hill and Mitchelson-Jacob, 1993; White and Bowyer, 1997). The direction of the SEC is predominantly poleward with a general northward increase in mean slope current speed and transport (Pingree et al., 1999; White and Bowyer, 1997). The Irish Shelf Front (ISF) is a salinity front along the 35.3 salinity contour located between the 150-200m isobath (Huang et al., 1991; White and Bowyer, 1997). Fernand et al. (2006) observed a well-defined and persistent baroclinic coastal current with jet-like flows along the west coast of Ireland, associated with bottom fronts during summer stratification. The SEC and fronts play an important role in physical exchange processes at the shelf break and cross-shelf fluxes of heat, salt, organic and inorganic materials between oceanic and Irish coastal waters (Huthnance, 1995; McMahon et al., 1995). The River Shannon, the longest river in Ireland, is the largest single source of freshwater to the western Irish shelf (long term average discharge $209 m^3 s^{-1}$). The River Fergus is a smaller river flowing into the Shannon estuary. The next most significant discharge, the River Corrib, flows into Galway Bay and has a long term average discharge of $105 m^3 s^{-1}$.

This paper looks at the distribution of one of the primary ocean acidification parameters – total alkalinity which represents the waters buffering capacity – in outer

estuarine, coastal, shelf and open ocean waters around Ireland. Riverine chemistry data from the Environment Protection Agency (EPA, 2010) and the Northern Ireland Environment Agency (NIEA, personal communication) have been analysed to compare A_T and nutrient concentrations between riverine and coastal water. Data are compared with values predicted from the North Atlantic algorithm developed by Lee et al. (2006) and allow different provinces to be delineated based on the alkalinity/salinity space, which may be key to understanding the varying severity of ocean acidification effects on marine ecosystems in nearshore waters.

2. Method

Sampling was carried out on a number of surveys as part of a pilot project initiating research into ocean carbon processes in Irish marine waters (O'Dowd et al., 2011). Dates of surveys and number of A_T samples are shown in Table 1 and station positions in Figure 1. Salinity and dissolved inorganic nutrient samples were taken together with every A_T sample. Dissolved inorganic carbon and oxygen were also sampled on some of these surveys but are not included here.

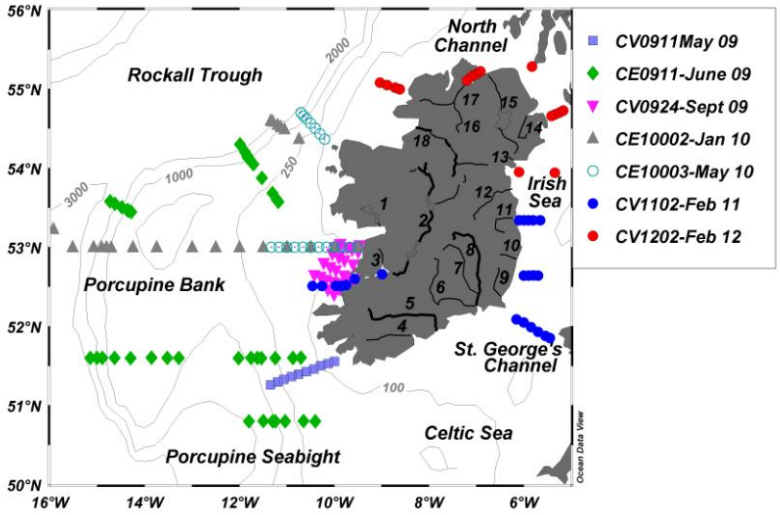

Figure 1 The study area with station positions where A_T measurements were made, labelled bathymetry and principal Irish rivers numbered (1) Corrib, (2) Shannon, (3) Fergus, (4) Lee, (5) Blackwater, (6) Suir, (7) Nore, (8) Barrow, (9) Slaney, (10) Avoca, (11) Liffey, (12) Boyne, (13) Newry, (14) Lagan, (15) Lower Bann, (16) Mourne, (17) Foyle and (18) Erne.

Table 1 Details of surveys discussed in the paper, with number of A_T samples. CE and CV refer to RV Celtic Explorer and RV Celtic Voyager respectively.

Survey	Date	A_T
CV0911	3-7 May 09	23
CE0911	14-22 June 09	172
CV0924	7-12 Sept 09	21
CE10002	5-17 Feb 10	95
CE10003	17-22 May 10	38
CV1102	29 Jan-10 Feb 11	33
CV1202	1-11 Feb 12	14

On all surveys a Seabird SBE 911 CTD rosette system was employed. The temperature, salinity and oxygen sensors deployed with the CTD were calibrated annually with the manufacturers.

A_T was analysed by potentiometric titration (Dickson et al., 2007) at NUI, Galway, on a VINDTA-3C (Versatile INstrument for the Determination of Total inorganic carbon and titration Alkalinity), manufactured by Marianda (Mintrop et al., 2000). The system was calibrated by running duplicate Certified Reference Materials with every batch of samples (CRMs provided by A. Dickson, Scripps Institute of Oceanography, USA). The precision of both CRMs and samples was calculated as the standard deviation of the difference between duplicate samples; A_T precision was ±2μmol kg^{-1} across all surveys. Salinity samples from CV0924 were analysed at NUIG on a Guildline Autosal salinometer. Samples from the other surveys were analysed on a Guildline Portasal salinometer (Model 8410A) at the Marine Institute (MI). Nutrient samples were filtered and frozen on board, and later analysed for total oxidised nitrogen (TOxN), nitrite (NO_2), silicate (Si) and phosphate (PO_4) on Skalar San^{++} continuous flow analyser by accredited standard colorimetric methods, also at the MI. Results from 7 QUASIMEME proficiency testing exercises (42 samples) between July 2008 and May 2011 gave an average z-score of ≤0.5 for TOxN, NO_2, PO_4, Si and salinity, ensuring high quality nutrient and salinity data..

The equation for calculating A_T from sea surface salinity (SSS) and sea surface temperature (SST), derived by Lee et al. (2006) for the North Atlantic is:

$$A_T = 2305 + 53.97(SSS–35) + 2.74(SSS–35)^2 – 1.16(SST–20) – 0.040(SST–20)^2 \quad (1)$$

where the uncertainty of the calculated A_T is 6.4μmol kg^{-1} for the N. Atlantic.

EPA samples were measured by titration with sulphuric acid to a pH colour indicated endpoint between 4.4 and 4.8, and results are reported in mg l^{-1} $CaCO_3$. To be able to compare the EPA data to our seawater alkalinity, the data were recalculated to µmol kg^{-1} total alkalinity by assuming that all the alkalinity in the freshwater is due to $CaCO_3$. The starting value is divided by the molar mass for $CaCO_3$ and multiplied by 2 since one mole of CO_3^{2-} equals 2 moles of alkalinity following the definition of total alkalinity by Dickson (1981). EPA methods to analyse total alkalinity can vary somewhat between laboratories so their data are treated as guideline values to give an indication of likely river end-member concentrations for our estuarine and coastal water samples. NIEA riverine A_T concentrations were also reported in mg l^{-1} and were converted to µmol kg^{-1} as outlined above and again are used only as guideline freshwater values.

The mineralogy of the river drainage basins were examined from the Geological Survey Ireland (GSI) map of Ireland's bedrock (http://www.gsi.ie/Programmes/Bedrock/Projects/).

3. Results and Discussion

3.1 Salinity, temperature, nutrients and oxygen

The salinity in the Irish Sea is clearly lower than in the western shelf and western coastal waters (Figure 2), and reflects the northward flow of Atlantic water which is freshened by rivers from the Irish and UK coasts (Bowden, 1980). This is also supported by lower salinity across the North Channel of the Irish Sea relative to St. George's Channel (Figure 2). Coldest temperatures were also measured in the Irish Sea during winter months, while surface temperatures of the western shelf and across Rockall measured during winter surveys were cooler relative to shelf surveys during spring and summer. Low salinities were measured at the mouth of the Shannon, extending out with the Shannon plume and at the mouth of the River Liffey in February 2011, and off Carlingford Lough and Lough Foyle in February 2012 (Table 2). Highest nutrient concentrations coincided with the low salinity waters, which decreased with increasing salinity due to dilution with coastal waters. Nitrate is the dominant inorganic nitrogen in all areas, with TOxN concentrations much higher than

nitrite, which was often not detected. All nutrient concentrations were higher in surface waters leaving the Irish Sea through the North Channel relative to water entering in the south due to river inputs. In offshore coastal waters, despite lower salinity in the Irish Sea, TOxN and PO_4 were generally higher on the western shelf which may be due to more of an oceanic influence in western areas and also denitrification in the Irish Sea (Hydes et al., 2004). The high silicate measured in the Shannon estuary (Table 2) is likely due to the large load of this river. Despite having higher salinity than other estuaries sampled in February 2011, samples measured at the mouth of the River Liffey had higher phosphate than any other region; concentrations were over 1.4µmol l^{-1} at four stations in the outer estuary. This is supported by EPA riverine data where maximum concentrations were mostly above 2.6µmol l^{-1} in the Liffey, reaching above 8µmol l^{-1} in some areas (Table 3), while maximum concentrations were generally below 1µmol l^{-1} in the Shannon. Where measured, the water columns in all areas were well oxygenated, with supersaturation in surface waters of spring-summer surveys due to photosynthesis. This supports findings by O'Boyle et al. (2009) who found no evidence of hypoxia or anoxia in Irish estuarine or coastal waters.

3.2 Total alkalinity (A_T) distribution

A_T is generally higher on the western shelf coinciding with higher salinities (Figure 2). West of 11ºW the average A_T concentration is 2335µmol kg^{-1} at an average salinity of 35.50. Concentrations decrease towards the coast together with salinity, highlighting the dominant role in physical processes on the A_T distribution. The average A_T across the southern transect in St. George's Channel is 2329µmol kg^{-1} at salinity 35.04; however it is higher on the Irish side of the Channel (2333µmol kg^{-1}) relative to the UK side (2321µmol kg^{-1}), despite similar salinity and nutrient concentrations across the Channel. This is suggestive of an A_T source on the Irish side of the Channel, likely from the Barrow, Nore and Suir flowing into the Celtic Sea which all have high A_T concentrations (Table 3). Such high A_T is likely due to a large part of the river catchments draining a limestone-rich bedrock in the centre of Ireland (GSI). The input from these rivers would increase the buffer capacity of the inner Celtic Sea, and may also be transported into the Irish Sea with residual currents.

Despite its large flow, the Blackwater delivers a smaller A_T load since with a mean concentration of 1978µmol kg^{-1} at the seaward end.

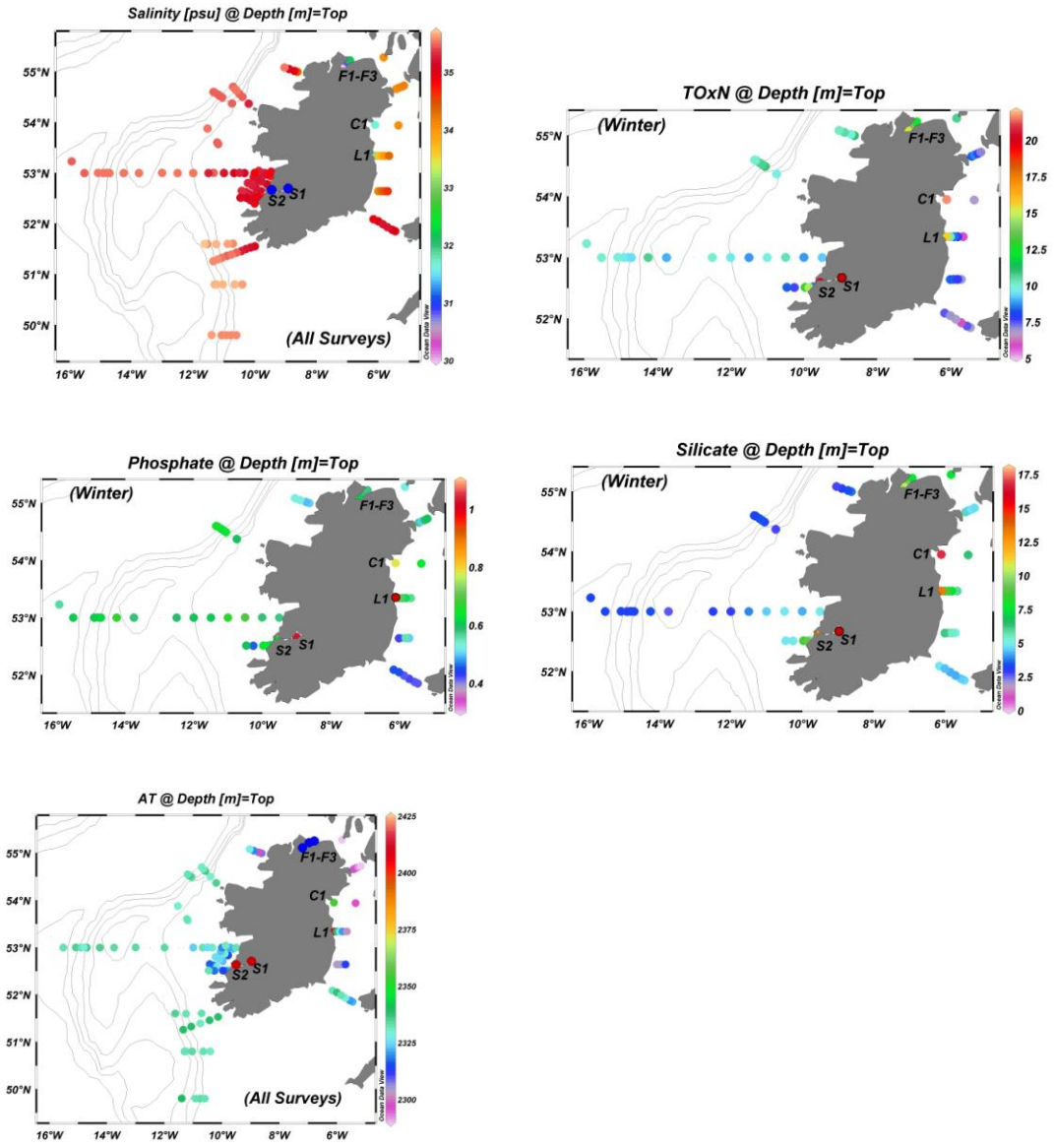

Figure 2 Surface distribution of (a) salinity (b) winter TOxN (c) winter phosphate (d) winter silicate and (e) total alkalinity. Nutrient concentrations were negligible during summer months. Nutrients are in µmol l^{-1}, while A_T is in µmol kg^{-1}. Actual values of winter inshore coastal waters are given in Table 2.

Table 2 Concentrations of chemical parameters in near-shore coastal waters at the mouth of the Shannon (S1 and S2), Liffey (L1), Carlingford Lough (C1) and Lough Foyle (F1-F3), as seen in Figure 2. Nutrients are in μmol l^{-1} and A_T is in μmol kg^{-1}.

	Salinity	Temp°C	TOxN	Phosphate	Silicate	A_T
S1	15.86	7.09	52.78	1.03	40.82	2864
S2	28.44	7.79	19.70	0.64	13.02	2432
L1	31.92	5.39	15.64	1.42	13.37	2412
C1	31.62	3.73	21.55	0.78	16.81	2354
F1	29.70	6.20	15.49	0.60	10.59	2111
F2	30.80	6.56	13.76	0.58	9.34	2146
F3	32.12	6.99	12.57	0.57	7.59	2208

Table 3 Riverine data from a number of Irish rivers from either the Irish Environment Protection Agency (EPA) or the Northern Ireland Environment Agency (NIEA). The EPA flow rate is the long term average up to 2010 (personal communication), while total alkalinity (A_T), total oxidised nitrogen (TOxN) and phosphate (PO_4) are the mean concentrations at the most seaward freshwater sampling site between 2007 and 2009 (EPA, 2010). NIEA A_T and TOxN are the mean concentrations between 2009 and 2011 at their fixed river sampling sites.

River	Flow rate $m^3 s^{-1}$	A_T μmol kg^{-1}	TOxN μmol l^{-1}	PO_4 μmol l^{-1}	Data Source
Boyne	39	5345	174.04	1.43	EPA
Liffey	17	4016	140.02	1.87	EPA
Avoca	22	233	113.86	0.21	EPA
Slaney	39	1332	324.40	1.01	EPA
Barrow	46	5107	286.31	1.41	EPA
Nore	42	5192	259.52	1.67	EPA
Suir	78	4460	224.29	0.83	EPA
Blackwater	87	1979	228.37	1.09	EPA
Shannon	209	3864	63.17	0.24	EPA
Fergus	19	4167	30.27	0.46	EPA
Corrib	105	2576	36.61	0.30	EPA
Newry		1558	190.06		NIEA
Lagan		2476	149.09		NIEA
L. Bann		2117	38.94		NIEA
Mourne		986	71.43		NIEA

Moving further north in the Irish Sea near Arklow, A_T again appears to be governed by factors affecting salinity, with lower A_T (2304µmol kg^{-1}) at stations closer to the coast (salinity 34.16), increasing to 2314µmol kg^{-1} in the centre of the Irish Sea (salinity 34.61). While river runoff results in lower salinity towards the coast in this area, it is not a high A_T source to the region. Both the River Slaney south of Arklow and the Avoca River flowing into Arklow have very low A_T concentrations (Table 3), as they flow through a granite bedrock catchment and therefore carbonate A_T is lower. A similar pattern was seen in the Baltic Sea where the A_T of rivers entering the southern Baltic Sea have higher A_T than those entering the northern part due to drainage basins rich in limestone, while further north granite dominates the bedrock (Hjalmarsson et al., 2008).

In the transect extending eastwards from the River Liffey, A_T is high at the mouth of the estuary (2413µmol kg^{-1}, salinity 31.80), and gradually decreases outwards along the transect to 2302µmol kg^{-1} at 34.32, due to mixing with more coastal waters (Figure 2). This is opposite to the pattern seen along the Arklow transect and indicates the Liffey is a high A_T source to the Irish Sea, despite its relatively small annual discharge. EPA A_T data supports these results with mean A_T concentrations of 4016µmol kg^{-1} at the most seaward freshwater sampling point in the Liffey. This high A_T water is diluted moving out from the coast with relatively low A_T coastal water. The high phosphate in this river may contribute to its higher A_T since it is part of Dickson's A_T definition (Dickson, 1981), but only a fraction of the magnitude of carbonate alkalinity. While the source of the Liffey is in a granite region south of Dublin, EPA riverine A_T steadily increases moving down river, likely due to the gradual addition of A_T from the limestone bedrock in the middle and lower parts of the river. The river Boyne, just north of the Liffey, has even higher A_T than the Liffey, as well as twice its average flow (Table 3).

Further north of the Liffey off Carlingford Lough, A_T concentrations are lower than at the mouth of the Liffey, despite similar salinity (Table 2). This coincides with lower A_T in the Newry River (Table 3) flowing into Carlingford Lough. There is a variety of different bedrocks in this region, including granite, sandstone and a small area of limestone (GSI). A_T across the North Channel is relatively low, with an average concentration of 2292µmol kg^{-1} in surface waters (salinity 34.12). This is partly due to physical processes as there is a gradual increase in A_T (5-6µmol kg^{-1}) with depth, coinciding with an increase in salinity. There is clearly an overall decrease in A_T and

salinity in offshore waters of the Irish Sea between St George's and the North Channel, highlighting again the predominantly northward flow through the Irish Sea. On the north coast, A_T is relatively low off Lough Foyle (<2210µmol kg^{-1}, Table 2) and coincides with a bedrock of schist, gneiss and quartzite (GSI), which unlike a limestone bedrock, would not contribute excess A_T. This is supported by NIEA riverine data with low A_T (<1000µmol kg^{-1}) in the Mourne River flowing into Lough Foyle. The A_T-salinity relationship for the North Coast (Figure 3) clearly highlights increasing A_T with salinity due to predominantly oceanic influence and minimal freshwater inputs. This relationship is similar to that reported by Muller et al. (1995), where the A_T of water in the Clyde estuary in western Scotland, which drains similar hard-rock geology to the north east of Ireland, was lower relative to surrounding coastal water. Muller et al. (1995) also found that A_T-salinity relationships were the only reliable method of determining the exact boundaries of the Clyde Plume, where at salinities lower than 32 significant variations were observed due to varying freshwater A_T inputs, precipitation and river discharge, while at salinities above 32 a permanent linear A_T-salinity relationship was observed.

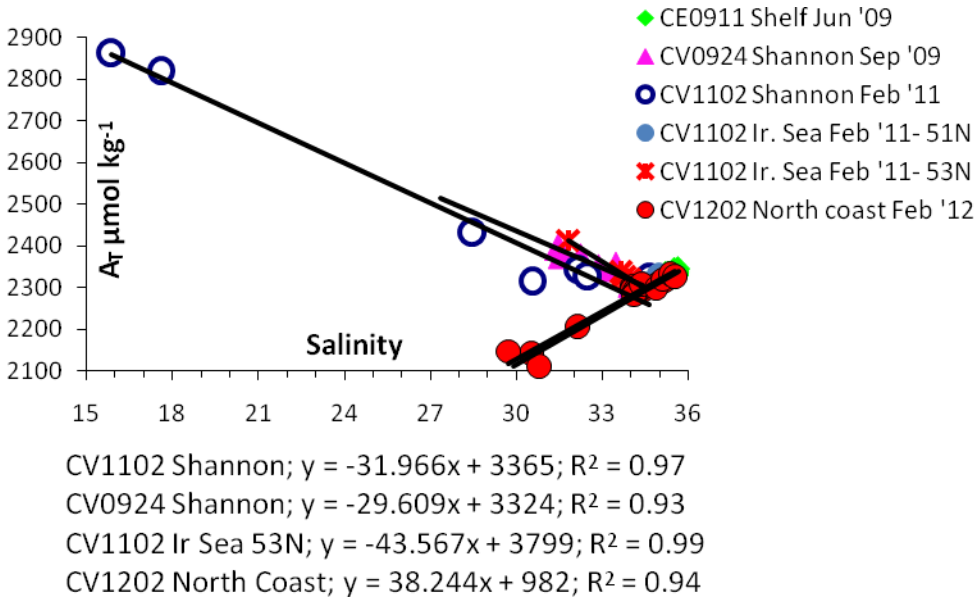

Figure 3 A_T versus salinity from four separate surveys, with predicted freshwater A_T concentrations from the A_T-salinity regressions. The River Shannon and Liffey are clearly A_T sources to coastal waters. The slope of the A_T-salinity regression of the North coast (CV1202) and the western shelf edge (CE0911) are almost identical indicating the predominantly oceanic influence in these regions with minimal freshwater A_T input.

On the west coast, the River Shannon has a high buffering capacity with the highest measured A_T values in the low salinity water of the outer estuary in Feb 2011 (CV1102); 2864µmol kg^{-1} in surface waters at a salinity of 15.87 and 2821µmol kg^{-1} in bottom waters at a salinity of 17.61 (Figure 2, Table 2). Concentrations decrease to 2432µmol kg^{-1} at salinity 28.44, and to 2318µmol kg^{-1} at salinity of 34.98. Due to the large annual discharge of this river, it has the capacity to carry greater A_T loads to the surrounding coastal water. Also, the Shannon drains an extensive limestone region in Ireland which is rich in calcium carbonate minerals and therefore it would be expected that total alkalinity would be high. This is likely the reason why the average A_T in the EPA riverine data gradually increases in the Shannon from the upper to the lower region. The mean concentrations of EPA riverine A_T in the lower Shannon ranged between 3278 and 4262µmol kg^{-1}, and despite the overall increase in A_T moving downstream along the river, A_T and nutrients start to decrease again at stations at the seaward end of the river relative to stations further upstream. This may indicate that the constituents are becoming more diluted closer to the coast. The River Fergus, despite its small discharge relative to the River Shannon, has high A_T levels where concentrations gradually increased downstream along the river's extensive limestone catchment (Table 3). A_T data from the transect extending out from the Shannon estuary (Feb 2011) predict a freshwater end-member concentration of 3365µmol kg^{-1}, while data in coastal waters west of the Shannon (Sept 2009) predict a freshwater end-member concentration of 3324µmol kg^{-1}, both calculated as the intercept of the regression line when salinity is plotted against A_T (Figure 3). These values fall within the A_T range for the River Shannon reported by the EPA between 2007 and 2009 of 3280 to 4060µmol kg^{-1}. Similar high A_T concentrations have been reported from other rivers with limestone bedrock; Hjalmarsson et al. (2008) reported A_T of 3244µmol kg^{-1} from the river Vistula flowing into the southeastern Baltic Sea, while A_T in the Nahr-Ibrahim River flowing into the Mediterranean Sea was 4250µmol kg^{-1} (Korfali and Davies, 2004). Similarly the UK's Derwent and Trent rivers have elevated A_T relative to other Humber rivers flowing into the North Sea due to calcareous soils and bedrock (Jarvie et al., 1997).

We conclude that the high A_T measured at the mouth of the Liffey and Shannon is primarily due to riverine inputs of A_T, mainly due to the rivers' limestone bedrock catchments. Denitrification is known to occur along the Irish shelf and into the Irish Sea (Hydes et al., 2004) and therefore may also contribute to A_T concentrations in

these waters (Thomas et al., 2009). However, the significance of the denitrification process is likely small relative to the differences in A_T between in-shore coastal waters influenced by different rivers; consider for example that the A_T in the Liffey is over 3000μmol kg^{-1} higher than in the Avoca River.

During the May surveys of 2009 and 2010 across the western shelf (CV0911 and CE10003), despite salinity increasing seaward along the transects, the A_T remains fairly constant, i.e. A_T normalised to constant salinity would be lower along the shelf edge relative to stations closer to the coast. While this may again be related to coastal A_T inputs, the nutrient concentrations and ratios indicate that there may be different phytoplankton species dominating in the shelf and coastal zones. In both surveys, all TOxN and PO_4 were generally depleted at stations in coastal waters, with low or depleted Si, while at the shelf edge, Si is depleted and TOxN and PO_4 are not. Diatoms require Si for their cell wall construction and are usually the first phytoplankton to bloom after spring stratification (Allen et al., 2005; Savidge et al., 1995). Once Si is depleted, as is seen along the shelf edge, it may result in a shift in phytoplankton community to calcifying species, such as coccolithophores (Sieracki et al., 1993). Calcifying phytoplankton play an important role in the carbonate biological pump and decrease A_T in surface waters through the precipitation of calcium carbonate. Massive blooms of *Emiliania huxleyi*, the most abundant and widespread species of coccolithophore, are observed annually extending for hundreds of km along the north western European continental shelf (Schmidt et al., 2012). Along the western edge of Ireland's continental shelf the E. *huxleyi* produces large seasonal blooms in early May (McGrane, 2007). The buffering capacity may therefore be lower along the shelf edge relative to coastal waters during the productive season due to reduced A_T concentrations.

Samples along 53ºN from CE10002 (Feb 2010) and CE10003 (May 2010) display varying A_T concentrations; in February, A_T averages 2331μmol kg^{-1}, while in May A_T averages 2339μmol kg^{-1}. The increase in A_T in May could be partly related to photosynthesis in the surface layer which tends to increase A_T due to the uptake of protons with nitrate by phytoplankton (Wolf-Gladrow et al., 2007). This is supported by depleted nutrients in May relative to February, with TOxN decreasing from 9.69μmol kg^{-1} to less than 0.26μmol kg^{-1} in May. The difference between summer and winter surface A_T across the Rockall Trough was also ~7μmol kg^{-1} due to

photosynthesis, since surface salinity was similar between surveys (McGrath et al., 2012). The average salinity along 53ºN is however lower in May (34.49) than February 2010 (35.33), which may also indicate more of a riverine influence and hence A_T input in May.

3.3 Investigation into the use of the Lee et al. (2006) A_T algorithm

There are large discrepancies between the calculated A_T following L'06 (Eq. 1) and measured A_T (Figure 4), where the discrepancy generally increases with decreasing salinity and temperature. The L'06 algorithm is said to work in open ocean surface waters of the North Atlantic with a sea surface salinity between 31 and 37 and a sea surface temperature between 0 and 20ºC. This is clearly not applicable in Irish coastal waters where the algorithm underestimates A_T in regions where there are significant inputs of high-alkalinity river water. With the exception of data from the North coast, between a salinity of 31 and 34, L'06 underestimates A_T by an average of 153µmol kg^{-1} (ranging between 61 and 245µmol kg^{-1}), and between a salinity of 34 and 35, it underestimates A_T by an average of 31µmol kg^{-1} (ranging between 6 and 71µmol kg^{-1}). It is generally above a salinity of 35.2 where calculated A_T falls within the given uncertainty of L'06 for the North Atlantic of 6.4µmol kg^{-1}. This somewhat coincides with the Irish Shelf Front along the 35.3 salinity contour which separates Irish coastal and oceanic water (Huang et al., 1991). In the CV1202 dataset (North coast), the A_T of samples with comparable salinity to surveys further south is underestimated to a much lesser extent, suggesting that freshwater A_T sources may not be as important in this area. For example off Lough Foyle, the calculated A_T in samples with salinity <32 were underestimated between 8 and 28µmol kg^{-1}, whereas at similar salinity in near shore waters of the Shannon and the Liffey, calculated A_T was underestimated by over 200µmol kg^{-1}. In other regions around the North coast the calculated A_T was closer to the measured value than elsewhere around Ireland. This again can be attributed to the bedrock of rivers in the north of Ireland supplying lower carbonate A_T to the river water, since most do not have a limestone bedrock. Due to such large variability in the freshwater end-member A_T concentrations in Irish rivers (Table 3), the intercept of the A_T-S relation used by Friis et al. (2003) in the calculation of normalised A_T (NA_T) can not be used in Irish coastal waters and must instead be calculated for individual regions around the coast.

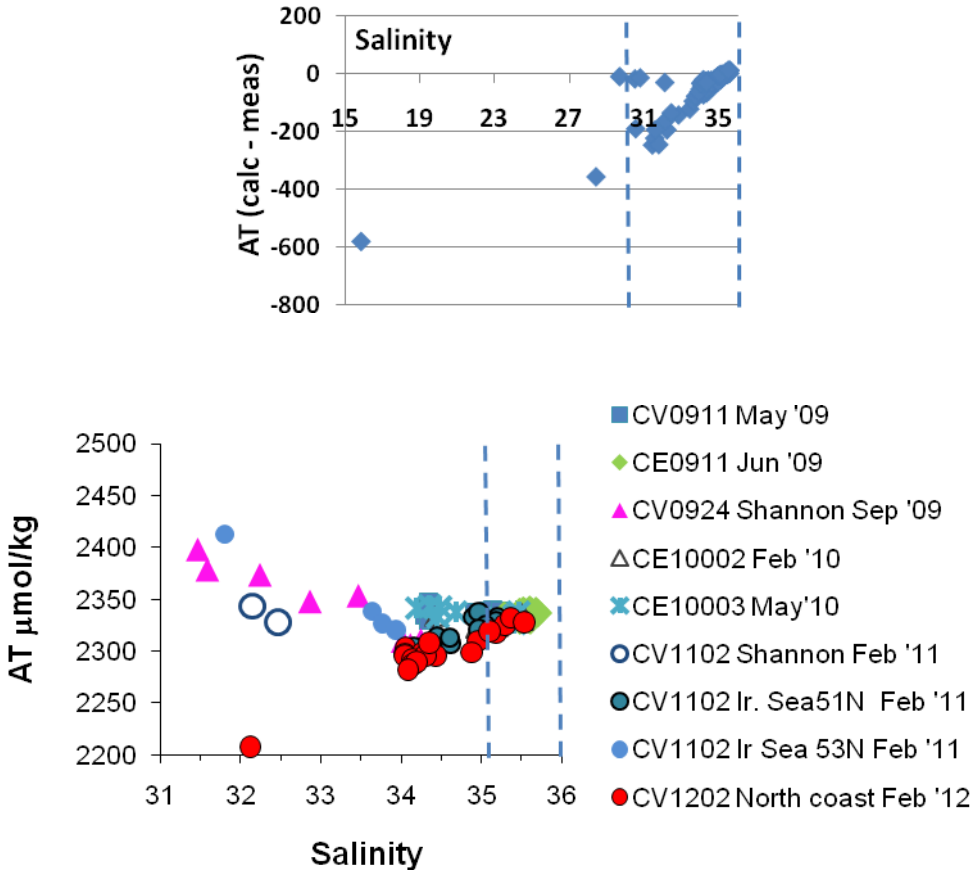

Figure 4 (a) A_T residuals (calculated A_T using L'06 minus measured A_T) vs. salinity, where the dotted lines indicate the full limits to the Lee et al. (2006) algorithm (b) A_T versus salinity for all surveys, the dotted lines indicate where our data fall within the uncertainty given by Lee et al. (2006).

Where calculated A_T was within the given L'06 uncertainty, the algorithm generally overestimates A_T along the western shelf by an average of 2µmol kg^{-1} in CE0911 and 4µmol kg^{-1} in CE10002. The algorithm better predicts A_T along the shelf edge during summer surveys (CE0911 and CE10003) relative to winter, with two stations from CE10003 having zero residuals. Calculated A_T by L'06 in the surface mixed layer across the Rockall Trough was overestimated by an average of 7µmol kg^{-1} in February 2010 (CE10002) and by 5µmol kg^{-1} in a similar WOCE transect in November 1996 (AR24) (McGrath et al., 2012). The only difference between surface waters of CE10002 and AR24 is cooler temperatures in 2010; salinity and A_T are the same. At constant temperature, pressure, salinity, C_T and nutrients, and at values similar to those across the Rockall Trough in winter 2010, an overestimation of A_T by 5-7µmol kg^{-1} leads to an underestimation of pCO_2 of 20-24µatm and in both cases lead to an overestimation in pH by 0.02 units, the average rate of decadal pH decline

in a number of carbon time series (Solomon et al., 2007). In the Rockall Trough, A_T tends to decrease from surface waters to ~1500m (McGrath et al., 2012) and therefore the overestimation in this region may be due to high rates of convective mixing during winter, which bring lower-A_T subsurface waters to the surface. While the algorithm can accurately predict A_T in tropical oceans (Lee et al., 2008), predicted A_T in the Rockall Trough is less robust since differences between measured and calculated A_T are close to or above the given uncertainty of the algorithm.

Results indicate that the L'06 algorithm should not be used to predict A_T in river-dominated coastal waters due to processes other than those governing salinity and temperature playing an important role in the A_T distribution. However, departures of measured alkalinity-salinity relationships from the algorithms provided by Lee et al. (2006) may provide valuable information on both the sources and magnitudes of the different fresh water inputs to the oceans. The physical and chemical discrimination of riverine-influenced coastal waters from open ocean waters will become particularly important for any large scale calculation of A_T, e.g. in the Arctic Ocean where low salinity waters can occur both as a result of melting sea ice and ice shelves (where salinity changes alone govern A_T), and from increasing volumes of riverine inputs due to ongoing climate change, whose input of dissolved organic material (e.g. Holmes et al., 2008) may strongly influence A_T.

4. Conclusion

We have highlighted various processes affecting A_T concentrations in Irish estuarine, coastal and shelf waters. The mineralogy of the river drainage basin in Ireland has a large influence on the riverine A_T signal, where rivers flowing over limestone bedrock have a high A_T signal due to the addition of carbonate minerals from the limestone. High A_T was measured at the mouth of both the Liffey and Shannon rivers, and therefore their plumes have high buffering capacity and will be able to better resist local changes in pH. Their surrounding coastal waters may therefore potentially act as 'refugia' for marine organisms as these waters will be less impacted by ocean acidification. Coastal waters surrounding Lough Foyle and the Avoca rivers have low buffering capacity, therefore ecosystems in these regions may be more prone to stress from ocean acidification. This paper highlights that on-going monitoring of total

alkalinity in river systems and surrounding coastal water is fundamental to the study of the impacts of ocean acidification on marine ecosystems.

One of the objectives of the paper was to test the L'06 algorithm for the N. Atlantic Ocean against our data in order to see in which regions the algorithm is valid and where it breaks down. We expected the algorithm to be robust for open ocean waters across the Rockall Bank and Rockall Trough, but might break down in more productive waters closer to the coast, where riverine inputs and the presence of organic acids might be expected to play a role. We have found that along the shelf and shelf edge above a salinity of 35.2, the calculated A_T from the L'06 algorithm are within the given uncertainty (although consistently low), however below this salinity the algorithm underestimates A_T. While the L'06 A_T calculation for the N. Atlantic is likely to be very useful in describing regional variation of surface water A_T across the basin, the size of the calculation uncertainty means that without substantial ground-truthing, it is unlikely to be able to accurately describe inter-annual variation in surface water alkalinity, and therefore pH in the region. However, where monitoring data are available, the algorithm may be very useful for discriminating between fresh water sources in coastal and Arctic waters.

Acknowledgements

We would like to thank the Irish Environmental Protection Agency (EPA) and the Northern Ireland Environment Agency (NIEA) for their riverine data and supporting information, which was a substantial contribution to the paper. This study was funded by the Irish Government, under the Marine Institute's Rapid Climate Change Programme project "Impacts of Increased Atmospheric CO_2 on Ocean Chemistry and Ecosystems", with Colin O'Dowd as PI and carried out under the Sea Change strategy with the support of the Marine Institute and the Marine Research Sub-Programme of the National Development Plan 2007- 2013. Surveys CV0911, CE10002, CE10003 and CV11020 were funded by the Irish government's National Development Plan 2007-2013. Shiptime for CV0924 was provided by the Marine Institute as part of NUIG's shiptime student training programme. We are grateful to the officers, crew and scientists on the surveys referred to in this paper. We thank Eileen Joyce for her help with figures.

References

Allen, J.T., Brown, L., Sanders, R., Mark Moore, C., Mustard, A., Fielding, S., Lucas, M., Rixen, M., Savidge, G., Henson, S. and Mayor, D., 2005. Diatom carbon export enhanced by silicate upwelling in the northeast Atlantic. Nature, 437(7059): 728-732.

Andersson, A.J., Mackenzie, F.T. and Lerman, A., 2005. Coastal ocean and carbonate systems in the high CO2 world of the Anthropocene. American Journal of Science, 305: 875-918.

Beldowski, J., Löffler, A., Schneider, B. and Joensuu, L., 2010. Distribution and biogeochemical control of total CO2 and total alkalinity in the Baltic Sea. Journal of Marine Systems, 81(3): 252-259.

Bowden, K.F., 1980. Chapter 12 Physical and Dynamical Oceanography of the Irish Sea. In: F.T. Banner, M.B. Collins and K.S. Massie (Editors), The North-west European Shelf Seas: The Sea Bed and the Sea in Motion II. Physical and chemical oceanography, and physical resources. Elsevier Oceanography Series, pp. 391-413.

Broecker, W.S. and Peng, T.H., 1982. Tracers in the sea. Columbia University Press, Palisades, NY, 690 pp.

Brown, J. and Gmitrowicz, E.M., 1995. Observations of the transverse structure and dynamics of the low frequency flow through the North Channel of the Irish Sea. Continental Shelf Research, 15(9).

Cai, W.-J., Hu, X., Huang, W.-J., Jiang, L.-Q., Wang, Y., Peng, T.-H. and Zhang, X., 2010. Alkalinity distribution in the western North Atlantic Ocean margins. Journal of Geophysical Research, 115(C8): C08014.

Chen, C.-T., 2002. Shelf-vs. dissolution-generated alkalinity above the chemical lysocline. Deep-Sea Research II, 49: 5365-5375.

Chen, C.-T. and Wang, S.-L., 1999. Carbon, alkalinity and nutrient budgets on the East China Sea continental shelf. Journal of Geophysical Research, 104: 20675-20686.

Dickson, A.G., 1981. An exact definition of total alkalinity and a procedure for the estimation of alkalinity and total inorganic carbon from titration data. Deep Sea Research Part A. Oceanographic Research Papers, 28(6): 609-623.

Dickson, A.G., Sabine, C.L. and Christian, J.R., 2007. Guide to best practices for ocean CO2 measurements. PICES Special Publication 3: 1-191.

Doney, S.C., Tilbrook, B., Roy, S., Metzl, N., Le Quéré, C., Hood, M., Feely, R.A. and Bakker, D., 2009. Surface-ocean CO2 variability and vulnerability. Deep Sea Research Part II: Topical Studies in Oceanography, 56(8-10): 504-511.

EPA, 2010. Water Quality in Ireland 2007-2009, Environmental Protection Agency, Wexford.

Fernand, L., Nolan, G.D., Raine, R., Chambers, C.E., Dye, S.R., White, M. and Brown, J., 2006. The Irish coastal current: A seasonal jet-like circulation. Continental Shelf Research, 26(15): 1775-1793.

Friis, K., Körtzinger, A. and Wallace, D.W.R., 2003. The salinity normalization of marine inorganic carbon chemistry data. Geophysical Research Letters, 30(2): 1085.

Gillooly, M., O'Sullivan, G., Kirkwood, D. and Aminot, A., 1992. The establishment of a database for trend monitoring of nutrients in the Irish Sea.

Hernández-Ayón, J.M., Belli, S.L. and Zirino, A., 1999. pH, alkalinity and total CO_2 in coastal seawater by potentiometric titration with a difference derivative readout. Analytica chimica acta, 394: 101-108.

Hill, A.E. and Mitchelson-Jacob, E.G., 1993. Observations of a poleward-flowing saline core on the continental slope west of Scotland. Deep Sea Research Part I: Oceanographic Research Papers, 40(7): 1521-1527.

Hjalmarsson, S., Wesslander, K., Anderson, L.G., Omstedt, A., Perttilä, M. and Mintrop, L., 2008. Distribution, long-term development and mass balance calculation of total alkalinity in the Baltic Sea. Continental Shelf Research, 28(4-5): 593-601.

Holmes, R.M., McClelland, J.W., Raymond, P.A., Frazer, B.B., Peterson, B.J. and Stieglitz, M., 2008. Lability of DOC transported by Alaskan rivers to the Arctic Ocean. Geophysical Research Letters, 35(L03402).

Holt, J., Harle, J., Proctor, R., Michel, S., Ashworth, M., Batstone, C., Allen, I., Holmes, R., Smyth, T., Haines, K., Bretherton, D. and Smith, G., 2009. Modelling the global coastal ocean. Philosophical Transactions of the Royal Society A: Mathematical, Physical and Engineering Sciences, 367(1890): 939-951.

Horsburgh, K.J., Hill, A.E. and Brown, J., 1998. A summer jet in the St. George's Channel of the Irish Sea. Estuarine, Coastal and Shelf Science, 47: 285-294.

Howland, R.J.M., Tappin, A.D., Uncles, R.J., Plummer, D.H. and Bloomer, N.J., 2000. Distributions and seasonal variability of pH and alkalinity in the Tweed Estuary, UK. Science of The Total Environment, 251/252(0): 125-138.

Hu, X. and Cai, W.-J., 2011. The impact of denitrification on the atmospheric CO2 uptake potential of seawater. Marine Chemistry, 127(1-4): 192-198.

Huang, W.G., Cracknell, A.P., Vaughan, R.A. and Davies, P.A., 1991. A Satellite and Field View of the Irish Shelf Front. Continental Shelf Research, 11(6): 543-562.

Huthnance, J.M., 1995. Circulation, exchange and water masses at the ocean margin: the role of physical processes at the shelf edge. Progress In Oceanography, 35(4): 353-431.

Hydes, D.J., Gowen, R.J., Holliday, N.P., Shammon, T. and Mills, D., 2004. External and internal control of winter concentrations of nutrients (N, P and Si) in north-west European shelf seas. Estuarine Coastal and Shelf Science, 59(1): 151-161.

Hydes, D.J. and Hartman, S., 2012. Seasonal and inter-annual variability in alkalinity in Liverpool Bay (53.5° N, 3.5° W) and in major river inputs to the North Sea. Ocean Dynamics, 62(321-333).

Jarvie, H.P., Neal, C., Leach, D.V., Ryland, G.P., House, W.A. and Robson, A.J., 1997. Major ion concentrations and the inorganic carbon chemistry of the Humber rivers. The Science of the Total Environment, 194/195: 285-302.

Kim, H.-C., Lee, K. and Choi, W., 2006. Contribution of phytoplankton and bacterial cells to the measured alkalinity of seawater. Limnology and Oceanography, 51(1): 331-338.

Korfali, S.I. and Davies, B.E., 2004. Speciation of metals in sediment and water in a river underlain by limestone: role of carbonate species for purification capacity of rivers. Advances in Environmental Research, 8(3-4): 599-612.

Lee, H.-W., Lee, K. and Lee, B.-Y., 2008. Prediction of Surface Ocean pCO2 from Observations of Salinity, Temperature and Nitrate: the Empirical Model Perspective. Ocean Science Journal, 43(4): 195-208.

Lee, K., Tong, L.T., Millero, F.J., Sabine, C.L., Dickson, A.G., Goyet, C., Park, G.H., Wanninkhof, R., Feely, R.A. and Key, R.M., 2006. Global relationships of total alkalinity with salinity and temperature in surface waters of the world's oceans. Geophysical Research Letters, 33(19).

McGrane, P.B., 2007. Extant coccolithophores in Irish shelf waters of the Northeast Atlantic, National University of Ireland, Galway 359 pp.

McGrath, T., Kivimae, C., Tanhua, T., Cave, R.R. and McGovern, E., 2012. Inorganic carbon and pH levels in the Rockall Trough 1991-2010. Deep Sea Research Part I: Oceanographic Research Papers, 68(0): 79-91.

McMahon, T., Raine, R., Titov, O. and Boychuk, S., 1995. Some oceanographic features of northeastern Atlantic waters west of Ireland Ices Journal of Marine Science, 52(2): 221-232.

Millero, F.J., Feistel, R., Wright, D.G. and McDougall, T.J., 2008. The composition of Standard Seawater and the definition of the Reference-Composition Salinity Scale. Deep Sea Research Part I: Oceanographic Research Papers, 55(1): 50-72.

Millero, F.J., Lee, K. and Roche, M., 1998. Distribution of alkalinity in the surface waters of the major oceans. Marine Chemistry, 60(1-2): 111-130.

Mintrop, L., Pérez, F.F., Gonzalez-Dávila, M., Santana-Casiano, J.M. and Körtzinger, A., 2000. Alkalinity determination by potentiometry: intercalibration using three different methods. Ciencias Marinas, 26(1): 23-37.

Muller, F.L.L., Balls, P.W. and Tranter, M., 1995. Processes controlling chemical distributions in the Firth of Clyde (Scotland). Oceanographic Literature Review, 43(9): 872.

Muller, F.L.L. and Bleie, B., 2008. Estimating the organic acid contribution to coastal seawater alkalinity by potentiometric titrations in a closed cell. Analytica Chimica Acta, 619(2): 183-191.

O'Boyle, S., McDermott, G. and Wilkes, R., 2009. Dissolved oxygen levels in estuarine and coastal waters around Ireland. Marine Pollution Bulletin, 58(11): 1657-1663.

O'Dowd, C., Cave, R., McGovern, E., Ward, B., Kivimae, C., McGrath, T., Stengel, D. and Westbrook, G., 2011. Impacts of Increased Atmospheric CO2 on Ocean Chemistry and Ecosystems.

Paulmier, A., Kriest, I. and Oschlies, A., 2009. Stoichiometries of remineralisation and denitrification in global biogeochemical ocean models. Biogeosciences, 6: 923–935.

Pingree, R.D. and Griffiths, C., 1980. Currents driven by a steady uniform wind stress on the shelf seas around the British Isles. Oceanologica Acta, 3.

Pingree, R.D., Holligan, P.M. and Mardell, G.T., 1978. The effects of vertical stability on phytoplankton distributions in the summer on the northwest European shelf. Deep Sea Research, 25: 1011–1028.

Pingree, R.D. and Le Cann, B., 1989. Celtic and Armorican slope and shelf residual currents. Progress in Oceanography, 23(308-338).

Pingree, R.D., Sinha, B. and Griffiths, C.R., 1999. Seasonality of the European slope current (Goban Spur) and ocean margin exchange. Continental Shelf Research, 19(7): 929-975.

Raine, R., O'Mahony, J., McMahon, T. and Roden, C., 1990. Hydrography and phytoplankton of waters off south-west Ireland. Estuarine, Coastal and Shelf Science, 30(6): 579-592.

Raymond, P.A. and Cole, J.J., 2003. Increase in the export of alkalinity from North America's largest river. Science, 301: 88-91.

Savidge, G., Boyd, P., Pomroy, A., Harbour, D. and Joint, I., 1995. Phytoplankton production and biomass estimates in the northeast Atlantic Ocean, May-June 1990. Deep Sea Research Part I: Oceanographic Research Papers, 42(5): 599-617.

Schmidt, S., Harlay, J., Borges, A.V., Groom, S., Delille, B., Roevros, N., Christodoulou, S. and Chou, L., 2012. Particle export during a bloom of Emiliania huxleyi in the North-West European continental margin. Journal of Marine Systems, doi:10.1016/j.jmarsys.2011.12.005.

Sieracki, M.E., Verity, P.G. and Stoecker, D.K., 1993. Plankton community response to sequential silicate and nitrate depletion during the 1989 North Atlantic spring bloom. Deep Sea Research Part II: Topical Studies in Oceanography, 40(1-2): 213-225.

Solomon, S., Qin, D., Manning, M., Chen, Z., Marquis, M., Averyt, K.B., Tignor, M. and (eds.), H.L.M., 2007. Climate Change 2007: The Physical Science Basis. Contribution of Working Group I to the Fourth Assessment Report of the Intergovernmental Panel on Climate Change, Cambridge University Press, Cambridge, United Kingdom and New York, NY, USA.

Takahashi, T., Broecker, W.S., Bainbridge, A.E. and Weiss, R.F., 1980. Carbonate chemistry of the Atlantic, Pacific and Indian Oceans: The Results of the GEOSECS Expedition, 1972-1978.

Thomas, H., Suykens, K., Koné, Y.M.J., Shadwick, E.H., Prowe, A.E.F., Bozec, Y., de Baar, H.J.W. and Borges, A., 2009. Enhanced ocean carbon storage from anaerobic alkalinity generation in coastal sediments. Biogeosciences, 6: 1-8.

White, M. and Bowyer, P., 1997. The shelf-edge current north-west of Ireland. Annales Geophysicae-Atmospheres Hydrospheres and Space Sciences, 15(8): 1076-1083.

Wolf-Gladrow, D.A., Zeebe, R.E., Klaas, C., Körtzinger, A. and Dickson, A.G., 2007. Total alkalinity: The explicit conservative expression and its application to biogeochemical processes. Marine Chemistry, 106(1-2): 287-300.

Zeebe, R.E. and Wolf-Gladrow, D., 2003. CO_2 in seawater: Equilibrium, kinetics, isotopes. Elsevier Oceanography Series, 65. Elsevier, 346 pp.

Appendices

Appendix 1 Ocean Acidification Project Overview

"Impacts of Increased Atmospheric CO_2 on Ocean Chemistry and Ecosystems" – Project Overview

Lead Partner: Dr. Colin'O Dowd[1]
Work package/Task leaders: Dr. Evin McGovern[2], Dr. Rachel Cave[1], Dr. Brian Ward[1], Dr. Dagmar Stengel[l], Dr. Glenn Nolan[2] and Dr. Guy Westbrook[2]
[1] National University of Ireland, Galway; [2] Marine Institute

This was a pilot project initiating research in ocean carbon processes in Irish marine waters, carried out by the National University of Ireland, Galway (NUI Galway) and the Marine Institute, Ireland (MI), between February 2008 and August 2010. It was carried out under the Sea Change strategy with the support of the Marine Institute and the Marine Research Sub- Programme of the National Development Plan 2007–2013.

The main objectives of the project were to:

- Initiate research into ocean carbon processes in Irish shelf Sea waters, including investigation of CO_2 fluxes
- Establish high-quality chemical measurement capabilities to describe inorganic carbon chemistry in seawater
- Deploy automated systems on moorings and shipboard systems for measurement of pCO_2 in seawater
- To investigate potential indicators of ecological impact of ocean acidification
- To make recommendations for future Irish research and long-term monitoring in this field

The project addressed these objectives in five work packages:

- Establish network of autonomous pCO_2 measurement systems
- Establish capabilities for measuring TA, TCO_2, pH and validate
- Establish baseline monitoring
- CO_2 flux quantification including seasonal processes in Irish Shelf waters
- Potential ecological impacts and indicators of ocean acidification for Irish maritime area and recommendations

Throughout the duration of the project a highly skilled interdisciplinary research team was developed with NUIG and the MI, developing expertise in CO_2 air-sea exchange and ocean carbon chemistry. The project has developed the capabilities for measuring pCO_2, CO_2 fluxes and inorganic carbon chemistry and pH in Irish waters. The overall findings of the project are published in O'Dowd et al. (2011).

Using equipment procured under the work programme, methodologies were optimised and validated to measure the inorganic carbon system (A_T, C_T ,pCO_2, and calculated pH – from other parameters) in Irish shelf waters with the high level of precision required given the relatively small annual change in oceanic pH expected. Excellent use of existing infrastructure and resources was made through collaboration with ongoing research programmes and surveys, allowing for the sampling of carbonate

parameters in Irish coastal, shelf and deeper waters. During the project carbonate parameters were sampled on five deepwater surveys and five coastal water surveys on the RV Celtic Explorer and RV Celtic Voyager (Chapter 2, Table 2.1, and Figure 2.1). Sampling was extended beyond the scope of the project on two extra surveys in 2011, one deepwater and one coastal. The inorganic carbonate system in key water masses to the west of Ireland was described (McGrath et al., in press) along with the baseline state of inorganic carbon chemistry in Irish coastal waters (Kivimäe et al., in prep; McGrath et al., in prep; O'Dowd et al., 2011) . This will provide a basis for longer-term assessment of future changes in the carbonate system in the Irish marine environment.

During the project pCO_2 and CO_2 flux data from the coastal buoy at Mace Head Atmospheric Research Station was analysed for seasonal trends. pCO_2 concentrations illustrated a summer-maximum-winter-minimum seasonal cycle. Maximum fluxes were observed in winter months, thought to be due to the increased wind speeds and lower temperatures promoting a higher flux, while the secondary peak observed in summer is likely due to biological activity. Overall, coastal fluxes were higher than those previously reported over open oceans. Techniques were developed to derive CO_2 fluxes from instruments mounted on the Celtic Explorer.

A desk study was carried out to review ecological impacts of ocean acidification that are likely to occur in Irish waters. The study examined the current state of knowledge, the potential consequences and nationally relevant policy considerations including monitoring and research needs. A comprehensive report was produced and published as a Marine Institute Foresight report in May 2010, outlining potential indicators of ocean acidification and species and ecosystems at risk (Ní Longphuirt et al., 2010). Ocean acidification may either directly or indirectly alter keystone species which could culminate in ecosystem shifts with untold impacts on economically important organisms. Organisms for which acidification may have direct or indirect economic ramifications include zooplankton and phytoplankton which are a food source for pelagic and benthic commercial species, harvested shellfish and those which support fish species such as deep-water corals and macroalgal beds (wrack, kelp, maërl). Calcifying species at risk include mussels and oysters, which are important for Irish aquaculture.

Recommendations for future Irish research and monitoring, along with essential facts for policy development on ocean acidification in Irish waters were outlined in Ní Longphuirt et al. (2010). This information is essential to develop mitigation and adaptation management policies including risk analysis. In summary it was recommended that "a long-term multi-disciplinary ocean acidification and marine climate change monitoring and research programme is established to support policy decisions on mitigation and adaptation. Specialist expertise and capacity developed under this programme should be sustained to deliver a viable and cost-effective monitoring programme into the future", (O'Dowd et al., 2011).

Appendix 2 Offset in CE0903 total alkalinity data

The A_T data from CE0903 (Feb 2009) is ~7-8µmol kg^{-1} lower through the water column than the CE10002 (Feb 2010) A_T across the Rockall Trough, see Paper II. The CE0903 A_T is also lower than two WOCE transects across the Trough, AR24 (Nov 1996) and A24 (May 1997), Figure 1. The NA_T (normalised A_T to a salinity of 35) is clearly lower in CE0903 relative to the other years and is therefore not related to salinity. Vertical A_T profiles from along the shelf edge in June 2009 (CE0911) are also similar to the CE10002 data, despite a different location. Since CE10002 A_T is similar to a number of other surveys in the region and since we would not expect NA_T to vary considerably between subsequent years, we assume that the CE10002 results are correct. The CE0903 dissolved inorganic carbon (C_T) results were similar to CE10002, suggesting it is not due to sampling or storage issues, since C_T and A_T are sampled from the same bottle. An investigation was carried out to explain the reason for the negative offset in the CE0903 A_T data.

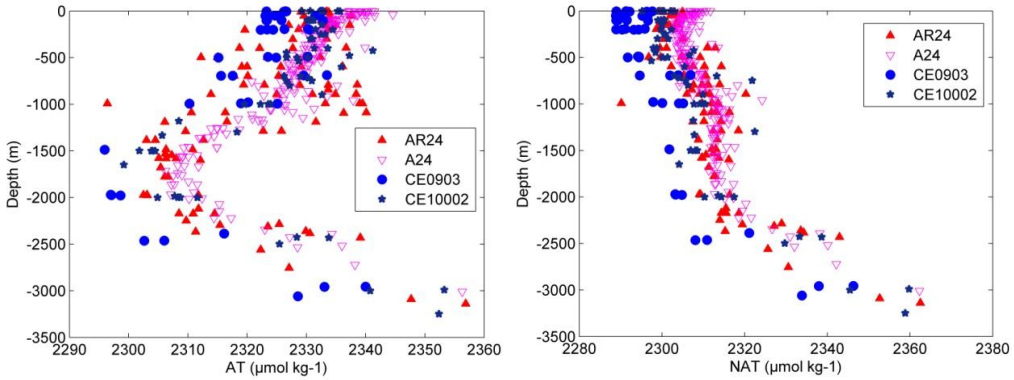

Figure 1. Vertical profiles of (a) A_T and (b) NA_T with depth for two WOCE surveys, AR24 and A24, and our CE0903 (2009) and CE10002 (2010) Rockall surveys. Profiles illustrate a negative offset in the CE0903 A_T data.

Potential reasons for offset

1. Sampling;

Inconsistencies in sampling of the CE0903 carbon samples would not result in a constant offset through the water column, but rather varying degrees of offset between samples. Also, since C_T samples (sampled from the same bottle) are more prone to contamination and errors in sampling, results would highlight any differences in the sampling technique, which was not the case. The same Duran bottles were used in CE0903 and CE10002 and were cleaned in the same manner before the surveys. Samples were poisoned with mercuric chloride in both years, which was generally in very low concentrations (0.02% volume). If there was a problem with deionised water that was used to make the mercuric chloride, A_T would have been added to the sample, however this would be minimal due to the small volume added. The headspace may have varied slightly between surveys; in CE0903, a plastic squeezy pipette was used to create headspace in the samples, while an accurate pipette, removing exactly 2ml from every sample, was used in CE10002. If headspace had an effect on the samples, we would not get a consistent offset through water column

since a squeezy pipette would not have removed the exact same volumes from every sample. If there was a larger headspace in the CE0903 A_T samples, we would expect to see higher A_T due to more evaporation. The same Apiezon grease was used in both surveys to seal the bottles. If the seal was not as effective in CE0903, we would expect more evaporation and hence higher A_T, rather than the lower A_T observed. Also, if there was a problem with the seal we would have seen a difference in C_T due to air contamination.

2. Storage;

All samples were stored in the same fridge at NUIG (~4ºC) after the surveys. Samples at sea were kept in the same fridge in the dark. In CE0903, the temperature of this fridge may have been set at a lower temperature (4-5ºC) than CE10002 (6-7ºC) for the duration of the survey. However, considering they were all stored at ~4ºC for the longer storage time period at NUIG, this should have minimal effect. The CE0903 A_T samples were stored for a longer time period than CE10002; however, the results from the sample storage plan (See Section 2.2.1) indicated that A_T concentration does not vary with time due to storage.

3. Analysis;

Samples were always placed in same water bath at the same temperature before analysis. The pipette volume was not changed at any time between surveys. For the CE10002 A_T analysis, ampoules of HCl were used to ensure exact concentration of the acid was added to the solution. These ampoules were not used for the CE0903 analysis and therefore acid concentration may not have been as precise. However, this would have also applied to the CRMs that were run with the CE0903 samples, and results would have been corrected with the CRM correction factor. CRMs were run with every batch of samples, and the CRM batches used for CE0903 (Batch 97 and 99) were also used in CE0911. The same electrode was used to monitor the pH; if there was a problem with the electrode we would not expect a consistent offset, but rather erratic results. Also, CE0903 A_T samples were analysed between CE0911 and CE10002; both of which have similar A_T profiles and results are similar to the WOCE A_T data. If there was any issue with the electrode, pipette or VINDTA software, there would be a date after which sample results would differ from previous samples rather than only the samples analysed in between surveys being problematic.

4. Data processing;

After A_T samples were run, the salinity of each sample was entered into the VINDTA software, which then re-calculated results based on the correct salinity. Bottle salinity versus CTD salinity results from both CE0903 and CE10002 surveys give an r-square of 0.9996, with an average difference of 0.01 between data sets, therefore we are confident that the salinity results are correct. The salinity-corrected A_T was then corrected for the daily CRM results by multiplying by the CRM correction factor (assigned value divided by measured value). The assigned values of the CRMs were checked that the correct value was used in the calculations, see Figure 2. Sample results from all surveys had to be corrected for HCl acid concentration since the VINDTA software assumes an acid concentration of 0.09822ml, rather than 0.1ml. Without this acid correction the A_T results would be much higher. To ensure data processing was not resulting in the large offset, some of the CRMs were treated as samples and processed in the same manner, i.e. correction for salinity and acid concentration, and while there were some very small changes between initial and

recalculated CRM results (~0.35µmol kg^{-1}), it could not account for the 7-8µmol kg^{-1} offset in the CE0903 A_T results.

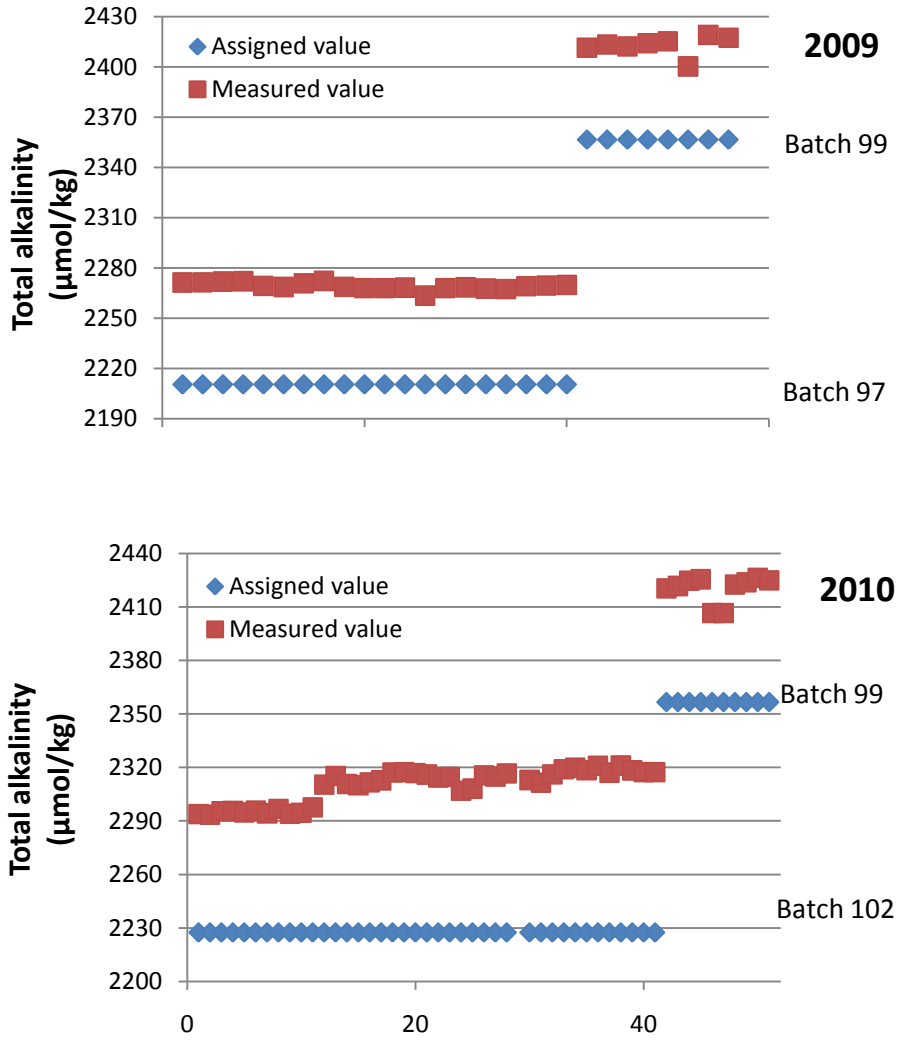

Figure 2. Measured concentrations verses the certified values for the CRMs analysed with the CE0903 and CE10002 total alkalinity samples.

Conclusion

No cause could be identified for the offset in the CE0903 A_T data and therefore results have not been used in this thesis. Total alkalinity for 2009 was instead calculated using multiple linear regression in Paper II.